The Role of OPA1 and Interacting Proteins in Mitochondrial Function

David A Patten

Thesis submitted to the

Faculty of Graduate and Postdoctoral Studies

in partial fulfillment of the requirements

for the Doctorate in Philosophy degree in Neuroscience

Department of Cellular and Molecular Medicine

Neuroscience Graduate Program

Faculty of Medicine

University of Ottawa

Authorization

This thesis contains parts of published and unpublished work.

The following publication is included in its entirety (specifically the second paragraph of the abstract, the last paragraph of chapter 1.4.6, chapters 2, 3.1, 4.1 and the first paragraph of 4.5):

> **Patten DA**, Wong J, Khacho M, Soubannier V, Mailloux RJ, Pilon-Larose K, MacLaurin JG, Park DS, McBride HM, Trinkle-Mulcahy L, Harper ME, Germain M, Slack RS (2014) OPA1-dependent cristae modulation is essential for cellular adaptation to metabolic demand. Embo J 33: 2676-2691

The following published works were appended to the thesis and referenced herein, with excerpts from Patten el al. 2010 used to introduce reactive oxygen species in section 1.8.1:

> **Patten DA**, Germain M, Kelly MA, Slack RS. Reactive oxygen species: stuck in the middle of neurodegeneration. J Alzheimers Dis. 2010;20 Suppl 2:S357-67.
>
> Khacho M, Tarabay M, **Patten D**, Khacho P, MacLaurin JG, Guadagno J, Bergeron R, Cregan SP, Harper ME, Park DS, Slack RS (2014) Acidosis overrides oxygen deprivation to maintain mitochondrial function and cell survival. Nature communications 5: 3550
>
> Germain M, Nguyen AP, Khacho M, **Patten DA**, Screaton RA, Park DS, Slack RS (2013) LKB1-regulated adaptive mechanisms are essential for neuronal survival following mitochondrial dysfunction. Hum Mol Genet 22: 952-962

Permissions for use of these publications, as well as permission for the use of Figure 6 (Palmieri, 2013), are included in Appendix A: Licences.

Chapters on CLUH (Chapter 3.2) and Glutathione (Chapter 3.3) remain at present unpublished.

Abstract

The cell possesses a number of vital mechanisms to respond to different stressors. Mitochondria are dynamic organelles which undergo constant changes in length, transport and inner membrane structure and curvature. Invaginations of this inner membrane, cristae, have been known to respond to the energetic state of mitochondria, but the regulation of these changes as well as the consequences thereof remain undetermined. We find that Optic Atrophy 1 (OPA1), a protein involved in inner membrane fusion and cristae maintenance during cell death, can respond to the energetic state of mitochondria and the cell. Moreover, OPA1-dependent changes in cristae structure are required for resistance to starvation induced cell death, proper functioning of the electron transport chain, for growth in galactose media and for maintenance of ATP synthase assembly. Interestingly, we demonstrate that select members of the mitochondrial solute carriers (SLC25A) interact with OPA1 and affect the response of OPA1 to substrate levels. Taken together, we propose an SLC25A-dependent role for OPA1 in sensing energy substrate availability and responding to alter cristae, bioenergetics and cellular survival.

We also identified KIAA0664 as a novel OPA1-interacting protein, describe its subcellular localization and investigate its role in mitochondrial fusion and in mitochondrial localization. Finally, since both known carriers of mitochondrial glutathione were demonstrated to interact with OPA1, we investigated the role of OPA1 in cellular glutathione redox. OPA1 depleted cells demonstrated both increased total cellular glutathione and a shift in redox to its reduced form. The role of OPA1 in glutathione levels and redox ratios required GTPase activity, but surprisingly not fusion. Since glutathione is

a master regulator of reactive oxygen species detoxification, these findings may shed light on the role of OPA1 in ROS-induced cell death pathways.

Table of contents

List of Tables

List of Figures

List of Abbreviations Used

Aβ	Amyloid β
AD	Alzheimer's disease
ADP	Adenosine diphosphate
AIF	Apoptosis inducing factor
AGC	Mitochondrial aspartate-glutamate transporter (1&2)
AICAR	5-aminoimidiazole-4-carboxamide ribonucleotide (AMP kinase activator)
ALS	amyotrophic lateral sclerosis
AMPK	5' AMP-activated protein kinase
ANT	Adenine nucleotide translocator
aPKC	atypical Protein Kinase C
ATP	Adenosine triphosphate
BM	2-Butylmalonate (inhibitor of the DIC)
BME	Beta-mercaptoethanol
BMH	Bismaleimidohexane (crosslinker)
BN-PAGE	Blue-Native PAGE
BSA	Bovine serum albumin
Ca2+	Calcium Ion
CC	Coiled coil (domain)
CCCP	Carbonyl cyanide 3-chlorophenylhydrazone (uncoupler of OXPHOS)
CL	Cardiolipin
CLUH	Clustered Mitochondria (CluA/CLU1) Homolog
ClO^-	Hypochlorite
CoQ	Coenzyme Q_{10} (ubiquinone)
CytC	Cytochrome c
DIC	Differential interference contrast
DIC	Dicarboxylate carrier

Dig	Digitonin
DMEM	Dulbecco's Modified Eagle Medium
DNA	Deoxyribonucleic Acid
DOA	Dominant Optic Atrophy
DRP-1	Dynamin related protein 1
EBSS	Earle's balanced salt solution
EDC	1-ethyl-3-(3-dimethylaminopropyl)carbodiimide hydrochloride (crosslinker)
ENDOG	Endonuclease G
EGTA	Ethylene glycol tetraacetic acid (chelating agent)
EM	Electron microscopy
ER	Endoplasmic reticulum
ESC	Embryonic stem cells
ETC	Electron transport chain
F_1	Fraction 1 (ATP synthase portion is within the membrane)
F_o	Oligomycin binding fraction (ATP synthase portion within matrix)
FACS	Fluorescence-activated cell sorting
$FADH_2$	Flavin adenine dinucleotide
FBS	Fetal bovine serum
FCCP	Carbonyl cyanide-p-trifluoromethoxyphenylhydrazone (uncoupler of OXPHOS)
GAPDH	Glyceraldehyde-3-Phosphate Dehydrogenase
GED	GTP effector domain
GFP	Green fluorescent protein
GTP	Guanosine triphosphate
GTPase	Guanosine triphosphate hydrolase
GPx	Glutathione peroxidase
GSH	Glutathione (reduced)
GSSG	Glutatione
H_2O_2	Hydrogen peroxide

HeLa	Cervical cancer cell line (Henrietta Lacks)
HO_2^-	Hydroperoxyl radicals
HD	Huntington's disease
HEPES	4-(2-hydroxyethyl)-1-piperazineethanesulfonic acid (buffering agent)
IBM	Inner boundary membrane
IM	Inner membrane [mitochondrial]
IMS	Intermembrane space
KRB	Kreb's ringer buffer
LC-MS	Liquid chromatography–mass spectrometry
Lgl	Lethal(2) giant larvae (Drosophila mutant)
MEF	Mouse embryonic fibroblasts
MFF	Mitochondrial fission factor
MFN1	Mitofusin 1
MFN2	Mitofusin 2
Mgm1	Mitochondrial genome maintenance 1 (Yeast OPA1 homologue)
MPP	Mitochondrial processing peptidase
MPTP	1-methyl-4-phenyl-1,2,3,6-tetrahydropyridine (neurotoxin)
MTS	Mitochondrial targeting sequence
mtDNA	Mitochondrial deoxyribonucleic acid
mtROS	Mitochondrial reactive oxygen species
mtHSP70	Mitochondrial heat shock protein 70kDa
NADH	Nicotinamide adenine dinucleotide
NADPH	Nicotinamide adenine dinucleotide phosphate
$^1O_2$	singlet oxygen
O_2^-	Superoxide
OGC	2-Oxoglutarate carrier
OH	Hydroxyl radical
OM	Outer membrane [mitochondrial]
OPA1	Optic atrophy 1

OXPHOS	Oxidative phosphorylation
PARL	Presenilin-associated rhomboid-like protein
PD	Parkinson's disease
PDGF	Platelet-derived growth factor
PGC-1α	Peroxisome proliferator-activated receptor gamma coactivator 1-alpha
PHB	Prohibitin
PHD	HIF prolyl-hydroxylases
PhS	2-Phenylsuccinate (inhibitor of OGC)
PINK1	PTEN-induced putative kinase 1
PI3K	Phosphoinositide 3-kinase
PI	Phosphatidylinositol
PMF	Proton motive force
qPCR	Quantitative polymerase chain reaction
RGC	Retinal Ganglion Cells
RNA	Ribonucleic acid
RNAi	RNA interference
ROS	Reactive oxygen species
RT-PCR	Reverse transcription polymerase chain reaction
SDS-PAGE	Sodium Dodecyl Sulfate - Polyacrylamide Gel Electrophoresis
SEM	Standard error of the mean
SILAC	Stable isotope labelling of amino acids in cell culture
SLC25As	Mitochondrial solute linked carriers
SOD	Superoxide dismutase
SS	Szeto-Schiller peptides
TCA	Tricarboxylic acid [cycle]
TEM	Transmission electron microscopy
TM	Transmembrane segment (or domain)
Tom20	Translocase of the outer membrane 20kDa
VDAC	Voltage-dependent anion channel

VSMC	Vascular smooth muscle cell
WT	Wild type

Acknowledgements

The research environment that Dr. Ruth Slack's laboratory harbours is truly impressive. As such, I have been privy to very exciting research questions and studies, to state of the art equipment and techniques, to phenomenal colleagues and to outstanding collaborators. I would like to thank you Ruth for all your support, for your accessibility, for your exceptional research insight, and for providing me the guided freedom to pursue new research avenues as they have presented themselves. Because of your guidance in both research and non-research capacities, I believe that I have grown as a scientist and as a person. Jason MacLaurin is truly an exceptional lab manager/senior research technician, pivotal to the Slack research team. Jason is perhaps the world's best multitasker, is exceptional at prioritizing and maintains the highest level of availability and approachability for all members of the Slack lab. Thank you Jason for countless technical assistances, brainstorming sessions when problems arose, and for molecular cloning and viral productions.

My PhD research training has been highly enhanced through working closely with two top-notch scientists at opposing ends of the research ladder: a brilliant PDF (now professor) Dr. Marc Germain, and a talented Masters student Jacob Wong. Marc, thank you for your teachings, for productive brainstorming sessions, for your guidance with research projects and text revisions, and for your original findings which (with Dr. Karine Pilon-Larose) sparked much of this research. Jacob, thank you for your positive attitude, your great work ethic and all of your help with respect to the roles of the mitochondrial solute carriers in OPA1 function and the CLUH stories. And thank you both for your friendships.

I apologize that for the sake of brevity, the following past and present labmates will be clumped together. In a perfect world, you would all be highlighted, since many of you provided technical assistance, some of you reviewed different texts and manuscripts and some of you offered important ideas or criticisms. Thank you for the great time I have spent with all of you, the scientific discussions and for your friendships: Matthew Andrusiak, Nastaran Ahmadi, Ujval Anilkumar, Joelle Azzi, Alysen Clark, Delphie Dugal-Tessier, Ruthann Duivesteyn, Bensun Fong, Raghda Gemae, Noel Ghanem, Carmen Hamze, Linda Jui, Lisa Julien, Melissa Kelly, Mireille Khacho, Curtis McCloskey, Cynthia Meghaizel, Angela Nguyen, Catherine Pakenham, Karine Pilon-Larose, Larisa Romanova, Kristen Stevens, Devon Svoboda, Michelle Tarabay, Renaud Vandenbosch and Meysam Yazdankhan. I would also like to thank members of other labs for insightful research comments and technical assistance: Sarah Hewitt, Paul Marcogliese, Maxime Rousseaux, Alvin Joselin, Dianbo Qu, Skye McBride, Ghadi Antoun and others I may have failed to recall.

I have been so fortunate to have had such exceptional collaborations. My sincerest thanks to: Dr. Mary-Ellen Harper and Dr. Ryan Mailloux for assistance and access to instrumentation for the analysis of oxygen consumption; Dr. Laura Trinkle-Mulcahy and Dephine Chamousset for SILAC-based proteomics; Dr. Heidi McBride and Dr. Vincent Soubannier for help developing the BN-PAGE technique; Dr. Mary-Ellen Harper and Ghadi Antoun for glutathione quantifications via HPLC; and Dr. David Park and Steven Callaghan for research insight, help with methods and research materials. I would also like to thank Dr. Peter Rippstein for great electron microscopy services and technical assistance. And thank you to my research advisory committee for insightful comments and

research guidance: Drs. Heidi McBride, Laura Trinkle-Mulcahy, Jean-Claude Beïque and Johnny Ngsee.

Thank you to my parents Robert and Eveline and my two brothers Christopher and Tyler for a terrific family and childhood, and instilling in me need to constantly ask the big questions: why and how. Thank you again for your continued support and encouragement. While often challenging and stressful, the years I've spent here at the University of Ottawa have been the best and most impactful of my life. During this time, I engaged and married the love of my life, bought my first home and had my first child. Véronique thank you for your support, love, understanding, and for tolerating that leaving in 30 minutes usually means multiplying "lab time" by three. Elizabeth, thank you for putting everything in perspective and for sleeping pretty well during the time I've written my thesis ;).

Finally I would like to acknowledge sources of funding that made my thesis possible: Shelby Hayter Pass the Baton Graduate Fellowship from the Parkinson's Research Consortium, Focus on Stroke Doctoral Research Award from the Heart and Stroke Foundation, Ontario Graduate Scholarship in Science and Technology, Ontario Graduate Scholarship, CIHR training program in lipidomics scholarship, and entrance and excellence scholarships from the University of Ottawa.

Author Contributions

Unless otherwise stated for the published sections 2.1, 3.1, and 4.1, I designed all experiments, acquired data, analyzed and interpreted data, and drafted and revised the manuscript with Dr. Ruth Slack. Dr. Marc Germain contributed to the design of experiments, data acquisition (specifically Figure 7C) and interpretation, and revised the manuscript. Jacob Wong contributed to the design of experiments, data acquisition and interpretation (specifically replicates for Figure 8C&E, replicates for Figure 16A, Figure 18A-E, replicates for Figure 22A-D), and revised the manuscript. Drs. Mireille Khacho, Vincent Soubannier and Ryan Mailloux contributed to the design of experiments (specifically VS with help on the BN-PAGE technique, and RM with help on oxygen consumption measurements), interpretation of data and revision of the manuscript. Dr. Karine Pilon-Larose contributed to the design of experiments, data acquisition (specifically Figure 8F) and interpretation of results. Jason MacLaurin contributed to the design of experiments and data acquisition (specifically generation of retroviruses and help with cloning). Drs. David S Park, Heidi M McBride, Laura Trinkle-Mulcahy and Mary-Ellen Harper contributed to the design of experiments, contributed critical reagents and revised the manuscript. Dr. Laura Trinkle-Mulcahy also analyzed LC-MS data for Figure 17 and Table 2.

For sections 3.2, I designed all experiments, acquired data, analyzed and interpreted data, with the exception of Figures 23A&B and 24A where Jacob Wong helped performed replicate experiments.

For section 3.3, I designed all experiments, acquired data, analyzed and interpreted data, in collaboration with Ghadi Antoun and Dr. Mary-Ellen Harper. Ghadi Antoun helped in the HPLC analysis of glutathione in Figures 27, 29A-B, 29E-F, 30B-C and 30E-F.

Chapter 1. Introduction

1.1 Introduction: Life with Oxygen

An explosion in photosynthesis 2.2 billion years ago resulted in the Great Oxidation Event (Bekker et al, 2004; Lyons et al, 2014). The ensuing oxygenation of earth's atmosphere and water resulted in earth's first known mass extinction. Many anaerobic organisms were unable to cope with the toxic levels of oxygen and were lost. However, aerobic organisms evolved in their place, thriving in this new world. The endosymbiotic theory explains how some of these simple prokaryotic cells evolved with eubacteria, generating the first eukaryotes around 1.5 billion years ago (Javaux et al, 2001). Host cells that took up eubacteria likely gained an energetic advantage, allowing for an explosion of more complex life forms. One of these early eubacteria likely became the energy producing organelle present in almost all human cells and critical for mammalian life: the mitochondrion. Since mitochondria are positioned at the center of cellular life and death signaling and are dysfunctional in many diseases, understanding this organelle may lead to breakthroughs in our understanding of basic cell biology, but also in the treatments of neurodegeneration, ageing, cancer and many other ailments.

Here, we examine the mitochondrial shaping protein OPA1 in mitochondrial function(s) and investigate the roles of some additional OPA1-interacting partners. To begin, a brief introduction in mitochondrial biology will be provided, emphasizing its vital role in the brain. Then, the dynamic nature of mitochondria will be discussed, focusing on the central role of OPA1. Novel OPA1-interacting proteins, CLUH and mitochondrial solute carriers, will be presented along with their known biological functions. And finally, reactive oxygen species generation and clearance will be discussed with emphasis on the glutathione

system.

1.2 Mitochondria

Mitochondria were discovered in the mid-1800s and named in 1898 by Carl Benda from the greek roots, “mito” for thread and “chondrion” for granule (Ernster & Schatz, 1981). Indeed, this nomenclature was given because of the filamentous, interconnected reticulum, or independent granule shapes that mitochondria could adapt. As such, their size and shape is largely context and cell-type specific, but are generally on the order of 500nm wide and 500nm-5μm long. Mitochondria are abundant organelles, accounting for 10-20% of most cell type’s mass, with more energy-dependent cell types containing a greater amount of mitochondria (Karp, 2002). Mitochondria perform a variety of essential cellular functions including: energy production through oxidative phosphorylation, cell death signaling, heme synthesis and calcium buffering (Duchen, 2004). However, a recent explosion of research interest has expanded the role of mitochondria to many other cellular processes including stem cell differentiation, cell proliferation, steroidogenesis *et cetera* (Kasahara & Scorrano, 2014; Teslaa & Teitell, 2015; Xavier et al, 2015).

1.2.1 Mitochondrial Structure and Oxidative Phosphorylation

Mitochondria are double membrane organelles: likely evidence of their evolutionary origin and imperative to their various function(s). The mitochondrial outer membrane (OM) is in contact with the cytoplasm and encloses mitochondria. The inner membrane (IM) isolates the mitochondrial matrix, the location of numerous key metabolic reactions, from the intermembrane space. While the OM is fairly permeable to a number of small molecules, the IM is relatively impermeable. Compared to the OM which is very phospholipid rich, the IM is especially protein rich, as up to a 6 fold difference in protein-phospholipid ratio

has been observed between the two membranes (Simbeni et al, 1991; Sperka-Gottlieb et al, 1988). The lipid composition of the IM is also quite unique, consisting of high levels (≈20%) of cardiolipin where other membranes contain only trace amounts (Ardail et al, 1990; Schlame et al, 2000; Simbeni et al, 1991; Sperka-Gottlieb et al, 1988). Cardiolipin has many mitochondrial functions and may be deregulated in human disease (Chicco & Sparagna, 2007)(further discussed in section 1.5.3). Due to these described differences in membrane compositions, the inner membrane is much less fluid than the outer membrane, which may dictate its function. The IM is further divided into two regions: internalizations of the membrane, termed cristae; and boundary membranes, the connections between cristae. Far from simple invaginations, cristae form pockets of inner membrane enriched for the machinery of energy production (Mannella, 2006; Vogel et al, 2006).

As the primary source of energy production in most eukaryotic cells, mitochondria are popularly nicknamed the "powerhouse of the cell". This energy production is due to their ability to couple oxidation events with the generation of adenosine triphosphate (ATP), the energy currency of the cell. Although the cell can utilize a number of substrates for energy production, the monosaccharide glucose will be used to briefly describe cellular respiration (Figure 1). Glucose enters the cell and is metabolized into pyruvate through the process of glycolysis. This process yields a net production of 2 ATP molecules and fuels mitochondria with pyruvate and NADH. Pyruvate is carried into the mitochondrial matrix and is oxidized to acetyl-CoA. Acetyl-CoA is metabolized through the 8-step tricarboxylic acid (TCA) cycle, or Krebs cycle (Krebs & Johnson, 1980). For every starting molecule of glucose, the TCA cycle yields 6 molecules of the reducing energy substrate NADH, 2 molecules of

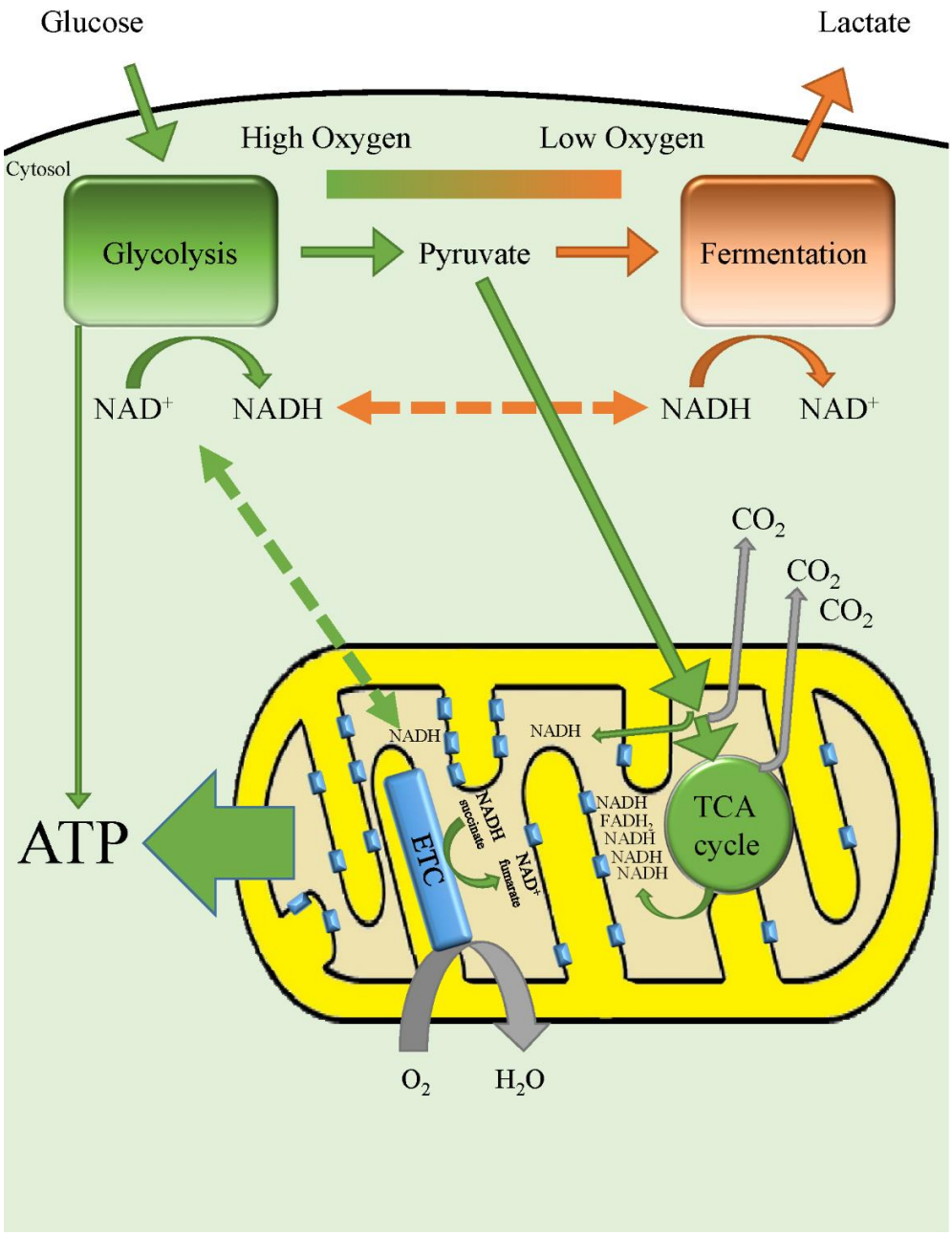

Figure 1. Cellular respiration.

Under normal (high) oxygen levels, the majority of healthy cells undergo aerobic respiration (green). For glucose metabolism, glycolysis yields a small amount of ATP, NADH and pyruvate. Pyruvate is transported into mitochondria, and oxidized through a number of steps in the mitochondrial matrix (TCA cycle). The resulting reducing equivalents, NADH and $FADH_2$, are used by the electron transport chain to create a proton gradient which is used for ATP production. Under low oxygen conditions (or certain cell types or pathologies) cells undergo anaerobic respiration (orange) where, in mammalian cells, pyruvate is converted to lactate and NADH is recycled.

$FADH_2$ and 2 molecules of ATP. NADH and $FADH_2$ provide reducing equivalents to the electron transport chain, which couple electron transport to the generation of a proton gradient across the IM. Oxygen, the final electron acceptor, is consumed in this process to form water. Protons from the resulting proton gradient are transported back into the matrix in a process coupled to ATP production (Mitchell, 1961). Alternatively, cells may undergo anaerobic respiration, in which pyruvate bypasses mitochondria, and is instead converted to lactic acid. Aerobic respiration, however, yields about 15 times more ATP per glucose molecule than anaerobic respiration (Lodish, 2000).

1.2.2 The Electron Transport Chain

In 1961, amidst competing models of mitochondrial ATP generation, Mitchell proposed his chemiosmotic hypothesis: where protons are pumped across the IM, in an electrogenic process, driving ATP synthesis (Mitchell, 1961). In the following decades, an overwhelming wealth of evidence supports his proton motive force (PMF) driven ATP-production hypothesis, earning him a Nobel prize in 1978. Among these evidences were the discoveries and characterizations of the four electron transport complexes and associated factors, and the ATP synthase. In fact, pioneering work on the ATP synthase by Paul Boyer (reviewed in (Boyer, 1997)) along with structural confirmations by John Walker, won them half of the Nobel prize in 1997. Our knowledge of the electron transport chain (ETC) and oxidative phosphorylation (OXPHOS) is now extremely well developed and characterized (Figure 2), although mechanisms altering its function continue to be discovered.

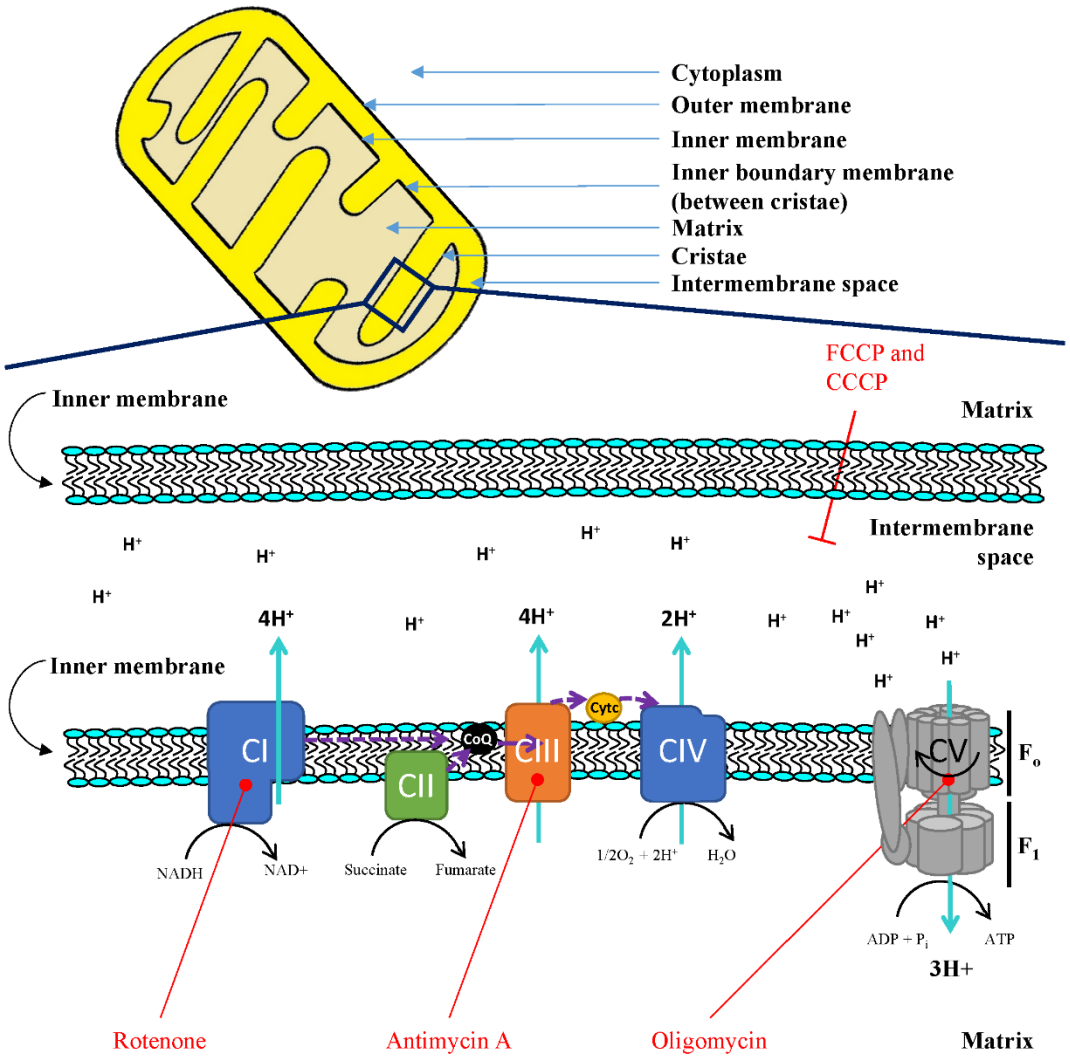

Figure 2. The electron transport chain.

Top panel: The key structures of a mitochondrion. Bottom panel: Electrons donated from NADH or succinate are transported from complex I or II respectively, to complex III through coenzyme Q. Cytochrome C receives these electrons from complex III and transfers them to complex IV, where molecular oxygen is the final electron acceptor. During this process, complexes I, III and IV pump protons into the intermembrane space, creating a proton gradient. This gradient forces protons through the ATP synthase (CV) which transfers this potential energy to ATP production. The ATP synthase is composed of two large subunits, F_o and F_1. In red are sites of ETC inhibitors used in this work.

Briefly: Complex I (NADH dehydrogenase) receives a pair of electrons from NADH and transfers the electrons to Coenzyme Q (CoQ or ubiquinone) (Ernster et al, 1969). Complex I is the largest of the OXPHOS complexes, with four antiporter-like subunits effectively transporting four protons across the IM for every pair of electrons it shuttles (Baradaran et al, 2013). Complex II (succinate dehydrogenase) is the only ETC component also integral to the TCA cycle, transforming succinate to fumarate. Succinate donates a pair of electrons through $FADH_2$ to Complex II, which donates its electrons to CoQ. Complex II does not transport protons, so $FADH_2$ reducing equivalents produce less of a PMF (and thus ATP generation) than NADH. Complex III (ubiquione-cytochrome c reductase) accepts electrons from CoQ, pumps four protons across the IM and transfers electrons to Cytochrome C (CytC) (Wikstrom, 2004). Cytochrome C shuttles electrons to complex IV (cytochrome c oxidase), pumping two protons across the IM and catalyzing the final acceptance of electrons to oxygen, producing water. The rather complex rotational molecular motor, the ATP synthase, then uses the PMF to drive ATP synthesis from ADP and inorganic phosphate (Boyer, 1997).

ATP synthase is a particularly "splendid molecular machine" (Boyer, 1997). The ATP synthase is a large complex (≈700 kDa) with two main portions, a smaller membrane bound F_o portion and the catalytic F_1 portion, located within the matrix. The F_o portion consists of subunits A (mtATP6), B, C, d, e, f, g, F6 and A6l(mtATP8); while the F_1 portion consists of subunits α, β, γ, δ, and ε (Jonckheere et al, 2012). Interestingly, mtATP6 and mtATP8 (A6l) are the only two proteins encoded by mitochondrial DNA (Anderson et al, 1981). In other words, the entire F_1 subunit is nuclear encoded. For ATP generation, protons are passed through the C-ring of the F_o portion, causing its rotation, along with γ, δ and ε in

F_1. Together these components make up the rotor, while the stator anchors the ATP synthase and consists of the subunits α, β, A, B, d, F6. This rotation is coupled to ATP hydrolysis originally described by Boyer (Boyer, 1975), at the interface of the α, β subunits within the F_1 (Devenish et al, 2008).

Providing isolated mitochondria with different energy substrates (such as in Chapter 3.1) energizes different ETC complexes. For example, glutamate and malate generates NADH from the TCA cycle, which electrons to Complex I. In contrast, when succinate is provided, Complex II is energized directly with reducing equivalents through $FADH_2$. In addition, many ETC inhibitors have been utilized to investigate OXPHOS, five are used in this publication: rotenone (complex I inhibitor), antimycin A (complex III inhibitor), oligomycin (ATP synthase inhibitor) and FCCP and CCCP which dissipate the mitochondrial membrane potential and the PMF.

1.2.3 Mitochondrial DNA

The large majority of mitochondrial proteins are encoded by nuclear DNA and imported via the outer and inner membrane translocases, TOM and TIM complexes (Neupert, 1997). However, many members of the ETC are encoded by the mitochondrial genome, located within the matrix. Specifically, of over 80 human ETC components, the mitochondrial genome encodes for 13 (Chen & Butow, 2005). MtDNA is essential to higher eukaryotic life. In its absence, respiratory complexes do not assemble, mitochondria fail to respire and fail to produce ATP. The human mitochondrial genome is 16.5 kb: comparatively tiny (0.0005%) to the nuclear genome (Anderson et al, 1981; Holt et al, 2007). However, the mitochondrial genome is also highly polyploid (upwards of 1000 per cell) and accounts for ≈1% of total DNA (Takamatsu et al, 2002). In addition to the 13 proteins involved in

respiratory complexes I, III, IV and V, the mitochondrial genome also encodes 2 rRNAs and 22 tRNAs, which are essential for the translation of mtDNA encoded proteins.

Mammalian mtDNA is packaged into discrete protein-DNA globular foci called mitochondrial nucleoids, tethered to the IM (Garrido et al, 2003; Kaufman et al, 2000; Mao & Holt, 2009; Wang & Bogenhagen, 2006). Multiple mtDNA copies are frequently contained within one nucleoid, implying that gene mutations in multiple copies of mtDNA are required to exert phenotypic change in mitochondrial function (Kukat et al, 2011; Legros et al, 2004; Satoh & Kuroiwa, 1991; Taylor & Turnbull, 2005).

MtDNA may be maintained through mtDNA replication, through nucleoid stabilization, and through mtDNA repair. Instability of the mitochondrial genome is associated with numerous human pathologies. Mutations in twinkle helicase, DNA polymerase γ 1 and 2, optic atrophy 1 and the adenine nucleotide translocator 1 cause progressive external ophthalmoplegia (PEO), an adult-onset neuromuscular disease associated with mtDNA instability and mtDNA deletions, molecules that have lost large sections of the mtDNA genome (Agostino et al, 2003; Hudson et al, 2008; Kaukonen et al, 2000; Spelbrink et al, 2001; Van Goethem et al, 2001). In addition, the concept of mtDNA instability in neurodegenerative diseases has been gaining support. Evidence for mtDNA instability is present in Alzheimer's disease (de la Monte et al, 2000; Wang et al, 2005), amyotrophic lateral sclerosis (Wiedemann et al, 2002) and Parkinson's disease (Bender et al, 2006; Lin et al, 2012).

1.2.4 Mitochondrial dysfunction in Neurodegeneration

Mitochondrial dysfunction in neurodegenerative disease clearly extends beyond defects in mtDNA [reviewed in (Lin & Beal, 2006)]. Likely due to their dependence on OXPHOS for energy production, neurons seem particularly sensitive to defects in mitochondrial dysfunction. Although beyond the scope of this thesis, the literature surrounding mitochondrial dysfunction in neurodegeneration is expanding at a rapid pace, with oxidative stress playing a central role, reviewed in [(Figure 3) and in (Patten et al, 2010) – Appendix C].

Using Parkinson's disease (PD) as an example, the following selected evidence for mitochondrial dysfunction in PD exist: increased oxidative stress has been reported in PD (Alam et al, 1997); PD-related genes are associated with mitochondrial function (Bueler, 2010) and defective mitochondrial clearance, termed mitophagy (Narendra et al, 2008); ETC inhibitors MPTP and rotenone cause PD-like disease in humans and in animal models (Cannon et al, 2009; Langston et al, 1984; Porras et al, 2012); and α-synuclein, the primary component of Lewy bodies (a common idiopathic PD hallmark), induces mitochondrial dysfunction and increased oxidative stress (Devi et al, 2008; Martin et al, 2006). Moreover, ageing is strongly associated with accumulated oxidative stress and mitochondrial dysfunction making it the number one risk factor for Parkinson's disease and other neurodegenerative diseases (Lu et al, 2004; Navarro & Boveris, 2010).

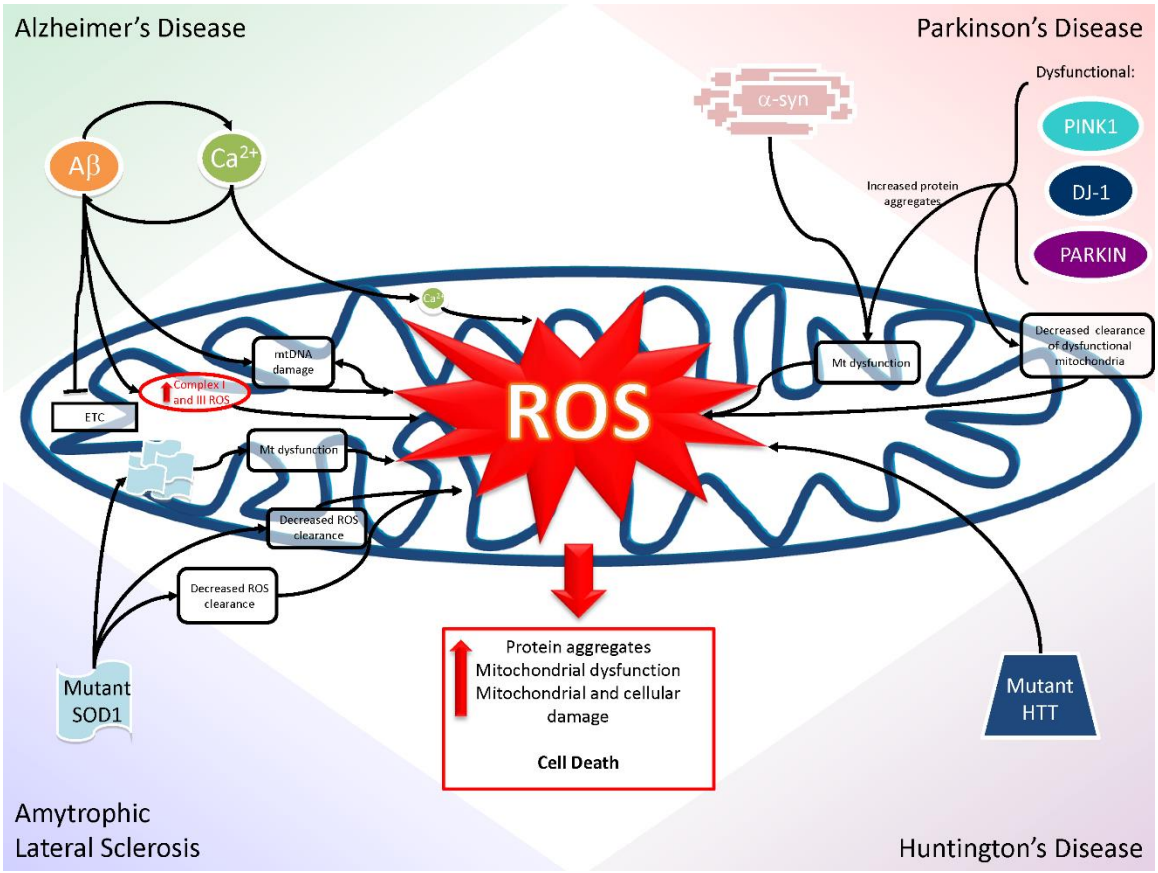

Figure 3. "Schematic of factors affecting mtROS in neurodegenerative diseases." (Patten et al., 2010)

"Multiple pathways in neurodegenerative disease converge on the mitochondria to induce the production of mtROS. In the case of AD, Aβ accumulation is toxic to mitochondrial respiration and increases mtDNA damage and mtROS. In addition, deregulated Ca2+ levels are also detrimental to proper mitochondrial function. These two components are not mutually exclusive in that Aβ accumulation can deregulate Ca2+ levels and vice versa. Mutations in PD-related genes cause protein aggregation leading to mitochondrial dysfunction and oxidative stress. In addition, dysfunctional mitochondria are not appropriately disposed of by mitophagy, further increasing mtROS production. Aberrant levels of the mutant form of the protein huntingtin causes ROS generation in HD. Finally, mutations in SOD1 in FALS hinder ROS clearance and create toxic mitochondrial aggregates. Generation of ROS may in turn lead to further protein aggregation, mitochondrial dysfunction, cell damage, and cell death."

Since the ability of the brain to regenerate is limited, neurons possess many adaptive mechanisms to survive different stressors. For example, oxidative stress activates NRF2, a master regulator of antioxidant genes (Bell et al, 2015). Peroxisome proliferator-activated receptor gamma coactivator 1-alpha (PGC-1α) is also activated by oxidative stress to increase mitochondrial biogenesis and respiration (Lin et al, 2004). 5' AMP-activated protein kinase (AMPK) is a master regulator of energy metabolism, sensing changes in the ATP/AMP ratio and responding by activating catabolic pathways and shunting anabolic ones (Culmsee et al, 2001; Williams et al, 2011). Moreover, we have provided evidence of an LKB1-dependent adaptive response to mitochondrial dysfunction initiated by the deletion of the mitochondrial protein Apoptosis Inducing Factor (AIF) [(Germain et al, 2013) – Appendix D]. Haploinsufficiency of the LKB1 gene product was sufficient to hinder the compensatory increased mitochondrial biogenesis and glycolysis, leading to increased neuronal cell death.

As our understanding of mitochondrial function increases, so too do the number of targetable sites for therapeutic intervention. In this regard, targeting mitochondrial dynamics, the focus of this thesis, is quickly becoming an attractive candidate for the treatment of neurodegenerative disease (Itoh et al, 2013; Khacho & Slack, 2015). Mitochondrial dynamics will now be presented, highlighting its implications in neurodegenerative disease.

1.3 Mitochondrial Dynamics

One of the fascinating aspects of mitochondria is that they constantly undergo changes to their shape: through fission and fusion events, through movement along cytoskeletal tracks or by regulating their cristae ultrastructure.

1.3.1 The Machinery

Fission and fusion is regulated by a group of mitochondrial dynamin GTPases (Figure 4). Mitochondrial fusion requires the mitofusins (MFN1 and MFN2) for outer membrane fusion and optic atrophy 1 (OPA1) for inner membrane fusion (Chen et al, 2003; Meeusen et al, 2006). Mitofusins are tethered to the outer membrane through two transmembrane domains, with both their N-terminal and C-terminal facing the cytoplasm. Mitofusins can function as either homodimers (Mfn1-Mfn1) or heterodimers (Mfn1-Mfn2) on adjacent mitochondria (Koshiba et al, 2004). With respect to their essential role in fusion, MFN1 and MFN2 are functionally redundant, since one alone may still result in some fusion activity (Chen et al, 2003). However, MFN1 is likely the more pro-fusion isoform since it possesses higher GTPase activity and mitochondrial tethering efficiency (Cipolat et al, 2004; Ishihara et al, 2004). The GTPase domain is located at the N-terminal of both MFN1 and MFN2, and GTPase activity is likely required for membrane fusion (Ishihara et al, 2004; Santel et al, 2003). OPA1 is the only known inner membrane protein known to regulate mitochondrial fusion, which is believed to require both an inner membrane tethered form and a shorter soluble form [(Akepati et al, 2008) further explained in section 1.4]. The outer and inner membrane fusion events are tightly coordinated, but independent events, as exemplified by slight outer membrane fusion in the complete absence of inner membrane fusion (Song et al, 2009). Although the precise molecular nature of mitochondrial fusion has yet to be elucidated, it is believed that these dynamins dimerize in a trans configuration and pull together their respective membranes by a SNARE-like mechanism (Koshiba et al, 2004).

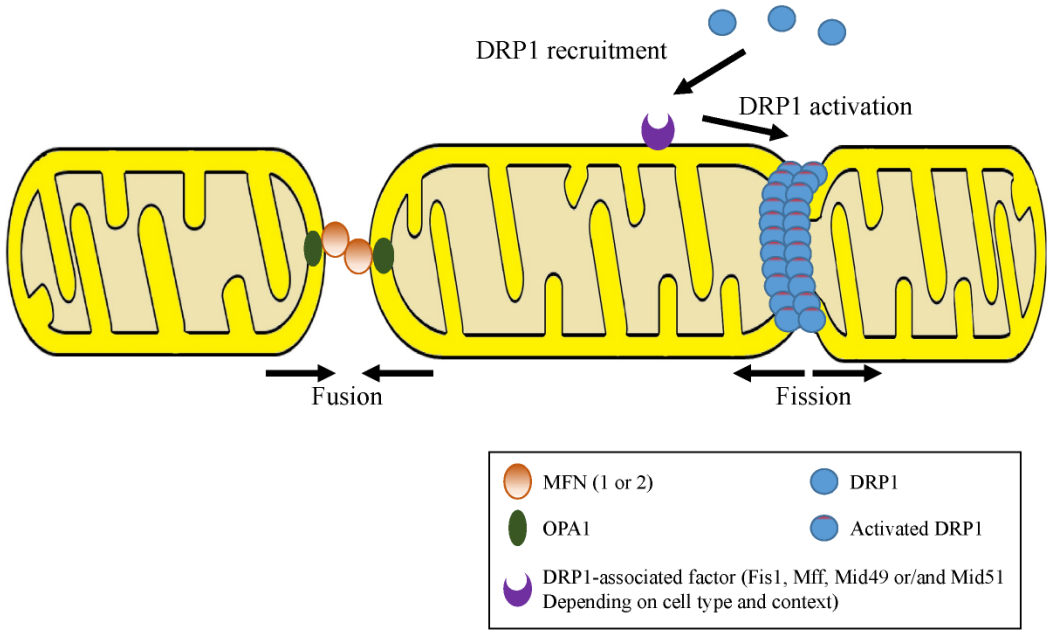

Figure 4. Mitochondrial dynamics is regulated by a group of GTPases.

Mitochondrial fusion is mediated by OPA1 and by MFN1 or 2 (as either homo- or heterodimers). Mitochondrial fission involves DRP1 which is recruited by either Fis1, Mff, Mid49 or Mid51, assemble into rings, are activated by posttranslational modifications and constrict mitochondria via GTP-dependent conformational changes.

It is currently not known how outer and inner membrane fusion are mechanistically linked. While interaction between MFN1, MFN2 and OPA1 has been reported and could represent a direct link between both fusion events (Guillery et al, 2008), their interactions remain to be corroborated by other groups. Furthermore, based on their localizations and the small portion of mitofusins spanning the intermembrane space, a yet to be discovered intermediate interacting protein seems more likely.

Conversely, mitochondrial fission is mediated by dynamin-related protein (DRP1, or dynamin 1 like, DNM1L) (Bleazard et al, 1999; Smirnova et al, 2001) and its associated factors: Fis1 (Yoon et al, 2003), Mff (Otera et al, 2010), MiD49 and MiD51 (Palmer et al, 2013). DRP1 acts only on the outer mitochondrial membrane, suggesting either that DRP1 acts by constricting mitochondria across both membranes, or that the mitochondrial inner membrane fission machinery has yet to be discovered. DRP1 requires a GTPase domain, GTPase effector domain and a middle domain for its function in mitochondrial fission (Pitts et al, 2004). Following recruitment to the site of fission by its associated factors and DRP1 activation, DRP1 oligomerizes forming a spiral ring that constricts mitochondria through GTP-dependent conformational changes (Ingerman et al, 2005; Mears et al, 2011; Smirnova et al, 2001). DRP1 activity is largely modulated by phosphorylation events. For example, phosphorylation of DRP1 at serine-616 by cyclin dependent kinase (Cdk1) enhances fission during mitosis (Taguchi et al, 2007). Phosphorylation of serine-637 by PKA conversely decreases GTP activity and fission, whereas calcineurin dephosphorylates this residue, in turn activating DRP1 (Cereghetti et al, 2008; Chang & Blackstone, 2007; Cribbs & Strack, 2007). DRP1 activity is also regulated by ubiquitination (Park et al, 2010), sumoylation (Zunino et al, 2009) or S-nitrosylation (Cho et al, 2009). The relative

importance of the four identified DRP1 associated proteins may be context and cell-type specific; however Mff is likely the major player in DRP1 recruitment in the majority of contexts (Loson et al, 2013; Otera et al, 2010). Interestingly, the endoplasmic reticulum may mark the sites for mitochondrial division and may aid in their constriction (Friedman et al, 2011; Naon & Scorrano, 2014).

Mitochondrial fusion and fission are extremely important conserved processes for cells and organisms. In this regard, genetic deletion of the fusion or fission machinery in mice is embryonically lethal: at embryonic day 13.5 for OPA1 (Davies et al, 2007), at embryonic day 12.5 for MFN1 (Chen et al, 2003), at embryonic day 11.5 for MFN2 (Chen et al, 2003) and at embryonic day 12.5 for DRP1 (Ishihara et al, 2009).

1.3.2 The Function of Mitochondrial Dynamics

Mutations in the fission/fusion machinery underlie a number of human pathologies. Mutations in OPA1 cause dominant optic atrophy (described in Chapter 1.4.1) (Alexander et al, 2000; Delettre et al, 2000), while mutations in MFN2 cause Charcot-Marie-Tooth neuropathy type 2A (CMT2A) (Zuchner et al, 2004). A *de novo* lethal DRP1 mutation has been reported to cause abnormal brain development, optic atrophy and lactic acidemia in a neonate (Chang et al, 2010; Waterham et al, 2007). Defects in mitochondrial dynamics may also underlie other more common neurodegenerative diseases including Parkinson's disease, Alzheimer's disease and Huntington's disease [reviewed in (Itoh et al, 2013)]. In Parkinson's disease for example, mutations in many PD-associated genes results in increased DRP-1 mediated fission and subsequently mitochondrial fragmentation (Dagda et al, 2009; Deng et al, 2008; Wang et al, 2011). Inhibition of mitochondrial fission by the DRP1 inhibitor mdivi-1 (Cui et al, 2010) or increased fusion through overexpression of

MFN2 or OPA1 (Lutz et al, 2009), alleviates the mitochondrial dysfunctions associated with PD-associated gene mutations, suggesting that mitochondrial dynamics plays a central role in mitochondrial dysfunction associated PD. Furthermore, ETC inhibitors associated with Parkinsonism also cause widespread mitochondrial fragmentation (Betarbet et al, 2006). Finally, PD-associated genes PINK1 and Parkin mutations underlie defects in the selective degradation of mitochondria, also termed mitophagy (Pickrell & Youle, 2015). Mitophagy is initiated by PINK1, which accumulates on mitochondria that have lost membrane potential (Narendra et al, 2010). Parkin is then recruited by PINK1 and ubiquitinates the outer membrane, targeting it for selective degradation (Geisler et al, 2010; Matsuda et al, 2010; Vives-Bauza et al, 2010). DRP1 mediated mitochondrial fission is required for mitophagy (Tanaka et al, 2010), without which large mitochondria cannot be engulfed by autophagosomes for their degradation (Gomes et al, 2011; Itoh et al, 2013). Parkin may play an additional role in mitochondrial dynamics by targeting MFN1 and MFN2 for proteasomal degradation (Tanaka et al, 2010).

While the importance of mitochondrial fusion and fission is highlighted by its conserved machinery, required for mammalian life and mutated in human disease; their cellular functions and relative contributions to human disease is less evident. For example, mitochondrial fusion is required for maintenance of the mitochondrial genome (Chen et al, 2010). However, while it is postulated that mitochondrial fusion could allow for complementation of mtDNA molecules, evidence for this model, and mechanistic insight is lacking. Mitochondrial fusion is also clearly required for resistance to different stressors, including UV irradiation, actinomycin D, cell starvation or neuronal hypoxia (Gomes et al, 2011; Khacho et al, 2014; Tondera et al, 2009) (Appendix E). However, since many of

these changes in mitochondrial length are accompanied by changes in mitochondrial cristae structure, it is currently unclear which structural change is required for the observed protection. Finally, mitochondrial fusion also has a described role in mitochondrial respiration. While in theory defective fusion could lead to mitochondrial fragments lacking mtDNA, and thus OXPHOS deficiencies; even short-term knockdown of the fusion machinery, without mtDNA depletion, results in defective respiration (Cogliati et al, 2013). This suggests that the role of mitochondrial fusion in respiration precedes defects in mtDNA. We believe that work presented here may help clarify some of these outstanding issues.

Another controversial role for mitochondrial dynamics its role in apoptosis. It is well-accepted that mitochondria fragment during apoptosis (Frank et al, 2001; Gao et al, 2001; Jahani-Asl et al, 2007; Lee et al, 2004), but whether this facilitates the cell death process or is merely a consequence thereof, is disputed (Sheridan & Martin, 2010). Overexpression of dominant negative DRP1 or DRP1 downregulation inhibits cytochrome c release and delays cell death (Breckenridge et al, 2003; Frank et al, 2001; Germain et al, 2005). OPA1 knockdown has the opposite effect where cytochrome c is more easily released and cells are sensitized to apoptosis (Lee et al, 2004). However, these results have not been confirmed by all groups (Sheridan et al, 2008; Sheridan & Martin, 2010). There may be tissue/cell type specific effects responsible for this sensitivity to cell death stimuli or the effects may involve other known, or yet to be discovered pathways.

Movement of mitochondria along the cytoskeletal network is another important aspect of mitochondrial dynamics, critical for mitochondrial localization. Mitochondrial transport is especially important in neurons for ATP production and calcium buffering at synapses,

where these functions are in high demand. Here, the non-redundant roles of the mitofusins emerge since MFN2, but not MFN1, interacts with Milton and a calcium-binding GTPase MIRO, connecting the microtubule motor kinesin with mitochondria for anterograde transport (Misko et al, 2010). This process is necessary for axonal transport of mitochondria and may explain the specificity of MFN2 CMT2A mutations in the degeneration of neurons with long axons. Moreover, characterization of CMT2A associated MFN2 mutations alter mitochondrial fusion, neuronal mitochondrial transport and axonal degeneration (Misko et al, 2012). Interestingly, while OPA1 depletion also caused mitochondrial fragmentation, mitochondrial transport and axonal degeneration was unaffected. DRP1 dependent mitochondrial fission is also required for mitochondrial transport since long-interconnected mitochondria are sterically unable to be transported (Li et al, 2004; Verstreken et al, 2005). Altered mitochondrial transport may also underlie other neurodegenereative diseases, such as ALS (De Vos et al, 2007).

MFN2, but not MFN1, is also required in mammals for tethering mitochondria to the endoplasmic reticulum (ER) (de Brito & Scorrano, 2008). It is believed that mitochondrial-ER tethering facilitates mitochondrial calcium buffering and metabolism in healthy cells (Bravo et al, 2011), which in some instances may facilitate apoptosis (Szabadkai et al, 2004). Additionally, mitochondria-ER association may also be required for mitochondrial fission (Friedman et al, 2011). While the importance of the mitochondrial-ER contacts is not in question, the requirement for MFN2 has recently become debated (Cosson et al, 2012; Filadi et al, 2015). Regardless the association between mitochondria and ER clearly regulates its function, although mammalian tethering components likely remain to be discovered.

Mitochondrial dynamics also encompasses ultrastructural cristae changes. Cristae, being invaginations of the inner membrane, form internal compartments which are connected to the inner boundary membrane (IBM) by tight cristae junctions (Mannella et al, 1994). Cristae possess different proteins than the IBM arguing that they are functionally distinct compartments (Gilkerson et al, 2003; Vogel et al, 2006; Wurm & Jakobs, 2006). In this respect, ETC complexes are more localized within cristae, while mitochondrial protein import machinery is more highly localized to the IBM. For example, by gold immunolabeling coupled electron microscopy, 94% of all Complex III and ATP synthase has been estimated to be within cristae (Gilkerson et al, 2003). OPA1, one of the major known players in cristae regulation, mitochondrial fusion, ETC function and mitochondrial DNA maintenance, and central to this thesis, will now be thoroughly discussed.

1.4 OPA1

1.4.1 Autosomal Dominant Optic Atrophy and Optic Atrophy "Plus" Phenotypes

Autosomal Dominant Optic Atrophy (ADOA) is an inherited disease affecting the retinal ganglion cells (RGC), leading to their degeneration and ascending atrophy of the optic nerve. ADOA was first described by Dr. Poul Kjer (Kjer, 1959), and has an estimated prevalence of up to 1:12000, depending on the population studied (Yu-Wai-Man & Chinnery, 2013). ADOA patients generally experience a slow progressive bilateral decrease in vision during childhood, resulting in a variable irreversible loss of vision (Lenaers et al, 2012). To date, 8 loci have been associated with ADOA, three of which encode mitochondrial inner membrane proteins: OPA1, OPA3 and OPA7 (Lenaers et al, 2012).

Like many other neurodegenerative disease, why a particular cell type is most affected in ADOA remains largely a mystery. Additionally, the principle pathway leading to RGC degeneration also remains to be elucidated. ADOA does however remain a direct example of how defects in mitochondrial structure can underlie human disease. OPA1 mutations account for at least 75% of cases of ADOA, while the other known loci account for an estimated 1% of all cases combined (Lenaers et al, 2012). As such, OPA1 is the primary gene product responsible for ADOA and has received the largest amount of research interest, due in part to its fascinating roles in mitochondrial physiology. For OPA1, 27% of gene mutations are missense mutations, present in many different domains (Figure 5); while the remainder are splice variants, frame shifts, nonsense, deletion or duplications – likely causing non-functional/degraded protein products. The nature of OPA1 mutations suggest that DOA is caused by haploinsufficiency of the OPA1 gene product.

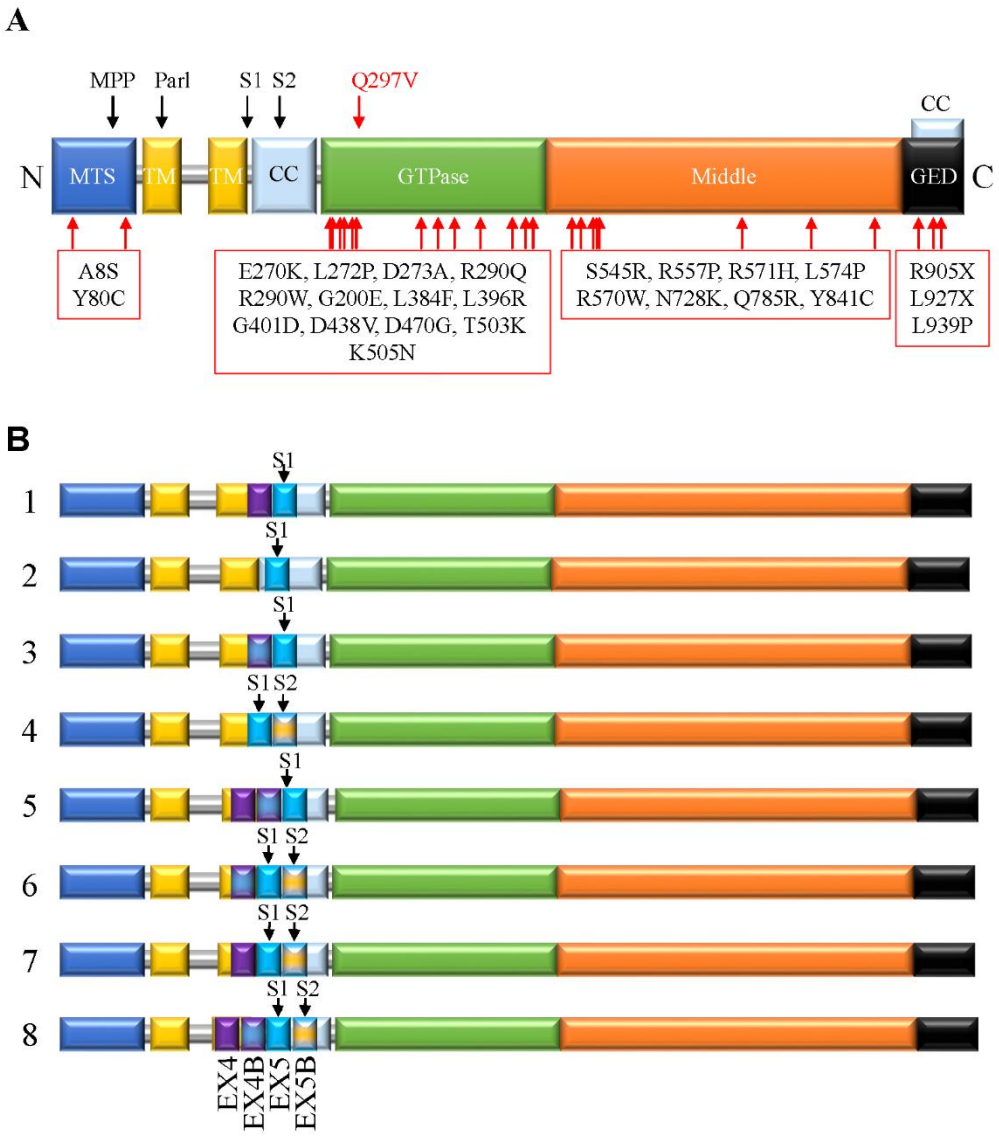

Figure 5. OPA1 structure and mRNA splice isoforms.

A Schematic of OPA1's major protein domains, sites of cleavage and mutation used in this work. Cleavage at only the mitochondrial processing peptidase (MPP) site leads to long, l-OPA1; while further cleavage at S1 or S2 leads to short, s-OPA1. Sites of human mutations described in patients with DOA are shown, while nonsense mutations or deletions are not. **B** OPA1 transcription yields 8 different human variants though alternative splicing or exons 4, 4B and 5B. Mitochondrial targeting sequence (MTS), transmembrane domain (TM), S1 and S2 are sites for cleavage, coiled coil domain (CC), GTPase effector domain (GED). Data for this figure was adapted from (Liesa et al, 2009) and (Olichon et al, 2007).

Since OPA1 has described roles in mitochondrial fusion, cristae structure and mtDNA maintenance (described below), it is perhaps not surprising that several patients with OPA1 mutations also present with additional symptoms. These ADOA-plus phenotypes are predominantly neuromuscular, including deafness, progressive external ophthalmoplegia, ataxia, myopathy and peripheral neuropathy (Amati-Bonneau et al, 2008; Hudson et al, 2008; Stewart et al, 2008). These extra-ocular neurological complications are present in as many as 20% of all ADOA patients (Yu-Wai-Man et al, 2010). Interestingly, OPA1 mutations in ADOA-plus are mostly within the GTPase and GTPase effector domains, hinting at a dominant-negative mode of action (Amati-Bonneau et al, 2008; Ranieri et al, 2012).

With mitochondrial dysfunction, mtDNA instability and altered quality control mechanisms underlying both DOA-plus and Parkinson's disease, it is particularly interesting that OPA1 mutations were discovered in two Italian families with parkinsonism (Carelli et al, 2015). In truth, the link between OPA1 and PD had been previously suggested. For example, the PD-associated gene parkin was previously demonstrated to regulate mitochondrial integrity by ubiquitinating NEMO, altering OPA1 transcriptional regulation (Muller-Rischart et al, 2013). Moreover, OPA1 overexpression can rescue mitochondrial defects induced by parkin or PINK1 loss of function (Lutz et al, 2009) and can rescue dopaminergic cell death in MPTP-treated mice (Ramonet et al, 2013). As such, new understandings into OPA1 function and dysfunction could be utilized to design therapeutic interventions in the treatments of DOA, DOA-plus and PD.

1.4.2 OPA1 Structure

Human OPA1 possess a number of notable domains and is alternatively spiced to form 8 ubiquitously expressed human isoforms (Figure 5) (Delettre et al, 2001; Olichon et al, 2007). Mouse OPA1 alternative splicing however, only generates 4 isoforms (Akepati et al, 2008). OPA1 isoform 1 and 7 are predominantly expressed in humans (Delettre et al, 2001; Olichon et al, 2007).

Like many mitochondrial proteins, OPA1 has a mitochondrial targeting sequence (MTS) allowing for import of OPA1 and sorting into the mitochondrial inner membrane, dependent on the transporter outer membrane (TOM) complex, transporter inner membrane (TIM) complex and the sorting and assembly machinery (SAM) complex (Branda & Isaya, 1995). Once imported, the MTS is cleaved by the mitochondrial processing peptidase (MPP). OPA1 has two transmembrane domains, orienting both the N- and C-terminals towards the intermembrane space with only a small region in the mitochondrial matrix. OPA1's GTPase domain is essential for its fusion activity, where GTP hydrolysis likely provides the energy required for membrane merging (Cipolat et al, 2004). The coiled coil domain consists of helical structures likely regulating OPA1's oligomerization and protein-protein interactions (Lupas, 1996). The GTP effector domain (GED) contains a second coiled coil domain which also regulates OPA1's oligomerization, along with its GTPase activity (Cipolat et al, 2004). OPA1's large conserved middle domain is relatively uncharacterized, but may regulate protein-protein interactions and retention of OPA1 within mitochondria (Moore et al, 2010).

1.4.3 OPA1 Processing

In addition to its cleavage by MPP, OPA1 long-forms (l-OPA1) are further processed by mitochondrial proteases to yield shorter soluble forms of OPA1 (s-OPA1) (Song et al, 2007). There is still much discrepancy in the literature with regard to OPA1 proteases (Belenguer & Pellegrini, 2013). The first identified rhomboid protease PARL may generate small amounts of s-OPA1 (Cipolat et al, 2006). Due to the discovery of mAAA-proteases discovered in yeast (Duvezin-Caubet et al, 2007), mammalian mAAA-proteases were defined including paraplegin (cutting at cleavage site S1) (Ishihara et al, 2006) and YME1L (cutting at S2) (Griparic et al, 2007; Song et al, 2007). Constitutive cleavage of OPA1 at S2 by YME1L is generally well accepted in the literature and yields both l-OPA1 and s-OPA1, since only 4 splice variants contain the cleavage site. Cleavage at S1, common to all splice variants, undergoes a complex membrane potential regulated cleavage (McBride & Soubannier, 2010). OMA1 is involved in this cleavage site, potentially through regulating expression of mAAA proteases or through direct OPA1 cleavage (Anand et al, 2014; Ehses et al, 2009; Head et al, 2009; Quiros et al, 2012). Finally, deletion of prohibitin 2 (PHB2) also results in OPA1 processing, mitochondrial fragmentation and cristae loss (Merkwirth et al, 2008). PHB2 likely serves as a scaffolding protein, organizing lipid domains, which may regulate recruitment of mAAA proteases for OPA1 processing (McBride & Soubannier, 2010). The requirement for OPA1 processing in OPA1 function(s) is debated as described below.

1.4.4 OPA1 in Mitochondrial Fusion

As previously stated, OPA1 is absolutely required for mitochondrial inner membrane fusion. In fact, OPA1 is the only known mammalian inner membrane protein directly involved in fusion. Mitochondrial fusion is believed to require both l-OPA1 and s-OPA1 since only OPA1 isoforms 1, 2, 4 and 7, which can undergo cleavage to produce both long and short forms, rescue fusion in OPA1 KO MEFs (Song et al, 2007). However, recent work suggests that OPA1 processing is dispensable for fusion (Anand et al, 2014). This was recently demonstrated in OPA1 cleavage incompetent cell lines that l-OPA1 alone can maintain mitochondrial fusion. Moreover, through clever mutational analysis the authors suggest that s-OPA1 possesses an additional pro-fission role (Anand et al, 2014). In conflict with these findings, Mishra and colleagues demonstrate how ETC-activity dependent cleavage of OPA1 stimulates mitochondrial fusion (Mishra et al, 2014). Further work is needed to resolve these differences. Regardless, based on mutants that do not fuse mitochondria, OPA1 likely requires both oligomerization and GTPase activity for fusion (Ban et al, 2010; Frezza et al, 2006). Finally, GTPase activity may be modified by the ability of OPA1 to bind cardiolipin, which may regulate its oligomerization (Ban et al, 2010).

1.4.5 OPA1 in mtDNA Maintanance

Mutations in ADOA and ADOA-plus phenotypes first linked mtDNA stability with OPA1 (Amati-Bonneau et al, 2008; Hudson et al, 2008; Kim et al, 2005). Surprisingly, these studies found multiple mtDNA deletions and mtDNA depletions associated with OPA1 mutations. Ablation of OPA1 in MEFs also significantly decreases mtDNA levels, and likely depends upon mitochondrial fusion, since ablation of both MFN1 and MFN2 also

resulted in a similar decrease in mtDNA levels (Chen et al, 2010). OPA1 variants containing exon 4b have been linked to mtDNA stability and may interact with nucleoids (Elachouri et al, 2011). Surprisingly however, little else is known concerning the role of mitochondrial fusion in mtDNA stability. It is long believed that fusion can allow for complementation of defective mtDNA molecules and their protein products, and some evidence indeed supports this hypothesis (Hori et al, 2011; Vidoni et al, 2013; Yang et al, 2015a). However, how complementation could rescue mtDNA depletion, and more grossly how cells regulate and maintain mtDNA copy number in general is largely unknown.

1.4.6 OPA1 in Cristae Structure

In addition to fusion, OPA1 and Mgm1, the yeast homologue of OPA1, are required for cristae structure, as their disruption drastically affects cristae morphology (Amutha et al, 2004; Frezza et al, 2006; Meeusen et al, 2006). Similar to mitochondrial fusion, the role of OPA1 in cristae morphogenesis likely requires its GED domain (Meeusen et al, 2006), GTPase domains (Amutha et al, 2004) and coiled-coil domains (Frezza et al, 2006). Moreover, maintenance of cristae structure by OPA1 requires its oligomerization since during apoptosis, disruption of OPA1 oligomers is necessary for cristae junction opening and cytochrome c mobilization (Frezza et al, 2006). While OPA1 overexpression maintained tight cristae junctions and protected cells from cell death, mitofusins were not required for these effects, suggesting that cristae modulation during cell death can be separated from mitochondrial fusion (Frezza et al, 2006). Another group corroborated these findings and demonstrated that cytochrome c release and apoptosis could be inhibited by overexpressing mutant OPA1(Q297V), which mimics OPA1's GTP-bound state and remains self-assembled (Yamaguchi et al, 2008). However, in contrast to Frezza,

Yamaguchi demonstrated that this protection and cytochrome c correlated with an apparent widening of cristae junctions. This apparent discrepancy has yet to be resolved, although one interpretation is that the major role of OPA1 in cristae structure may not be specifically at cristae junctions. In this regard, it would be of interest to revisit these ultrastructural studies and investigate other aspects of cristae structure, including cristae width. While these studies describe the essential role of OPA1 in cristae mediated changes during cell death, the impact of physiological metabolic changes on OPA1 assembly, cristae and mitochondrial respiration is unknown.

Here, we demonstrate that OPA1 dynamically regulates cristae shape in healthy cells and that this process is required to maintain mitochondrial activity under conditions of low energy substrate availability. Specifically, lack of energy substrates induced OPA1 oligomerization and narrowing of cristae, which was required to promote ATP synthase assembly and to maintain ATP linked respiration. Importantly, these changes were independent of mitochondrial fusion and essential for cell survival. We also identified a group of mitochondrial solute carriers that interact with OPA1 to regulate its function.

1.5 Cristae structure regulation

1.5.1 History

In the 1960's Hackenbrock's thesis work illustrated through electron microscopy how isolated mitochondria can adopt different configurations (Hackenbrock, 1966; Hackenbrock, 1968b). Hackenbrock took advantage of Chance and William's description of five states of a mitochondrial suspension (Chance & Williams, 1955) to investigate their role in mitochondrial ultrastructure. In summary, Hackenbrock described how in state III respiration, when mitochondria are respiring at a high rate and substrate levels are high,

the matrix was very compacted and cristae were dilated. By contrast, when mitochondria were left in a sucrose buffer with little substrates and low respiration (state I), the matrix was much less condensed (electron poor) and the cristae were tight. These structural configurations were termed "condensed" for the condensed matrix in state III mitochondria and "orthodox" mitochondria for those with nice tight cristae, similar to the shape of mitochondria following *in situ* fixation. These structural changes came at a time when the generation of ATP by mitochondria was a major question in cell biology. As such, Hackenbrock along with others advocated for, (in his words) "an energy-linked mechanochemical process which may reside in a multienzyme respiratory assembly which carries out electron transport and oxidative phosphorylation" (Powell, 2005). While we now know that ATP is generated by the proton gradient passing through the ATP synthase (the chemiosmotic theory), it remains unknown whether changes in cristae structure can tune metabolic rates to the cellular state. Within this work we confront this significant question in mitochondrial biology.

1.5.2 Cristae structure function

The function of cristae structural changes remains largely unknown. Tight cristae, and their junctions, may limit diffusion of small molecules and membrane proteins in and out of cristae (Mannella, 2006; Mannella et al, 2013; Sukhorukov & Bereiter-Hahn, 2009). This hypothesis is based on computer modeling where simulations of mitochondria in the tight orthodox conformation could lead to reduced local ADP levels. Likely due to technical hurdles, experimental evidence for this model is at present lacking. More recently, mitochondrial ultrastructure has been linked to stabilization of ETC supercomplexes which may represent another way in which mitochondrial function can be adjusted (Cogliati et al,

2013). Finally, changes in cristae structure have been noted during apoptosis, where cristae junction widening is required to mobilize cytochrome c stores for release upon outer membrane permeabilization (Frezza et al, 2006; Germain et al, 2005; Scorrano et al, 2002). Moreover, overexpression of OPA1 was able to maintain cristae structure and protect cells from apoptosis (Frezza et al, 2006).

The ETC fluid model, as proposed by Hackenbrock, suggests that independent ETC complexes interact randomly in a fluid membrane (Hackenbrock et al, 1986). While this model is attractively simple (and used in Figure 2 for simplicity), recent biochemical techniques have made it possible to visualize higher order conformations of ETC complexes. Specifically, Blue-Native PAGE and Clear-Native PAGE have revealed that ETC complexes self-associate and associate with others to form larger complexes, popularly called ETC supercomplexes (Acin-Perez et al, 2008; Cruciat et al, 2000; Schagger & Pfeiffer, 2000; Wittig & Schagger, 2009). For example, Schagger and colleagues demonstrated that CI assembles with CIII and CIV, and that CIII can assemble with CIV, in different stoichiometric configurations (Schagger & Pfeiffer, 2000). ETC supercomplexes can also contain CoQ and cytochrome c (Acin-Perez et al, 2008). While it had been proposed that supercomplex assembly may affect electron transfer efficiency, the literature failed to convincingly demonstrate the functional significance of these supercomplexes, leaving some to doubt if they were artifacts of the native-PAGE techniques (Barrientos & Ugalde, 2013). These doubts have been mostly resolved due to the recent discovery of ETC supercomplex assembly factors affecting mitochondrial respiration (Lapuente-Brun et al, 2013), and the regulation of ROS production by supercomplex assembly (Maranzana et al, 2013). The landmark *Science* paper by

Lapuente-Brun also describes how different supercomplexes determine how electrons are passed from one complex to another, creating two different pools of CoQ, one that accepts electrons from NADH and one that accepts electrons from $FADH_2$ (Lapuente-Brun et al, 2013). In addition, Scorrano and colleagues have demonstrated that inner membrane structure alters ETC supercomplex assembly (Cogliati et al, 2013). Furthermore, our own BN-PAGE analyses have revealed that neuronal extracellular acidification, like that Fassociated with stroke, increases ETC supercomplex assembly—representing one of the first known physiological modifiers of ETC assembly (Khacho et al. 2014).

These findings have led to our current understanding of the electron transport chain: the plasticity model, where different ETC supercomplexes assemble and disassemble in response to physiological cues in order to regulate electron transfer efficiency and ROS production (Acin-Perez & Enriquez, 2014). Due to their attractiveness as modifiers of mitochondrial respiration, many groups have investigated novel factors required for the assembly of ETC supercomplexes including: Cox7A2l/COX7RP/SCAF1 (Ikeda et al, 2013; Lapuente-Brun et al, 2013), MCJ/DnaJC15 (Hatle et al, 2013) and C11orf83/UQCC3 (Desmurs et al, 2015; Wanschers et al, 2014).

Although the mammalian ATP synthase does not assemble with the other ETC complexes, in many contexts it self-assembles, forming dimers and oligomers (Paumard et al, 2002). In yeast, ATP synthase dimers regulate membrane curvature and efficiency of ATP production (Minauro-Sanmiguel et al, 2005; Paumard et al, 2002). Assembly and stability of the ATP synthase monomer represents another mechanism to regulate its function. For example, yeast lacking mgm1, the OPA1 homologue, have a deficiency in ATP synthase assembly and ATP production (Amutha et al, 2004). Mechanisms regulating ATP synthase

stability are currently lacking and represent an attractive target to regulate ATP synthesis.

1.5.3 Regulators of Cristae Structure

Proteins and lipids required for proper cristae folding have received substantial recent research attention. Mitofilin downregulation, for example, leads to concentric sheets of cristae in both yeast and mammalian cells (John et al, 2005). In addition, mitofilin is enriched at sites of cristae junctions (Rabl et al, 2009). Interestingly, the mitochondrial network was undisturbed in these cells. By Blue-Native PAGE and glycerol gradient centrifugation John *et al.* also discovered large a high-molecular-weight protein complex that has led to a recent explosion in research interest (John et al, 2005).

Through immunoprecipitation-coupled mass spectrometry of the yeast mitofilin homologue, quantitative proteomics of isolated cristae contact sites, *in silico* analysis and genetic interaction assays, four independent groups identified a master protein complex regulating cristae ultrastructure in yeast (Alkhaja et al, 2012; Harner et al, 2011; Hoppins et al, 2011; von der Malsburg et al, 2011). Mutations in components of this complex resulted in degradation of other components of the complex and obvious cristae defects, most notably onion-like structures with no visible cristae junctions. Originally given multiple names, researchers have opted to unify the nomenclature calling it MICOS for MItochondrial contact site and Cristae Organizing System. In addition to regulating the contact sites, other roles for the MICOS have been investigated including ETC supercomplex assembly, respiration and mitochondrial transcription (Alkhaja et al, 2012; Koob et al, 2015; Yang et al, 2015b). Interestingly, OPA1 was found to interact with members of the mammalian MICOS complex, namely CHCHD3, mitofilin and MICOS associated factor Sam50 [(Darshi et al, 2011) and data presented herein]. Future studies on

the MICOS complex will undoubtedly discover other protein members, their regulating factors and functional significance.

ATP synthase dimerization and oligomerization is also a major contributor to cristae curvature in yeast, particularly within cristae tips (Minauro-Sanmiguel et al, 2005; Paumard et al, 2002). Interestingly, this regulation of ATP synthase dimerization/oligomerization requires yeast subunits *e, g* and *b,* but are not required for ATP synthase function *per se* (Paumard et al, 2002; Soubannier et al, 2002). These results have been confirmed in human cancer cell lines, where *e* and *g* subunits (ATP5l and ATP5L respectively) are also required for ATP synthase stabilization, affecting cellular respiration and the mitochondrial network (Habersetzer et al, 2013). In contrast, yeast cells lacking ATP synthase subunit 6, have a marked reduction in ATP synthase activity and no defect in cristae structure (Rak et al, 2007). Taken together, the roles of the ATP synthase on ATP generation and cristae structure morphogenesis seem to be independent. The ATP synthase inhibitor factor (IF1) limits the backflow of protons through the ATP synthase during stress, allowing mitochondria to maintain membrane potential at the expense of ATP levels. This is believed to prevent cell death in cell types that undergo limited regeneration (ie. neurons). Recently, IF1 has been implicated in cristae structure, where its overexpression leads to an increase in ATP synthase oligomerization and cristae density (Campanella et al, 2008), and its downregulating decreases cristae density and sensitizes cells to apoptosis (Faccenda et al, 2013).

In addition to protein modifiers of cristae structure, cardiolipin, the vital inner membrane phospholipid, is also required for inner membrane curvature. The importance of cardiolipin is exemplified by Barth syndrome, a rare X-linked recessive disease, where mutations in

the tafazzin gene causes reduced and altered cardiolipin (Barth et al, 1983; Bione et al, 1996; Schlame & Ren, 2006). Barth syndrome manifests as a cardiomyopathy associated with skeletal muscle weakness, neutropenia, growth retardation, and a slight cognitive decline (Barth et al, 1983; Mazzocco & Kelley, 2001). Alterations in mitochondrial cardiolipin (decreased by about 80%) caused by tafazzin mutations are believed to underlie cristae and ETC defects in Barth syndrome (Schlame & Ren, 2006). The effect of cardiolipin on ETC function is likely due to its role in ETC supercomplex assembly (Pfeiffer et al, 2003; Zhang et al, 2002). In this regard, Barth Syndrome patient cell lines are associated with defects in ETC supercomplexes, and in a minimalist *in vitro* system ETC supercomplex function was dependent on cardiolipin (Bazan et al, 2013; McKenzie et al, 2006). Admittedly, probably not all of the defects associated with Barth Syndrome are dependent on cristae structural abnormalities, as cardiolipin is required for many other mitochondrial functions, including iron homeostasis and protein import [reviewed in (Raja & Greenberg, 2014)]. Still, cardiolipin likely enacts its role in cristae shaping through interactions with various proteins including OPA1 (Ban et al, 2010), Bid (Kim et al, 2004), cytochrome c (Tyurin et al, 2007) and members of the MICOS complex (Weber et al, 2013). With respect to OPA1 for example, cardiolipin stimulates its GTP hydrolysis, required for membrane tubulation and fusion (Ban et al, 2010). Interestingly, cardiolipin stimulated OPA1-GTPase activity correlated with the ability of OPA1 to oligomerize (Ban et al, 2010). DeVay *et al.* took advantage of this cardiolipin-stimulated oligomerization of OPA1/Mgm1 to describe how membrane associated Mgm1 self-assembles in trans between a l-Mgm1 and a s-Mgm1 (DeVay et al, 2009). Their work is suggestive of a model whereby l-Mgm1 dimers are GTPase inactive, but recruits s-Mgm1 to promote GTPase–

dependent fusion events (DeVay et al, 2009).

Research into cristae structural regulation is evolving at an astounding rate. For example, at the time of our first OPA1 interaction screen (presented herein), the MICOS complex had not yet been described. Since its first description in 2011, dozens of papers on the MICOS complex have defined new core components, regulating factors and their metabolic functions. Regardless, how and why mitochondrial shape changes occur during shifting metabolic demands remained unknown.

1.6 CLUH

Novel OPA1-interacting factors may shed light on mechanisms governing mitochondrial dynamics, cristae structure or mtDNA maintenance. For this reason, in this thesis we performed quantitative proteomic OPA1-interaction screen and identified numerous potentially novel interactors. Among this list, KIAA0664, the human clueless homologue (CLUH), of which little is known, was identified.

S. cerevisiae CLU1, and *Dictyostelium discoideum* cluA genes were previously demonstrated to regulate mitochondrial distribution, where mutants had clustered mitochondria (Fields et al, 1998; Zhu et al, 1997b). More recently, Drosophila *Clu* was demonstrated to regulate a similar mechanism in mitochondrial localization (Cox & Spradling, 2009; Sen et al, 2013). Drosophila with null mutations for *Clu* also showed multiple metabolic defects including shortened lifespan, complete sterility in both males and females, little movement and flight muscle defects (Cox & Spradling, 2009). Interestingly, despite clear defects in mitochondrial localization and cristae structure, they did not investigate a role of drosophila *Clu* within mitochondria. Many of the observed defects in Drosophila phenocopied those associated with *park* and *pink* mutations.

Moreover, double heterozygotes for *park* and *Clu* resulted in mitochondrial clustering while their respective heterozygote controls had no such effect. These results suggest that *park* and *Clu* genetically interact, implying that CLUH may represent a novel protein involved in processes associated with Parkinson's disease (Cox & Spradling, 2009). Human CLUH demonstrates 53% similar to Drosophila *clu*, with more conserved middle (85%) and tetratricopeptide repeats (TPR) (55%) domains. While the Clu domain has no ascribed function, the TPR domain is believed to regulate protein-protein interactions, and in the case of Drosophila *clu* may compete for TPR domains on kinesin light chain hindering its interaction with mitochondria (Cox & Spradling, 2009).

More recently, Cox and colleagues also found a developmental increase in *Clu* expression in developing neuroblasts, presumably responsible for the differentiation of neuronal cells (Sen et al, 2013). Furthermore, they demonstrate that the mitochondrial defects are downstream of the effect that *Clu* has on cellular ROS levels and suggest that the mitochondrial defects are simply a consequence of this oxidative damage. Since larvae depend mostly on glycolysis for energy production, defects are only apparent once reaching adulthood where the organism relies more on mitochondrial OXPHOS. Goh and colleagues proposed another role for *Drosphila clu* with respect to its role in PD associated phenotypes (Goh et al, 2013). They advocate that *clu* interacts with atypical Protein Kinase C (aPKC) regulating its activity, mislocalizing Miranda and Numb during neuroblast divisions. Moreover *clu* mutations rescued brain size in *lethal(2) giant larvae (lgl)* mutants, which present with defects dependent on aPKC inactivation. Since *park* mutant flies also present with defects in neuroblast asymmetric divisions and double *lgl/park* mutants also restored brain size, the authors provide tantalizing evidence for a link between minor early

neurogenesis defects leading to later neurodegeneration. They also failed to investigate a role for mitochondrial CLUH on mitochondrial function in their system.

A recent screen revealed CLUH as a novel PGC-1α target, providing the first insights into its regulation (Nsiah-Sefaa et al, 2014). Both overexpression of PGC-1α and its activation by AICAR resulted in the discovery of four novel target genes: *Mtfp1, Mrm1, Oxnad1* and *Cluh*. Notably, PGC-1α activation has roles in promoting mitochondrial mass, metabolism and antioxidants (St-Pierre et al, 2003; Wu et al, 1999), and all four novel PGC-1α regulated genes had some role in mitochondrial function (Nsiah-Sefaa et al, 2014).

Altogether, the research on CLUH and its various homologues point to a role in mitochondrial localization and function, although mitochondrial CLUH had not been demonstrated prior to our studies. Furthermore, many questions surrounding the role of CLUH in mitochondrial dynamics remains unanswered. Namely, does CLUH regulate mitochondrial length? How would its potential interaction with the fusion machinery affect mitochondrial function? And how conserved are the previously noted functions of CLUH homologues?

1.7 Mitochondrial Solute Linked Carriers (SLC25)

The solute linked carriers (SLC) are a large group of highly conserved membrane proteins which transport various substances across different cellular membranes. Located within the inner membrane, mitochondrial transporters (SLC25) represent a growing family of transporters, shuttling vital metabolites in and out of the matrix. Their discovery, functional characterization and regulation are advancing at a rapid pace.

The term transporters broadly refers to the transport of a substance across a membrane,

comprising of pumps, channels and carriers. SLC25s are therefore both transporters and carriers, although the term carrier is more specific and will be utilized here. Carriers can be further divided into various types transport: uniporters, symporters and antiporters. Uniporters transport molecules across a concentration gradient. Symporters cotransport two molecules in the same direction, one against its concentration gradient fueled by the movement of another down its gradient. Antiporters like symporters, cotransport two molecules, one along and one against its gradient, but in opposite directions (Lodish, 2000). The majority of SLC25 proteins are antiporters, also termed exchangers, but a few are uniporters or symporters or a combination antiporters and exchangers under certain conditions. Interestingly, the inner membrane shaping phospholipid, cardiolipin, is required for proper assembly and function of the mitochondrial solute carriers (Claypool, 2009).

1.7.1 SLC25 protein structure and function

SLC25 family proteins have a number of conserved features. Generally, they contain a tripartite structure, three repeats of homologous domains with two α-helix transmembrane motifs each (six in total) (Palmieri, 2013). Both N- and C-terminals face the intermembrane space with 3 long matrix loops and two short intermembrane space loops. SLC25 protein exists in one of two conformations: the cytoplasmic state (c-state) where the carrier can accept substrates from the cytoplasm, and the matrix state (m-state) where the carrier accepts substrates from the matrix. Although crystalizing SLC25s in their uninhibited states has proven difficult, two SLC25 members have had their structures solved. The crystal structure of the bovine ADP/ATP carrier with its inhibitor, carboxyatractyloside, locking the carrier in the c-state (Pebay-Peyroula et al, 2003). And more recently,

SLC25A8 (uncoupling protein 2, UCP2) was solved in a complex with GDP by nuclear magnetic resonance (Berardi et al, 2011). These studies revealed the six transmembrane α-helices with three α-helices within the matrix loops. Each transmembrane α-helix has two signature motifs, PX[D/E]XX[R/K] and [D/E]GXXXX[W/Y/F][R/K]G where the proline residue kinks the α-helix and charged residues form salt bridges, closing the cavity. A common substrate-binding domain likely exists between three contact points halfway within the even numbered transmembrane α-helices, each interacting with a single functional group of the transported substrate (Robinson & Kunji, 2006). These critical three residues provide substrate specificity and may even help predict potential substrates for uncharacterized SLC25 proteins. When substrates bind either the c-state or m-state of the carrier, the protein rearranges until the transition state is reached, dependent on the "flexible hinged helix movements" (Palmieri, 2013). As their structure and function suggests, mitochondrial carriers largely operate as monomers (Kunji & Crichton, 2010).

There are 54 identified SLC25 proteins, 24 of which are characterized, involved in transporting solutes required for almost all aspects of mitochondrial function (Figure 6). Many SLC25 proteins transport nucleotides including the ADP/ATP carriers (AAC), ATP-Mg/P_i carriers (APC), CoA and adenosine diphosphate carrier and others. ADP/ATP carriers are the most characterized mitochondrial solute carriers, due to their dual roles in regulating mitochondrial metabolism and cell death. In healthy cells, AACs exchange cytosolic ADP for matrix ATP, providing substrate for the ATP synthase, and energy to the rest of the cell. During cell death, AACs regulate the permeability transition pore (mPTP) through interactions with cyclophilin D and voltage-dependent anion channels (Crompton et al, 1998; Woodfield et al, 1998), although such a direct role of AACs in

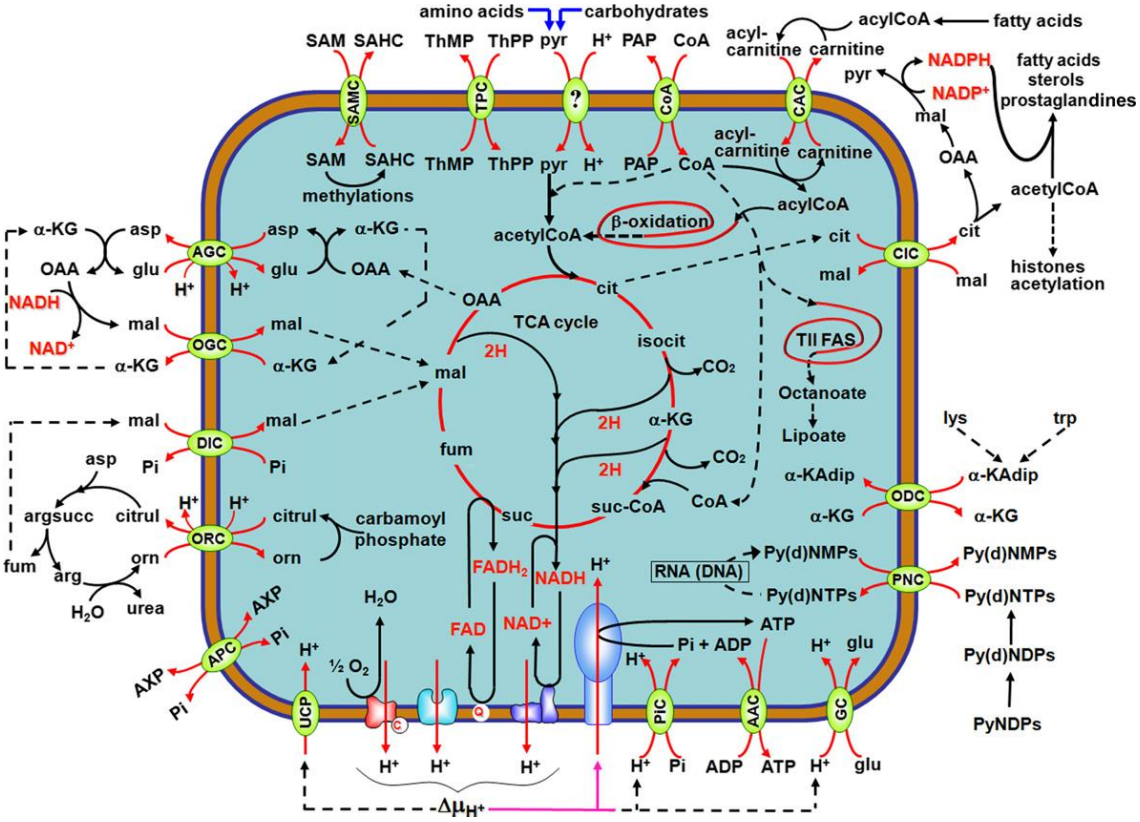

Figure 6. "Metabolic roles of MCs." From (Palmieri, 2013).

"The scheme shows 16 functionally identified MCs catalyzing metabolite, nucleotide or coenzyme transport through the inner mitochondrial membrane. These carriers are involved, with partial overlap, in: oxidative phosphorylation (AAC, PiC, UCP); oxidation/reduction pathways (AGC, OGC, DIC, CIC, CAC); synthesis and breakdown of mitochondrial DNA and RNA (PNC); homeostasis of the intramitochondrial adenine nucleotide pool (APC); methylation of mtDNA, mtRNA and some intramitochondrial proteins (SAMC); import of thiamine pyrophosphate (ThPP) required for pyruvate- and oxoglutarate-dehydrogenase complex activities (TPC); import of coenzyme A (CoA) required for fatty acid (FA) b-oxidation, Krebs cycle, biosynthesis of heme, branched-chain amino acid catabolism, urea cycle and mitochondrial type II FA synthase (CoA carrier); and amino acid metabolism (AGC, ORC, GC, ODC). The scheme does not include all of the carriers listed in Table 1 and does not show all the metabolic pathways in which the already identified carriers are involved. AAC, ADP/ATP carrier; AGC, aspartate glutamate carrier; APC, ATP-Mg/Pi carrier; CAC, carnitine-acylcarnitine carrier; CIC, citrate (tricarboxylate) carrier; CoA, coenzyme A carrier; DIC, dicarboxylate carrier; GC, glutamate carrier; ODC, oxoadipate carrier; OGC, oxoglutarate carrier; ORC, ornithine carrier; PiC, phosphate carrier; PNC, pyrimidine nucleotide carrier; SAMC, S-adenosylmethionine carrier; TPC, thiamine pyrophosphate carrier; UCP, uncoupling protein."

mPTP regulation is highly debated (Kokoszka et al, 2004). Another large group of SLC25 carriers transports amino acids, including the aspartate glutamate carriers (AGC1 and AGC2) and 14 others. The oxoglutamate carrier (OGC), the dicarboxylate carrier (DIC), the citrate carrier (CIC) are among the carboxylate carrier class of SLC25 proteins. Finally, uncoupling proteins (UCP) make up a last group of solute carriers, facilitating transport of protons across the inner membrane dissipating the proton gradient without the generation of ATP. This dissipation produces heat, predominantly in brown adipose tissue, as well as decreases oxidative stress at the expense of ATP generation (reviewed in (Mailloux & Harper, 2011).

1.7.2 SLC25 in disease

As SLC25 function is pivotal to mitochondrial function, their dysfunction leads to numerous genetic disorders. These disorders are characterized by specific metabolic manifestations, of which 11 have been described. They are mostly autosomal recessive diseases with the exception of autosomal dominant progressive external ophthalmoplegia (adPEO). AdPEO can be caused by mutations in ANT1 and other non-SLC25 proteins. The disorder manifests usually during adulthood with symptoms of eye muscle weakness and exercise intolerance, characterized by multiple mtDNA deletions in skeletal muscle (Agostino et al, 2003). While research into rare genetic diseases is advancing at an incredible speed (Beaulieu et al, 2014), more novel disease gene mutations in SLC25 proteins will undoubtedly be discovered in the future. Research on four SLC25 carriers (AGC1, AGC2, DIC and OGC) will be discussed in greater detail.

1.7.3 AGC

AGC1 (SLC25A12/aralar) and AGC2 (SLC25A13/citrin) regulate amino acid transport of aspartate out of the matrix and glutamate and a hydrogen ion into the matrix (Palmieri et al, 2001). They are larger in size than other SLC25s due to their long N terminus containing multiple EF-hand motifs. As such, AGC1&2 are known to be regulated by calcium, where calcium increases their transport activity (Palmieri et al, 2001; Satrustegui et al, 2007). The AGCs are central to both the urea cycle and the malate-aspartate shuttle. The urea cycle produces urea from toxic ammonia in the liver of mammals. This process requires 5 steps, two within mitochondria and three within the cytosol. Mitochondrial aspartate, shuttled to the cytosol by AGC, is converted with citrulline to arginosuccinate that is then converted to arginine, the substrate for urea synthesis. The by-products from these reactions, malate and orthinine, are then imported into the matrix and, through a series of reactions, reconverted to aspartate and citrulline respectively using ammonia in the process (Satrustegui et al, 2007). The malate-aspartate shuttle (MAS) is a very important process by which cytosolic NADH is imported into mitochondria through a series of reactions. This increased mitochondrial NADH is particularly important during glycolysis and lactate metabolism. Both AGC and the OGC are critical for the MAS, the net effect of which is that cytosolic NADH is oxidized to NAD^+ and matrix NAD^+ is reduced to NADH (LaNoue et al, 1973).

While both AGCs are expressed very early on during embryogenesis (del Arco et al, 2002), AGC1 is expressed in the diaphragm, skeletal muscle, heart, brain and kidney, but is not detected in the liver; while AGC2 is expressed mainly in the liver, kidney and heart, but is not detected in the brain (Begum et al, 2002). This tissue specificity helps explain the

different clinical manifestations of diseases caused by mutations in AGC1 and AGC2. AGC1 deficiency causes complete lack of function of AGC in the brain and is associated with a very poor clinical prognosis. Infants present with halted psychomotor development, muscle weakness and seizures (Wibom et al, 2009). Since *N*-acetyl aspartate is a myelin lipid precursor AGC1 deficiency leads to hypomyelination. Interestingly, there is also a strong relationship between certain AGC1 mutations and the development of autism (Aoki & Cortese, 2015). In contrast, since AGC2 is normally the only AGC present in the liver, AGC2 deficiency leads to a defect in the urea cycle and type II citrullinemia (CTLN2) associated with fatal hyperammonemia comas (Kobayashi et al, 1999).

1.7.4 DIC

The dicarboxylic carrier (SLC25A10/DIC) exchanges malate or succinate from the matrix for inorganic phosphate from the cytosol (Palmieri et al, 1971; Palmieri et al, 1996). As such, the DIC supplies substrates for Krebs cycle, gluconeogenesis, urea synthesis, sulfur metabolism and glucose-stimulated insulin secretion (Fiermonte et al, 1998; Huypens et al, 2011). The DIC, along with the OGC, has also been implicated in mitochondrial glutathione transport (Chen & Lash, 1998; Chen et al, 2000). This mechanism of glutathione transport was confirmed in brain mitochondria where the inhibitor and short hairpin RNA knockdown of the DIC increased ROS content and impaired complex I activity (Kamga et al, 2010). Although there is mounting evidence to support the OGC and the DIC as glutathione carriers (Lash et al, 2002; Wilkins et al, 2014; Wilkins et al, 2013; Zhong et al, 2008), recent work has cast doubt on the direct transport of glutathione by OGC and DIC (Booty et al, 2015). Future work will need to establish the precise role of these carriers in mitochondrial glutathione transport and resolve these discrepancies.

1.7.5 OGC

The oxoglutarate carrier (SLC25A11/OGC) is responsible for the import of malate into the matrix for 2-oxoglutarate (Fiermonte et al, 1993; Indiveri et al, 1987; Palmieri et al, 1972). As such the OGC also plays a pivotal role in MAS, shuttling the reducing equivalents from malate into the matrix for NADH generation. The OGC is also involved in glucose-stimulated insulin secretion (Odegaard et al, 2010) and the oxoglutarate-citrate (isocitrate) shuttle resulting in NADPH reducing equivalents being shuttled from the matrix to the cytoplasm (Monne et al, 2013). OGC has also been linked to mitochondrial dynamics, cristae structure and apoptosis (Gallo et al, 2011). Like many other SLC proteins, OGC is not completely selective and may also transport malonate, maleate, succinate, oxaloacetate, 2-oxopimelate and, like DIC, may transport glutathione (Monne et al, 2013).

1.8 Reactive Oxygen Species and Glutathione

1.8.1 General Introduction

ROS are a group of small oxygen-containing free radicals that are extremely reactive due to their unpaired valence electrons. ROS are generally formed by the primary ROS superoxide ($O_2^{\cdot-}$), which is chiefly converted to hydrogen peroxide (H_2O_2) by superoxide dismutases (SOD) but may also be protonated to form hydroperoxyl radicals (HO^{2-}). H_2O_2 can be transformed into a number of other ROS including hydroxyl radicals (OH•), hydroxyl anions (HO−), singlet oxygen ($^1O_2$) and hypochlorite (ClO^-). There are many generators of cellular ROS including the mitochondrion, nicotinamide adenine dinucleotide phosphate (NADPH) oxidase (reviewed in (Babior, 2000)), xanthine oxidase (Yokoyama et al, 1990), and uncoupled endothelial nitric oxide synthase (eNOS) (Dijkstra et al, 1998). In the majority of cell types, the mitochondrion is the major source of ROS.

Superoxide production, due to inefficiencies in oxidative phosphorylation, accounts for up to 2% of the total oxygen consumed by mitochondria (Orrenius, 2007). Mitochondrial-generated ROS (mtROS) are mainly produced at complex I and complex III of the electron transport chain, although a total of nine sites have been identified (Andreyev et al, 2005). Complex I produces superoxide solely in the matrix while complex III generates superoxide in both the matrix and the intermembrane space (Muller et al, 2004).

One cannot discuss ROS without discussing its clearance. Cells possess a number of antioxidant defences chiefly to protect the cell from oxidative stress, but there are also involved in other functions including cellular signaling. As a charged molecule, superoxide is generally membrane impermeable and is a particularly damaging molecule. It is however rapidly converted to H_2O_2 by superoxide dismutases: copper/zinc superoxide dismutase (SOD1) in the cytoplasm and mitochondrial intermembrane space; and by manganese superoxide dismutase (SOD2) in the mitochondrial matrix (Zhang & Gutterman, 2007). The importance of superoxide detoxification is highlighted by the fact that SOD2 knockout mice live only weeks (Lebovitz et al, 1996). H_2O_2, however, is membrane permeable and is likely the main signaling molecule in ROS-mediated pathways. H_2O_2 is detoxified in cells by glutathione peroxidase (GPx), and in some cases by catalase, to form water (Zhang & Gutterman, 2007). Prolonged high levels of ROS that surpass the cell's antioxidant capacity result in oxidative stress.

1.8.2 Glutathione

As stated above, cells have a number of processes to detoxify H_2O_2, notably by the glutathione system. Glutathione (GSH) is a very abundant (around 1-10 mM) tripeptide antioxidant (Mari et al, 2013), central to cellular antioxidant defense and other functions including: cell cycle progression, apoptosis, cysteine storage and modulation of immune function (Hutter et al, 1997; Lu, 2009; Pallardo et al, 2009; Suthanthiran et al, 1990). Its structure consists of glutamic acid, cysteine and glycine, where the cysteine amino acid provides the thiol side chain (-SH) and antioxidant function. Due to its unusual γ-carboxyl bond between the glutamic acid and cysteine, GSH is resistant to intracellular degradation, and is instead excreted by cells for degradation by GGT-mediated cleavage of the γ-glutamyl bond (Meister & Anderson, 1983).

H_2O_2 scavenging requires two GSH molecules in the presence of glutathione peroxidase (GPx), which efficiently reduces H_2O_2 to water and oxidizes two GSH molecules together at their thiol side chains, creating glutathione disulfide (GSSG). GSSG can, in turn, be reduced by glutathione reductase, in a reaction which requires reducing equivalents from NADPH. The products, two GSH molecules, are thus recycled and may continue their antioxidant function. Due to its central role in antioxidant function, the ratio between GSH and GSSG states is often used as an indicator of oxidative stress. In addition to its conversion to GSSG, GSH can also mediate antioxidant activity through protein s-glutathionylation on cysteine –SH groups. Protein s-glutathionylation generally occurs under high oxidative stress and is a post-translational modification demonstrated to regulate aspects of mitochondrial metabolism and function (Mailloux & Willmore, 2014). For example, uncoupling proteins 2 and 3 may be glutathionylated during prolonged

oxidative stress, decreasing their activity (Mailloux et al, 2011). This glutathionylation may be critical to maintain membrane potential and to prevent apoptosis. Proteins can also be deglutathionylated by glutaredoxin, requiring GSH, when the cell's oxidative status returns to normal (Liu & Gaston Pravia, 2010).

Since cysteine is extremely unstable in the extracellular environment, due to its ability to auto-oxidize, one of the primary functions of glutathione is to supply the cell with cysteine residues (Meister & Anderson, 1983). In a series of reactions, Meister described and named the γ-glutamyl cycle (Meister & Anderson, 1983). To begin, GSH is excreted (primarily by the liver) through cellular glutathione transporters. GSH is then transported to various tissues. GSH is broken down extracellularly by GGT and dipeptidase, resulting in free cysteine amino acids ready for import into mitochondria. Synthesis of GSH in the cytoplasm requires this source of cysteine and takes place through two ATP dependent reactions (Lu, 2000). The rate-limiting first step utilises l-glutamate and l-cysteine to form γ-glutamyl-l-cysteine, which is catalyzed by glutamate cysteine ligase (Yan & Meister, 1990). This step is regulated by feedback inhibition of GSH (Richman & Meister, 1975) (Huang et al, 1988) and by cysteine availability (Meister & Anderson, 1983). The second step in GSH synthesis involves ligation of γ-glutamyl-l-cysteine and l-glycine, catalyzed by GSH synthase (Oppenheimer et al, 1979). This second step is not rate-limiting since GSH synthase overexpression does not increase GSH production (Grant et al, 1997) and cellular levels of γ-glutamyl-l-cysteine are very low (Dalton et al, 2004).

Mitochondria contain a similar concentration of GSH to the rest of the cell (Ribas et al, 2014). Accordingly, mitochondria contain around 10% of the total glutathione pool, and higher amounts in certain tissues (Meredith & Reed, 1982). Since GSH is made exclusively

in the cytosol and GSH cannot diffuse into the mitochondrial matrix, GSH transport mechanisms are required (Mari et al, 2013). Mitochondrial transport of GSH is vital to proper metabolism and function (Mari et al, 2013). Interestingly, only two proteins have been implicated in mitochondrial GSH transport: the oxoglutarate carrier (OGC) and the dicarboxylate carrier (DIC) (Chen & Lash, 1998). There may be tissue specificity for mitochondrial GSH transport as both carriers have been demonstrated to transport GSH in liver mitochondria, while only DIC transports GSH in neurons (Kamga et al, 2010). Moreover, mitochondrial GSH transport through OGC and DIC regulates neuronal susceptibility to oxidative stress (Wilkins et al, 2014; Wilkins et al, 2013). Here, we demonstrate that OPA1 interacts with both of these carriers and investigate a novel role of OPA1 in glutathione regulation.

1.9 Objectives and Hypotheses

Maintenance of mitochondrial ultrastructure during apoptosis has previously been demonstrated to regulate cell survival (Frezza et al, 2006; Yamaguchi et al, 2008). This cristae-dependent protection required the mitochondrial fusion protein OPA1. **We hypothesize here that OPA1-dependent changes in cristae structure, under non-apoptotic conditions, could represent a novel mechanism by which the cell can respond to its environment and dictate mitochondrial function.** My principal objectives are: to determine whether OPA1 controls mitochondrial metabolism and function by modulating cristae structure during different energy states; and to identify novel OPA1 interacting factors and signaling pathways that control OPA1 function.

OPA1 deoligomerization is a key step in the dissolution of cristae structure during cell death (Frezza et al, 2006). We therefore begin by investigating whether OPA1's oligomerization status changes in response to changing energetic conditions and if this mechanism could regulate mitochondrial cristae structure and ETC function in response to the energetic demand of the cell. We also described the fusion-dependent and fusion-independent roles of OPA1 in the response to cellular starvation, respiration and assembly of the ATP synthase. Finally, through the investigation of OPA1-interacting proteins we highlight a novel mechanism by which OPA1 can respond to metabolic demand.

Also, from the screens outlined in this work we identified CLUH as a novel OPA1 interactor. Since the Drosophila orthologue of CLUH is known to regulate mitochondrial dynamics, we hypothesize that the OPA1-CLUH interaction may regulate mitochondrial dynamics in mammals. Here we characterize this interaction, probing its role in mitochondrial fusion.

Since we demonstrate that OPA1 interacts with both the known mitochondrial transporters of glutathione (OGC and DIC) (Chen & Lash, 1998), that ablation of OGC affects OPA1 function and that it has been demonstrated that OPA1 mutations sensitize cells to ROS induced cell death (Tang et al, 2009); we hypothesize that OPA1 affects mitochondrial glutathione redox in order to regulate mitochondrial function. To this end we propose to confirm that OGC deletion affects the cellular GSH/GSSG ratio, to determine whether OPA1 regulates GSH redox levels and to determine if mitochondrial fusion is required to regulate this function.

Chapter 2. Materials and Methods

Cell culture, transfections, and viral production. HeLa and MEF cells were cultured in DMEM supplemented with 10 % FBS (Wisent), 50 u/ml penicillin and streptomycin, and 2 mM of glutamine (Gibco). Galactose media was prepared from glucose/pyruvate free DMEM supplemented as above with 10 mM galactose (Sigma). Cells were transfected using Lipofectamine 2000 (Invitrogen), or with the indicated siRNA using siLentFect (Bio-Rad) according to the manufacturer's protocol. Viral vectors were prepared as previously described (Jahani-Asl et al, 2011; Tashiro et al, 2006). All constructs used are listed in (**Table 1**). To generate the long term expression cultures, OPA1 KO cells were infected with viruses encoding for WT OPA1, OPA1(Q297V) or GFP as control and WT cells were infected with control GFP. Following transduction, cells were selected with puromycin and FACS sorted for GFP expression. These cell lines were maintained and used between 4-12 weeks after stable expression for all experiments.

Mitochondrial isolation. Mouse liver was dissected from young CD-1 or C57BL/6 mice euthanized with sodium pentobarbital. Cells or mouse liver were rinsed with PBS and lysed in mitochondrial isolation buffer (200 mM mannitol, 70 mM sucrose, 10 mM HEPES, pH 7.4, 1 mM EGTA). The isolation was performed in its entirety on ice or at 4ºC. Cells were homogenized with a 25G needle 15 times; while liver were Dounce homogenized 10 times. Nuclei and cell debris were pelleted by centrifugation at 1000 rpm for 9 minutes. The supernatant was then centrifuged at 9000rpm for 9 minutes to pellet mitochondria. These two spins are repeated to further enrich mitochondria in this heavy membrane fraction. Mitochondrial purity was confirmed by western blot and EM.

Western Blot Analysis. Western blots were performed as previously described (Germain et al, 2013), with the following antibodies: mouse anti-actin and anti-flag (Sigma-Aldrich); mouse anti-OPA1 and anti-cytochrome c (BD bioscience); mouse anti-p62 (SQSTM1) and rabbit anti-TOM20 (Santa Cruz Biotechnologies); mouse anti-ATP5A and anti-Complex II (Invitrogen); mouse anti-mtHSP70 (ABR Bioreagents) and rabbit anti-OGC (ABCAM).

Analysis of OPA1 oligomers. To analyse rapid changes in OPA1 oligomerization in whole cells, we used the cell permeable BMH (Thermo Scientific) (1 mM) for 20 minutes at 37°C. After crosslinking, cells were quenched and washed in PBS with 0.1% beta-mercaptoethanol (BME) twice. Cells were then lysed in lysis buffer with BME and subjected to western blot on NuPAGE Novex 3-8% Tris-acetate gradient gels (Life Technologies). For mitochondrial experiments, isolated liver or MEF mitochondria were suspended in the indicated buffer (200 mM sucrose, 10 mM Tris-Mops pH 7.4, 2 mM K_2HPO_4, 0.080 mM ADP, 10 µM EGTA-Tris) at 0.5-1 µg of mitochondrial protein/µL. Substrates and drugs were also added or not as follows: malate, glutamate, succinate and glucose (5 mM) (Sigma), rotenone (2 µM) (Sigma), carbonylcyanide-3-chlorophenylhydrazone (CCCP)(10 µM)(Sigma). All drugs and substrates were adjusted to pH 7.4. Samples were then incubated on a 37°C heating block for 30 minutes or 1 hour. After incubation, EDC (1 mM) (Thermo Scientific) or BMH (10 mM) was added for 30 minutes at room temperature and quenched with BME. Samples were then analysed by gradient gel western blot.

Table 1. Constructs and primers used in this work

Plasmids	**Backbone and cloning strategy**	**Publication**
adOPA1-YFP	OPA1-YFP (Kind gift from Dr. McBride) cloned into pShuttle-CMV via Xho1 and Xba1	Jahani-Asl et al., 2011
adMito-YFP	cDNA for mito-YFP was cloned into the OPA1-YFP vector	This publication
Mito-YFP	Kind gift from Dr. McBride	Braschi et al., 2009
GFP	eGFP-C3	Clonetek
OPA1	Since our WT OPA1 plasmid gave strikingly less OPA1 following transient transfections than OPA1(Q297V) (Yamaguchi et al., 2008), we cloned the WT OPA1 into OPA1(Q297V) mutant using BSPE1 internal restriction sites flanking the mutation	This publication
OPA1(Q297V)	Kind gift from Dr. Newmeyer. In pcna3.1flag	Yamaguchi et al., 2008
lvGFP	Plasmid 12258: pWPXLd (Addgene)	
rvOPA1	cDNA was cloned into MSCV-PIG (Ref Addgene plasmid 18751 Scott Lowe) Gibson assembly cloning Nat. Methods daniel gibson	This publication
rvOPA1(Q297V)	cDNA was cloned into MSCV-PIG (Ref Addgene plasmid 18751 Scott Lowe) Gibson assembly cloning Nat. Methods daniel gibson	This publication
mito-YFP-3xflag	cDNA from of mito-YFP was PCRed out of and cloned into the intermediate pGEM-t-easy to generate restriction sites and inserted with EcoRI restriction sites into p3XFLAG-CMV-14 (Addgene E7908)	This publication
SLC25A10-3xflag	cDNA from mouse SCL25A10 from Open Biosystems (CloneID:3482316) was PCRed out of the pCMV-SPORT6 vector, pasted into pGEM-T-easy and cut and pasted with EcoRI restriction sites into p3XFLAG-CMV-14 (Addgene E7908)	This publication
SLC25A11-3xflag	cDNA from human SCL25A11 from Open Biosystems (CloneID:3911858) was PCRed out of the pCMV-SPORT6 vector, pasted into pGEM-T-easy and cut and pasted with EcoRI restriction sites into p3XFLAG-CMV-14 (Addgene E7908)	This publication
SLC25A12-3xflag	cDNA from human SCL25A12 from Open Biosystems (CloneID:4420100) was PCRed out of the pCMV-SPORT6 vector, pasted into pGEM-T-easy and cut and pasted with Not1 restriction sites into p3XFLAG-CMV-14 (Addgene E7908)	This publication
SLC25A13-3xflag	cDNA from human SCL25A13 from Open Biosystems (CloneID:3600909) was PCRed out of thepCMV-SPORT6 vector, pasted into pGEM-T-easy and cut and pasted with EcoRI restriction sites into p3XFLAG-CMV-14 (Addgene E7908)	This publication
Oligonucleotides	**Company**	**Validation**
siCtrl	Silencer Select Negative Control #1 (Invitrogen)	This publication
siOGC	Silencer Select SLC25A11 s85783 (Invitrogen)	This publication
siOPA1	Silencer Select OPA1 s92343 (Invitrogen)	This publication
Primers	**Sequence**	**Validation**
COI forward	5'-GCCCCAGATATAGCATTCCC-3'	Tal et al., 2009
COI reverse	5'-GTTCATCCTGTTCCTGCTCC-3'	Tal et al., 2009
18S forward	5'-TAGAGGGACAAGTGGCGTTC-3'	Tal et al., 2009
18S reverse	5'-CGCTGAGCCAGTCAGTGT-3'	Tal et al., 2009
ATP5b1 forward	5'-CCGTGAGGGCAATGATTTATAC-3'	Gomes et al., 2013
ATP5b1 reverse	5'-GTCAAACCAGTCAGAGCTACC-3'	Gomes et al., 2013
ATP5a1 forward	5'-CATTGGTGATGGTATTGCGC-3'	Gomes et al., 2013
ATP5a1 reverse	5'-TCCCAAACACGACAACTCC-3'	Gomes et al., 2013
ATP6 forward	5'-TCCCAATCGTTGTAGCCATC-3'	Gomes et al., 2013
ATP6 reverse	5'-TGTTGGAAAGAATGGAGTCGG-3'	Gomes et al., 2013
GAPDH forward	5'-GGTGAAGGTCCGTGTGAACG-3'	Gomes et al., 2013
GAPDH reverse	5'-CTCGCTCCTGGAAGATGGTG-3'	Gomes et al., 2013

Cytochrome C retention assay. As a readout for changes in mitochondrial ultrastructure, mitochondria were assayed for their ability to retain cytochrome c. Mitochondria were incubated as described, then incubated with low digitonin (1 mg/mg of protein at 0.1%), at 4 ºC for 30 minutes to mobilize their inner cristae stores dependent on cristae ultrastructure. Mitochondria are then centrifuged for 10 minutes at 10,000 RPM (4 ºC) to separate the released proteins. The resulting supernatants and pellets (volume equivalents from 12.5 µg of starting mitochondria) were analysed by western blot.

Immunofluorescence and cell death assays. Cells were washed twice with PBS and fixed with 4% paraformaldehyde for 20 minutes and analysed with the indicated primary antibodies. Coverslips were then washed and incubated with their corresponding secondary antibodies (anti-mouse and anti-rabbit Alexa Fluor 488/Alexa Fluor 594). Hoechst stain (Sigma) was added with the secondary where noted to visualize the nucleus. Coverslips were then washed and mounted using Gel Mount Aqueous mounting medium (Sigma).

To analyse cell death during starvation, 24 hours after transfection, cells were starved for 6 hours and stained using propidium iodide (PI) and Hoechst stain for 20 minutes. All dead (PI+) were counted and expressed as a percentage of all cells (Hoechst+). Cell death was also quantified as the percent of condensed nuclei to total nuclei. Images were taken of at least six fields of view on a 20x objective, containing an average of 200 cells each (>1000 cells total).

Immunoprecipitations. 24 hours following transfection, cells were lysed (50 mM tris HCl, 150 mM NaCl, 1 mM EDTA, 1 % Triton X-100, and 1:1000 PIC at pH 7.4), and proteins (2 mg) were immunoprecipitated with ANTI-FLAG M2 magnetic beads (Sigma-Aldrich) according to the manufacturers protocol. Samples were incubated overnight and

the beads were washed four times with TBS (50 mM tris-HCl, 150 mM NaCl, and 1:1000 PIC at pH 7.4). Immunoprecipitated protein was then eluted from the magnetic beads twice with elution buffer (50 mM tris-HCl, and 150 mM NaCl, at pH 7.4 containing 150 ng/µl FLAG peptides). Endogenous immunoprecipitation of OPA1 was performed on isolated MEF or liver mitochondria with CHAPS containing buffer (50 mM tris HCl, 150 mM NaCl, 1 mM EDTA, 1 % CHAPS and 1:1000 PIC at pH 7.4) at 4^{o}C overnight with no antibody, normal mouse IgG, or mouse monoclonal anti-OPA1 (BD Biosciences). OPA1 complexes were then immunoprecipitated with 20 µl of A/G magnetic beads (Pierce) at RT for 1 hour, washed with TBS 4 times, eluted with SDS loading dye for 20 minutes and analysed by western blot.

Transmission electron microscopy. To analyse rapid cristae structure changes during cell starvation, cells were adhered to square glass coverslips, grown to confluence, treated and rapidly fixed with a combination of 2 % paraformaldehyde and 1.6 % gluteraldehyde. Fixed cells were floated off their cover slips, and samples were processed as previously described (Jahani-Asl et al, 2011). For structural quantification, the cristae diameter and mitochondrial width were measured from all mitochondria from ten cells for each condition in two independent cultures. For analysis of cristae structure in isolated mitochondria, mitochondria were treated as indicated, fixed with 2 % gluteraldehyde for 20 at RT, and analysed by EM.

Blue-Native Analysis of ETC complexes ATP synthase assembly was analysed from whole cells and isolated mitochondria by Blue-Native PAGE (BN-PAGE) electrophoresis according to (Wittig et al, 2006). The digitonin extraction and BN-PAGE electrophoresis was performed entirely on ice or at 4 ºC. Cells were grown on 100 mm plates, washed with

PBS, and scraped in PBS. Cells were pelleted at 3000 RPM for 5 minutes or mitochondria were pelleted at 9000 RPM for 9 minutes and resuspended in digitonin extraction buffer (50 mM imidazole/HCl pH 7.0, 50 mM NaCl, 5 mM 6-aminohexanoic acid, 1 mM EDTA with 1% digitonin). Final protein to digitonin ratios were 1:4 w/w for cells and 1:8 w/w for mitochondria. Protein was extracted on ice for 1 hour (for cells) or 30 minutes (for mitochondria) and cleared at 14,000 RPM for 30 minutes. Protein was quantified and 150 µg of protein (or 75 µg from mitochondria) was loaded with 5% glycerol and 1:10 dye:digitonin ratio of Coomassie blue G-250 in 500 mM 6-aminohexanoic acid onto home-made 3-13% large gels. Gels were run 2 hours in a high Coomassie blue G-250 cathode buffer at 150V at 4ºC then switched to a low G-250 buffer overnight at 4ºC. Pictures of the gels were taken to confirm proper loading, and gels were transferred to nitrocellulose membrane at 500mA for 2 hours. The resulting membranes were western blotted as per above.

mtDNA and mRNA Quantification. DNA was extracted by phenol-chloroform-isoamylalcohol extraction according to (Guo et al, 2009), followed by qPCR with SYBR Green FastMix (Quanta Biosciences) according to the manufacturers protocol with the indicated primers in Table 1. RNA was extracted with TRIzol (Life Technologies) and analysed by RT-PCR according to (Gomes et al, 2013) with the indicated primers in Table 1.

Analysis of Oxygen consumption rates. To assess mitochondrial respiration, oxygen consumption was measured with the XF24 Analyzer (Seahorse Biosciences). Cells (50,000-experimentally optimized) were seeded onto 24 well XF24 cell culture plates. On the following day, cells were starved or not for 2 hours. Cells were then washed and

incubated with modified Kreb's Ringer Buffer (KRB) (KRB: 128 mM NaCl, 4.8 mM KCl, 1.2 mM KH_2PO_4, 1.2 mM $MgSO_4$, 25 mM $CaCl_2$, 0.1% BSA (fatty acid free); completed on the day of the experiment with 10 mM glucose and 1 mM sodium pyruvate and pH 7.4) for 15 minutes at 37°C prior to cartridge loading in the XF Analyser. Following resting respiration, cells were treated sequentially with: oligomycin (0.2 µg/µL), for nonphophorylating OCR; FCCP (1 µM), for maximal OCR; and antimycin A (2.5 µM) with rotenone (1 µM), for extramitochondrial OCR. Measurements were taken over 2 minute intervals, proceeded by a 2 minute mixing and a 2 minute incubation. Three measurements were taken for the resting OCR, three for nonphosphorylating OCR, two for maximal OCR and two for extramitochondrial OCR. All data was compiled by the XF software, normalized to protein levels per well and analysed with Microsoft Excel.

Stable Isotope Labelling with Amino Acids in Cell Culture (SILAC) coupled Immunoprecipitation and Mass Spectrometry. SILAC coupled immunoprecipitation and MS was performed as previously described (Trinkle-Mulcahy, 2012). HeLa cells were grown in DMEM minus arginine and lysine, supplemented with: 10% dialysed FBS, 100 U/ml penicillin/streptomycin and either "light" L-arginine and L-lysine or "heavy" L-arginine^{13}C and L-lysine 4,4,5,5-D4. Cells were grown and passaged for 10 days to allow for incorporation of isotopic amino acids. Cells were then transduced with control adenovirus (mito-YFP) in the light conditions and with OPA1-YFP adenovirus in the heavy condition. Cells were harvested 24 hours after transduction and lysed in RIPA buffer (50mM Tris-HCl pH7.5, 150mM NaCl, 1% NP-40, 0.5% deoxycholate and protease inhibitors). Proteins were immunoprecipitated with GFP-Trap_A (Chromotek) and combined during immunoprecipitation washes and eluted together. Proteins were then

reduced with 10 mM DTT, alkylated with 50mM iodoacetamide and separated on pre-cast SDS-PAGE gels (Invitrogen). Bands were cut, digested with trypsin and peptides were recovered. Peptides were analysed by liquid chromatography-mass spectrometry (LC-MS) using an LTQ-Oribitrap mass MS system coupled to a Dionex 3000 nano-LC system. Raw data files were analysed using the UniProt human database. Quantitation was performed using the MaxQuant software package (Cox & Mann, 2008). Positive OPA1 interactors were identified as being enriched in the heavy condition.

Additional Materials and Methods to investigate CLUH function:

CLUH cDNA from Open Biosystems (CloneID: 6193982) was PCRed out of the pCMV-SPORT6 vector (adding a leading GCCACC Kozak sequence) and assembled into p3XFLAG-CMV-14 (Addgene E7908) via Gibson assembly cloning (Gibson et al, 2009). Western blotting, immunoprecipitations, and immunofluorescence was performed as above with rabbit polyclonal CLUH(eIF3X) antibody (Novus biologicals). For transient CLUH knockdown, siRNAs s23461 and s23461 from Life Technologies were used. For RT-PCR analysis the following primers were used:

CLUH-For1 5’ TACATCATGGGCGACTACGC
CLUH-Rev1 5’ GGCCAGGTGCATGTATTCCT
CLUH-For2 5’ CCAGGATGAAGTTCGGGACC
CLUH-Rev2 5’ ATGCAGTCCTTCACCAAGCC

Subcellular fractionation experiments were performed as above, keeping the first supernatant after the 9,000 RPM spin for the crude cytoplasmic fraction. Saponin solubilization of cytoplasmic proteins prior to fixation and immunofluorescence was performed according to (Hudder et al, 2003). Cells were washed with PBS and permeabilized at room temperature in saponin permeabilization buffer (130mM sucrose,

50mM potassium acetate, 20mM HEPES, pH 7.4) for 1 minute. Cells were then washed with PBS, fixed in 4% PFA and immunofluorescence was performed as above.

GSH and GSSG determinations by High Performance Liquid Chromatography

GSH, GSSG and their ratio was calculated with an Agilent HPLC system (Mailloux et al, 2014). Cells were grown in 100mm tissue culture plates with the indicated treatments, harvested with trypsin and washed twice with ice cold PBS. Cells were counted and lysed on ice for 20 minutes in: 125mM sucrose, 1.5mM EDTA, 5mM Tris, 0.1% TFA and 0.5% MPA in mobile phase (10% HPLC grade methanol, 0.09% TFA – 0.2 micron filtered). Homogenates were cleared by centrifugation for 20 min at 14,000 g at 4°C. Each sample was run in duplicate on a Pursuit5 C18 column (150 × 4.6 mm, 5 μm; Agilent Technologies, Santa Clara, CA) with a 1 mL/min flow rate and detected at 215nm. Standards were prepared at the indicated concentrations in the same buffer and used to interpolate absolute quantities of GSH and GSSG in the samples.

For DMFN KD cells, MEFs were isolated from E13.5 $MFN1^{flox/flox}MFN2^{flox/flox}$ mice as previously described (Zindy et al, 1997). Resulting primary MEFs were transformed via SV40 transfection and grown for multiple passages. Immortalized $DMFN^{flox/flox}$ ($MFN1^{flox/flox}MFN2^{flox/flow}$) MEFs were then infected with either a control (LVX-EF1-mCherry-N1) or Cre (LVX-EF1-cre-mCherry-N1) (Clonetech) lentiviruses at 10 MOI and were selected with puromycin.

Chapter 3. Results

3.1 OPA1-dependent cristae modulation is essential for cellular adaptation to metabolic demand

3.1.1 OPA1 responds rapidly and reversibly to metabolic demand

Although mitochondrial structural changes in response to energetic states have been documented for decades, their regulation and functional significance have remained largely unknown. To ask if cristae structure responds to changes in nutrient conditions, mouse embryonic fibroblasts (MEFs) were starved with EBSS for two hours and cristae were measured. We observed a significant thinning of cristae width and mitochondrial width in response to starvation (Figure 7A). While untreated cells had an average cristae width of 17.6 nm, starved cells had an average width of only 11.9 nm. Since the deoligomerization of OPA1 regulates cristae widening during cell death signaling (Frezza et al, 2006), we assessed the oligomerization status of OPA1 in response to starvation. Starved MEFs exhibited significantly more oligomerized OPA1 than fed controls (Figure 7B & 1D). At longer time points we also observed that mitochondria elongate from an average length of 3.3 to 4.2 μm $p = 0.022$ (distribution in Figure 7C). This previously documented elongation has been substantiated by a decrease in mitochondrial fission through DRP-1 inhibition leading to unopposed mitochondrial fusion (Gomes et al, 2011; Rambold et al, 2011). Unlike elongation, the oligomerization of OPA1 in response to starvation was rapid (within one hour), and preceded activation of the autophagic pathway as indicated by p62 degradation (Figure 7D).

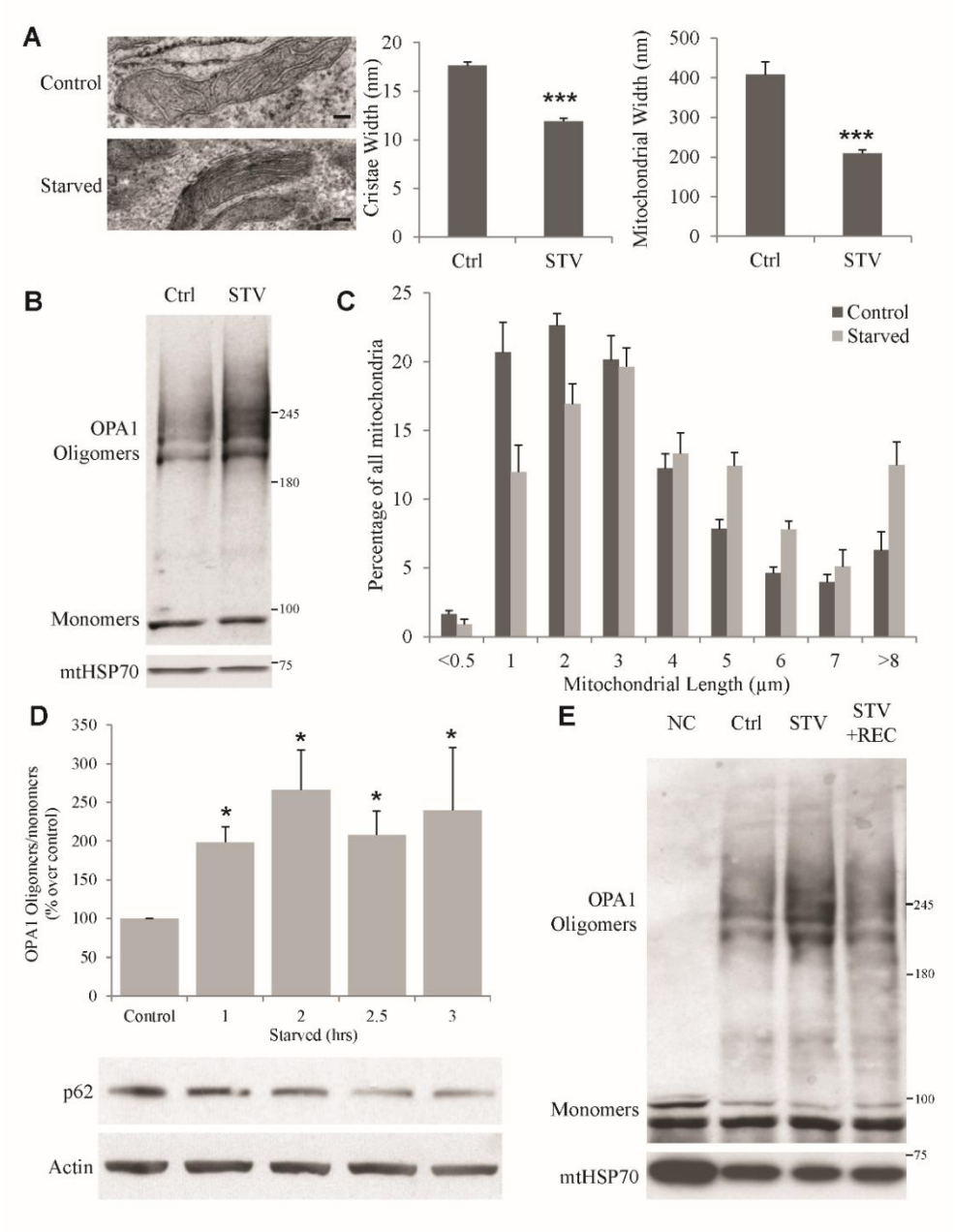

Figure 7. Cristae condense, mitochondria elongate and OPA1 oligomerizes rapidly and reversibly during cell starvation.

A MEFs were starved (STV) or not (Ctrl) for 2 hours, fixed with 2% PFA and 1.6% glutaraldehyde and analysed by EM. Cristae and mitochondrial width were quantified from mitochondria and cristae within 10 cells from 2 independent cultures (n=20). Scale bars: 100 nm. **B** Cells were starved or not for 2 hours, crosslinked with BMH (1mM) and OPA1 oligomerization was analysed by gradient gel western blot. **C** MEFs were starved for 4 hours, fixed and mitochondrial length was measured by immunofluorescence using Tom20 antibodies (averages ± SEM of 3 independent experiments). **D** Time course experiment of EBSS starvation on OPA1 oligomerization status as performed in B (averages ± SEM of 4 independent experiments). Whole cell lysates of a parallel experiment were analysed by western blot. **E** After 2 hours of EBSS starvation, MEFs were recovered (REC) in regular growth media for 30 minutes or not and OPA1 oligomers were then analysed as above. A non-crosslinked control (NC) is also included. Student t-tests were performed relative to control, *p<0.05, ***p<0.005.

Furthermore, changes in OPA1 oligomerization were rapidly reversible, since incubation of starved MEFs for only 30 minutes in recovery media (regular growth media) reversed the increase in oligomerized OPA1 (Figure 7E). Together, these data suggest that changes in OPA1 oligomers are linked to changes in cristae structure not only during cell death as previously demonstrated (Frezza et al, 2006), but also in healthy cells following changes in energy substrate availability.To assess how OPA1 responds to changes in fuel substrate availability, we turned to an *in vitro* system. Isolated mitochondria were incubated in the absence or the presence of ETC substrates and crosslinked. When mitochondria were fed with complex I and II substrates (malate plus glutamate or succinate respectively), OPA1 oligomerization was dramatically reduced compared to no-substrate, starved controls [Figure 8A (EDC cross-linking) and Figure 9A (BMH cross-linking)]. As we would predict, the same concentration of glucose, the principal glycolysis substrate, had no effect on OPA1 oligomerization (Figure 8A). As in starved cells, OPA1 oligomerization was rapidly reversible upon the addition or removal of complex I substrates (Figure 8B). Next, we asked whether changes in OPA1 oligomerization correlated with altered mitochondrial structure. This was assessed by mitochondrial inter-cristae cytochrome c retention, as a readout of cristae structure, since an increase in releasable cytochrome c following outer membrane solubilisation correlates with wider cristae (Scorrano et al, 2002; Wasilewski et al, 2012). Following the addition of a low concentration of digitonin to specifically solubilize the outer membrane [1 µg/µg mitochondria, at 0.1 % w/v - experimentally determined (Figure 9B)], significantly more cytochrome c was mobilized when

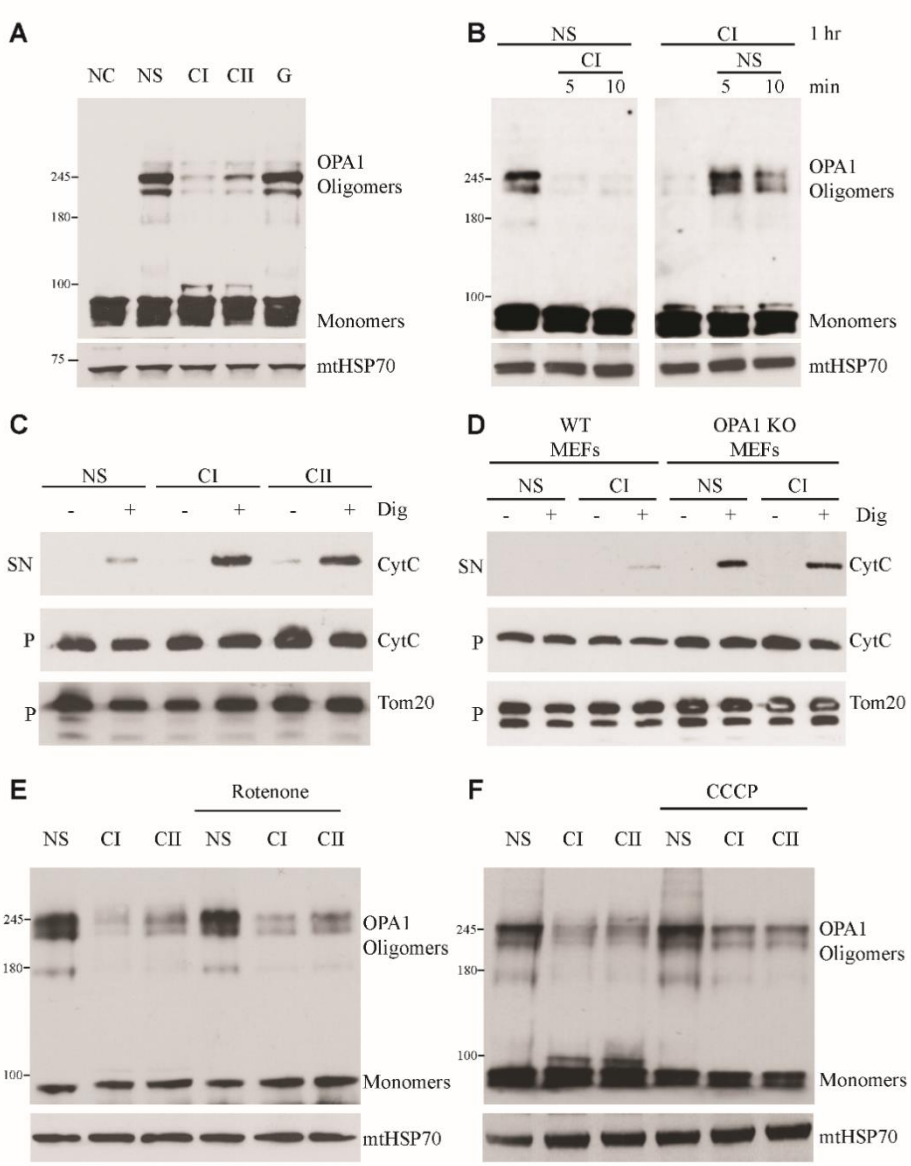

Figure 8. OPA1 responds to energy substrate availability and responds by oligomerizing and maintaining cytochrome c in isolated mitochondria

A OPA1 oligomerization was analysed in isolated mouse liver mitochondria incubated with or without the indicated ETC substrates [NC: non crosslinked control; NS: no substrate control; CI: Complex I, malate and glutamate; CII: Complex II, succinate; G: Glucose control all at 5 mM each] for 1 hour at 37ºC and subsequently cross-linked with EDC for 30 minutes at room temperature. OPA1 oligomers were then analysed by gradient gel western blot. **B** Mitochondria were incubated with or without complex I substrates, spun down and resuspended in the indicated buffer for 5 and 10 minutes and analysed as above. **C** Mitochondrial ultrastructure was analysed as the distribution of intercristal cytochrome c from liver mitochondria, and solubilized with low digitonin concentrations (1µg/µg mitochondria, 0.1%). Mobilized cytochrome c was separated by centrifugation and visualized by western blot analysis where released CytC was redistributed from the pellet (P) to the supernatant (SN) fraction. **D** Cytochrome c mobilization was analysed on mitochondria isolated from WT and OPA1 KO MEFs treated as indicated. **E** Liver mitochondria were incubated with or without indicated substrates as above with or without rotenone (2 µM), an ETC complex I poison. **F** Liver mitochondria were incubated with or without indicated substrates as above with or without CCCP (10 µM), a mitochondrial uncoupler.

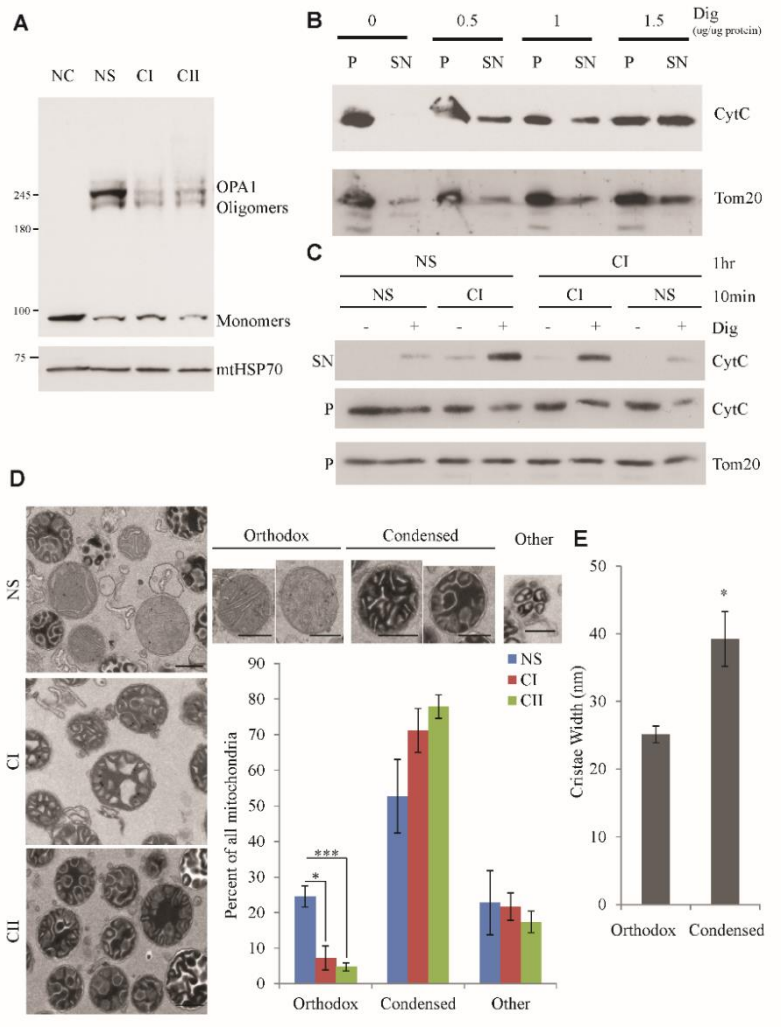

Figure 9. Supplement to Figure 8.

A OPA1 oligomerization was analysed in isolated mouse liver mitochondria incubated with or without the indicated ETC substrates as Figure 2A for 1 hour at 37ºC and subsequently cross-linked with BMH [10 mM] for 30 minutes at room temperature and quenched with BME. OPA1 oligomers were then analysed by gradient gel western blot. **B** The effect of varying digitonin concentrations on the mobilization of cytochrome C from intracristae stores. Mitochondria were incubated in a no substrate buffer for 1 hour, and then varying concentrations of digitonin (0.5 µg/µg mitochondria, 0.05 %; 1 µg/µg mitochondria, 0.1%; 1.5 µg/µg mitochondria, 0.15 %) were incubated with the mitochondria for 30 minutes at 4ºC on a rotator. Mobilized cytochrome c was then separated from retained CytC by centrifugation and analysed by western blot where released CytC was mobilized from the pellet (P) to the supernatant (SN) fraction. The highest concentration of digitonin that showed no change in Tom20 release (1ug/ug protein) was used in subsequent experiments. **C** The reversibility of cytochrome c mobilization was analysed as previously described where mitochondria were incubated with or without complex I substrates, spun down and resuspended in the indicated buffer for 10 minutes and analysed for cytochrome c retention. **D** Isolated liver mitochondria were incubated for 1 hour in the indicated buffers and processed for electron microscopy. Left panel, representative EM images from samples incubated with the indicated buffer. Right panel, quantification of orthodox, condensed and other mitochondria from 50 images per condition (over 500 mitochondria per condition) (averages ± SEM of 3 independent experiments). **E** Cristae width was quantified from orthodox and condensed mitochondria from 10 fields of no substrate incubated mitochondria (minimum 25 mitochondria per class per experiment) (averages ± SEM of 3 independent experiments). Student t-tests were performed as indicated *$p<0.05$, ***$p<0.005$.

mitochondria were incubated in the presence of complex I and II substrates, compared to the absence of substrates (Figure 8C). Furthermore, this increase in cytochrome c mobilization, indicative of cristae widening, was reversible (Figure 9C), correlating with the decrease in OPA1 oligomerization and a decrease in orthodox mitochondria, which demonstrates tighter cristae morphology (Figure 9D&E). The regulation of cytochrome c retention was OPA1-dependent, since mitochondria from OPA1 KO cells had very high levels of mobilized cytochrome c independently of the presence of complex I substrates (Figure 8D). We next asked whether the substrate-dependent changes in OPA1 oligomerization were secondary to changes in electron transport chain (ETC) activity. To this end, we added rotenone, a complex I poison, and CCCP, a mitochondrial uncoupler, to the mitochondrial preparations. Neither rotenone nor CCCP altered OPA1 oligomerization (Figure 8E and F), suggesting that OPA1 responds to energy substrate availability upstream of changes in mitochondrial respiration and ETC function.

These studies reveal a strict correlation between energy substrate level, cristae structure and OPA1 oligomerization in which: mitochondria enriched with substrates show low levels of OPA1 oligomers and mobilized cytochrome c from cristae stores, and starved mitochondria show high levels of OPA1 oligomers and tight cristae. We next sought out the physiological relevance of this cristae regulation as well as the mechanism by which OPA1 senses energy substrate availability.

3.1.2 OPA1 is required for regulation of cristae structure and cell survival during starvation

To address the physiological importance of OPA1-dependent cristae remodelling in response to changes in energy substrate conditions, we first asked whether OPA1 KO cells, devoid of cristae, could survive cellular starvation. While WT MEFs were minimally affected by 6 hours of EBSS starvation; OPA1 KO MEFs showed a dramatic increase in cell death, as recently published (Figure 10A, Figure 11A and Figure 11B)(Gomes et al, 2011). As survival of starved cells has been suggested to require mitochondrial elongation through unopposed fusion (Gomes et al, 2011), we isolated the roles of fusion and cristae structure using a mutant form of OPA1 that fails to mediate fusion. OPA1(Q297V) mimics the GTP-bound state of OPA1, allowing oligomerization, but defective in GTPase activity, which is required to mediate fusion (Misaka et al, 2002; Yamaguchi et al, 2008). To assess their ability to rescue mitochondrial fusion and cristae structure, isoform 1 of WT OPA1 and OPA1(Q297V) were reintroduced in OPA1 KO MEFs by transient transfections, resulting in the expression of mostly the long form with some cleaved short form (Figure 10B). While WT OPA1 rescued fusion, the OPA1(Q297V) mutant was completely fusion-incompetent, despite that it was expressed at slightly higher levels than WT OPA1 (Figure 10B and C). To assess whether OPA1(Q297V) can rescue the cristae structural defects seen in OPA1 KO cells, we performed transmission electron microscopy (EM). Both WT and OPA1(Q297V) rescued the severe cristae defects found in OPA1 KO MEFs (Figure 10D), and rescued survival of OPA1 KO MEFs during starvation (Figure 10E & Figure 11C). These results suggest that OPA1 protects against starvation-induced cell death independently of its fusion activity.

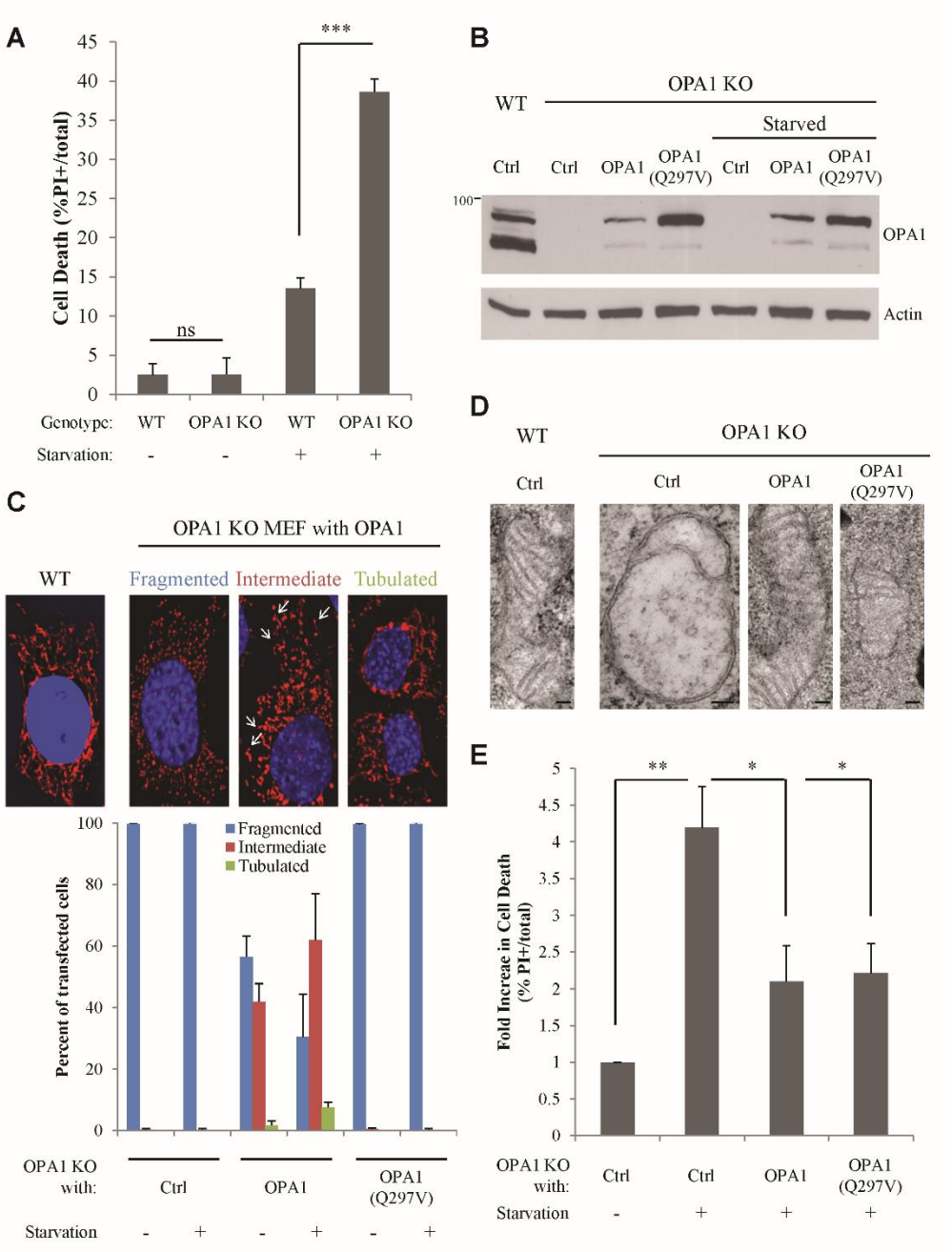

Figure 10. OPA1 is required for resistance to starvation induced cell death, independently of its fusion activity.

A Cell death of WT and OPA1 KO cells starved or not for 6 hours was analysed with propidium iodide (PI) and Hoechst (averages ± SEM of 4 independent experiments). **B** Representative western blot of OPA1 expression in the transient transfection experiments performed in C-E. **C** OPA1 KO MEFs were transiently transfected for 48 hours with the indicated plasmids and mitochondrial length was binned according to the top panels by immunofluorescence where cells that had any long mitochondria were binned as intermediate (averages ± SEM of 3 independent experiments). **D** Representative EM of mitochondria from cells transfected as indicated. Scale bars: 100 nm. **E** OPA1 KO MEFs were transfected as indicated for 48 hours and starved or not for 6 hours and cell death was analysed as in A (averages ± SEM of 4 independent experiments). Student t-tests were performed as indicated, *p<0.05, **p<0.01 and ***p<0.005.

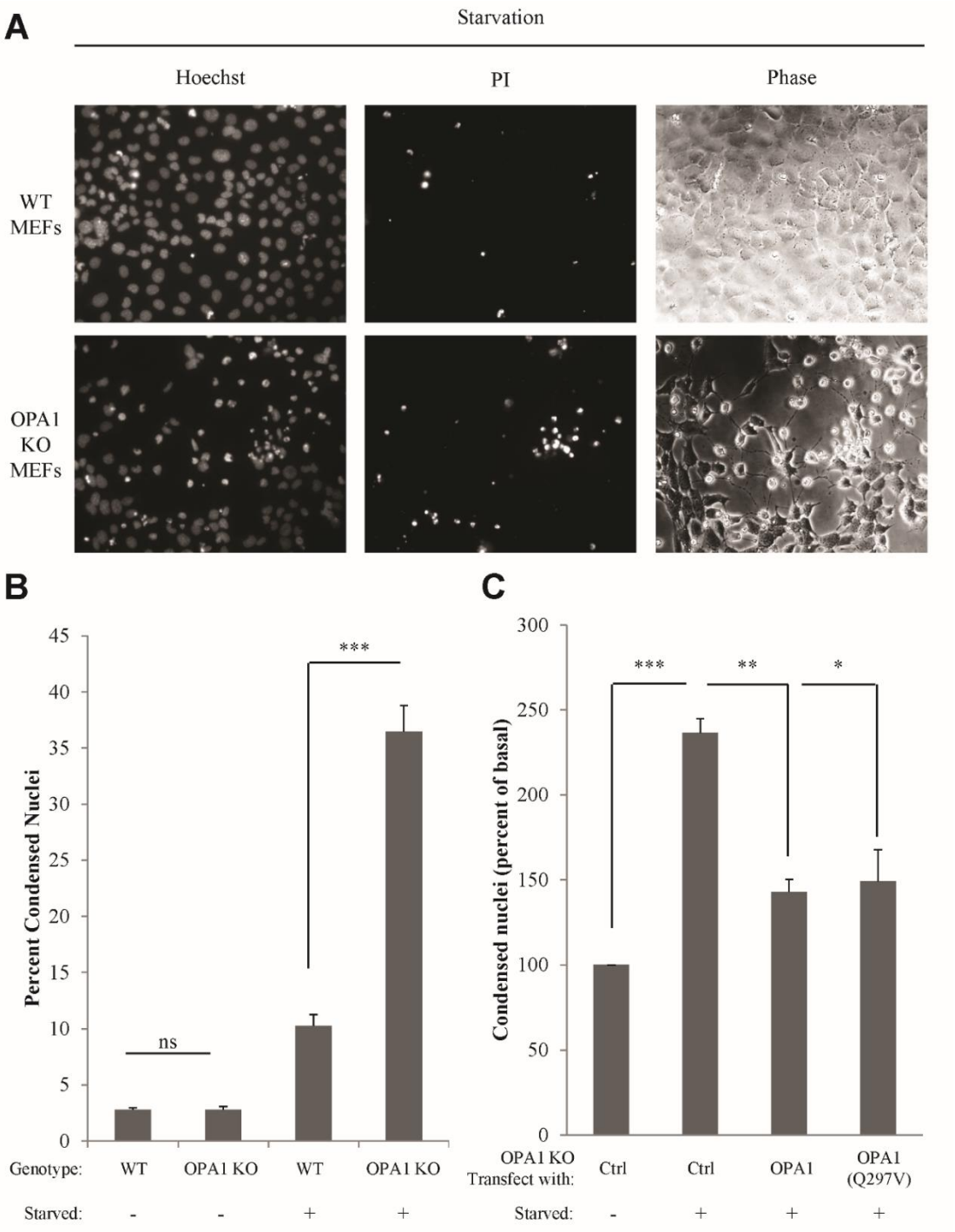

Figure 11. OPA1 dependent starvation-induced cell death.

A Representative images of cells quantified in Figure 3A and S1B, live-cell stained with Hoechst and PI. **B** Cells were treated as in Figure 3A, but quantified as the percent condensed nuclei (averages ± SEM of 3 independent experiments). **C** Cells were treated as in Figure 3E, but quantified as the percent condensed nuclei (averages ± SEM of 3 independent experiments). Student t-tests were performed as indicated, *$p<0.05$, **$p<0.01$ and ***$p<0.005$.

3.1.3 OPA1 maintains mitochondrial function independently of its fusion activity

The rescue of cristae structure and cell survival by OPA1 and a fusion incompetent mutant suggests that cristae modulation is a key determinant of cellular survival under changing energetic demands. To assess whether OPA1 mediated cristae alterations alone can affect cellular metabolism, we generated MEFs stably expressing OPA1 or OPA1(Q297V), resulting in high expression of both the long and short isoforms of OPA1 (Figure 12A). As in the transient system, OPA1(Q297V) rescued cristae structure in OPA1 deficient MEFs but not mitochondrial fusion (Figure 13A&B). In addition, both WT and OPA1(Q297V) oligomerized and responded to substrate level changes in isolated mitochondria from stable cell lines (Figure 12B). To address how OPA1-mediated control of cristae modulates mitochondrial energetics, we assessed cellular oxygen consumption characteristics after OPA1 reintroduction using a Seahorse XF-24 analyzer (Figure 12C-E). Under fuel rich conditions, a modest difference in ATP-linked respiration (the difference between the initial resting respiration and the respiration in the presence of oligomycin, a complex V inhibitor) was observed between WT and OPA1 KO MEFs (Figure 12, Figure 14A&B). However, starvation increased the difference in ATP-linked oxygen consumption between WT and OPA1 KO cells (Figure 12D, Figure 14A&B), consistent with a requirement for OPA1 to maintain mitochondrial ATP levels under starvation (Gomes et al, 2011). We next addressed whether OPA1(Q297V) rescued oxygen consumption. Under resting (fed) conditions, only expression of the WT form of OPA1 significantly increased ATP-linked respiration of OPA1 KO MEFs (Figure 12C and quantified in E). However, after starvation both the WT and OPA1(Q297V) significantly increased ATP-linked oxygen consumption (Figure 12D&E). Only WT OPA1 reintroduction completely rescued maximal

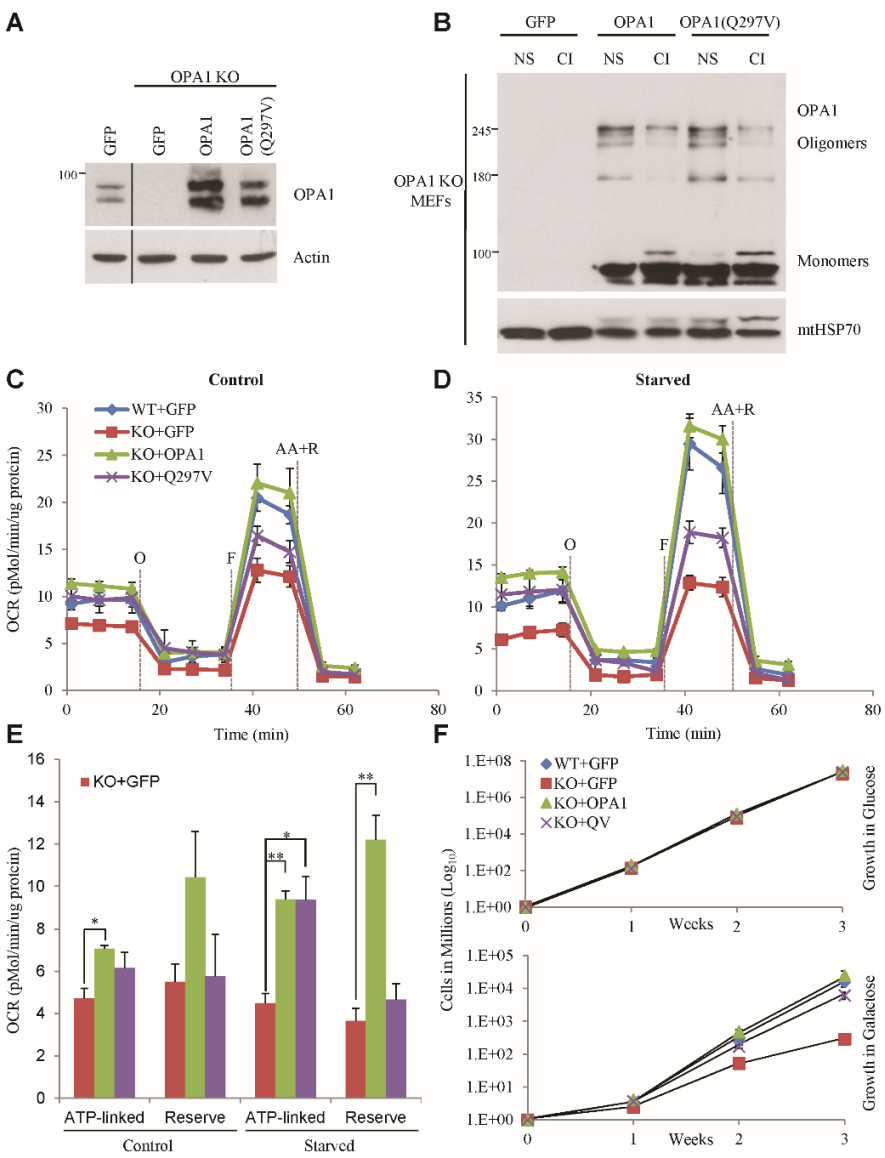

Figure 12. OPA1 regulates mitochondrial metabolism independently of mitochondrial fusion.

A WT and OPA1 knockout MEFs were infected with viruses encoding, GFP, OPA1 or OPA1(Q297V) with dual promoters expressing GFP to allow for puromycin selection and FACS sorting cells for GFP expression. The resulting cultures were lysed, analysed by western blot analysis and used for all subsequent experiments. **B** OPA1 oligomers were analysed from isolated mitochondria incubated with no substrate or complex I substrates. **C** To assess the impact of the fusion incompetent OPA1 mutant on mitochondrial bioenergetics we studied cells in a Seahorse XF-24 analyzer. Cells were plated on Seahorse TC plates 24 hours prior to analysis, washed and incubated for 15 minutes in modified KRB and analysed. At the indicated times, oligomycin (O), FCCP (F), and antimycin A (AA) with rotenone (R) were injected (averages ± SEM of 3 independent experiments). **D** The same cells were pre-starved for 2 hours before identical analysis (averages ± SEM of 3 independent experiments). **E** Quantification of ATP-linked OCR (resting OCR minus oligomycin insensitive OCR) and reserve OCR (Maximal minus resting) in C and D. **F** Long-term cell cultures were grown in glucose (top panel) or galactose media (bottom panel). Cells were passaged as required, media was changes every 3 days if required, and cell number was determined once per week (averages ± SEM of 4 independent experiments). Student t-tests were performed relative to control, *p<0.05 **P<0.01

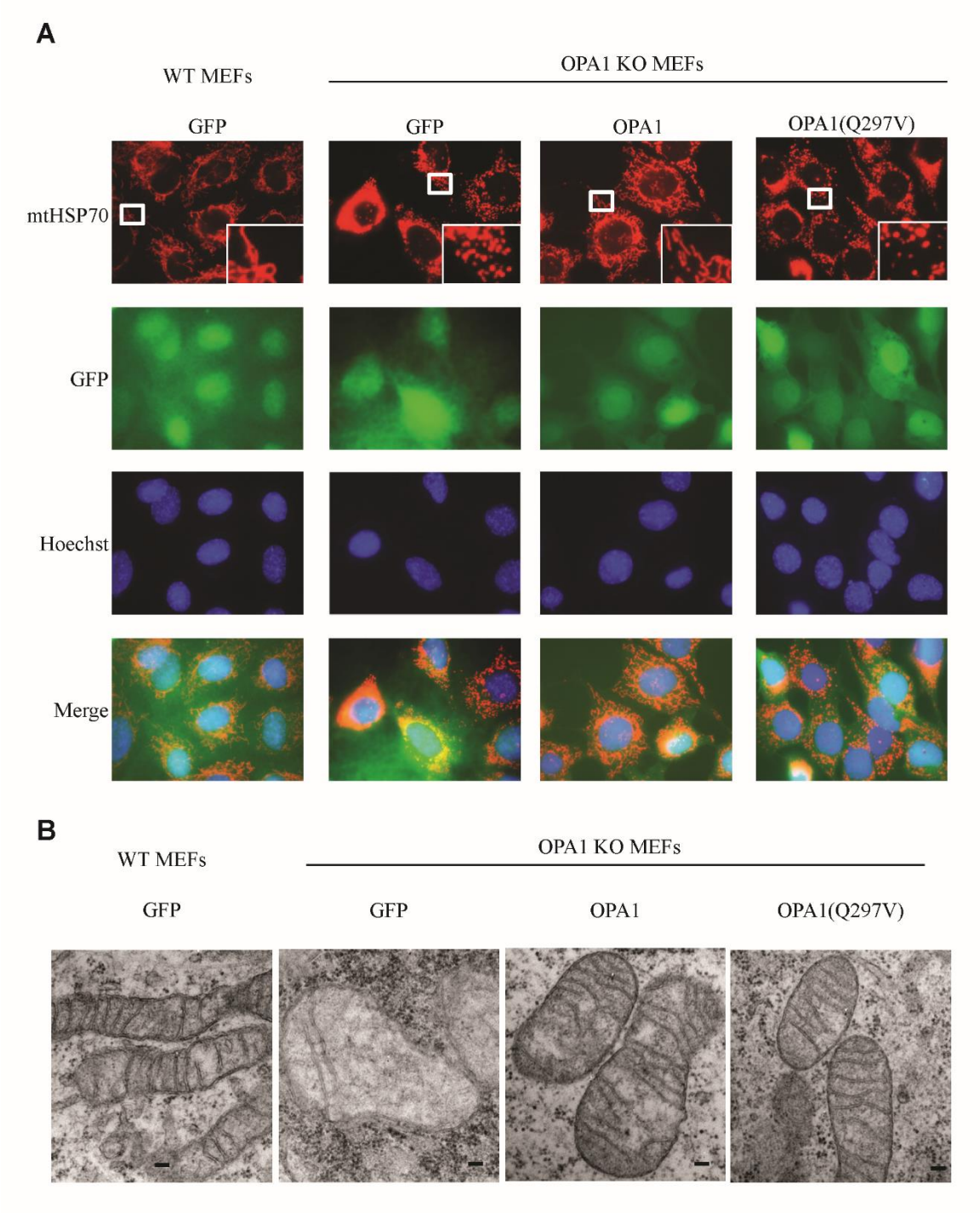

Figure 13. OPA1(Q297V) after long-term reintroduction is fusion incompetent, but rescues cristae structure.

A Longterm reintroduced OPA1 KO cells were seeded on glass coverslips 24 hours prior to fixation and analysed for mitochondrial length by immunofluoresecnce for mtHSP70. **B** Parallel cultures were seeded onto square coverslips, fixed, and mitochondrial cristae structure was assessed by EM.

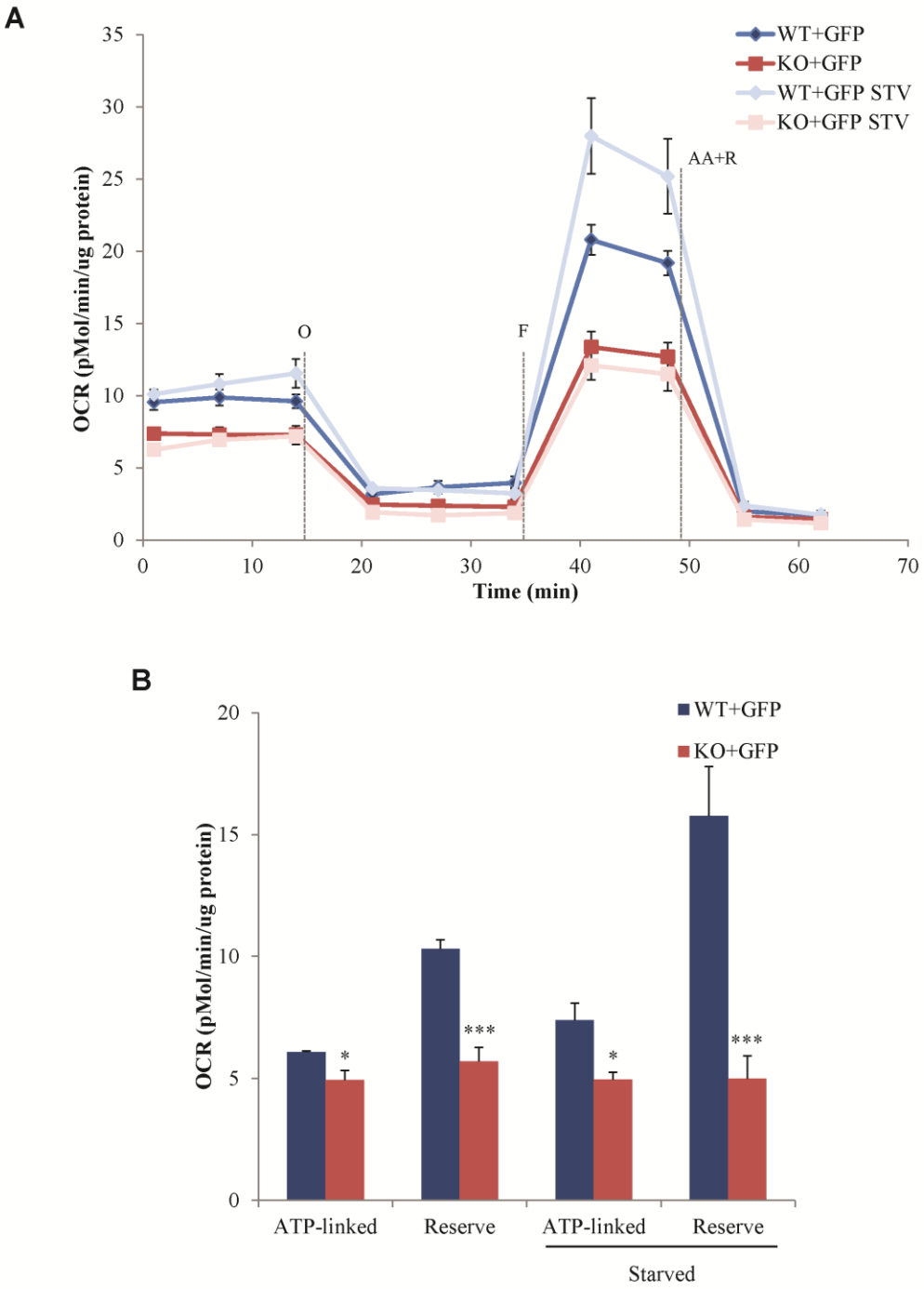

Figure 14. OPA1 is required for ATP-linked and reserve OCR.

A WT and OPA1 KO MEFs transiently or stably expressing GFP, starved or not for 2 hours, were analysed with the Seahorse XF-24 analyzer. At the indicated times, oligomycin (O), FCCP (F), and antimycin A (AA) with rotenone (R) were injected (averages ± SEM of 4 independent experiments). **B** Quantification of ATP-linked (resting OCR minus oligomycin insensitive OCR) and reserve OCR (Maximal minus resting) in A (averages ± SEM of 4 independent experiments). Student t-tests were performed as indicated, *p<0.05 and ***p<0.005.

respiration (oligomycin and FCCP, a mitochondrial uncoupler) and thus the reserve capacity (the difference between the resting and maximal respiration) (Figure 12E). These functional studies demonstrate that the critical role of OPA1 in regulating mitochondrial metabolism is fusion independent; however, mitochondrial fusion is required for full maximal oxygen consumption, possibly through maintenance of mtDNA (see below), which may be important following other various stressors.

To further investigate the role of cristae and mitochondrial fusion in mitochondrial function, cells were grown in a galactose medium in which they must rely on OXPHOS for ATP production (Aguer et al, 2011; Cogliati et al, 2013). While WT and OPA1 KO MEFs grew at similar rates in glucose media, OPA1 KO cells were growth retarded in galactose media compared to WT MEFs (Figure 12F). In fact, in the third week of growth in galatose media, it took more than twice as long for OPA1 KO cells to double their numbers (Figure 15). Reintroducing WT or OPA1(Q297V) rescued growth retardation in OPA1 KO MEFs (Figure 12F, Figure 15), providing further evidence that OPA1 can maintain mitochondrial function to support cell growth, independently of mitochondrial fusion.

As Mgm1 and OPA1 are required for the assembly of the ATP synthase (Amutha et al, 2004; Gomes et al, 2011), we asked if this assembly is modified by energy substrate availability and in a fusion-independent fashion. To this end, Blue-Native PAGE (BN-PAGE) was performed on isolated mitochondria treated with substrates affecting OPA1 oligomerization and cytochrome c retention. When mitochondria are fed with complex I substrates, which decrease OPA1 oligomers (Figure 8), both ATP synthase oligomers and monomers are decreased (Figure 16A), without a decrease in ATP5A subunits themselves (Figure 16B).

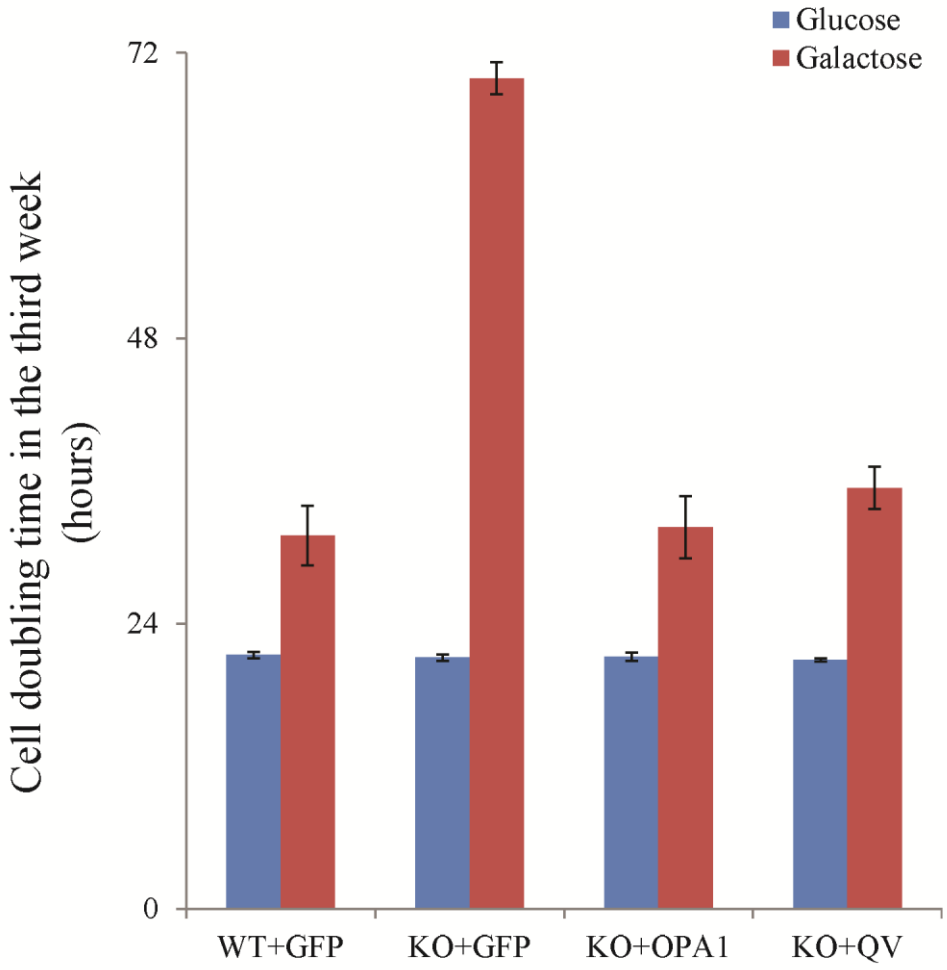

Figure 15. WT and OPA1(Q297V) rescue cell growth in galactose media.

Cell doubling times were calculated within the second week of growth in either glucose or galactose medium from Figure 12F using http://www.doubling-time.com/compute.php.

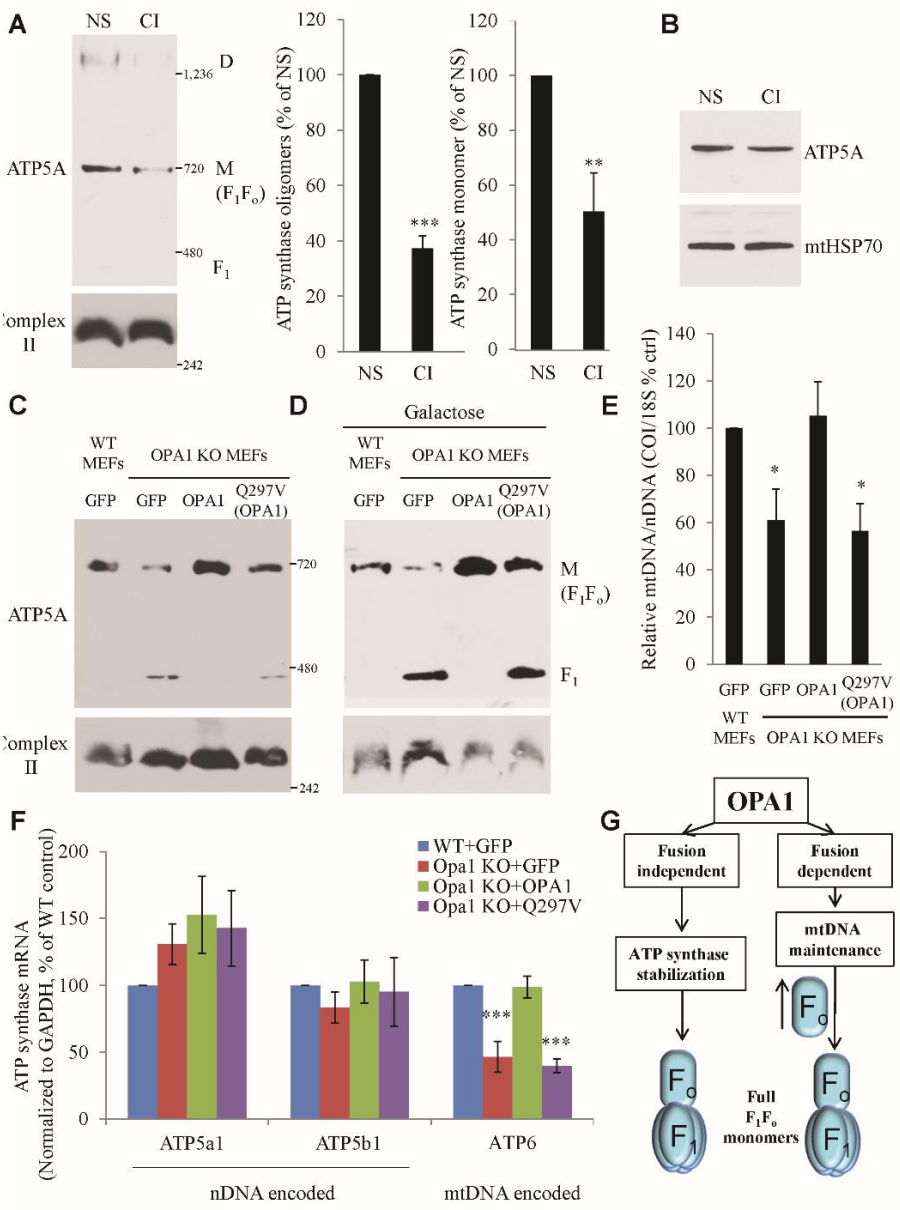

Figure 16. The dual role of OPA1 in regulating the ATP synthase.

A Isolated mitochondria incubated with complex I substrates were analysed by BN-PAGE and blotted for ATP5A of the ATP synthase. The oligomers [mostly dimers (D)] and monomer (M) of the ATP-synthase were quantified as relative to complex II monomer (averages ± SEM of 5 independent experiments). **B** Isolated liver mitochondria incubated with or without complex I in parallel with Figure 5A, lysed and analysed for ATP5A by straight western blot. **C** Long-term cell cultures were extracted for BN-PAGE directly from cells and blotted for ATP5A and complex II. **D** Cells grown for 1-2 weeks in galactose were analysed by BN-PAGE identically to C. **E** DNA was extracted from long-term cultures and mtDNA was analysed by qPCR relative to nDNA (averages ± SEM of 3 independent experiments). **F** RNA was extracted from long-term cultures and nuclear and mtDNA encoded ATP synthase transcripts were analysed by rtPCR (averages ± SEM of 4 independent experiments). **G** Schematic demonstrating the dual roles of OPA1 on the F_1F_o ATP synthase where OPA1 regulates the stabilization of the ATP synthase independently of its fusion activity and regulates mtDNA stability which is required for ATP6 (F_o subunit) expression and thus full F_1F_o ATP synthase assembly. Student t-tests were performed relative to control, *p<0.05, **p<0.01 and ***p<0.005.

BN-PAGE analysis in whole cells demonstrated that in WT MEFS, all ATP synthase subunits were assembled to form the monomer (very little dimer was detected); however, OPA1 KO MEFs had substantially less assembled ATP synthase monomers and an increase in free F_1 (Figure 16C). Reconstitution with either WT OPA1 or OPA1(Q297V) increased ATP synthase assembly, most notably when cells were forced to rely on OXPHOS for ATP production (galactose media, Figure 16C&D). While WT OPA1 completely rescued the assembly of the F_1 portion into F_1F_o monomers, OPA1(Q297V) cells still exhibited a significant level of free F_1, even in galactose media (Figure 16C&D). The persistence of free F_1 correlated with the inability of OPA1(Q297V) to rescue the loss of mtDNA caused by OPA1 deletion (Figure 16E), consistent with the requirement of mitochondrial fusion for mtDNA maintenance (Chen et al, 2010). While all of the subunits of the F_1 are nuclear encoded, the F_o portion contains two subunits, ATP6 and ATP8, encoded by mtDNA. Since OPA1 KO and OPA1(Q297V) cells, have decreased mtDNA levels, unassembled F_1 is likely due to a lack of mitochondrial encoded F_o subunits. Interestingly, human mutations affecting expression of both mtDNA F_o subunits demonstrate increased free F_1 relative to monomer by BN-PAGE (Jonckheere et al, 2008; Pitceathly et al, 2012). Indeed, decreased levels of the mtDNA encoded F_o subunit ATP6 in OPA1 KO and OPA1(Q297V) cells were confirmed by rtPCR (Figure 16F). Since the OPA1(Q297V) mutant was unable to rescue mtDNA or mtDNA-encoded transcripts, here we propose a novel fusion-independent role of OPA1 on ATP synthase stability. Thus, assembly of a functional F_1F_o monomer depends dually on OPA1 for its stability, and for fusion-dependent, mtDNA encoded F_o subunit expression (Figure 16G).

3.1.4 Solute carriers interact with OPA1 and regulates its sensing of mitochondrial energy substrates

Our results revealed that OPA1 responds to changes in fuel substrate conditions by modifying its oligomerization, and that this is required for the adaptation and survival of cells during starvation. To determine the mechanism by which substrate levels modify OPA1 function we performed a proteomics screen in search of OPA1 interacting factors. Stable isotope labelling of amino acids in cell culture (SILAC) combined with immunoprecipitation and mass spectroscopy was used as a quantitative and sensitive technique to identify novel OPA1 protein interactors that may be required for substrate sensing (Trinkle-Mulcahy, 2012)(Figure 17A). A log SILAC ratio of 1 was set as the cut-off for validation since it gave a confidence interval of 95% (Figure 17B). Of the 35 hits above a log SILAC ratio of 1: 18 (51%) were mitochondrial, 8 were ribosomal and 9 were either unknown or neither mitochondrial nor ribosomal (Figure 17C and Table 2). Highly relevant to fuel substrate sensing, a number of mitochondrial carrier proteins (SLC25A) were identified as OPA1-interacting proteins. Mitochondrial solute carriers are mitochondrial inner-membrane proteins that catalyze the transfer of diverse substrates across the mitochondrial inner membrane [for a review see (Palmieri, 2013)]. Importantly, some of these solute carriers are involved in shuttling the mitochondrial substrates utilized in Figure 2, namely malate and succinate by SLC25A10 [the dicarboxylate carrier (DIC)], malate by SLC25A11 [the oxoglutarate carrier (OGC)] and glutamate by SLC25A12 and SLC25A13 [the aspartate/glutamate carriers 1 (AGC1) and 2 (AGC2)]. Given the requirement for OPA1-mediated cristae regulation in response to starvation, we asked if

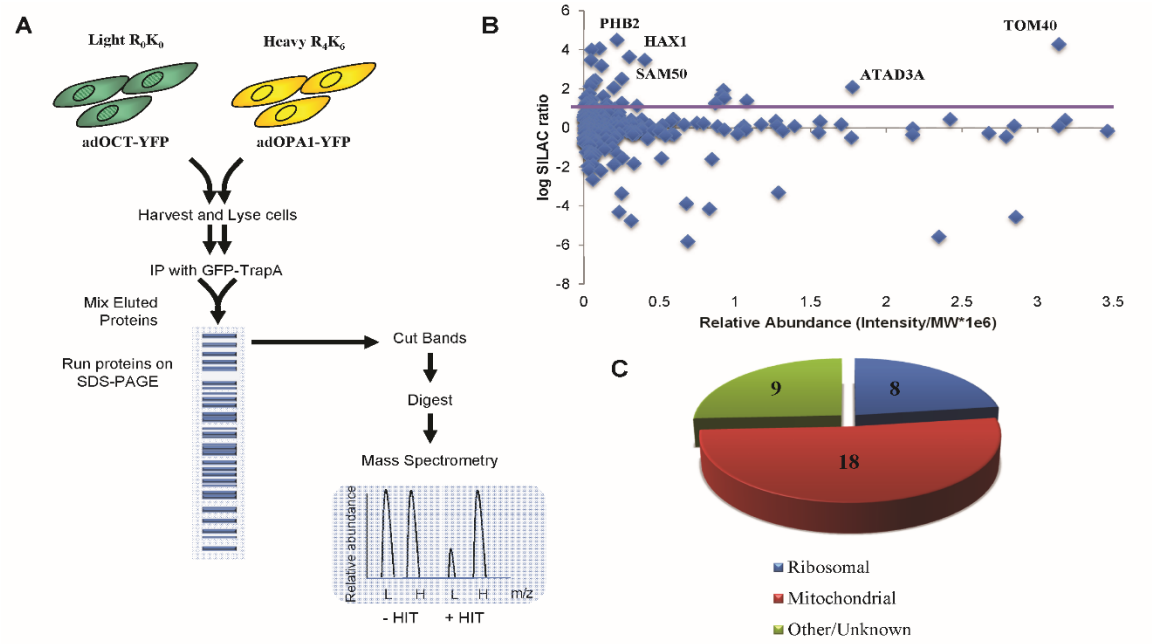

Figure 17. OPA1 interacting partner identification by Stable Isotope Labeling by Amino Acids in Cell Culture (SILAC).

A Schema of SILAC experiment to identify OPA1 binding partners. **B** Representation of the mass spectroscopy data as the relative abundance of the peptide fragments to the log SILAC ratio of the heavy to light fraction. A log SILAC ratio of 1 was set as the threshold for putative interactors to consider validating and previously reported or functionally suggested OPA1 interacting partners are identified on the graph. **C** Pie graph representing the localization of the 35 potential OPA1 interactors identified from this screen.

Table 2. Putative OPA1 interactors revealed by quantitative IP coupled MS

Gene Name	Protein Name	Peptides	Log(Normalized Ratio H/L)	Intensity/ MW10^6
HSPB1	Heat shock protein beta-1	2	4.52	0.22
TOMM40	Translocase of outer mitochondrial membrane 40 homolog	15	4.30	3.14
PHB2	Prohibitin-2	4	4.09	0.10
CHCHD3	Coiled-coil-helix-coiled-coil-helix domain-containing protein 3	3	4.02	0.05
HAX1	HCLS1-associated protein X-1	8	3.65	0.30
NAP1L1	Nucleosome assembly protein 1-like 1	4	3.49	0.40
RPS3	40S ribosomal protein S3	3	3.19	0.12
OPA1	Optic atrophy 1 (autosomal dominant)	108	2.85	83.41
BAG2	BAG family molecular chaperone regulator 2	7	2.52	0.25
TMEM33	Transmembrane protein 33	2	2.47	0.08
ATP5C1	ATP synthase subunit gamma	4	2.41	0.06
ERAB	3-hydroxyacyl-CoA dehydrogenase type-2	2	2.31	0.05
GPSN2	highly similar to Synaptic glycoprotein SC2	2	2.14	0.04
ATAD3A	ATPase family AAA domain-containing protein 3A	22	2.10	1.78
CLPB	Caseinolytic peptidase B protein homolog	11	2.06	0.20
SLC25A5	ADP/ATP translocase 2	10	1.96	0.92
SURF4	Surfeit locus protein 4	2	1.77	0.04
RPS11	40S ribosomal protein S11	8	1.71	0.91
SLC25A6	ADP/ATP translocase 3	10	1.64	0.13
CAV1	Caveolin	1	1.56	0.01
RPL23	60S ribosomal protein L23	6	1.54	0.93
SAMM50	SAMM50 sorting and assembly machinery component	4	1.43	0.05
RPS15A	40S ribosomal protein S15a	7	1.40	1.08
TIMM50	Translocase of inner mitochondrial membrane 50 homolog	2	1.34	0.04
ATP5B	ATP synthase subunit beta	8	1.30	0.25
MYO1B	Myosin-Ib	4	1.29	0.02
RPS27	Ribosomal protein S27	3	1.27	0.87
RPL10	Ribosomal protein L10	4	1.25	0.15
KIAA0664	Protein KIAA0664	4	1.18	0.01
ATP5A1	ATP synthase subunit alpha	15	1.16	0.35
ISG15	Interferon-induced 17 kDa protein	2	1.14	0.05
SLC25A3	Phosphate carrier protein	6	1.09	0.06
ARF4	ADP-ribosylation factor 4	3	1.08	0.07
RPS13	40S ribosomal protein S13	2	1.08	0.07
RPS14	40S ribosomal protein S14	3	1.06	0.15

these solute carriers were responsible for modulating OPA1 in response to substrate concentrations.

To first validate the OPA1–SLC25A protein interactions, C-terminally 3xflag tagged solute carrier protein constructs (AGC1, AGC2, OGC and DIC) were overexpressed in MEFs and their mitochondrial localization was confirmed by immunofluorescence (Figure 19A). Immunoprecipitation of tagged AGC1, AGC2, OGC and DIC revealed an interaction with endogenous OPA1 (Figure 18A); in line with the SILAC experiment where tagged OPA1 immunoprecipitated endogenous SLC25 proteins. Furthermore, immunoprecipitation of endogenous OPA1 from both isolated MEF and liver mitochondria also revealed an interaction with endogenous OGC, but not other control mitochondrial proteins (Figure 18B & Figure 19B). In addition, the interaction between OPA1 and OGC was decreased, by 59.4% ± 10.7 (SEM, n=3) when an OGC competitive inhibitor (phenylsuccinate) was added to the immunoprecipitation buffer suggestive of a dynamic interaction (Figure 18B & Figure 19B). To further study this interaction and the role of solute carriers in the regulation of OPA1 assembly and function we used both a genetic and pharmaceutical approach. To deplete OGC, MEFs were subjected to two rounds of siRNA transfection for a total of 120 hours (Figure 18C). Neither OGC depletion nor OGC overexpression had an observable effect on mitochondrial length (Figure 20A&B). In addition to mitochondrial length, OGC depletion had no effect on gross mitochondrial structure (Figure 21A), OCR rates in regular growth conditions (Figure 18F&H) or cell survival in starvation (Figure 21B&C), indicating that decreasing OGC levels does not disrupt overall mitochondrial structure and function. As our hypothesis is that OGC (and other SLC25A proteins) regulate OPA1 under changing substrate levels, we then measured

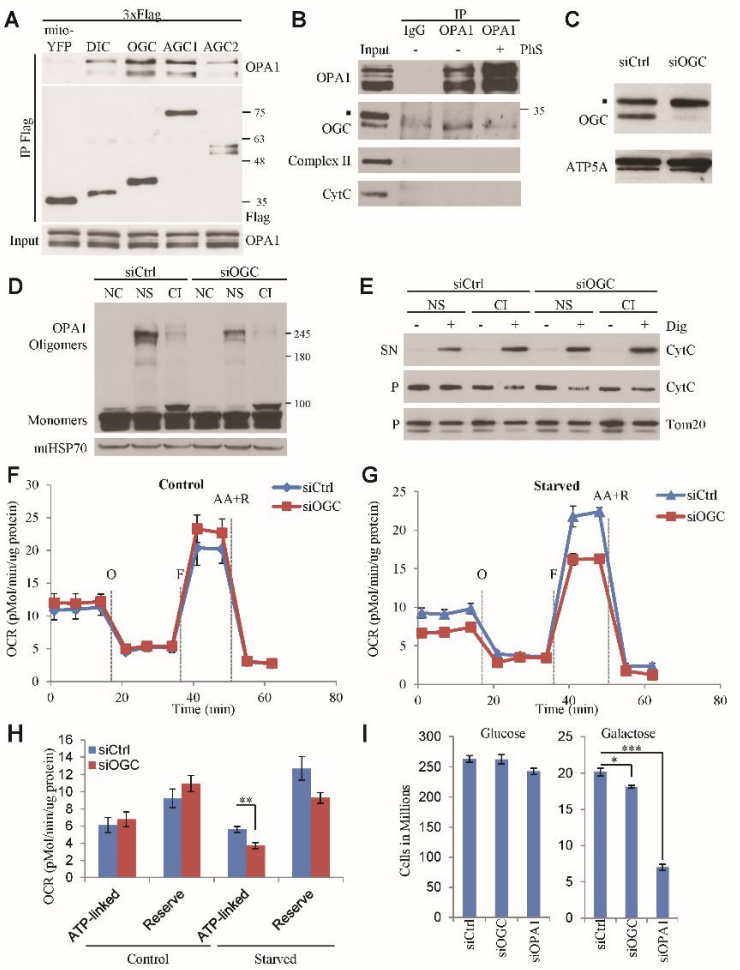

Figure 18. OPA1 interacts with SLC25 proteins that regulate OPA1's response to starvation.

A Mito-YFP-3xflag, DIC-3xflag, OGC-3xflag, AGC1-3xflag and AGC2-3xflag constructs were transiently transfected into MEFs. 24 hours post-transfection, cells were lysed, immunoprecipitated with anti-flag antibodies and analysed by western blot. **B** Endogenous OPA1 was immunoprecipitated from MEF mitochondrial lysates with or without 15 mM phenylsuccinate (PhS) and the eluted samples were analysed by western blot. Complex II and CytC were used as negative controls. **C** Representative OGC knockdown for experiments 18D-H, 20B & 21A-E. MEFs were transfected twice with siOGC for 120 hrs total and mitochondrial lysates were analysed by western blot. **D** Isolated mitochondria from siOGC-treated cells were incubated with the indicated ETC substrates [NC: non crosslinked control; NS: no substrate control; CI: Complex I, malate and glutamate at 5 mM each] for 30 minutes at 37ºC, cross-linked with EDC, and OPA1 oligomers were then analysed by gradient gel western blot. **E** Isolated mitochondria from siOGC and siCtrl cells were incubated in no substrate and complex I buffers for 30 minutes and analysed for cytochrome c retention. **F** SiOGC and siCtrl cells were plated onto Seahorse TC plates 24 hours prior to analysis, washed and incubated for 15 minutes in modified KRB and analysed by the XF analyzer. At the indicated times, oligomycin (O), FCCP (F), and Antimycin A (AA) with Rotenone (R) were injected. **G** The same cells were pre-starved for 2 hrs before identical analysis. **H** Quantification of ATP-linked (resting OCR minus oxygen leak) and reserve OCR (maximal minus resting OCR) in F and G (averages ± SEM of 4 independent experiments). **I** MEFs were grown for one week in galactose media, to revert to a more oxidative phenotype, or in regular glucose media, and these cells (1 000 000) were transfected with either siCtrl, siOGC, or siOPA1 and maintained in their respective media. Cells were then left to grow, passaged where required and cell number in regular growth medium (left panel) or galactose media (right panel) was counted 6 days later (averages ± SEM of 4 independent experiments). Student t-tests were performed as indicated *p<0.05,

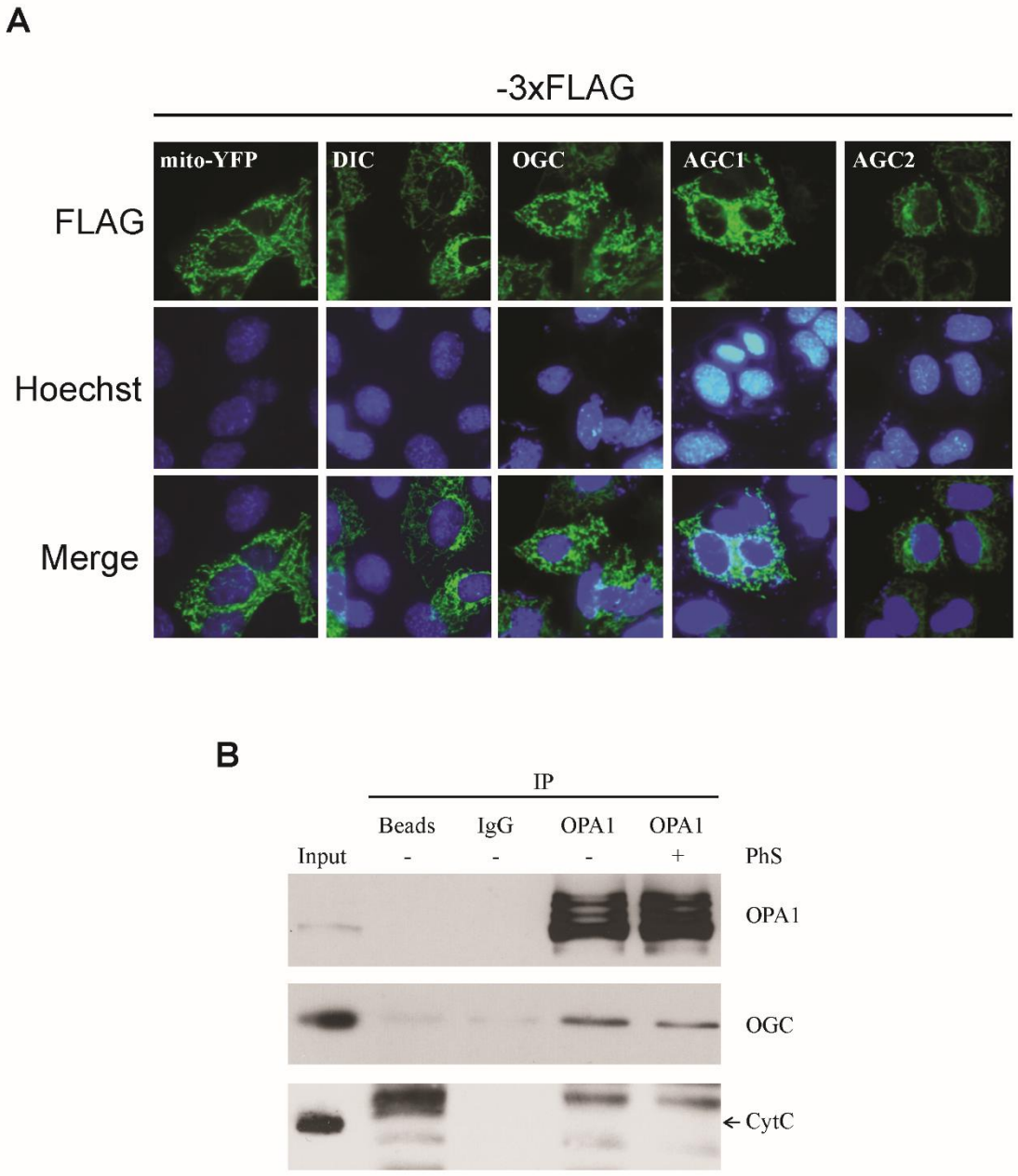

Figure 19. Fusion proteins for DIC, OGC, AGC1, and AGC2 are all mitochondrially targeted.

A MEFs were transiently transfected with mito-YFP-3xFLAG, DIC-3xFLAG, OGC-3xFLAG, AGC1-3xFLAG, and AGC2-3xFLAG for 24 hours, seeded onto coverslips for 24 hours, fixed and analysed by immunofluorescence with anti-flag antibodies. **B** Endogenous OPA1 was immunoprecipitated from mouse liver mitochondrial lysates with or without 15 mM phenylsuccinate (PhS) and the eluted samples were analysed by western blot.

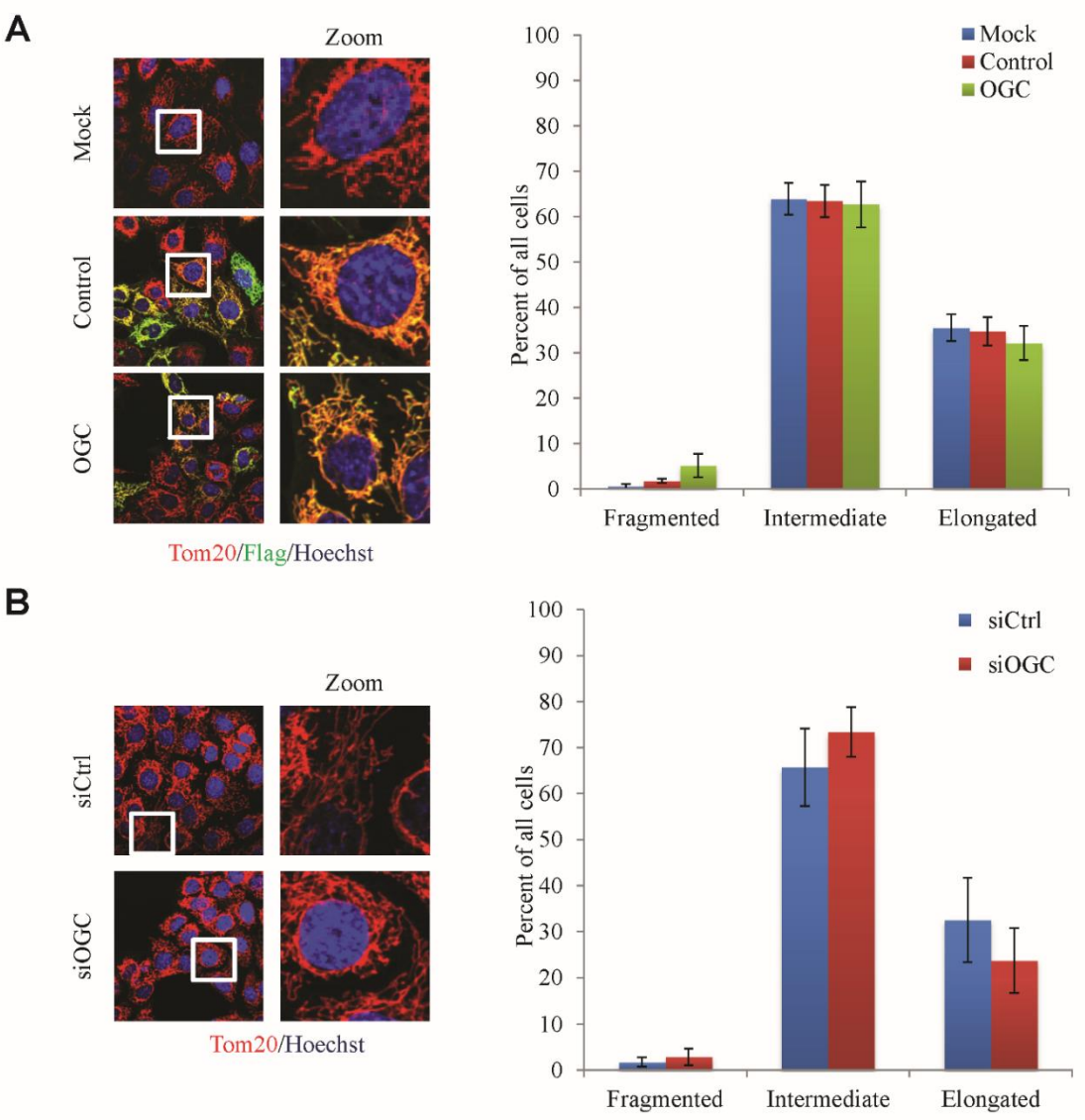

Figure 20. Overexpression or knockdown of OGC does not affect mitochondrial length.

A MEFs were transiently transfected with no plasmid, mito-YFP-3xFlag, or OGC-3xFlag for 48 hours. Mitochondrial morphology was then analysed by Tom20 immunofluorescence and binned as fragmented, intermediate or elongated (right panels, averages ± SEM of 3 independent experiments). **B** MEFs were transfected twice with siOGC for 120 hrs total and mitochondrial morphology was then analysed by Tom20 immunofluorescence and binned as fragmented, intermediate or elongated (right panels, averages ± SEM of 3 independent experiments).

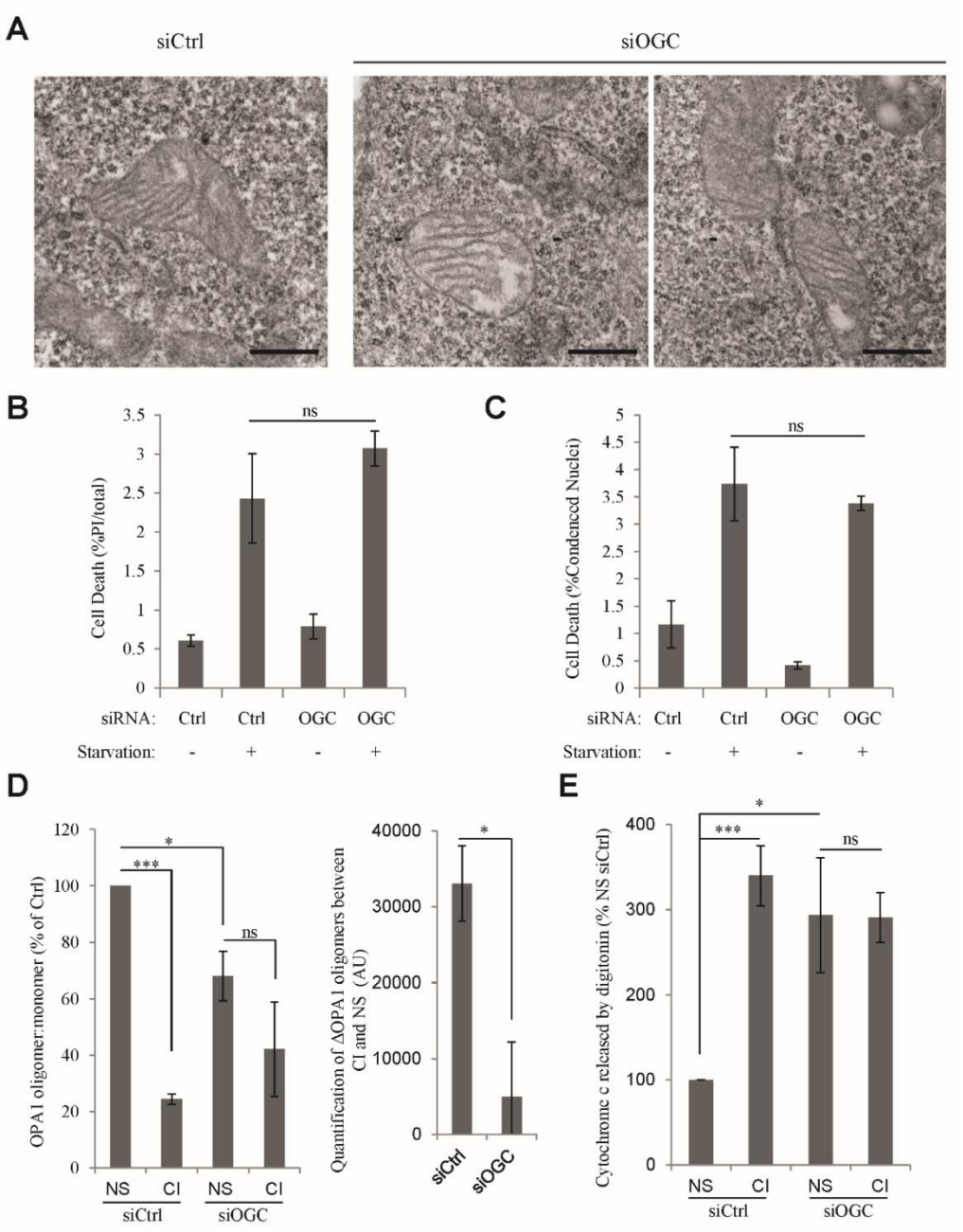

Figure 21. Supplement to Figure 18.

A Representative EM images of mitochondria from siCtrl or siOGC MEFs. Scale bars : 500 nm. **B** Cell death of siCtrl or siOGC MEFs starved or not for 6 hours was analysed following PI and Hoechst staining where dead cells are expressed as the percentage of PI^+ to all cells ($Hoechst^+$) (averages ± SEM of 3 independent experiments). **C** Cells were treated as in Figure E9B, but quantified as the percent condensed nuclei (averages ± SEM of 3 independent experiments). **D** Quantification of Figure 6D of the OPA1 oligomer to monomer ratio, percent of control (averages ± SEM of 4 independent experiments). Right panel, quantification of same experiments, but expressed as the change in OPA1 oligomers from incubation with complex I substrates to no substrates (AU: Arbitraty Units). **E** Quantification of Figure 6E of the ratio of cytochrome c in the supernatants to that remaining in the pellets after incubation with digitonin and expressed as percent of siCtrl with NS (averages ± SEM of 4 independent experiments). Student t-tests were performed as indicated *p<0.05, ***p<0.005.

the response of siOGC mitochondria to substrate availability *in vitro*. Incubation of siOGC mitochondria in the absence of substrates reduced OPA1 oligomerization, also reducing the difference in OPA1 oligomerization between fed and no substrate conditions (Figure 18D & Figure 21D). Additionally when isolated mitochondria were incubated in the absence of energy substrates, siOGC mitochondria were unable to retain as much cytochrome c, indicative of their inability to respond to changing substrate levels (Figure 18E & Figure 21C).

Next, we investigated the consequences of OGC depletion on the response to starvation. Starvation of siOGC cells significantly reduced their ATP-linked oxygen consumption rate (Figure 18G&H), indicating an impaired response to changes in substrate availability. In addition, siOGC cells displayed a modest but reproducible decrease in cell growth in galactose media (Figure 18I). These results indicate that OGC plays a role in the adaptation of mitochondria to changing energy substrate levels, possibly by regulating OPA1 oligomerization.

To confirm that OPA1 senses substrate availability through the SLC25A proteins, we utilized competitive inhibitors of the DIC and OGC in order to mimic substrate binding in the complete absence of actual energy substrates. Strikingly, both the DIC inhibitor butylmalonate (BM) and the OGC inhibitor phenylsuccinate (PhS) alone drastically reduced OPA1 oligomerization mirroring the OPA1 response to substrate-rich conditions (Figure 22A). Again, this correlated with increased mobilization of cytochrome c stores, indicative of an increased cristae width (Figure 22B). Finally, since OPA1 regulates ATP synthase stability, we investigated the effect of the SLC25A inhibitors on the ATP synthase. Strikingly, both the dimer and the monomer of the ATP synthase were drastically

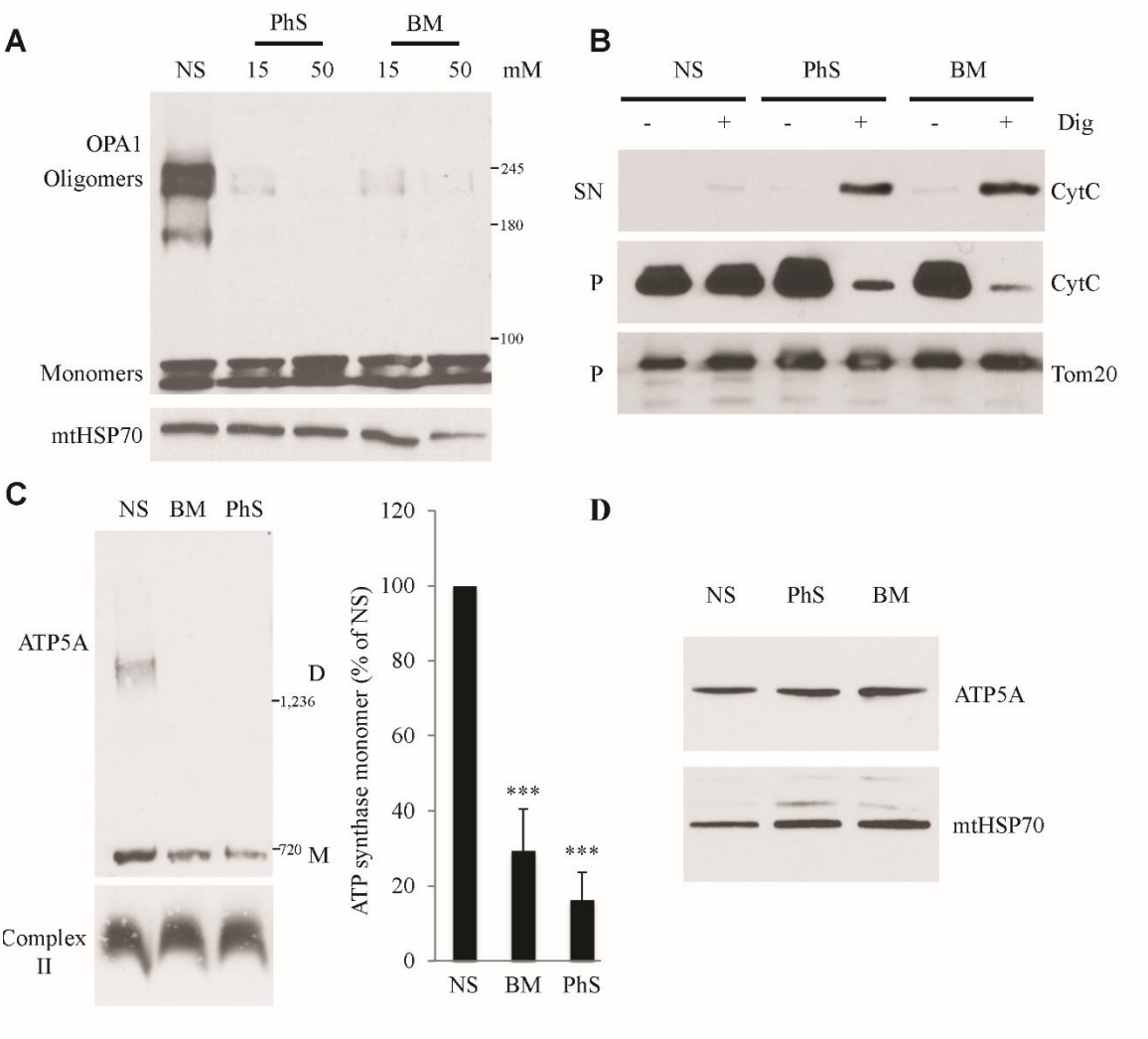

Figure 22. Pharmacological blockade of SLC25A proteins drastically inhibit OPA1 oligomerization and function.

A Isolated liver mitochondria were incubated with phenylsuccinate (PhS) or butylmalonate (BM) and OPA1 oligomerization was assessed as previously. **B** Mouse liver mitochondria were incubated with 50mM PhS or BM, then cytochrome c retention was analysed where released CytC was mobilized from the pellet (P) to the supernatant (SN) fraction. **C** Mouse liver mitochondria were incubated with 50mM PhS or BM and lysates were analysed by BN-PAGE. (Right panel) ATP synthase monomers were quantified relative to complex II monomer (averages ± SEM of 6 independent experiments). **D** Mouse liver mitochondria were prepared and incubated in parallel with 22C and analysed by regular western blot for ATP5A. Student t-tests were performed relative to control, ***p<0.005.

decreased following incubation with BM or PhS (Figure 22C). Importantly, the decrease in ATP synthase and increase in cytochrome c mobilization were specific, as cytochrome c was not mobilized in the absence of digitonin (Figure 22B), Complex II was not altered (Figure 22C), and BM and PhS did not alter total ATP5A levels (Figure 22D).

Altogether, these results indicate that OPA1 responds to changes in fuel substrate levels, influenced by SLC25A proteins, altering mitochondrial function through its role in cristae regulation and ATP synthase assembly.

3.2 The interaction between OPA1 and CLUH

From our SILAC-based proteomic interaction screen, we identified KIAA0664 (CLUH) as a potential novel interacting partner of OPA1. Since CLUH homologues are known to regulate mitochondrial dynamics in *Dictyostelium, Saccharomyces cerevisiae, Arabidopsis, Drosophila melanogaster* (Cox & Spradling, 2009; Fields et al, 1998; Logan et al, 2003; Zhu et al, 1997a), we investigated whether or not CLUH can regulate mitochondrial dynamics in mammalian cells. Furthermore, as OPA1 is a master regulator of mitochondrial dynamics, we questioned whether OPA1's effect on mitochondrial dynamics is regulated by CLUH. Since little is known on mammalian CLUH, we began our studies by investigating its function in an overexpression system.

3.2.1 OPA1 and CLUH co-immunoprecipitate

To confirm the OPA1-CLUH interaction, we created a construct in which full length CLUH was tagged on the C-terminal with 3xflag, as to not disturb mitochondrial transport, which is usually N-terminal-dependent. Overexpression of this construct (CLUH-3xflag) was expressed at high levels in different cell types at the predicted size (approximately 160 kDa, Figure 23A). However, other bands were also present with CLUH overexpression, including a significant band at 75 kDa. By immunofluorescence, we confirmed that overexpressed CLUH was mostly cytoplasmic with a slight overlap with the mitochondrial marker Tom20, while control, mito-YFP, was completely mitochondrial (Figure 23C).

Since our SILAC studies revealed an interaction with overexpressed OPA1-YFP and endogenous CLUH, we performed the opposite experiment where CLUH-flag overexpression was used to immunoprecipitate endogenous OPA1. When CLUH-flag was immunoprecipitated, we observed an interaction with OPA1 (Figure 23B). However mito-

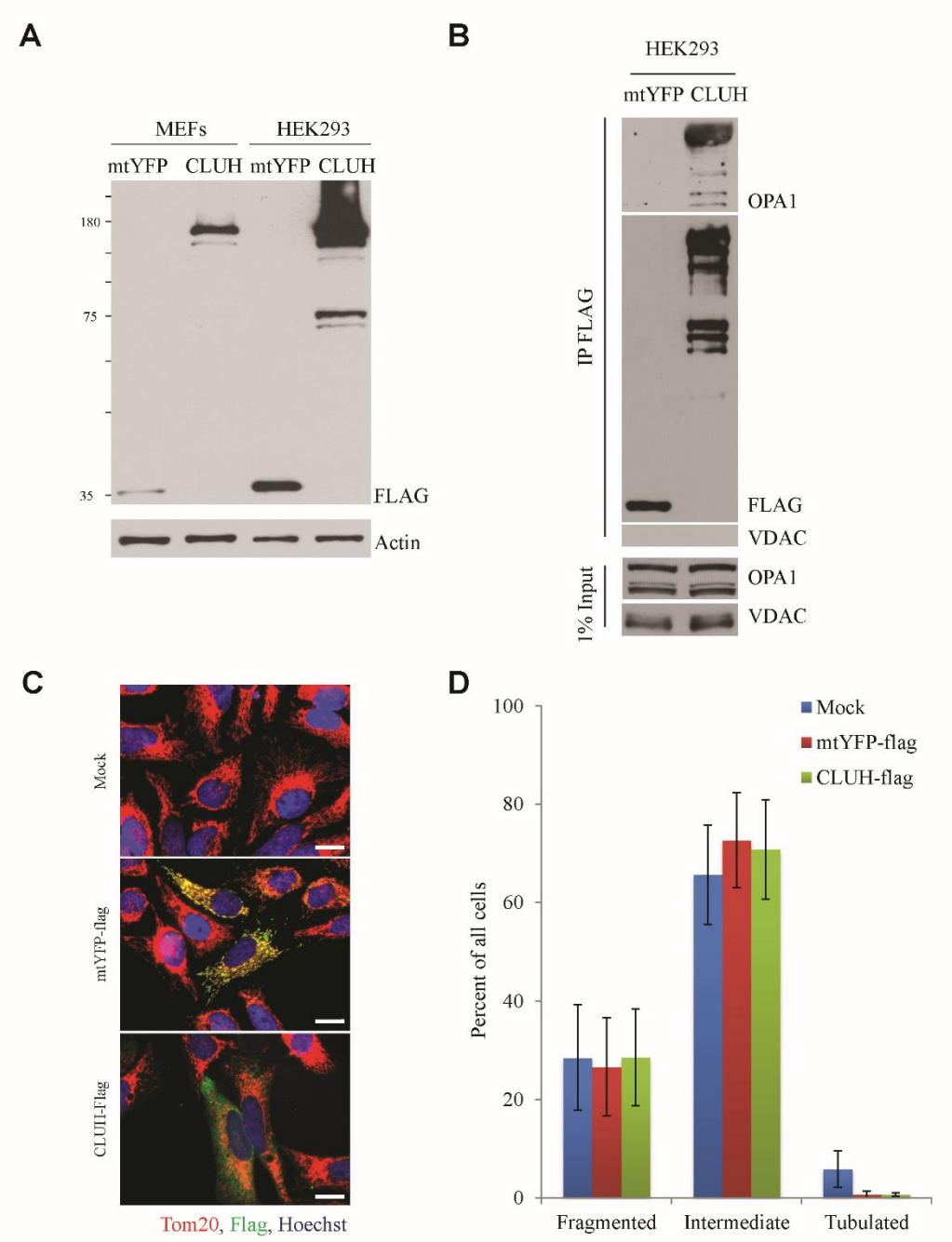

Figure 23. CLUH interacts with OPA1 and is expressed primarily in the cytoplasm.

A mtYFP-3xflag and CLUH-3xflag constructs were transiently transfected into the indicated cell lines. 48 hours post-transfection, cells were lysed and analysed by western blot with the indicated antibody. **B** HeLa cells were transfected with the indicated constructs for 48 hours. Cells were then fixed and analyzed by immunofluorescence with anti-Tom20, anti-flag antibodies and Hoechst. These cells were then quantified for mitochondrial length and binned as fragmented, intermediate or elongated (minimum of 100 cells per experiment, averages ± SEM of 3 independent experiments). **C** Mito-YFP-3xflag and CLUH-3xflag constructs were transiently transfected in HEK297 cells for 48 hours. Cells were then lysed, immunoprecipitated with anti-flag magnetic beads and analysed by western blot with the indicated antibody. Scale bars: 20 µm.

YFP did not pull down OPA1 and CLUH-flag did not pull down the control mitochondrial protein VDAC. These results confirm a potential novel interaction between OPA1 and CLUH. The functional significance of this relationship remains to be elucidated.

3.2.2 A subpopulation of CLUH is mitochondrial

Since we demonstrated that CLUH interacts with OPA1, a protein exclusively localized to mitochondria, and that CLUH-3xflag immunofluorescence overlapped slightly with the mitochondrial marker Tom20, we further investigated this previously unknown mitochondrial localization of CLUH. Firstly, we isolated mitochondria and cytoplasm by differential centrifugation in HeLa cells overexpressing either CLUH-flag or control, mitoYFP-flag. We confirmed that the mitochondrial isolation was appreciably pure since lactase dehydrogenase (LDH) was present exclusively in the cytosolic fraction, while Tom20 and OPA1 were present exclusively in the mitochondrial fraction (Figure 24A). From these cellular fractionation experiments, we uncovered a significant amount of CLUH-flag present in the mitochondrial fraction (Figure 24A). Moreover, we found this mitochondrial CLUH-flag was mostly full length (≈160 kDa).

We next corroborated these findings with confocal imaging of endogenous CLUH in the presence of a weak detergent to solubilize cytoplasmic proteins. An experimentally determined concentration and timing of saponin (75µg/mL) solubilisation was used prior to cell fixation to remove soluble cytoplasmic proteins, including CLUH. Interestingly, this technique revealed a co-localization of CLUH with mito-YFP used to visualize mitochondria (Figure 24B). Taken together these results suggest that a fraction of CLUH localizes to mitochondria.

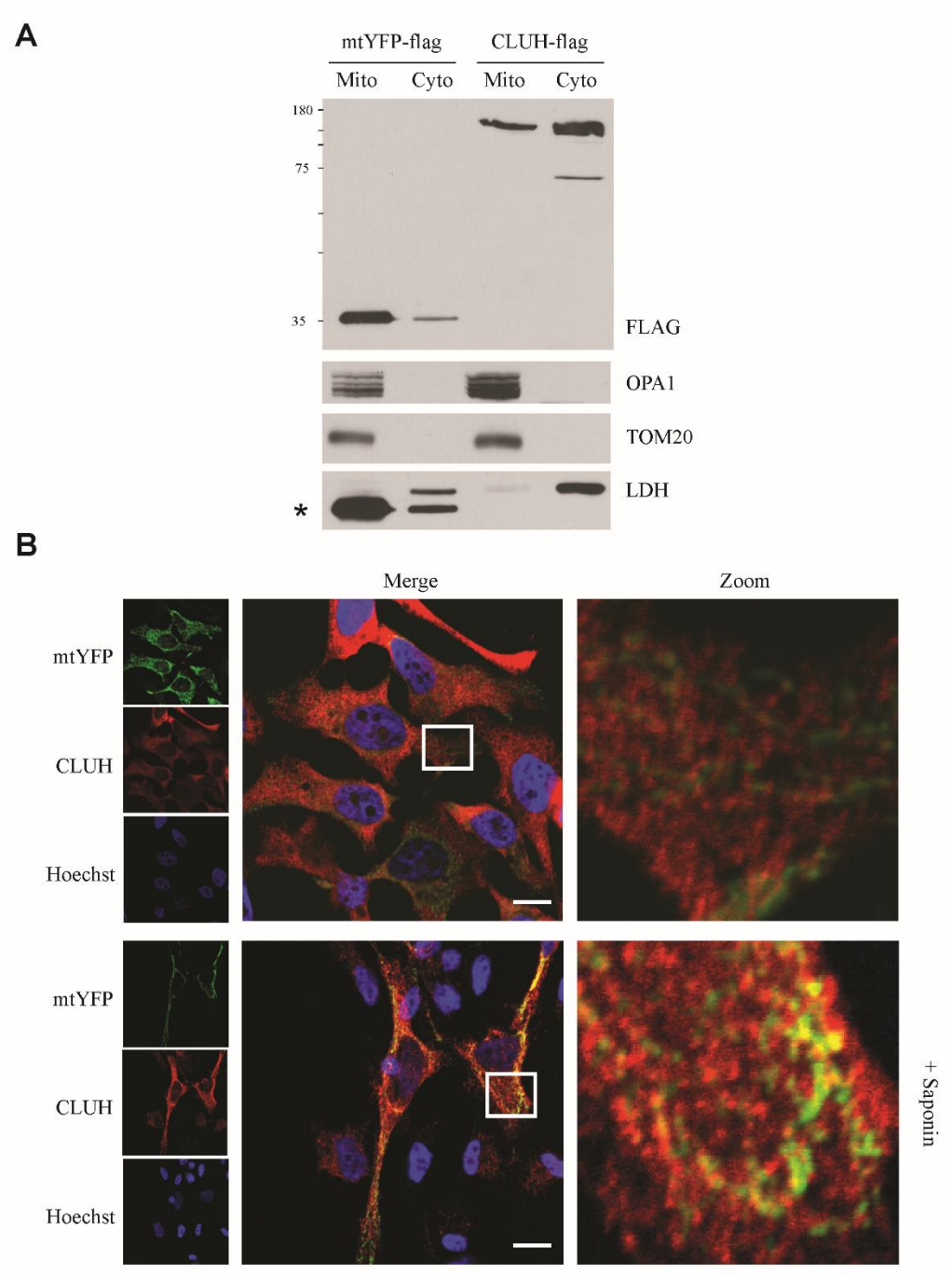

Figure 24. A subpopulation of CLUH is associated with mitochondria.

Mitochondrial and cytoplasmic fractions were isolated by differential centrifugation from cells expressing mito-YFP or CLUH-flag. The resulting fractions were analyzed by western blot with the indicated antibodies. **B** Cells were transfected with mtYFP to visualize mitochondria, plated on glass coverslips and then fixed regularly (top panels) or fixed following Saponin solubilisation for 1 minute (bottom panels). Fixed cells were then visualized by confocal microscopy flowing immunofluorescence with anti-CLUH antibodies and Hoechst. Scale bars: 20 µm.

3.3.3 CLUH does not alter mitochondrial dynamics or mitochondrial localization

Since OPA1 and CLUH interact, we asked if the expression of CLUH influences mitochondrial dynamics, a key function of OPA1. To determine whether CLUH regulates mitochondrial dynamics, mitochondrial length was quantified in the CLUH-3xflag overexpressing cells. There was no change in mitochondrial length when cells overexpressing CLUH were compared to controls (quantified in Figure 23D). To determine if absence of CLUH affects mitochondrial length, CLUH was ablated with two different siRNAs targeting CLUH, efficiently knocking down CLUH at the RNA and protein level by greater than 80% (Figure 25A&B). Of note, endogenous CLUH had a similar banding pattern to overexpressed CLUH-3xflag, suggesting that these bands are not an overexpression degradation artifact. CLUH immunofluorescence was almost completely absent in the majority of these cells, while few cells still possessed large amounts of CLUH (Figure 25C). Mitochondrial length was not different in siCLUH groups compared to their controls (Figure 25D and quantified in Figure 25E), confirming that CLUH does not affect mitochondrial length in these cells. In addition to changes in mitochondrial length, it has been noted that Drosophila *clu* regulates the localization of mitochondria within the cell. Specifically, mitochondria in *clu* mutant germ cells are clumped around the nucleus and are unable to reach the extremities of the cells (Cox & Spradling, 2009). However, with both mtHSP70 and Tom20 immunofluorescence and differential interference contrast (DIC) to delineate the cell boundaries, no change in mitochondrial localization was observed in the absence of CLUH (Figure 26). Mitochondria in cells devoid of CLUH were still able to occupy the periphery of the cell. This suggests that contrary to Drosophila, CLUH does not affect mitochondrial localization in HeLa cells.

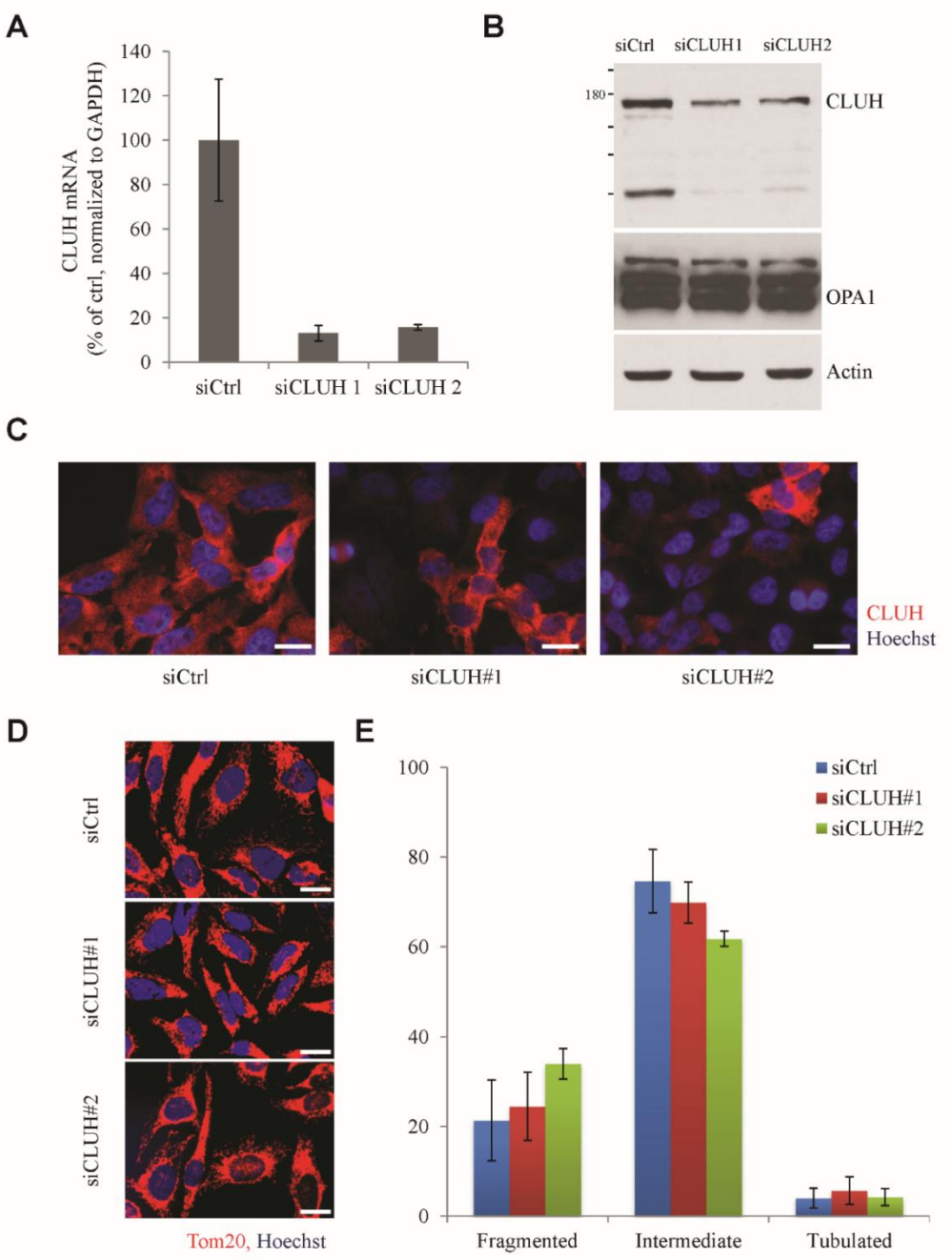

Figure 25. CLUH ablation does not affect mitochondrial length in HeLa cells.

A Hela cells were transfected with either control, non-targeting siRNA, or one of two siRNAs targeting CLUH for 48 hour. Cells were then harvested and RNA for CLUH and GAPDH was determined by RT-PCR (averages ± SEM of 4 technical replicates). **B** Cells were treated as in A, but lysed and analyzed by western blot with the indicated antibody. **C** Cells were treated as in A, but seeded onto coverslips and analyzed by immunofluorescence with anti-CLUH antibodies and Hoechst. **D** Cells were treated as in A, but seeded onto coverslips and analyzed by immunofluorescence with anti-Tom20 antibodies. **E** These cells were then quantified for mitochondrial length and binned as fragmented, intermediate or elongated (minimum of 100 cells per experiment, averages ± SEM of 3 independent experiments). Scale bars: 20 µm.

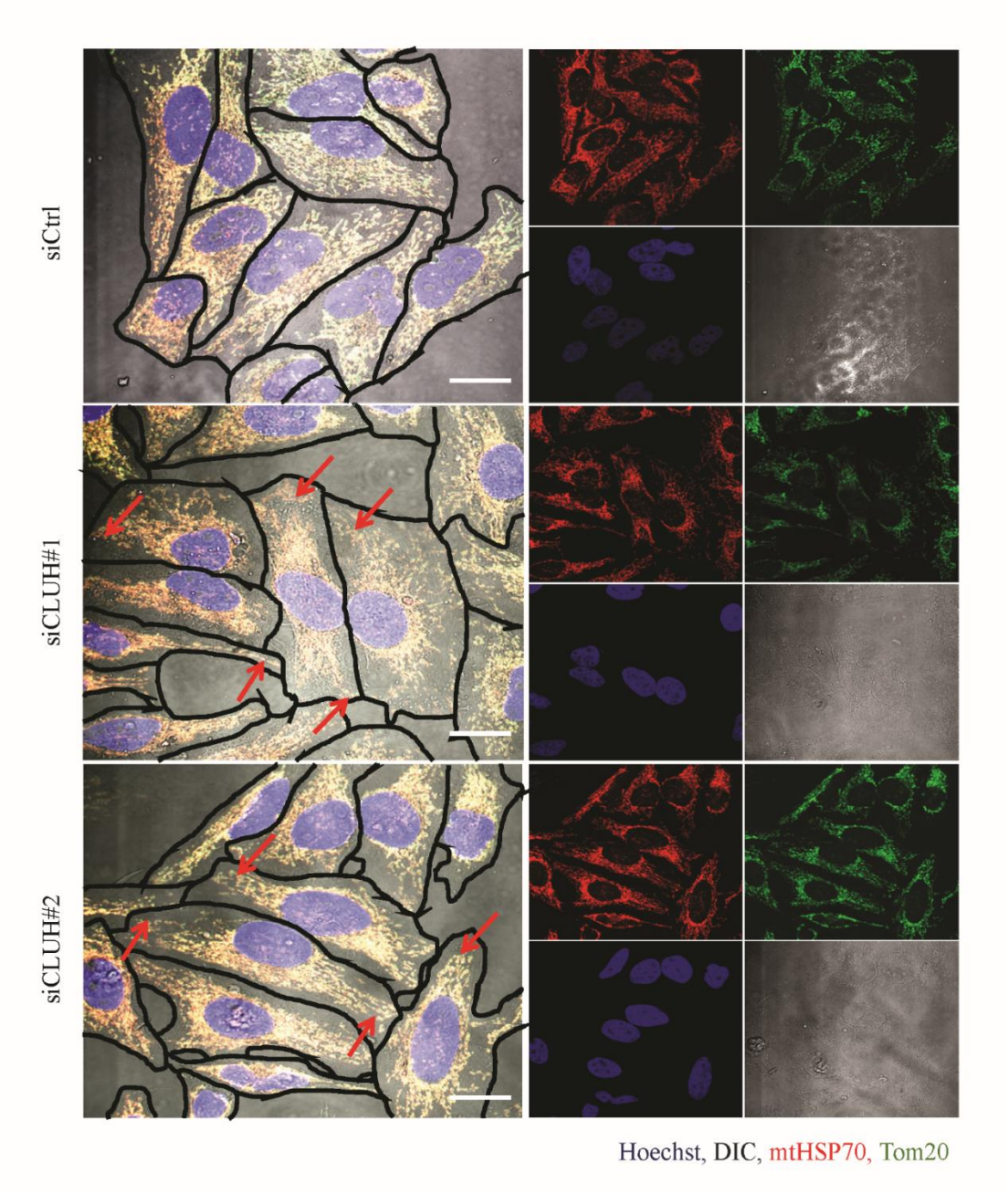

Figure 26. CLUH does not regulate mitochondrial localization in HeLa cells

Hela cells were transfected with either control non-targeting siRNA or one of two siRNAs targeting CLUH for 48 hour. Cells were seeded onto coverslips and analysed by immunofluorescence with confocal microscopy with mtHSP70 or Tom20 antibodies, Hoechst or with differential interference contrast. Arrows indicate mitochondria able to reach the outer bounds of the cytoplasm. Scale bars: 20 µm.

While CLUH interacts with OPA1 and a significant pool is located inside mitochondria we were unable to observe an effect on mitochondrial dynamics in human cells. Further investigation is therefore warranted to reveal the functionality of mitochondrial CLUH.

3.3 The role of OGC and OPA1 in glutathione redox state

3.3.1 OGC regulates cellular glutathione redox state in MEFs

In chapter 3.1 we described how OPA1 interacts with, and is regulated by OGC. OGC is known to regulate the transport of mitochondrial glutathione (Chen & Lash, 1998). OPA1 deletion sensitizes cells to oxidative stress associated forms of apoptosis (Frezza et al, 2006; Jahani-Asl et al, 2011). OPA1 is also regulated by glutathionalization (Shutt et al, 2012), therefore we next investigated the role of OPA1 in the regulation of glutathione.

Carriers for mitochondrial glutathione may be cell-type specific (Kamga et al, 2010) and previous studies used mainly overexpression and pharmaceutical approaches (Kamga et al, 2010; Wilkins et al, 2014; Wilkins et al, 2013), thus we first investigated whether OGC knockdown affected the levels and redox potential of glutathione in MEFs. To this end we utilized a high-performance liquid chromatography (HPLC) technique to quantify cellular glutathione in both its reduced (GSH) and oxidized (GSSG) states. Running standards containing both GSH and GSSG by HPLC yielded two clean peaks, and different concentrations were used to produce standard curves for efficient quantification of GSH and GSSG levels in subsequent experiments (Figure 27A&C). When whole cell MEF lysates were analyzed, notable peaks at similar retention times were observed, indicative of the GSH and GSSG products (Figure 27B). Moreover, control cells were treated with 1mM H_2O_2 to functionally confirm the GSH and GSSG peaks. As expected, during this treatment the ratio between reduced GSH to oxidized GSSG peaks was significantly decreased (Figure 27C). When OGC was transiently decreased (Figure 27D), the GSH/GSSG redox ratio was increased (Figure 27E). Since the total levels of glutathione

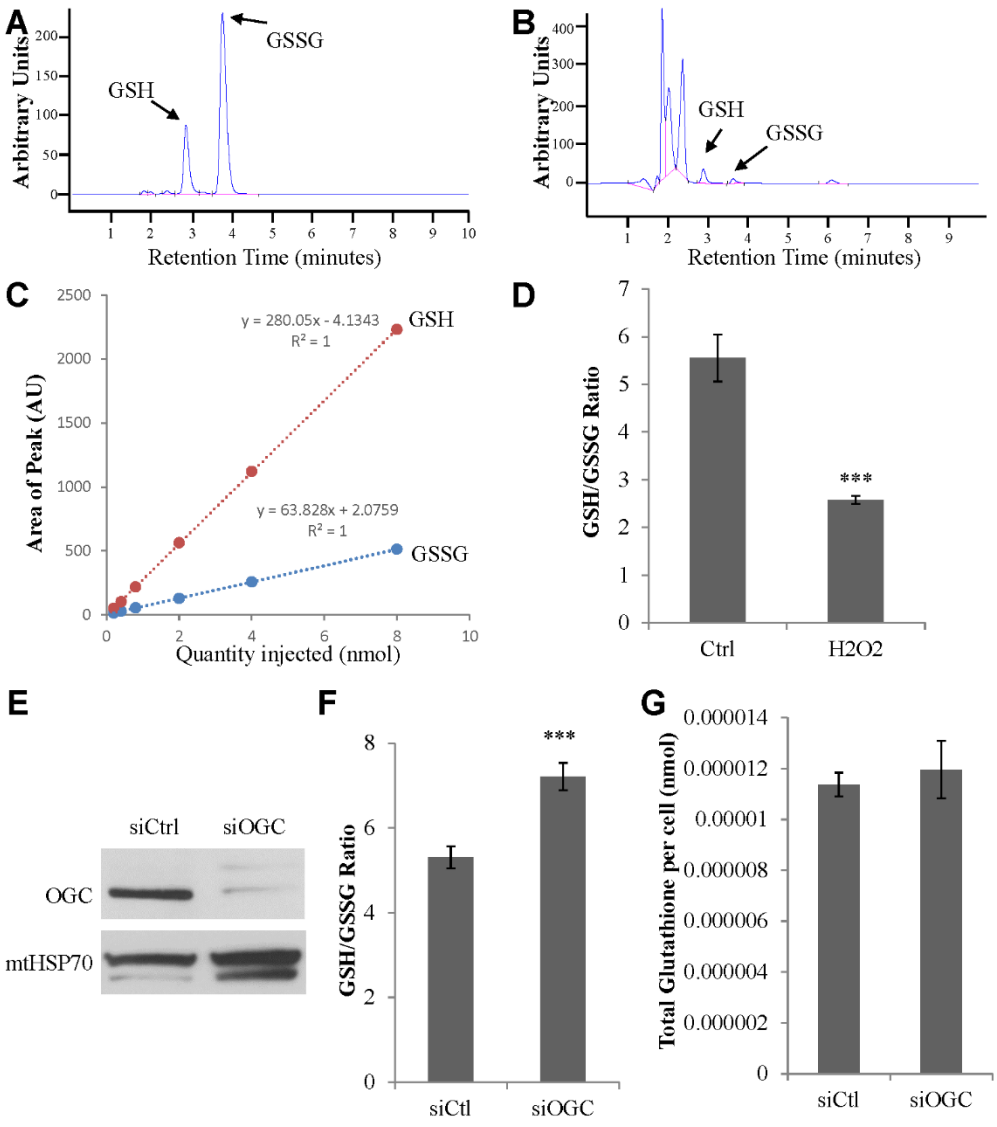

Figure 27. OGC controls the GSH/GSSG ratio in MEFs.

A. Representative HPLC analysis of standards containing GSH and GSSG. **B.** Representative analysis of whole cell GSH and GSSG levels by HPLC. **C.** Representative standard curves for the quantification of GSH and GSSG by HPLC. **D.** Control cells were treated with 1mM H2O2 or vehicle for 1 hour prior to quantification of GSH and GSSG by HPLC (averages ± SEM of 4 independent experiments). **E.** Western blot analysis of OGC following 120 hour siRNA knockdown (double transfections) used in subsequent experiments. **F.** Cells were treated with siRNA as D and analyzed by HPLC for whole cell GSH and GSSG quantity, expressed as a ratio (averages ± SEM of 4 independent experiments). **G.** The same experiments in E were analyzed for whole cell total GSH content ([GSH] + 2[GSSG]). Student's t-tests were performed relative to control, ***P < 0.005.

were unchanged (Figure 27F), the increase in GSH/GSSG ratio is consistent with decreased glutathione transport into the mitochondrial matrix, the major source of oxidative stress.

Although it has been demonstrated that reduced mitochondrial transport of glutathione by OGC can sensitize cells to ROS induced cell death (Wilkins et al, 2014; Wilkins et al, 2013), the consequence of OGC deletion in mitochondrial respiration in response to oxidative stress has not been investigated. Therefore, we analyzed the respiration of these cells in response to short-term H_2O_2 treatments. Although all parameters of respiration were unchanged following OGC knockdown (Figure 18 and Figure 28), following H_2O_2 treatment, OGC depleted cells had a decreased ability to maintain maximal respiration (Figure 28). In fact, under these conditions, OGC depleted cells have almost no reserve respiratory capacity, the ability of mitochondria to increase their respiration following membrane depolarization. How OGC depletion results in a decrease reserve capacity remains to be determined; however, it may be that the inability to properly buffer ROS within the matrix would lead to oxidation and inefficiencies within the electron transport chain.

3.3.2 OPA1 regulates cellular glutathione

With OGC confirmed to regulate the glutathione redox ratio in MEFs, we next asked whether OPA1 regulates glutathione redox. Surprisingly, in OPA1 knockout MEF cell lines, the GSH/GSSG ratio was drastically increased, much more so than the increase with OGC knockdown (Figure 29A). In addition, we observed a robust increase in total glutathione levels (Figure 29B). Thus two different mechanisms may regulate glutathione levels in OPA1 KO cells.

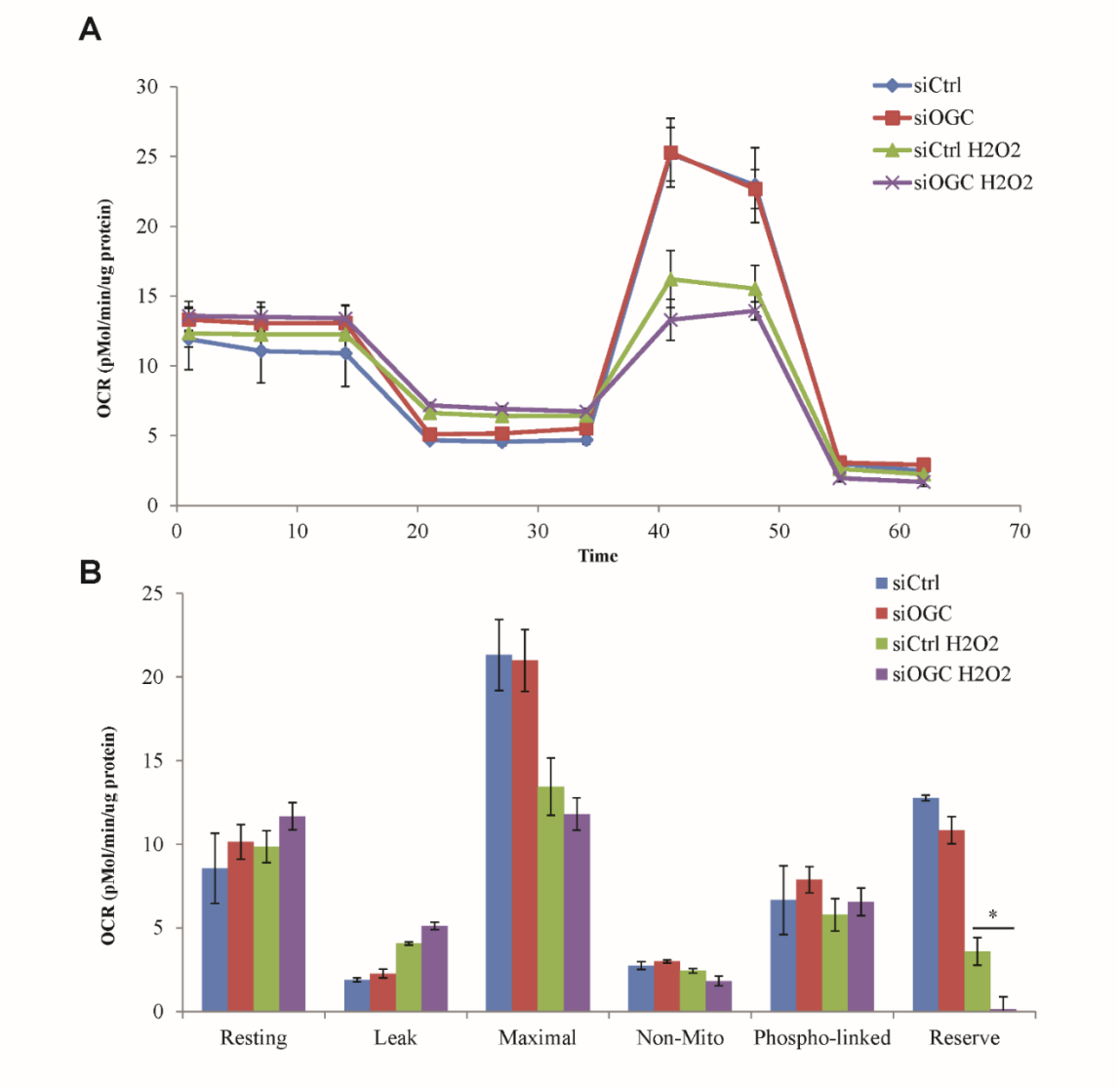

Figure 28. OGC depletion affects mitochondrial reserve respiration following H_2O_2 treatment

A To assess the impact of the OGC downregulation on the cell's response to H_2O_2 treatment we studied cells in a Seahorse XF-24 analyzer. Cells were plated on Seahorse TC plates 24 hours prior to analysis, stimulated or not with 1mM H_2O_2 for 1 hour, washed and incubated for 15 minutes in modified KRB, and analysed for OCR. At the indicated times, oligomycin (O), FCCP (F), and antimycin A (AA) with rotenone (R) were injected (averages ± SEM of 3 independent experiments). **B** Quantification of Resting OCR (Basal minus non-mitochondrial), Leak OCR (oligomycin insensitive minus non-mitochondrial), Maximal OCR (OCR in uncoupled mitochondria), phospho-linked OCR (resting OCR minus oligomycin insensitive OCR) and reserve OCR (Maximal minus resting) in A. (averages ± SEM of 3 independent experiments). Student t-tests were performed relative to control, *p<0.01

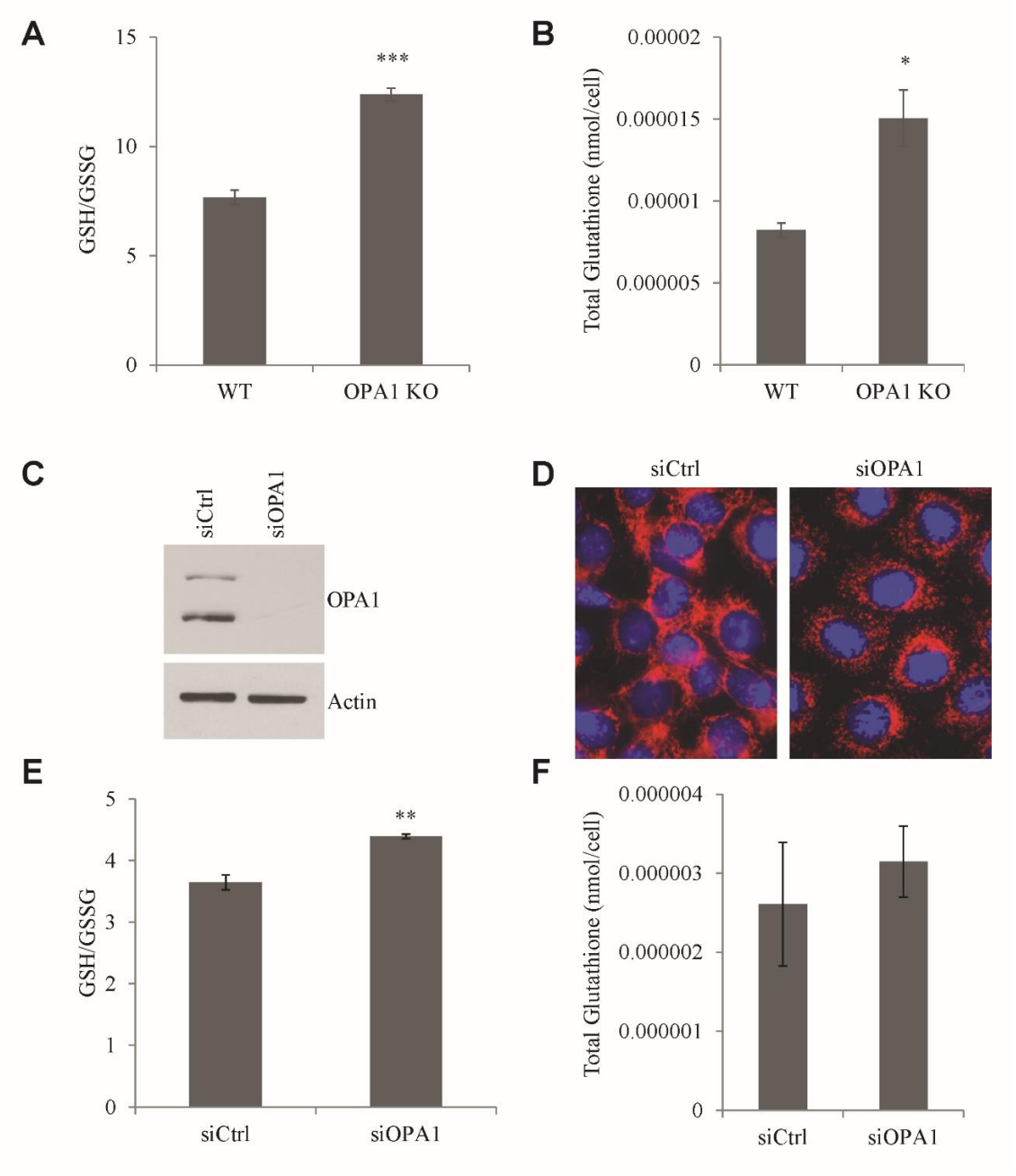

Figure 29. OPA1 dependent regulation of glutathione redox potential and quantity.

A. Control and OPA1 KO MEFs were analyzed by HPLC for whole cell GSH and GSSG quantity, expressed as a ratio (averages ± SEM of 3 independent experiments). **B.** The same experiments in A were analyzed for whole cell total GSH content ([GSH] + 2[GSSG]). **C**. Western blot analysis of OPA1 following 48 hour siRNA knockdown used in subsequent experiments. **D.** Cells were treated with siRNA as C and analysed for mitochondrial length by immunofluorescence with Tom20 antibodies (Red) and Hoescht stain (Blue). **E.** Cells were treated with siRNA as C and analyzed by HPLC for whole cell GSH and GSSG quantity, expressed as a ratio (averages ± SEM of 3 independent experiments). **F.** The same experiments in A were analyzed for whole cell total GSH content ([GSH] + 2[GSSG]). Student's t-tests were performed relative to control, *P < 0.05, **P < 0.01 and ***P < 0.005.

Since long-term deletion of OPA1 may result in multiple mitochondrial deficiencies, we transiently ablated OPA1 with siRNA. At this timepoint (48hrs), OPA1 was efficiently decreased (Figure 29C), and mitochondria were already considerably fragmented (Figure 29D). Under these conditions, the GSH/GSSG ratio was again significantly more reduced, in line with the hypothesis that OPA1 would regulate mitochondrial transport of GSH (Figure 29E). Total glutathione content was statistically unchanged (p=0.15) (Figure 29F). These results suggest that OPA1 has a two-pronged effect on glutathione, first an effect on the GSH/GSSG ratio (similar to OGC) and second a longer-term effect on whole glutathione levels, which may represent compensatory effects.

3.3.3 OPA1 regulation of cellular glutathione requires its GTPase activity

To confirm the role of OPA1 in the regulation of glutathione, we asked whether we could rescue the defects in OPA1 KO cells with WT OPA1. Furthermore, we asked if the GTPase function of OPA1 is required for this phenotype. In chapter 3.1 we rescued some characteristics of OPA1 function with a fusion-incompetent mutant of OPA1 that can still oligomerize and maintain cristae structure, the OPA1(Q297V) mutant. This mutant was able to oligomerize in response to substrate availability but could not rescue decreased mtDNA levels in OPA1 KO cells. We used these cells lines with overexpressed WT OPA1 or OPA1(Q297V) to investigate glutathione content and redox ratio. Overexpression of both WT OPA1 and OPA1(Q297V) in control cells had little effect on both the GSH/GSSG ratio or total glutathione levels (Figure 30A&B). There was however, a striking rescue in both the GSH/GSSG ratio and the total glutathione levels with WT OPA1 in the OPA1 KO MEFs, but the OPA1(Q297V) had no effect on either parameter.

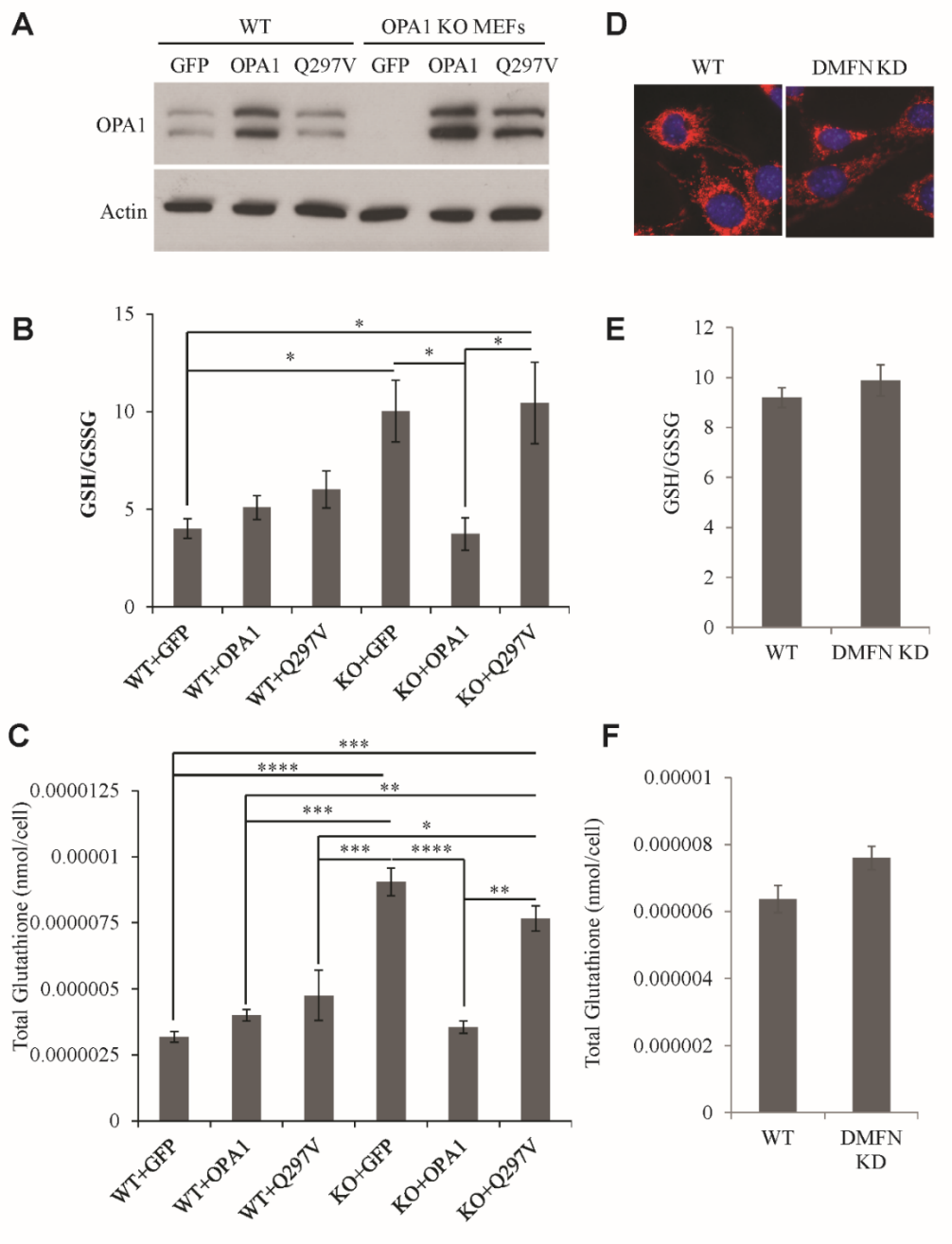

Figure 30. OPA1 dependent regulation of glutathione redox potential and quantity requires its GTPase activity.

A Longterm cultures of WT and OPA1 KO MEFs stably expressing the indicated constructs were analysed by western blot for OPA1 and Actin. **B** These cell lines were analyzed by HPLC for whole cell GSH and GSSG quantity, expressed as a ratio. **C** The same experiments in A were analyzed for whole cell total GSH content ([GSH] + 2[GSSG]). (averages ± SEM of 3 independent experiments) with one-way anova (Tukey post hoc test), *P < 0.05, **P < 0.01, ***P < 0.005 and ****P < 0.001. **D** WT and DMFN KD MEFs were plated on coverslips and mitochondrial length was analyzed with the live stain mitotracker and Hoechst. **E** These cells were analyzed by HPLC for whole cell GSH and GSSG quantity expressed as a ratio (averages ± SEM of 3 independent experiments). **F** The same experiments in E were analyzed for whole cell total GSH content. SEM of three independent experiments.

This data suggests that GTPase activity is required for the regulation of glutathione content and redox ratio. Since GTPase activity is also required for mitochondrial fusion, we asked whether affecting mitochondrial length alone was sufficient to induce changes in glutathione levels and redox ratios. To this end, we generated MEFs in which MFN1 and MFN2 were deleted. As expected, mitochondria were fragmented in these cells (Figure 30D), however neither the ratio of GSH/GSSG nor the total glutathione differed between DMFN KD or control cells (Figure 30E&F). Together these results suggest that OPA1 requires its GTPase activity to regulate glutathione levels and redox state, however, this function is not dependent on fusion alone.

Chapter 4. Discussion

4.1 The role of OPA1 in sensing substrate availability and responding by altering cristae structure

Cristae structural changes have been documented decades ago (Hackenbrock, 1966; Hackenbrock, 1968a; Hackenbrock, 1968b), but our understanding of how these changes occur and their functional consequence is largely unknown. Here, we demonstrate a novel mechanism by which cristae are physiologically regulated. Changes in energy substrate availability are sensed by mitochondrial SLC25A transporters, which in turn regulate OPA1 oligomerization. OPA1 oligomerization is then required to modulate cristae width and regulate assembly of the ATP synthase, in a mitochondrial fusion-independent manner. The physiological importance of this mechanism is highlighted by the demonstration that a fusion-incompetent form of OPA1 (Q297V) rescued OCR, ATP synthase assembly and cell growth of OPA1 KO MEFs in galactose media, which forces mitochondrial respiration for ATP production.

Although it is known that OPA1 oligomers disassemble during cell death leading to release of proapoptotic factors (Frezza et al, 2006), and recently that OPA1 oligomer disruption by cristae remodelling results in impaired respiration (Cogliati et al, 2013), physiological changes in OPA1 oligomers and their role in regulating cristae structure under non-cell death conditions remained poorly understood. Here we demonstrated in both cells and isolated mitochondria that starvation increases OPA1 oligomers rapidly and reversibly, correlating with tighter cristae width. These substrate dependent changes in OPA1 oligomers were upstream/independent of ETC function and membrane potential, known regulators of OPA1 processing and its fusion function (Mishra et al, 2014; Song et al,

2007). By taking advantage of the OPA1(Q297V) mutant we showed that, independently of mitochondrial fusion, OPA1 can maintain cristae structure, mitochondrial activity and adapt to the lack of nutrients during starvation. Our study therefore demonstrates that the roles of OPA1 in mitochondrial fusion and cristae maintenance can be separated and that cristae can be maintained in the absence of mitochondrial fusion.

How oligomerized OPA1 regulates cristae structure is still largely unknown. One proposed mechanism is through the oligomerization of two long and one short isomer of OPA1 (Frezza et al, 2006), although OPA1 oligomerization could also promote its interaction with other protein complexes required for cristae formation. In support of this hypothesis, our SILAC-based interaction screens revealed interactions with several factors critical for cristae structure maintenance: the ATP synthase, prohibitin, mitofilin, CHCHD3, Sam50 and the adenonucleotide transporters. In fact, recent ground-breaking studies have revealed protein complexes required for cristae maintenance termed MINOS, MitOS or MICOS (Harner et al, 2011; Hoppins et al, 2011; von der Malsburg et al, 2011). Indeed, disruption of these components may lead to cristae loss, decreased ETC complexes and a decrease in respiration. In addition, since it has been demonstrated that ATP synthase oligomerization mediates cristae morphogenesis (Habersetzer et al, 2013; Paumard et al, 2002) it is possible that OPA1 oligomer-dependent changes regulate the ATP synthase which then alters cristae structure. In any case, the fact that OPA1 interacts with cristae maintenance components, as well as the ATP synthase, highlight its central role in the coordinate regulation of mitochondrial structure and function.

One of the ways in which cristae structure may regulate ETC function is by controlling local substrate concentrations. From computer modeling experiments, it has been proposed

that these changes in cristae structure may regulate the diffusion of metabolites (Mannella, 2006). Scorrano's group has shown that OPA1 is required for the regulation of respiratory chain supercomplex assembly (Cogliati et al, 2013). These ETC supercomplexes may increase the efficiency of electron transfer and ATP production, and may decrease the toxic accumulation of reactive oxygen species (Lenaz & Genova, 2012; Wittig & Schagger, 2009). Here, we present non-cell death manipulations of healthy cells or mitochondria to demonstrate that in addition to regulating expression OPA1 is also required for full ATP synthase monomer stabilization independently of its fusion activity, the monomer being the functional unit of the ATP synthase. The starvation-induced rescue of ATP synthase assembly by OPA1 and OPA1(Q297V) clearly support a major role for these complexes in fine tuning mitochondrial function according to nutrient availability. However, we cannot exclude that part of the prosurvival role of OPA1(Q297V) is in preventing the release of proapoptotic factors from mitochondria, as previously suggested under apoptotic conditions (Yamaguchi et al, 2008). Interestingly, the OPA1(Q297V) mutant still responds to changes in fuel substrate availability without GTPase activity, potentially mimicking GTP binding (Yamaguchi et al, 2008), suggesting that OPA1 oligomerization is upstream of GTP binding and hydrolysis.

We identified members of the SLC25A family of mitochondrial solute carrier as being required for OPA1 oligomerization in response to changes in energy substrate levels. Since their pharmacological and genetic ablation resulted in disruption of OPA1 oligomers and cytochrome c mobilization, outside of transporting their respective substrates, SLC25As could represent a novel class of inner membrane shaping proteins. While our results suggest that OGC interacts with OPA1, we cannot exclude the possibility that it affects

OPA1 indirectly, by modulating some undefined mitochondrial process. Moreover, the mechanism governing how SLC25A proteins transport their cargo as well as relay information to OPA1 still remains to be determined. Work on other more characterized solute carriers, the amino acid transporters, suggest that they may act as sensors in addition to carrier functions by activating different cellular signaling pathways [reviewed in (Taylor, 2014)]. The transfer of this idea to SLC25A proteins is of interest, considering the effect of OGC depletion and SLC25 inhibition on OPA1 oligomerization and function. Additionally, since the effect on OPA1 oligomerization and cytochrome c mobilization with these drugs was so robust, it would be interesting to investigate if targeting SLC25As represent a novel mechanism to adjust the cell death program.

4.2 The OPA1-CLUH interaction

During the course of our studies, we identified the human homologue of the clueless gene product as a potentially novel OPA1-interacting protein. Since it was demonstrated in other organisms that CLUH homologues regulate mitochondrial dynamics and that mammalian fusion machinery likely lacks the identification of all its members (Zhao et al, 2013), we questioned if CLUH represents a novel mitochondrial fusion protein. We found that this was not the case in HeLa cells since neither CLUH overexpression nor its downregulation affected mitochondrial length. Previous mitochondrial ultrastructure work had demonstrated that cluA- mutants had thin connections between mitochondria, suggesting they likely had a defect in late phases of mitochondrial fission (Fields et al, 2002). By confocal microscopy we investigated localizations of both the outer membrane marker Tom20 and the matrix marker mtHSP70, and were unable to find marked differences when overexpressing or downregulating CLUH. In other words, so called “beads on a string”

mitochondria (Spinazzi et al, 2008), representative of a fusion defect, were not observed. In fact, the mitochondrial clustering phenotype for which the protein was named for was unchanged in HeLa cells following CLUH knockdown.

Despite its lack of effect on mitochondrial length and localization, we do provide evidence of an OPA1-CLUH interaction by immunoprecipitation studies. While we investigated mitochondrial fusion through mitochondrial length measurements, further experimentation is required to investigate the role of CLUH in other known functions of OPA1. For example, it would be of interest to investigate mitochondrial cristae structure, OXPHOS and mtDNA levels in cells where CLUH levels have been altered.

During the course of our studies, Gao *et al.* described a fascinating role for CLUH in mitochondrial biogenesis (Gao et al, 2014). In their work, they propose that CLUH is an mRNA-binding protein involved in translation of a specific subset of mitochondrial proteins. In agreement with our data they describe a CLUH population that is closely associated with mitochondria; however, since we demonstrate that CLUH interacts with OPA1 we would hypothesize that some CLUH would actually need to enter mitochondria. Under the model proposed by Gao and colleagues, a small portion of OPA1 interacting with CLUH could be immunoprecipitated during its translation. We found that even the short isoforms of OPA1 interact with CLUH. Since s-OPA1 requires mitochondrial located proteases it would be more likely that CLUH interacts with OPA1 in the intermembrane space.

The fact that only certain cell types demonstrate a mitochondrial clustered defect, may suggest that the mitochondrial distribution defect associated with CLUH could be secondary to another underlying phenotype. To this effect, Gao and colleagues demonstrate

that Cos7 and NSC34 cells had different amounts of mitochondrial clustering while MEF cells lacked an overt clustering phenotype (Gao et al, 2014). While it could be a secondary effect, another possibility is that a factor governing the role of CLUH in mitochondrial clustering is lacking in certain cell types. In support of mitochondrial clustering being a secondary effect to mitochondrial dysfunction, Sen and colleagues have reported that mitochondrial clustering occurs downstream of its role in suppressing oxidative damage in Drosophila mutant (Sen et al, 2013). Recognizing its associations with Parkinson's disease in animal models, it will be of interest to delineate the full role of CLUH in mitochondrial (dys)function.

4.3 OPA1: a regulator of glutathione

In the chapter 3.1 we demonstrate how OPA1 oligomerization is required, independently of mitochondrial fusion, for the cellular adaptation to metabolic demand. Our data suggests that this regulation is dependent upon OGC and DIC carrier function. Since these two carriers are the only known carriers for mitochondrial glutathione, and that OPA1 interacts with these two carriers, we investigated an OPA1-dependent regulation of the glutathione system. Our data confirm a role for OGC in glutathione status and mitochondrial function and reveal a new role for OPA1 in the regulation of glutathione. Specifically, deletion of OPA1 had two effects: first it phenocopied the effect of OGC on the GSH/GSSG ratio and secondly it drastically increased total levels of glutathione. The latter is perhaps due to a long-term compensatory upregulation of glutathione synthesis following mitochondrial dysfunction, since short-term deletion of OPA1 did not result in a significant increase in total glutathione levels. Interestingly, OPA1-dependent regulation of glutathione is GTPase dependent, since the OPA1(Q297V) mutant could not rescue the increased ratio

or levels of glutathione. However, knockdown of mitofusins, which caused mitochondrial fragmentation, had no effect on GSH levels or redox ratio suggesting that fragmented mitochondria alone does not regulate glutathione.

Since OGC is a well-documented transporter of mitochondrial glutathione, we believe the increased ratio of GSH to GSSG might reflect the inability of GSH to enter the mitochondrial matrix to be oxidized. It remains to be determined if the increased GSH/GSSG ratio in OPA1 knockout and knockdown cells is also due to a defect in mitochondrial GSH transport. Future mitochondrial transport assays may help isolate a specific role for OPA1 in GSH transport through the OGC carrier.

However, despite substantial evidence to the contrary, it has been recently proposed that glutathione is not transported by OGC and DIC (Booty et al, 2015). In their study, Booty *et al.* demonstrate that fused membrane vesicles of *Lactococcus lactis* expressing *Saccharomyces cerevisiae* DIC or human OGC are unable to transport glutathione. While this data does show that expression of DIC or OGC in a simple membranes is insufficient for glutathione transport alone, it doesn't rule out other ways in which these transporters can affect mitochondrial GSH transport. The simplest scenario would be that in this minimal system, OGC and DIC are not in their proper form for GSH transport. Perhaps these carriers require an essential protein cofactor, lipid composition, membrane structure or post-translational modification, not present in *Lactococcus lactis* fused membrane vesicles. Another possibility fitting the current literature, is that glutathione transport is only regulated by and not actively transported by OGC and DIC. Regardless, manipulations of these carriers clearly leads to defects in the glutathione content, sensitivity of cells to

oxidative stress, and defects in respiration following oxidative stress as we have demonstrated.

While OGC deletion in cells had no effect on all investigated parameters of respiration, when these cells were subjected to an oxidative stress we observed a significant decrease in reserve capacity. How oxidative stress affects the reserve capacity in these cells remains to be elucidated. Because mitochondrial GSH transport is likely affected, one interpretation is that the mitochondrial matrix is less able to buffer an oxidative stress, and that the OXPHOS machinery is damaged. Since reserve capacity is linked to ETC supercomplex assembly in other models (Cogliati et al, 2013; Khacho et al, 2014), it would be interesting to investigate ETC supercomplexes in this setting.

Shutt *et al*. have previously described a role for oxidative stress and glutathione status in the regulation of mitochondrial fusion (Shutt et al, 2012). In their study, they demonstrate how GSH and GSSG have opposing roles on *in vitro* mitochondrial fusion rates, where GSSG can induce a strong increase in MFN oligomerization, thus priming the fusion machinery. Interestingly, OPA1's oligomerization was also slightly increased in their study. Considering the aforementioned study and our data describing the GTPase-dependent role of OPA1 on the GSH redox ratio and GSH levels, OPA1 is both affected by, and affects the redox status of the glutathione pool. This is particularly interesting since OPA1 deletion has been known for some time to sensitize cells to forms of cell death in which oxidative damage is involved (Frezza et al, 2006; Jahani-Asl et al, 2011). Further studies are thus required to investigate this OPA1 dependent role of glutathione levels, redox ratios and potentially mitochondrial transport in different forms of cell death.

4.4 Additional General Discussion

In addition to our described cristae alterations during cellular starvation, mitochondria also elongate under these conditions (Gomes et al, 2011; Rambold et al, 2011). OPA1-dependent resistance to starvation induced cell death was thus attributed to this mitochondrial elongation. However, here we were able to dissect the relative roles of mitochondrial elongation with mitochondrial cristae structure changes with the OPA1(Q297V) mutant. We demonstrate that the role of OPA1 in maintaining cell viability during starvation does not require mitochondrial fusion. Since we also demonstrate the role of OPA1 oligomerization on cristae structure changes, it is tempting to speculate that these cristae alterations are required for resistance to starvation induced cell death by maintaining OXPHOS. However, since OPA1 could also play a direct role on apoptotic signaling, further experimentation will be required.

In this regard, many studies manipulate MFN1&2 in parallel with OPA1 to determine whether an effect is fusion-dependent or not. Caution should be employed when making such judgements since these are multifaceted proteins. In this regard, MFN2 has recently been described to regulate coenzyme Q levels, vital for OXPHOS function (Mourier et al, 2015). Thus, if OPA1 and MFN1&2 deletion cause a similar phenotype, it may be fusion-dependent, mtDNA-dependent, OXPHOS dependent or other undescribed processes.

How OPA1 regulates mitochondrial DNA is still unclear. It has been proposed that OPA1 regulates both mtDNA replication and distribution by an exon 4b-dependent function (Elachouri et al, 2011). Indeed, silencing of exon 4b containing OPA1 transcripts decreased mtDNA, which was reversed upon overexpression of a mitochondrially targeted exon4b fragment. Moreover, this 10-kDa fragment was demonstrated to interact with nucleoids,

mechanistically linking OPA1 to mtDNA. However, we, and recently others (Cogliati et al, 2013), reversed the mtDNA defects in OPA1 KO MEFs with isoform 1, which does not include exon 4b. We also demonstrate that the OPA1(Q297V) mutant is unable to rescue this mtDNA depletion. The fact that the OPA1(Q297V) mutant is fusion incompetent could suggest that OPA1 regulates mtDNA maintenance through a fusion-dependent mechanism. The literature seems to support this fusion-dependent interpretation. Human mutations in OPA1 and MFN2 which cause mtDNA depletions are located in their GTPase or GED domains, pivotal domains for their fusion functions (Vidoni et al, 2013). Also, deletion of MFN1 and MFN2 results in severe mtDNA depletion which can be completely reversed by expressing either MFN1 or MFN2 (Chen et al, 2010). In yeast, defects in mitochondrial fusion also cause mtDNA depletion and if mitochondrial length is maintained by decreasing mitochondrial fission, cells are able to maintain higher levels of mtDNA (Bleazard et al, 1999; Sesaki & Jensen, 2001).

Many outstanding questions remain with respect to mtDNA maintenance. For example if mtDNA maintenance indeed requires mitochondrial fusion, how would this mechanistically work? Trans-complementation has been described between mitochondria to mix protein, lipid and potentially repair damaged mtDNA in order to overcome mtDNA deletions (Takai et al, 1999). Nonetheless, how would trans-complementation result in an increase in the absolute number of mtDNA molecules? To understand how OPA1 could regulate mtDNA, we investigated our OPA1 interaction screens for modifiers of mtDNA and we identified ATAD3A as a potentially novel OPA1 interacting protein. ATAD3 had previously been demonstrated to interact with nucleoids and to dictate mtDNA replication (He et al, 2012; He et al, 2007). Our group confirmed that OPA1 and ATAD3A interact,

and hypothesized that ATAD3A could be the factor by which OPA1 regulates mitochondrial DNA. However, when ATAD3A was deleted, we did not observe a decrease in nucleoid numbers or mtDNA levels (Wong MSc Thesis, 2014). While these results suggest that ATAD3A likely does not link OPA1 function to mtDNA maintenance, other interesting candidates were also identified. These include the adenine nucleotide translocators and mitochondrial myosins, which may both affect mtDNA maintenance in different, though fairly uncharacterized manners (Kaukonen et al, 2000; Reyes et al, 2011).

Here we demonstrated a dual role for OPA1 in ATP synthase regulation. Fusion-dependent maintenance of the mtDNA genome is required for mtDNA-encoded transcripts in the F_o-subunit; while a fusion-independent role for OPA1 regulates the full assembly of the ATP synthase monomer. Interestingly, multiple subunits of the ATP synthase were also identified in our SILAC interactor screen. Further studies will therefore establish if a direct protein-protein interaction stabilizes the ATP synthase monomer. In this regard a number of components are already known to regulate the ATP synthase assembly, stability and oligomerization (Habersetzer et al, 2013; Wittig et al, 2010). As the ATP synthase is fundamental for eukaryotic life, its regulation and functions are likely highly complex and await further research. For example, a new role for the ATP synthase in the mitochondrial permeability transition pore opening has been recently discovered (Alavian et al, 2014; Giorgio et al, 2013). As both OPA1 and ATP synthase play such pivotal roles in cell death signaling, it remains to be determined if their direct interaction dictates this function.

While we did not observe an obvious defect in cristae structure in siOGC MEFs, the ability of OPA1 to respond to substrate availability and to maintain cytochrome c was impaired. However, when MISC-1, the *C. elegans* OGC orthologue, was mutated, cristae within the

head region were fewer in number and slightly blebbed under basal conditions (Gallo et al, 2011). This may indicate that the effect of OGC on OPA1 function may be more crucial in different organisms or cell types. In this regard, translating the findings of this thesis to *in vivo* models is imperative to advancing our knowledge of OPA1-mediated cristae changes. Perhaps, in more energy demanding cell types, such as neurons, the regulation of OXPHOS by OPA1-mediated cristae structure maybe even more crucial to their function. Two mouse models of OPA1 deficiency have been developed which will prove useful to investigate many of these questions *in vivo* (Alavi et al, 2007; Davies et al, 2007).

Fifteen years since the discovery of OPA1 mutations in ADOA, and amidst immense research progress, it is still unclear why OPA1 mutations cause selective loss of the RGCs. In fact, the neuronal selectivity for different mitochondrial dysfunctions in neurodegeneration remains a major research question. Are RGCs more prone to metabolic stress and starvation than other neurons? While there is ample evidence to suggest that defects in mitochondrial morphology underlies DOA, some DOA OPA1 mutations do not cause mitochondrial fragmentation, but do cause defects in respiration, and yet cristae structure has yet to be investigated with these mutants (Chevrollier et al, 2008). Finally, since OPA1 overexpression can rescue MPTP induced cell death (Ramonet et al, 2013), and that human OPA1 mutations have been linked to Parkinsonism (Carelli et al, 2015), increasing OPA1 function and/or oligomerization may be an attractive therapeutic target for PD or other forms of neurodegeneration.

4.5 Conclusions

In conclusion we propose a model in which OPA1 senses the presence of mitochondrial fuel substrates upstream and independently of ETC activity itself (Figure 31). The sensing of substrates lead to OPA1 oligomerization and tightening of cristae. These ultrastructural changes are accompanied by increased assembly of the ATP synthase which promotes the efficiency or capacity for ATP produced by oxidative phosphorylation. We believe that these cristae structural changes may be required for other physiological adaptations, which warrants further investigation. Finally, our findings strengthen the link between OPA1 and cristae maintenance and suggest another mechanism by which the cell can respond to its metabolic supply.

In addition, we identified CLUH as a previously unknown interactor of OPA1 and investigated its role in mitochondrial dynamics. Finally, our studies reveal a novel role of OPA1 in the regulation of glutathione. The role of OPA1 in glutathione levels and redox ratio required its GTPase domain, but was interestingly not fusion-dependent. The role of OPA1 in the regulation of glutathione warrants further investigation due to their interconnected roles in mitochondrial function and cell death signaling.

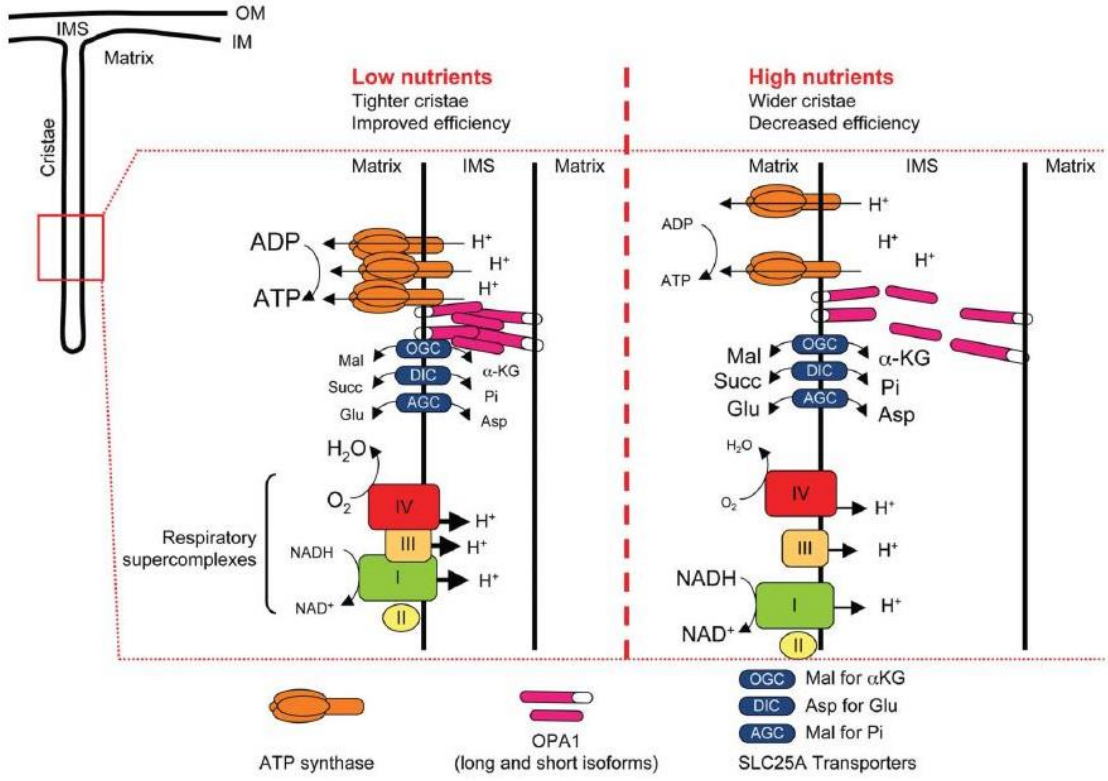

Figure 31. "Regulation of mitochondrial ATP production by OPA1." From (Germain, 2015)

"Members of the SLC25A family of mitochondrial inner membrane transporters sense the levels of mitochondrial metabolites. Starvation leads to a decrease in metabolites, promoting interaction between the transporters and OPA1. This leads to OPA1 oligomerization, reduced cristae width, increased assembly of the ATP synthase, and formation of respiratory supercomplexes, all of which improve mitochondrial efficiency. Conversely, when nutrient levels are high, less OPA1 oligomerizes and mitochondrial ATP production is less efficient. Importantly, these changes occur in a fusion-independent fashion. a-KG, a-ketoglutarate; AGC, aspartate/glutamate carrier; DIC, dicarboxylate carrier; Glu, glutamate; IM, inner membrane; IMS, intermembrane space; Mal, malate; OGC, oxoglutarate carrier; OM, mitochondrial outer membrane; Pi, phosphate; Succ, succinate."

References

Acin-Perez R, Enriquez JA (2014) The function of the respiratory supercomplexes: the plasticity model. *Biochim Biophys Acta* **1837:** 444-450

Acin-Perez R, Fernandez-Silva P, Peleato ML, Perez-Martos A, Enriquez JA (2008) Respiratory active mitochondrial supercomplexes. *Mol Cell* **32:** 529-539

Agostino A, Valletta L, Chinnery PF, Ferrari G, Carrara F, Taylor RW, Schaefer AM, Turnbull DM, Tiranti V, Zeviani M (2003) Mutations of ANT1, Twinkle, and POLG1 in sporadic progressive external ophthalmoplegia (PEO). *Neurology* **60:** 1354-1356

Aguer C, Gambarotta D, Mailloux RJ, Moffat C, Dent R, McPherson R, Harper ME (2011) Galactose enhances oxidative metabolism and reveals mitochondrial dysfunction in human primary muscle cells. *PLoS One* **6:** e28536

Akepati VR, Muller EC, Otto A, Strauss HM, Portwich M, Alexander C (2008) Characterization of OPA1 isoforms isolated from mouse tissues. *J Neurochem* **106:** 372-383

Alam ZI, Jenner A, Daniel SE, Lees AJ, Cairns N, Marsden CD, Jenner P, Halliwell B (1997) Oxidative DNA damage in the parkinsonian brain: an apparent selective increase in 8-hydroxyguanine levels in substantia nigra. *J Neurochem* **69:** 1196-1203

Alavi MV, Bette S, Schimpf S, Schuettauf F, Schraermeyer U, Wehrl HF, Ruttiger L, Beck SC, Tonagel F, Pichler BJ, Knipper M, Peters T, Laufs J, Wissinger B (2007) A splice site mutation in the murine Opa1 gene features pathology of autosomal dominant optic atrophy. *Brain* **130:** 1029-1042

Alavian KN, Beutner G, Lazrove E, Sacchetti S, Park HA, Licznerski P, Li H, Nabili P, Hockensmith K, Graham M, Porter GA, Jr., Jonas EA (2014) An uncoupling channel within the c-subunit ring of the F1FO ATP synthase is the mitochondrial permeability transition pore. *Proceedings of the National Academy of Sciences of the United States of America* **111:** 10580-10585

Alexander C, Votruba M, Pesch UE, Thiselton DL, Mayer S, Moore A, Rodriguez M, Kellner U, Leo-Kottler B, Auburger G, Bhattacharya SS, Wissinger B (2000) OPA1, encoding a dynamin-related GTPase, is mutated in autosomal dominant optic atrophy linked to chromosome 3q28. *Nat Genet* **26:** 211-215

Alkhaja AK, Jans DC, Nikolov M, Vukotic M, Lytovchenko O, Ludewig F, Schliebs W, Riedel D, Urlaub H, Jakobs S, Deckers M (2012) MINOS1 is a conserved component of mitofilin complexes and required for mitochondrial function and cristae organization. *Molecular biology of the cell* **23:** 247-257

Amati-Bonneau P, Valentino ML, Reynier P, Gallardo ME, Bornstein B, Boissiere A, Campos Y, Rivera H, de la Aleja JG, Carroccia R, Iommarini L, Labauge P, Figarella-Branger D, Marcorelles P, Furby A, Beauvais K, Letournel F, Liguori R, La Morgia C, Montagna P, Liguori M, Zanna C, Rugolo M, Cossarizza A, Wissinger B, Verny C, Schwarzenbacher R, Martin MA, Arenas J, Ayuso C, Garesse R, Lenaers G, Bonneau D, Carelli V (2008) OPA1 mutations induce mitochondrial DNA instability and optic atrophy 'plus' phenotypes. *Brain* **131:** 338-351

Amutha B, Gordon DM, Gu Y, Pain D (2004) A novel role of Mgm1p, a dynamin-related GTPase, in ATP synthase assembly and cristae formation/maintenance. *Biochem J* **381:** 19-23

Anand R, Wai T, Baker MJ, Kladt N, Schauss AC, Rugarli E, Langer T (2014) The i-AAA protease YME1L and OMA1 cleave OPA1 to balance mitochondrial fusion and fission. *J Cell Biol* **204:** 919-929

Anderson S, Bankier AT, Barrell BG, de Bruijn MH, Coulson AR, Drouin J, Eperon IC, Nierlich DP, Roe BA, Sanger F, Schreier PH, Smith AJ, Staden R, Young IG (1981) Sequence and organization of the human mitochondrial genome. *Nature* **290:** 457-465

Andreyev AY, Kushnareva YE, Starkov AA (2005) Mitochondrial metabolism of reactive oxygen species. *Biochemistry (Mosc)* **70:** 200-214

Aoki Y, Cortese S (2015) Mitochondrial Aspartate/Glutamate Carrier SLC25A12 and Autism Spectrum Disorder: a Meta-Analysis. *Molecular neurobiology*

Ardail D, Privat JP, Egret-Charlier M, Levrat C, Lerme F, Louisot P (1990) Mitochondrial contact sites. Lipid composition and dynamics. *J Biol Chem* **265:** 18797-18802

Babior BM (2000) The NADPH oxidase of endothelial cells. *IUBMB Life* **50:** 267-269

Ban T, Heymann JA, Song Z, Hinshaw JE, Chan DC (2010) OPA1 disease alleles causing dominant optic atrophy have defects in cardiolipin-stimulated GTP hydrolysis and membrane tubulation. *Human molecular genetics* **19:** 2113-2122

Baradaran R, Berrisford JM, Minhas GS, Sazanov LA (2013) Crystal structure of the entire respiratory complex I. *Nature* **494:** 443-448

Barrientos A, Ugalde C (2013) I function, therefore I am: overcoming skepticism about mitochondrial supercomplexes. *Cell Metab* **18:** 147-149

Barth PG, Scholte HR, Berden JA, Van der Klei-Van Moorsel JM, Luyt-Houwen IE, Van 't Veer-Korthof ET, Van der Harten JJ, Sobotka-Plojhar MA (1983) An X-linked mitochondrial disease affecting cardiac muscle, skeletal muscle and neutrophil leucocytes. *Journal of the neurological sciences* **62:** 327-355

Bazan S, Mileykovskaya E, Mallampalli VK, Heacock P, Sparagna GC, Dowhan W (2013) Cardiolipin-dependent reconstitution of respiratory supercomplexes from purified Saccharomyces cerevisiae complexes III and IV. *J Biol Chem* **288:** 401-411

Beaulieu CL, Majewski J, Schwartzentruber J, Samuels ME, Fernandez BA, Bernier FP, Brudno M, Knoppers B, Marcadier J, Dyment D, Adam S, Bulman DE, Jones SJ, Avard D, Nguyen MT, Rousseau F, Marshall C, Wintle RF, Shen Y, Scherer SW, Friedman JM, Michaud JL, Boycott KM (2014) FORGE Canada Consortium: outcomes of a 2-year national rare-disease gene-discovery project. *American journal of human genetics* **94:** 809-817

Begum L, Jalil MA, Kobayashi K, Iijima M, Li MX, Yasuda T, Horiuchi M, del Arco A, Satrustegui J, Saheki T (2002) Expression of three mitochondrial solute carriers, citrin, aralar1 and ornithine transporter, in relation to urea cycle in mice. *Biochim Biophys Acta* **1574:** 283-292

Bekker A, Holland HD, Wang PL, Rumble D, 3rd, Stein HJ, Hannah JL, Coetzee LL, Beukes NJ (2004) Dating the rise of atmospheric oxygen. *Nature* **427:** 117-120

Belenguer P, Pellegrini L (2013) The dynamin GTPase OPA1: more than mitochondria? *Biochim Biophys Acta* **1833:** 176-183

Bell KF, Al-Mubarak B, Martel MA, McKay S, Wheelan N, Hasel P, Markus NM, Baxter P, Deighton RF, Serio A, Bilican B, Chowdhry S, Meakin PJ, Ashford ML, Wyllie DJ, Scannevin RH, Chandran S, Hayes JD, Hardingham GE (2015) Neuronal development is promoted by weakened intrinsic antioxidant defences due to epigenetic repression of Nrf2. *Nature communications* **6:** 7066

Bender A, Krishnan KJ, Morris CM, Taylor GA, Reeve AK, Perry RH, Jaros E, Hersheson JS, Betts J, Klopstock T, Taylor RW, Turnbull DM (2006) High levels of mitochondrial DNA deletions in substantia nigra neurons in aging and Parkinson disease. *Nat Genet* **38:** 515-517

Berardi MJ, Shih WM, Harrison SC, Chou JJ (2011) Mitochondrial uncoupling protein 2 structure determined by NMR molecular fragment searching. *Nature* **476:** 109-113

Betarbet R, Canet-Aviles RM, Sherer TB, Mastroberardino PG, McLendon C, Kim JH, Lund S, Na HM, Taylor G, Bence NF, Kopito R, Seo BB, Yagi T, Yagi A, Klinefelter G, Cookson MR, Greenamyre JT (2006) Intersecting pathways to neurodegeneration in Parkinson's disease: effects of the pesticide rotenone on DJ-1, alpha-synuclein, and the ubiquitin-proteasome system. *Neurobiology of disease* **22:** 404-420

Bione S, D'Adamo P, Maestrini E, Gedeon AK, Bolhuis PA, Toniolo D (1996) A novel X-linked gene, G4.5. is responsible for Barth syndrome. *Nat Genet* **12:** 385-389

Bleazard W, McCaffery JM, King EJ, Bale S, Mozdy A, Tieu Q, Nunnari J, Shaw JM (1999) The dynamin-related GTPase Dnm1 regulates mitochondrial fission in yeast. *Nat Cell Biol* **1:** 298-304

Booty LM, King MS, Thangaratnarajah C, Majd H, James AM, Kunji ER, Murphy MP (2015) The mitochondrial dicarboxylate and 2-oxoglutarate carriers do not transport glutathione. *FEBS Lett* **589:** 621-628

Boyer PD (1975) A model for conformational coupling of membrane potential and proton translocation to ATP synthesis and to active transport. *FEBS Lett* **58:** 1-6

Boyer PD (1997) The ATP synthase--a splendid molecular machine. *Annu Rev Biochem* **66:** 717-749

Branda SS, Isaya G (1995) Prediction and identification of new natural substrates of the yeast mitochondrial intermediate peptidase. *J Biol Chem* **270:** 27366-27373

Bravo R, Vicencio JM, Parra V, Troncoso R, Munoz JP, Bui M, Quiroga C, Rodriguez AE, Verdejo HE, Ferreira J, Iglewski M, Chiong M, Simmen T, Zorzano A, Hill JA, Rothermel BA, Szabadkai G, Lavandero S (2011) Increased ER-mitochondrial coupling promotes mitochondrial respiration and bioenergetics during early phases of ER stress. *J Cell Sci* **124:** 2143-2152

Breckenridge DG, Stojanovic M, Marcellus RC, Shore GC (2003) Caspase cleavage product of BAP31 induces mitochondrial fission through endoplasmic reticulum calcium signals, enhancing cytochrome c release to the cytosol. *J Cell Biol* **160:** 1115-1127

Bueler H (2010) Mitochondrial dynamics, cell death and the pathogenesis of Parkinson's disease. *Apoptosis* **15:** 1336-1353

Campanella M, Casswell E, Chong S, Farah Z, Wieckowski MR, Abramov AY, Tinker A, Duchen MR (2008) Regulation of mitochondrial structure and function by the F1Fo-ATPase inhibitor protein, IF1. *Cell Metab* **8:** 13-25

Cannon JR, Tapias V, Na HM, Honick AS, Drolet RE, Greenamyre JT (2009) A highly reproducible rotenone model of Parkinson's disease. *Neurobiology of disease* **34:** 279-290

Carelli V, Musumeci O, Caporali L, Zanna C, La Morgia C, Del Dotto V, Porcelli AM, Rugolo M, Valentino ML, Iommarini L, Maresca A, Barboni P, Carbonelli M, Trombetta C, Valente EM, Patergnani S, Giorgi C, Pinton P, Rizzo G, Tonon C, Lodi R, Avoni P, Liguori R, Baruzzi A, Toscano A, Zeviani M (2015) Syndromic parkinsonism and dementia associated with OPA1 missense mutations. *Ann Neurol*

Cereghetti GM, Stangherlin A, Martins de Brito O, Chang CR, Blackstone C, Bernardi P, Scorrano L (2008) Dephosphorylation by calcineurin regulates translocation of Drp1 to

mitochondria. *Proceedings of the National Academy of Sciences of the United States of America* **105:** 15803-15808

Chance B, Williams GR (1955) Respiratory enzymes in oxidative phosphorylation. III. The steady state. *J Biol Chem* **217:** 409-427

Chang CR, Blackstone C (2007) Cyclic AMP-dependent protein kinase phosphorylation of Drp1 regulates its GTPase activity and mitochondrial morphology. *J Biol Chem* **282:** 21583-21587

Chang CR, Manlandro CM, Arnoult D, Stadler J, Posey AE, Hill RB, Blackstone C (2010) A lethal de novo mutation in the middle domain of the dynamin-related GTPase Drp1 impairs higher order assembly and mitochondrial division. *J Biol Chem* **285:** 32494-32503

Chen H, Detmer SA, Ewald AJ, Griffin EE, Fraser SE, Chan DC (2003) Mitofusins Mfn1 and Mfn2 coordinately regulate mitochondrial fusion and are essential for embryonic development. *The Journal of cell biology* **160:** 189-200

Chen H, Vermulst M, Wang YE, Chomyn A, Prolla TA, McCaffery JM, Chan DC (2010) Mitochondrial fusion is required for mtDNA stability in skeletal muscle and tolerance of mtDNA mutations. *Cell* **141:** 280-289

Chen XJ, Butow RA (2005) The organization and inheritance of the mitochondrial genome. *Nat Rev Genet* **6:** 815-825

Chen Z, Lash LH (1998) Evidence for mitochondrial uptake of glutathione by dicarboxylate and 2-oxoglutarate carriers. *The Journal of pharmacology and experimental therapeutics* **285:** 608-618

Chen Z, Putt DA, Lash LH (2000) Enrichment and functional reconstitution of glutathione transport activity from rabbit kidney mitochondria: further evidence for the role of the dicarboxylate and 2-oxoglutarate carriers in mitochondrial glutathione transport. *Archives of biochemistry and biophysics* **373:** 193-202

Chevrollier A, Guillet V, Loiseau D, Gueguen N, de Crescenzo MA, Verny C, Ferre M, Dollfus H, Odent S, Milea D, Goizet C, Amati-Bonneau P, Procaccio V, Bonneau D, Reynier P (2008) Hereditary optic neuropathies share a common mitochondrial coupling defect. *Ann Neurol* **63:** 794-798

Chicco AJ, Sparagna GC (2007) Role of cardiolipin alterations in mitochondrial dysfunction and disease. *Am J Physiol Cell Physiol* **292:** C33-44

Cho DH, Nakamura T, Fang J, Cieplak P, Godzik A, Gu Z, Lipton SA (2009) S-nitrosylation of Drp1 mediates beta-amyloid-related mitochondrial fission and neuronal injury. *Science* **324:** 102-105

Cipolat S, Martins de Brito O, Dal Zilio B, Scorrano L (2004) OPA1 requires mitofusin 1 to promote mitochondrial fusion. *Proceedings of the National Academy of Sciences of the United States of America* **101:** 15927-15932

Cipolat S, Rudka T, Hartmann D, Costa V, Serneels L, Craessaerts K, Metzger K, Frezza C, Annaert W, D'Adamio L, Derks C, Dejaegere T, Pellegrini L, D'Hooge R, Scorrano L, De Strooper B (2006) Mitochondrial rhomboid PARL regulates cytochrome c release during apoptosis via OPA1-dependent cristae remodeling. *Cell* **126:** 163-175

Claypool SM (2009) Cardiolipin, a critical determinant of mitochondrial carrier protein assembly and function. *Biochim Biophys Acta* **1788:** 2059-2068

Cogliati S, Frezza C, Soriano ME, Varanita T, Quintana-Cabrera R, Corrado M, Cipolat S, Costa V, Casarin A, Gomes LC, Perales-Clemente E, Salviati L, Fernandez-Silva P, Enriquez JA, Scorrano L (2013) Mitochondrial cristae shape determines respiratory chain supercomplexes assembly and respiratory efficiency. *Cell* **155:** 160-171

Cosson P, Marchetti A, Ravazzola M, Orci L (2012) Mitofusin-2 independent juxtaposition of endoplasmic reticulum and mitochondria: an ultrastructural study. *PLoS One* **7:** e46293

Cox J, Mann M (2008) MaxQuant enables high peptide identification rates, individualized p.p.b.-range mass accuracies and proteome-wide protein quantification. *Nat Biotechnol* **26:** 1367-1372

Cox RT, Spradling AC (2009) Clueless, a conserved Drosophila gene required for mitochondrial subcellular localization, interacts genetically with parkin. *Dis Model Mech* **2:** 490-499

Cribbs JT, Strack S (2007) Reversible phosphorylation of Drp1 by cyclic AMP-dependent protein kinase and calcineurin regulates mitochondrial fission and cell death. *EMBO Rep* **8:** 939-944

Crompton M, Virji S, Ward JM (1998) Cyclophilin-D binds strongly to complexes of the voltage-dependent anion channel and the adenine nucleotide translocase to form the permeability transition pore. *European journal of biochemistry / FEBS* **258:** 729-735

Cruciat CM, Brunner S, Baumann F, Neupert W, Stuart RA (2000) The cytochrome bc1 and cytochrome c oxidase complexes associate to form a single supracomplex in yeast mitochondria. *J Biol Chem* **275:** 18093-18098

Cui M, Tang X, Christian WV, Yoon Y, Tieu K (2010) Perturbations in mitochondrial dynamics induced by human mutant PINK1 can be rescued by the mitochondrial division inhibitor mdivi-1. *J Biol Chem* **285:** 11740-11752

Culmsee C, Monnig J, Kemp BE, Mattson MP (2001) AMP-activated protein kinase is highly expressed in neurons in the developing rat brain and promotes neuronal survival following glucose deprivation. *Journal of molecular neuroscience : MN* **17:** 45-58

Dagda RK, Cherra SJ, 3rd, Kulich SM, Tandon A, Park D, Chu CT (2009) Loss of PINK1 function promotes mitophagy through effects on oxidative stress and mitochondrial fission. *J Biol Chem* **284:** 13843-13855

Dalton TP, Chen Y, Schneider SN, Nebert DW, Shertzer HG (2004) Genetically altered mice to evaluate glutathione homeostasis in health and disease. *Free Radic Biol Med* **37:** 1511-1526

Darshi M, Mendiola VL, Mackey MR, Murphy AN, Koller A, Perkins GA, Ellisman MH, Taylor SS (2011) ChChd3, an inner mitochondrial membrane protein, is essential for maintaining crista integrity and mitochondrial function. *J Biol Chem* **286:** 2918-2932

Davies VJ, Hollins AJ, Piechota MJ, Yip W, Davies JR, White KE, Nicols PP, Boulton ME, Votruba M (2007) Opa1 deficiency in a mouse model of autosomal dominant optic atrophy impairs mitochondrial morphology, optic nerve structure and visual function. *Human molecular genetics* **16:** 1307-1318

de Brito OM, Scorrano L (2008) Mitofusin 2 tethers endoplasmic reticulum to mitochondria. *Nature* **456:** 605-610

de la Monte SM, Luong T, Neely TR, Robinson D, Wands JR (2000) Mitochondrial DNA damage as a mechanism of cell loss in Alzheimer's disease. *Laboratory investigation; a journal of technical methods and pathology* **80:** 1323-1335

De Vos KJ, Chapman AL, Tennant ME, Manser C, Tudor EL, Lau KF, Brownlees J, Ackerley S, Shaw PJ, McLoughlin DM, Shaw CE, Leigh PN, Miller CC, Grierson AJ (2007) Familial amyotrophic lateral sclerosis-linked SOD1 mutants perturb fast axonal transport to reduce axonal mitochondria content. *Human molecular genetics* **16:** 2720-2728

del Arco A, Morcillo J, Martinez-Morales JR, Galian C, Martos V, Bovolenta P, Satrustegui J (2002) Expression of the aspartate/glutamate mitochondrial carriers aralar1 and citrin during development and in adult rat tissues. *European journal of biochemistry / FEBS* **269:** 3313-3320

Delettre C, Griffoin JM, Kaplan J, Dollfus H, Lorenz B, Faivre L, Lenaers G, Belenguer P, Hamel CP (2001) Mutation spectrum and splicing variants in the OPA1 gene. *Human genetics* **109:** 584-591

Delettre C, Lenaers G, Griffoin JM, Gigarel N, Lorenzo C, Belenguer P, Pelloquin L, Grosgeorge J, Turc-Carel C, Perret E, Astarie-Dequeker C, Lasquellec L, Arnaud B,

Ducommun B, Kaplan J, Hamel CP (2000) Nuclear gene OPA1, encoding a mitochondrial dynamin-related protein, is mutated in dominant optic atrophy. *Nat Genet* **26:** 207-210

Deng H, Dodson MW, Huang H, Guo M (2008) The Parkinson's disease genes pink1 and parkin promote mitochondrial fission and/or inhibit fusion in Drosophila. *Proceedings of the National Academy of Sciences of the United States of America* **105:** 14503-14508

Desmurs M, Foti M, Raemy E, Vaz FM, Martinou JC, Bairoch A, Lane L (2015) C11orf83, a mitochondrial cardiolipin-binding protein involved in bc1 complex assembly and supercomplex stabilization. *Mol Cell Biol* **35:** 1139-1156

DeVay RM, Dominguez-Ramirez L, Lackner LL, Hoppins S, Stahlberg H, Nunnari J (2009) Coassembly of Mgm1 isoforms requires cardiolipin and mediates mitochondrial inner membrane fusion. *J Cell Biol* **186:** 793-803

Devenish RJ, Prescott M, Rodgers AJ (2008) The structure and function of mitochondrial F1F0-ATP synthases. *International review of cell and molecular biology* **267:** 1-58

Devi L, Raghavendran V, Prabhu BM, Avadhani NG, Anandatheerthavarada HK (2008) Mitochondrial import and accumulation of alpha-synuclein impair complex I in human dopaminergic neuronal cultures and Parkinson disease brain. *J Biol Chem* **283:** 9089-9100

Dijkstra G, Moshage H, van Dullemen HM, de Jager-Krikken A, Tiebosch AT, Kleibeuker JH, Jansen PL, van Goor H (1998) Expression of nitric oxide synthases and formation of nitrotyrosine and reactive oxygen species in inflammatory bowel disease. *J Pathol* **186:** 416-421

Duchen MR (2004) Roles of mitochondria in health and disease. *Diabetes* **53 Suppl 1:** S96-102

Duvezin-Caubet S, Koppen M, Wagener J, Zick M, Israel L, Bernacchia A, Jagasia R, Rugarli EI, Imhof A, Neupert W, Langer T, Reichert AS (2007) OPA1 processing reconstituted in yeast depends on the subunit composition of the m-AAA protease in mitochondria. *Molecular biology of the cell* **18:** 3582-3590

Ehses S, Raschke I, Mancuso G, Bernacchia A, Geimer S, Tondera D, Martinou JC, Westermann B, Rugarli EI, Langer T (2009) Regulation of OPA1 processing and mitochondrial fusion by m-AAA protease isoenzymes and OMA1. *J Cell Biol* **187:** 1023-1036

Elachouri G, Vidoni S, Zanna C, Pattyn A, Boukhaddaoui H, Gaget K, Yu-Wai-Man P, Gasparre G, Sarzi E, Delettre C, Olichon A, Loiseau D, Reynier P, Chinnery PF, Rotig A, Carelli V, Hamel CP, Rugolo M, Lenaers G (2011) OPA1 links human mitochondrial genome maintenance to mtDNA replication and distribution. *Genome research* **21:** 12-20

Ernster L, Lee IY, Norling B, Persson B (1969) Studies with ubiquinone-depleted submitochondrial particles. Essentiality of ubiquinone for the interaction of succinate dehydrogenase, NADH dehydrogenase, and cytochrome b. *European journal of biochemistry / FEBS* **9:** 299-310

Ernster L, Schatz G (1981) Mitochondria: a historical review. *The Journal of cell biology* **91:** 227s-255s

Faccenda D, Tan CH, Seraphim A, Duchen MR, Campanella M (2013) IF1 limits the apoptotic-signalling cascade by preventing mitochondrial remodelling. *Cell Death Differ* **20:** 686-697

Fields SD, Arana Q, Heuser J, Clarke M (2002) Mitochondrial membrane dynamics are altered in cluA- mutants of Dictyostelium. *Journal of muscle research and cell motility* **23:** 829-838

Fields SD, Conrad MN, Clarke M (1998) The S. cerevisiae CLU1 and D. discoideum cluA genes are functional homologues that influence mitochondrial morphology and distribution. *J Cell Sci* **111 (Pt 12):** 1717-1727

Fiermonte G, Palmieri L, Dolce V, Lasorsa FM, Palmieri F, Runswick MJ, Walker JE (1998) The sequence, bacterial expression, and functional reconstitution of the rat mitochondrial dicarboxylate transporter cloned via distant homologs in yeast and Caenorhabditis elegans. *J Biol Chem* **273:** 24754-24759

Fiermonte G, Walker JE, Palmieri F (1993) Abundant bacterial expression and reconstitution of an intrinsic membrane-transport protein from bovine mitochondria. *Biochem J* **294 (Pt 1):** 293-299

Filadi R, Greotti E, Turacchio G, Luini A, Pozzan T, Pizzo P (2015) Mitofusin 2 ablation increases endoplasmic reticulum-mitochondria coupling. *Proceedings of the National Academy of Sciences of the United States of America* **112:** E2174-2181

Frank S, Gaume B, Bergmann-Leitner ES, Leitner WW, Robert EG, Catez F, Smith CL, Youle RJ (2001) The role of dynamin-related protein 1, a mediator of mitochondrial fission, in apoptosis. *Dev Cell* **1:** 515-525

Frezza C, Cipolat S, Martins de Brito O, Micaroni M, Beznoussenko GV, Rudka T, Bartoli D, Polishuck RS, Danial NN, De Strooper B, Scorrano L (2006) OPA1 controls apoptotic cristae remodeling independently from mitochondrial fusion. *Cell* **126:** 177-189

Friedman JR, Lackner LL, West M, DiBenedetto JR, Nunnari J, Voeltz GK (2011) ER tubules mark sites of mitochondrial division. *Science* **334:** 358-362

Gallo M, Park D, Luciani DS, Kida K, Palmieri F, Blacque OE, Johnson JD, Riddle DL (2011) MISC-1/OGC links mitochondrial metabolism, apoptosis and insulin secretion. *PLoS One* **6:** e17827

Gao J, Schatton D, Martinelli P, Hansen H, Pla-Martin D, Barth E, Becker C, Altmueller J, Frommolt P, Sardiello M, Rugarli EI (2014) CLUH regulates mitochondrial biogenesis by binding mRNAs of nuclear-encoded mitochondrial proteins. *J Cell Biol* **207:** 213-223

Gao W, Pu Y, Luo KQ, Chang DC (2001) Temporal relationship between cytochrome c release and mitochondrial swelling during UV-induced apoptosis in living HeLa cells. *J Cell Sci* **114:** 2855-2862

Garrido N, Griparic L, Jokitalo E, Wartiovaara J, van der Bliek AM, Spelbrink JN (2003) Composition and dynamics of human mitochondrial nucleoids. *Molecular biology of the cell* **14:** 1583-1596

Geisler S, Holmstrom KM, Treis A, Skujat D, Weber SS, Fiesel FC, Kahle PJ, Springer W (2010) The PINK1/Parkin-mediated mitophagy is compromised by PD-associated mutations. *Autophagy* **6:** 871-878

Germain M (2015) OPA1 and mitochondrial solute carriers in bioenergetic metabolism. *Molecular & Cellular Oncology* **2**

Germain M, Mathai JP, McBride HM, Shore GC (2005) Endoplasmic reticulum BIK initiates DRP1-regulated remodelling of mitochondrial cristae during apoptosis. *Embo J* **24:** 1546-1556

Germain M, Nguyen AP, Khacho M, Patten DA, Screaton RA, Park DS, Slack RS (2013) LKB1-regulated adaptive mechanisms are essential for neuronal survival following mitochondrial dysfunction. *Human molecular genetics* **22:** 952-962

Gibson DG, Young L, Chuang RY, Venter JC, Hutchison CA, 3rd, Smith HO (2009) Enzymatic assembly of DNA molecules up to several hundred kilobases. *Nature methods* **6:** 343-345

Gilkerson RW, Selker JM, Capaldi RA (2003) The cristal membrane of mitochondria is the principal site of oxidative phosphorylation. *FEBS Lett* **546:** 355-358

Giorgio V, von Stockum S, Antoniel M, Fabbro A, Fogolari F, Forte M, Glick GD, Petronilli V, Zoratti M, Szabo I, Lippe G, Bernardi P (2013) Dimers of mitochondrial ATP synthase form the permeability transition pore. *Proceedings of the National Academy of Sciences of the United States of America* **110:** 5887-5892

Goh LH, Zhou X, Lee MC, Lin S, Wang H, Luo Y, Yang X (2013) Clueless regulates aPKC activity and promotes self-renewal cell fate in Drosophila lgl mutant larval brains. *Developmental biology* **381:** 353-364

Gomes AP, Price NL, Ling AJ, Moslehi JJ, Montgomery MK, Rajman L, White JP, Teodoro JS, Wrann CD, Hubbard BP, Mercken EM, Palmeira CM, de Cabo R, Rolo AP, Turner N, Bell EL, Sinclair DA (2013) Declining NAD(+) induces a pseudohypoxic state disrupting nuclear-mitochondrial communication during aging. *Cell* **155:** 1624-1638

Gomes LC, Di Benedetto G, Scorrano L (2011) During autophagy mitochondria elongate, are spared from degradation and sustain cell viability. *Nat Cell Biol* **13:** 589-598

Grant CM, MacIver FH, Dawes IW (1997) Glutathione synthetase is dispensable for growth under both normal and oxidative stress conditions in the yeast Saccharomyces cerevisiae due to an accumulation of the dipeptide gamma-glutamylcysteine. *Molecular biology of the cell* **8:** 1699-1707

Griparic L, Kanazawa T, van der Bliek AM (2007) Regulation of the mitochondrial dynamin-like protein Opa1 by proteolytic cleavage. *J Cell Biol* **178:** 757-764

Guillery O, Malka F, Landes T, Guillou E, Blackstone C, Lombes A, Belenguer P, Arnoult D, Rojo M (2008) Metalloprotease-mediated OPA1 processing is modulated by the mitochondrial membrane potential. *Biology of the cell / under the auspices of the European Cell Biology Organization* **100:** 315-325

Guo W, Jiang L, Bhasin S, Khan SM, Swerdlow RH (2009) DNA extraction procedures meaningfully influence qPCR-based mtDNA copy number determination. *Mitochondrion* **9:** 261-265

Habersetzer J, Larrieu I, Priault M, Salin B, Rossignol R, Brethes D, Paumard P (2013) Human F1F0 ATP synthase, mitochondrial ultrastructure and OXPHOS impairment: a (super-)complex matter? *PLoS One* **8:** e75429

Hackenbrock CR (1966) Ultrastructural bases for metabolically linked mechanical activity in mitochondria. I. Reversible ultrastructural changes with change in metabolic steady state in isolated liver mitochondria. *The Journal of cell biology* **30:** 269-297

Hackenbrock CR (1968a) Chemical and physical fixation of isolated mitochondria in low-energy and high-energy states. *Proceedings of the National Academy of Sciences of the United States of America* **61:** 598-605

Hackenbrock CR (1968b) Ultrastructural bases for metabolically linked mechanical activity in mitochondria. II. Electron transport-linked ultrastructural transformations in mitochondria. *The Journal of cell biology* **37:** 345-369

Hackenbrock CR, Chazotte B, Gupte SS (1986) The random collision model and a critical assessment of diffusion and collision in mitochondrial electron transport. *Journal of bioenergetics and biomembranes* **18:** 331-368

Harner M, Korner C, Walther D, Mokranjac D, Kaesmacher J, Welsch U, Griffith J, Mann M, Reggiori F, Neupert W (2011) The mitochondrial contact site complex, a determinant of mitochondrial architecture. *Embo J* **30:** 4356-4370

Hatle KM, Gummadidala P, Navasa N, Bernardo E, Dodge J, Silverstrim B, Fortner K, Burg E, Suratt BT, Hammer J, Radermacher M, Taatjes DJ, Thornton T, Anguita J, Rincon M (2013) MCJ/DnaJC15, an endogenous mitochondrial repressor of the respiratory chain that controls metabolic alterations. *Mol Cell Biol* **33:** 2302-2314

He J, Cooper HM, Reyes A, Di Re M, Sembongi H, Litwin TR, Gao J, Neuman KC, Fearnley IM, Spinazzola A, Walker JE, Holt IJ (2012) Mitochondrial nucleoid interacting proteins support mitochondrial protein synthesis. *Nucleic Acids Res* **40:** 6109-6121

He J, Mao CC, Reyes A, Sembongi H, Di Re M, Granycome C, Clippingdale AB, Fearnley IM, Harbour M, Robinson AJ, Reichelt S, Spelbrink JN, Walker JE, Holt IJ (2007) The AAA+ protein ATAD3 has displacement loop binding properties and is involved in mitochondrial nucleoid organization. *J Cell Biol* **176:** 141-146

Head B, Griparic L, Amiri M, Gandre-Babbe S, van der Bliek AM (2009) Inducible proteolytic inactivation of OPA1 mediated by the OMA1 protease in mammalian cells. *J Cell Biol* **187:** 959-966

Holt IJ, He J, Mao CC, Boyd-Kirkup JD, Martinsson P, Sembongi H, Reyes A, Spelbrink JN (2007) Mammalian mitochondrial nucleoids: organizing an independently minded genome. *Mitochondrion* **7:** 311-321

Hoppins S, Collins SR, Cassidy-Stone A, Hummel E, Devay RM, Lackner LL, Westermann B, Schuldiner M, Weissman JS, Nunnari J (2011) A mitochondrial-focused genetic interaction map reveals a scaffold-like complex required for inner membrane organization in mitochondria. *The Journal of cell biology* **195:** 323-340

Hori A, Yoshida M, Ling F (2011) Mitochondrial fusion increases the mitochondrial DNA copy number in budding yeast. *Genes Cells* **16:** 527-544

Huang CS, Moore WR, Meister A (1988) On the active site thiol of gamma-glutamylcysteine synthetase: relationships to catalysis, inhibition, and regulation. *Proceedings of the National Academy of Sciences of the United States of America* **85:** 2464-2468

Hudder A, Nathanson L, Deutscher MP (2003) Organization of mammalian cytoplasm. *Mol Cell Biol* **23:** 9318-9326

Hudson G, Amati-Bonneau P, Blakely EL, Stewart JD, He L, Schaefer AM, Griffiths PG, Ahlqvist K, Suomalainen A, Reynier P, McFarland R, Turnbull DM, Chinnery PF, Taylor RW (2008) Mutation of OPA1 causes dominant optic atrophy with external

ophthalmoplegia, ataxia, deafness and multiple mitochondrial DNA deletions: a novel disorder of mtDNA maintenance. *Brain* **131:** 329-337

Hutter DE, Till BG, Greene JJ (1997) Redox state changes in density-dependent regulation of proliferation. *Experimental cell research* **232:** 435-438

Huypens P, Pillai R, Sheinin T, Schaefer S, Huang M, Odegaard ML, Ronnebaum SM, Wettig SD, Joseph JW (2011) The dicarboxylate carrier plays a role in mitochondrial malate transport and in the regulation of glucose-stimulated insulin secretion from rat pancreatic beta cells. *Diabetologia* **54:** 135-145

Ikeda K, Shiba S, Horie-Inoue K, Shimokata K, Inoue S (2013) A stabilizing factor for mitochondrial respiratory supercomplex assembly regulates energy metabolism in muscle. *Nature communications* **4:** 2147

Indiveri C, Palmieri F, Bisaccia F, Kramer R (1987) Kinetics of the reconstituted 2-oxoglutarate carrier from bovine heart mitochondria. *Biochim Biophys Acta* **890:** 310-318

Ingerman E, Perkins EM, Marino M, Mears JA, McCaffery JM, Hinshaw JE, Nunnari J (2005) Dnm1 forms spirals that are structurally tailored to fit mitochondria. *J Cell Biol* **170:** 1021-1027

Ishihara N, Eura Y, Mihara K (2004) Mitofusin 1 and 2 play distinct roles in mitochondrial fusion reactions via GTPase activity. *J Cell Sci* **117:** 6535-6546

Ishihara N, Fujita Y, Oka T, Mihara K (2006) Regulation of mitochondrial morphology through proteolytic cleavage of OPA1. *Embo J* **25:** 2966-2977

Ishihara N, Nomura M, Jofuku A, Kato H, Suzuki SO, Masuda K, Otera H, Nakanishi Y, Nonaka I, Goto Y, Taguchi N, Morinaga H, Maeda M, Takayanagi R, Yokota S, Mihara K (2009) Mitochondrial fission factor Drp1 is essential for embryonic development and synapse formation in mice. *Nat Cell Biol* **11:** 958-966

Itoh K, Nakamura K, Iijima M, Sesaki H (2013) Mitochondrial dynamics in neurodegeneration. *Trends in cell biology* **23:** 64-71

Jahani-Asl A, Cheung EC, Neuspiel M, MacLaurin JG, Fortin A, Park DS, McBride HM, Slack RS (2007) Mitofusin 2 protects cerebellar granule neurons against injury-induced cell death. *J Biol Chem* **282:** 23788-23798

Jahani-Asl A, Pilon-Larose K, Xu W, MacLaurin JG, Park DS, McBride HM, Slack RS (2011) The mitochondrial inner membrane GTPase, optic atrophy 1 (Opa1), restores mitochondrial morphology and promotes neuronal survival following excitotoxicity. *J Biol Chem* **286:** 4772-4782

Javaux EJ, Knoll AH, Walter MR (2001) Morphological and ecological complexity in early eukaryotic ecosystems. *Nature* **412:** 66-69

John GB, Shang Y, Li L, Renken C, Mannella CA, Selker JM, Rangell L, Bennett MJ, Zha J (2005) The mitochondrial inner membrane protein mitofilin controls cristae morphology. *Molecular biology of the cell* **16:** 1543-1554

Jonckheere AI, Hogeveen M, Nijtmans LG, van den Brand MA, Janssen AJ, Diepstra JH, van den Brandt FC, van den Heuvel LP, Hol FA, Hofste TG, Kapusta L, Dillmann U, Shamdeen MG, Smeitink JA, Rodenburg RJ (2008) A novel mitochondrial ATP8 gene mutation in a patient with apical hypertrophic cardiomyopathy and neuropathy. *J Med Genet* **45:** 129-133

Jonckheere AI, Smeitink JA, Rodenburg RJ (2012) Mitochondrial ATP synthase: architecture, function and pathology. *Journal of inherited metabolic disease* **35:** 211-225

Kamga CK, Zhang SX, Wang Y (2010) Dicarboxylate carrier-mediated glutathione transport is essential for reactive oxygen species homeostasis and normal respiration in rat brain mitochondria. *Am J Physiol Cell Physiol* **299:** C497-505

Karp G (2002) *Cell and molecular biology : concepts and experiments*, 3rd edn. New York: J. Wiley.

Kasahara A, Scorrano L (2014) Mitochondria: from cell death executioners to regulators of cell differentiation. *Trends in cell biology* **24:** 761-770

Kaufman BA, Newman SM, Hallberg RL, Slaughter CA, Perlman PS, Butow RA (2000) In organello formaldehyde crosslinking of proteins to mtDNA: identification of bifunctional proteins. *Proceedings of the National Academy of Sciences of the United States of America* **97:** 7772-7777

Kaukonen J, Juselius JK, Tiranti V, Kyttala A, Zeviani M, Comi GP, Keranen S, Peltonen L, Suomalainen A (2000) Role of adenine nucleotide translocator 1 in mtDNA maintenance. *Science* **289:** 782-785

Khacho M, Slack RS (2015) Mitochondrial dynamics in neurodegeneration: from cell death to energetic states. *AIMS Molecular Science* **2:** 161-174

Khacho M, Tarabay M, Patten D, Khacho P, MacLaurin JG, Guadagno J, Bergeron R, Cregan SP, Harper ME, Park DS, Slack RS (2014) Acidosis overrides oxygen deprivation to maintain mitochondrial function and cell survival. *Nature communications* **5:** 3550

Kim JY, Hwang JM, Ko HS, Seong MW, Park BJ, Park SS (2005) Mitochondrial DNA content is decreased in autosomal dominant optic atrophy. *Neurology* **64:** 966-972

Kim TH, Zhao Y, Ding WX, Shin JN, He X, Seo YW, Chen J, Rabinowich H, Amoscato AA, Yin XM (2004) Bid-cardiolipin interaction at mitochondrial contact site contributes to mitochondrial cristae reorganization and cytochrome C release. *Molecular biology of the cell* **15:** 3061-3072

Kjer P (1959) Infantile optic atrophy with dominant mode of inheritance: a clinical and genetic study of 19 Danish families. *Acta ophthalmologica Supplementum* **164:** 1-147

Kobayashi K, Sinasac DS, Iijima M, Boright AP, Begum L, Lee JR, Yasuda T, Ikeda S, Hirano R, Terazono H, Crackower MA, Kondo I, Tsui LC, Scherer SW, Saheki T (1999) The gene mutated in adult-onset type II citrullinaemia encodes a putative mitochondrial carrier protein. *Nat Genet* **22:** 159-163

Kokoszka JE, Waymire KG, Levy SE, Sligh JE, Cai J, Jones DP, MacGregor GR, Wallace DC (2004) The ADP/ATP translocator is not essential for the mitochondrial permeability transition pore. *Nature* **427:** 461-465

Koob S, Barrera M, Anand R, Reichert AS (2015) The non-glycosylated isoform of MIC26 is a constituent of the mammalian MICOS complex and promotes formation of crista junctions. *Biochim Biophys Acta* **1853:** 1551-1563

Koshiba T, Detmer SA, Kaiser JT, Chen H, McCaffery JM, Chan DC (2004) Structural basis of mitochondrial tethering by mitofusin complexes. *Science* **305:** 858-862

Krebs HA, Johnson WA (1980) The role of citric acid in intermediate metabolism in animal tissues. *FEBS Lett* **117 Suppl:** K1-10

Kukat C, Wurm CA, Spahr H, Falkenberg M, Larsson NG, Jakobs S (2011) Super-resolution microscopy reveals that mammalian mitochondrial nucleoids have a uniform size and frequently contain a single copy of mtDNA. *Proceedings of the National Academy of Sciences of the United States of America* **108:** 13534-13539

Kunji ER, Crichton PG (2010) Mitochondrial carriers function as monomers. *Biochim Biophys Acta* **1797:** 817-831

Langston JW, Forno LS, Rebert CS, Irwin I (1984) Selective nigral toxicity after systemic administration of 1-methyl-4-phenyl-1,2,5,6-tetrahydropyrine (MPTP) in the squirrel monkey. *Brain research* **292:** 390-394

LaNoue KF, Walajtys EI, Williamson JR (1973) Regulation of glutamate metabolism and interactions with the citric acid cycle in rat heart mitochondria. *J Biol Chem* **248:** 7171-7183

Lapuente-Brun E, Moreno-Loshuertos R, Acin-Perez R, Latorre-Pellicer A, Colas C, Balsa E, Perales-Clemente E, Quiros PM, Calvo E, Rodriguez-Hernandez MA, Navas P, Cruz R, Carracedo A, Lopez-Otin C, Perez-Martos A, Fernandez-Silva P, Fernandez-Vizarra E,

Enriquez JA (2013) Supercomplex assembly determines electron flux in the mitochondrial electron transport chain. *Science* **340:** 1567-1570

Lash LH, Putt DA, Matherly LH (2002) Protection of NRK-52E cells, a rat renal proximal tubular cell line, from chemical-induced apoptosis by overexpression of a mitochondrial glutathione transporter. *The Journal of pharmacology and experimental therapeutics* **303:** 476-486

Lebovitz RM, Zhang H, Vogel H, Cartwright J, Jr., Dionne L, Lu N, Huang S, Matzuk MM (1996) Neurodegeneration, myocardial injury, and perinatal death in mitochondrial superoxide dismutase-deficient mice. *Proceedings of the National Academy of Sciences of the United States of America* **93:** 9782-9787

Lee YJ, Jeong SY, Karbowski M, Smith CL, Youle RJ (2004) Roles of the mammalian mitochondrial fission and fusion mediators Fis1, Drp1, and Opa1 in apoptosis. *Molecular biology of the cell* **15:** 5001-5011

Legros F, Malka F, Frachon P, Lombes A, Rojo M (2004) Organization and dynamics of human mitochondrial DNA. *J Cell Sci* **117:** 2653-2662

Lenaers G, Hamel C, Delettre C, Amati-Bonneau P, Procaccio V, Bonneau D, Reynier P, Milea D (2012) Dominant optic atrophy. *Orphanet journal of rare diseases* **7:** 46

Lenaz G, Genova ML (2012) Supramolecular organisation of the mitochondrial respiratory chain: a new challenge for the mechanism and control of oxidative phosphorylation. *Adv Exp Med Biol* **748:** 107-144

Li Z, Okamoto K, Hayashi Y, Sheng M (2004) The importance of dendritic mitochondria in the morphogenesis and plasticity of spines and synapses. *Cell* **119:** 873-887

Liesa M, Palacin M, Zorzano A (2009) Mitochondrial dynamics in mammalian health and disease. *Physiological reviews* **89:** 799-845

Lin J, Wu PH, Tarr PT, Lindenberg KS, St-Pierre J, Zhang CY, Mootha VK, Jager S, Vianna CR, Reznick RM, Cui L, Manieri M, Donovan MX, Wu Z, Cooper MP, Fan MC, Rohas LM, Zavacki AM, Cinti S, Shulman GI, Lowell BB, Krainc D, Spiegelman BM (2004) Defects in adaptive energy metabolism with CNS-linked hyperactivity in PGC-1alpha null mice. *Cell* **119:** 121-135

Lin MT, Beal MF (2006) Mitochondrial dysfunction and oxidative stress in neurodegenerative diseases. *Nature* **443:** 787-795

Lin MT, Cantuti-Castelvetri I, Zheng K, Jackson KE, Tan YB, Arzberger T, Lees AJ, Betensky RA, Beal MF, Simon DK (2012) Somatic mitochondrial DNA mutations in early Parkinson and incidental Lewy body disease. *Ann Neurol* **71:** 850-854

Liu RM, Gaston Pravia KA (2010) Oxidative stress and glutathione in TGF-beta-mediated fibrogenesis. *Free Radic Biol Med* **48:** 1-15

Lodish HF (2000) *Molecular cell biology*, 4th edn. New York: W.H. Freeman.

Logan DC, Scott I, Tobin AK (2003) The genetic control of plant mitochondrial morphology and dynamics. *The Plant journal : for cell and molecular biology* **36:** 500-509

Loson OC, Song Z, Chen H, Chan DC (2013) Fis1, Mff, MiD49, and MiD51 mediate Drp1 recruitment in mitochondrial fission. *Molecular biology of the cell* **24:** 659-667

Lu SC (2000) Regulation of glutathione synthesis. *Current topics in cellular regulation* **36:** 95-116

Lu SC (2009) Regulation of glutathione synthesis. *Mol Aspects Med* **30:** 42-59

Lu T, Pan Y, Kao SY, Li C, Kohane I, Chan J, Yankner BA (2004) Gene regulation and DNA damage in the ageing human brain. *Nature* **429:** 883-891

Lupas A (1996) Coiled coils: new structures and new functions. *Trends in biochemical sciences* **21:** 375-382

Lutz AK, Exner N, Fett ME, Schlehe JS, Kloos K, Lammermann K, Brunner B, Kurz-Drexler A, Vogel F, Reichert AS, Bouman L, Vogt-Weisenhorn D, Wurst W, Tatzelt J, Haass C, Winklhofer KF (2009) Loss of parkin or PINK1 function increases Drp1-dependent mitochondrial fragmentation. *J Biol Chem* **284:** 22938-22951

Lyons TW, Reinhard CT, Planavsky NJ (2014) The rise of oxygen in Earth's early ocean and atmosphere. *Nature* **506:** 307-315

Mailloux RJ, Harper ME (2011) Uncoupling proteins and the control of mitochondrial reactive oxygen species production. *Free Radic Biol Med* **51:** 1106-1115

Mailloux RJ, Seifert EL, Bouillaud F, Aguer C, Collins S, Harper ME (2011) Glutathionylation acts as a control switch for uncoupling proteins UCP2 and UCP3. *J Biol Chem* **286:** 21865-21875

Mailloux RJ, Willmore WG (2014) S-glutathionylation reactions in mitochondrial function and disease. *Frontiers in cell and developmental biology* **2:** 68

Mailloux RJ, Xuan JY, McBride S, Maharsy W, Thorn S, Holterman CE, Kennedy CR, Rippstein P, deKemp R, da Silva J, Nemer M, Lou M, Harper ME (2014) Glutaredoxin-2 is required to control oxidative phosphorylation in cardiac muscle by mediating deglutathionylation reactions. *J Biol Chem* **289:** 14812-14828

Mannella CA (2006) Structure and dynamics of the mitochondrial inner membrane cristae. *Biochim Biophys Acta* **1763:** 542-548

Mannella CA, Lederer WJ, Jafri MS (2013) The connection between inner membrane topology and mitochondrial function. *Journal of molecular and cellular cardiology* **62:** 51-57

Mannella CA, Marko M, Penczek P, Barnard D, Frank J (1994) The internal compartmentation of rat-liver mitochondria: tomographic study using the high-voltage transmission electron microscope. *Microscopy research and technique* **27:** 278-283

Mao CC, Holt IJ (2009) Clinical and molecular aspects of diseases of mitochondrial DNA instability. *Chang Gung Med J* **32:** 354-369

Maranzana E, Barbero G, Falasca AI, Lenaz G, Genova ML (2013) Mitochondrial respiratory supercomplex association limits production of reactive oxygen species from complex I. *Antioxid Redox Signal* **19:** 1469-1480

Mari M, Morales A, Colell A, Garcia-Ruiz C, Kaplowitz N, Fernandez-Checa JC (2013) Mitochondrial glutathione: features, regulation and role in disease. *Biochim Biophys Acta* **1830:** 3317-3328

Martin LJ, Pan Y, Price AC, Sterling W, Copeland NG, Jenkins NA, Price DL, Lee MK (2006) Parkinson's disease alpha-synuclein transgenic mice develop neuronal mitochondrial degeneration and cell death. *J Neurosci* **26:** 41-50

Matsuda N, Sato S, Shiba K, Okatsu K, Saisho K, Gautier CA, Sou YS, Saiki S, Kawajiri S, Sato F, Kimura M, Komatsu M, Hattori N, Tanaka K (2010) PINK1 stabilized by mitochondrial depolarization recruits Parkin to damaged mitochondria and activates latent Parkin for mitophagy. *J Cell Biol* **189:** 211-221

Mazzocco MM, Kelley RI (2001) Preliminary evidence for a cognitive phenotype in Barth syndrome. *American journal of medical genetics* **102:** 372-378

McBride H, Soubannier V (2010) Mitochondrial function: OMA1 and OPA1, the grandmasters of mitochondrial health. *Curr Biol* **20:** R274-276

McKenzie M, Lazarou M, Thorburn DR, Ryan MT (2006) Mitochondrial respiratory chain supercomplexes are destabilized in Barth Syndrome patients. *J Mol Biol* **361:** 462-469

Mears JA, Lackner LL, Fang S, Ingerman E, Nunnari J, Hinshaw JE (2011) Conformational changes in Dnm1 support a contractile mechanism for mitochondrial fission. *Nature structural & molecular biology* **18:** 20-26

Meeusen S, DeVay R, Block J, Cassidy-Stone A, Wayson S, McCaffery JM, Nunnari J (2006) Mitochondrial inner-membrane fusion and crista maintenance requires the dynamin-related GTPase Mgm1. *Cell* **127:** 383-395

Meister A, Anderson ME (1983) Glutathione. *Annu Rev Biochem* **52:** 711-760

Meredith MJ, Reed DJ (1982) Status of the mitochondrial pool of glutathione in the isolated hepatocyte. *J Biol Chem* **257:** 3747-3753

Merkwirth C, Dargazanli S, Tatsuta T, Geimer S, Lower B, Wunderlich FT, von Kleist-Retzow JC, Waisman A, Westermann B, Langer T (2008) Prohibitins control cell proliferation and apoptosis by regulating OPA1-dependent cristae morphogenesis in mitochondria. *Genes & development* **22:** 476-488

Minauro-Sanmiguel F, Wilkens S, Garcia JJ (2005) Structure of dimeric mitochondrial ATP synthase: novel F0 bridging features and the structural basis of mitochondrial cristae biogenesis. *Proceedings of the National Academy of Sciences of the United States of America* **102:** 12356-12358

Misaka T, Miyashita T, Kubo Y (2002) Primary structure of a dynamin-related mouse mitochondrial GTPase and its distribution in brain, subcellular localization, and effect on mitochondrial morphology. *J Biol Chem* **277:** 15834-15842

Mishra P, Carelli V, Manfredi G, Chan DC (2014) Proteolytic cleavage of Opa1 stimulates mitochondrial inner membrane fusion and couples fusion to oxidative phosphorylation. *Cell Metab* **19:** 630-641

Misko A, Jiang S, Wegorzewska I, Milbrandt J, Baloh RH (2010) Mitofusin 2 is necessary for transport of axonal mitochondria and interacts with the Miro/Milton complex. *J Neurosci* **30:** 4232-4240

Misko AL, Sasaki Y, Tuck E, Milbrandt J, Baloh RH (2012) Mitofusin2 mutations disrupt axonal mitochondrial positioning and promote axon degeneration. *J Neurosci* **32:** 4145-4155

Mitchell P (1961) Coupling of phosphorylation to electron and hydrogen transfer by a chemi-osmotic type of mechanism. *Nature* **191:** 144-148

Monne M, Miniero DV, Iacobazzi V, Bisaccia F, Fiermonte G (2013) The mitochondrial oxoglutarate carrier: from identification to mechanism. *Journal of bioenergetics and biomembranes* **45:** 1-13

Moore BA, Gonzalez Aviles GD, Larkins CE, Hillman MJ, Caspary T (2010) Mitochondrial retention of Opa1 is required for mouse embryogenesis. *Mammalian genome : official journal of the International Mammalian Genome Society* **21:** 350-360

Mourier A, Motori E, Brandt T, Lagouge M, Atanassov I, Galinier A, Rappl G, Brodesser S, Hultenby K, Dieterich C, Larsson NG (2015) Mitofusin 2 is required to maintain mitochondrial coenzyme Q levels. *J Cell Biol* **208:** 429-442

Muller-Rischart AK, Pilsl A, Beaudette P, Patra M, Hadian K, Funke M, Peis R, Deinlein A, Schweimer C, Kuhn PH, Lichtenthaler SF, Motori E, Hrelia S, Wurst W, Trumbach D, Langer T, Krappmann D, Dittmar G, Tatzelt J, Winklhofer KF (2013) The E3 ligase parkin maintains mitochondrial integrity by increasing linear ubiquitination of NEMO. *Mol Cell* **49:** 908-921

Muller FL, Liu Y, Van Remmen H (2004) Complex III releases superoxide to both sides of the inner mitochondrial membrane. *J Biol Chem* **279:** 49064-49073

Naon D, Scorrano L (2014) At the right distance: ER-mitochondria juxtaposition in cell life and death. *Biochim Biophys Acta* **1843:** 2184-2194

Narendra D, Tanaka A, Suen DF, Youle RJ (2008) Parkin is recruited selectively to impaired mitochondria and promotes their autophagy. *J Cell Biol* **183:** 795-803

Narendra DP, Jin SM, Tanaka A, Suen DF, Gautier CA, Shen J, Cookson MR, Youle RJ (2010) PINK1 is selectively stabilized on impaired mitochondria to activate Parkin. *PLoS Biol* **8:** e1000298

Navarro A, Boveris A (2010) Brain mitochondrial dysfunction in aging, neurodegeneration, and Parkinson's disease. *Frontiers in aging neuroscience* **2**

Neupert W (1997) Protein import into mitochondria. *Annu Rev Biochem* **66:** 863-917

Nsiah-Sefaa A, Brown EL, Russell AP, Foletta VC (2014) New gene targets of PGC-1alpha and ERRalpha co-regulation in C2C12 myotubes. *Molecular biology reports* **41:** 8009-8017

Odegaard ML, Joseph JW, Jensen MV, Lu D, Ilkayeva O, Ronnebaum SM, Becker TC, Newgard CB (2010) The mitochondrial 2-oxoglutarate carrier is part of a metabolic pathway that mediates glucose- and glutamine-stimulated insulin secretion. *J Biol Chem* **285:** 16530-16537

Olichon A, Elachouri G, Baricault L, Delettre C, Belenguer P, Lenaers G (2007) OPA1 alternate splicing uncouples an evolutionary conserved function in mitochondrial fusion from a vertebrate restricted function in apoptosis. *Cell Death Differ* **14:** 682-692

Oppenheimer L, Wellner VP, Griffith OW, Meister A (1979) Glutathione synthetase. Purification from rat kidney and mapping of the substrate binding sites. *J Biol Chem* **254:** 5184-5190

Orrenius S (2007) Reactive oxygen species in mitochondria-mediated cell death. *Drug Metab Rev* **39:** 443-455

Otera H, Wang C, Cleland MM, Setoguchi K, Yokota S, Youle RJ, Mihara K (2010) Mff is an essential factor for mitochondrial recruitment of Drp1 during mitochondrial fission in mammalian cells. *J Cell Biol* **191:** 1141-1158

Pallardo FV, Markovic J, Garcia JL, Vina J (2009) Role of nuclear glutathione as a key regulator of cell proliferation. *Mol Aspects Med* **30:** 77-85

Palmer CS, Elgass KD, Parton RG, Osellame LD, Stojanovski D, Ryan MT (2013) Adaptor proteins MiD49 and MiD51 can act independently of Mff and Fis1 in Drp1 recruitment and are specific for mitochondrial fission. *J Biol Chem* **288:** 27584-27593

Palmieri F (2013) The mitochondrial transporter family SLC25: identification, properties and physiopathology. *Mol Aspects Med* **34:** 465-484

Palmieri F, Prezioso G, Quagliariello E, Klingenberg M (1971) Kinetic study of the dicarboxylate carrier in rat liver mitochondria. *European journal of biochemistry / FEBS* **22:** 66-74

Palmieri F, Quagliariello E, Klingenberger M (1972) Kinetics and specificity of the oxoglutarate carrier in rat-liver mitochondria. *European journal of biochemistry / FEBS* **29:** 408-416

Palmieri L, Palmieri F, Runswick MJ, Walker JE (1996) Identification by bacterial expression and functional reconstitution of the yeast genomic sequence encoding the mitochondrial dicarboxylate carrier protein. *FEBS Lett* **399:** 299-302

Palmieri L, Pardo B, Lasorsa FM, del Arco A, Kobayashi K, Iijima M, Runswick MJ, Walker JE, Saheki T, Satrustegui J, Palmieri F (2001) Citrin and aralar1 are Ca(2+)-stimulated aspartate/glutamate transporters in mitochondria. *Embo J* **20:** 5060-5069

Park YY, Lee S, Karbowski M, Neutzner A, Youle RJ, Cho H (2010) Loss of MARCH5 mitochondrial E3 ubiquitin ligase induces cellular senescence through dynamin-related protein 1 and mitofusin 1. *J Cell Sci* **123:** 619-626

Patten DA, Germain M, Kelly MA, Slack RS (2010) Reactive oxygen species: stuck in the middle of neurodegeneration. *Journal of Alzheimer's disease : JAD* **20 Suppl 2:** S357-367

Patten DA, Wong J, Khacho M, Soubannier V, Mailloux RJ, Pilon-Larose K, MacLaurin JG, Park DS, McBride HM, Trinkle-Mulcahy L, Harper ME, Germain M, Slack RS (2014) OPA1-dependent cristae modulation is essential for cellular adaptation to metabolic demand. *Embo J* **33:** 2676-2691

Paumard P, Vaillier J, Coulary B, Schaeffer J, Soubannier V, Mueller DM, Brethes D, di Rago JP, Velours J (2002) The ATP synthase is involved in generating mitochondrial cristae morphology. *Embo J* **21:** 221-230

Pebay-Peyroula E, Dahout-Gonzalez C, Kahn R, Trezeguet V, Lauquin GJ, Brandolin G (2003) Structure of mitochondrial ADP/ATP carrier in complex with carboxyatractyloside. *Nature* **426:** 39-44

Pfeiffer K, Gohil V, Stuart RA, Hunte C, Brandt U, Greenberg ML, Schagger H (2003) Cardiolipin stabilizes respiratory chain supercomplexes. *J Biol Chem* **278:** 52873-52880

Pickrell AM, Youle RJ (2015) The roles of PINK1, parkin, and mitochondrial fidelity in Parkinson's disease. *Neuron* **85:** 257-273

Pitceathly RD, Murphy SM, Cottenie E, Chalasani A, Sweeney MG, Woodward C, Mudanohwo EE, Hargreaves I, Heales S, Land J, Holton JL, Houlden H, Blake J, Champion M, Flinter F, Robb SA, Page R, Rose M, Palace J, Crowe C, Longman C, Lunn MP, Rahman S, Reilly MM, Hanna MG (2012) Genetic dysfunction of MT-ATP6 causes axonal Charcot-Marie-Tooth disease. *Neurology* **79:** 1145-1154

Pitts KR, McNiven MA, Yoon Y (2004) Mitochondria-specific function of the dynamin family protein DLP1 is mediated by its C-terminal domains. *J Biol Chem* **279:** 50286-50294

Porras G, Li Q, Bezard E (2012) Modeling Parkinson's disease in primates: The MPTP model. *Cold Spring Harbor perspectives in medicine* **2:** a009308

Powell K (2005) Were mitochondrial contractions driving the cellular energy cycle? *The Journal of Cell Biology* **169:** 217-218

Quiros PM, Ramsay AJ, Sala D, Fernandez-Vizarra E, Rodriguez F, Peinado JR, Fernandez-Garcia MS, Vega JA, Enriquez JA, Zorzano A, Lopez-Otin C (2012) Loss of mitochondrial protease OMA1 alters processing of the GTPase OPA1 and causes obesity and defective thermogenesis in mice. *Embo J* **31:** 2117-2133

Rabl R, Soubannier V, Scholz R, Vogel F, Mendl N, Vasiljev-Neumeyer A, Korner C, Jagasia R, Keil T, Baumeister W, Cyrklaff M, Neupert W, Reichert AS (2009) Formation of cristae and crista junctions in mitochondria depends on antagonism between Fcj1 and Su e/g. *J Cell Biol* **185:** 1047-1063

Raja V, Greenberg ML (2014) The functions of cardiolipin in cellular metabolism-potential modifiers of the Barth syndrome phenotype. *Chemistry and physics of lipids* **179:** 49-56

Rak M, Tetaud E, Godard F, Sagot I, Salin B, Duvezin-Caubet S, Slonimski PP, Rytka J, di Rago JP (2007) Yeast cells lacking the mitochondrial gene encoding the ATP synthase

subunit 6 exhibit a selective loss of complex IV and unusual mitochondrial morphology. *J Biol Chem* **282:** 10853-10864

Rambold AS, Kostelecky B, Elia N, Lippincott-Schwartz J (2011) Tubular network formation protects mitochondria from autophagosomal degradation during nutrient starvation. *Proceedings of the National Academy of Sciences of the United States of America* **108:** 10190-10195

Ramonet D, Perier C, Recasens A, Dehay B, Bove J, Costa V, Scorrano L, Vila M (2013) Optic atrophy 1 mediates mitochondria remodeling and dopaminergic neurodegeneration linked to complex I deficiency. *Cell Death Differ* **20:** 77-85

Ranieri M, Del Bo R, Bordoni A, Ronchi D, Colombo I, Riboldi G, Cosi A, Servida M, Magri F, Moggio M, Bresolin N, Comi GP, Corti S (2012) Optic atrophy plus phenotype due to mutations in the OPA1 gene: two more Italian families. *Journal of the neurological sciences* **315:** 146-149

Reyes A, He J, Mao CC, Bailey LJ, Di Re M, Sembongi H, Kazak L, Dzionek K, Holmes JB, Cluett TJ, Harbour ME, Fearnley IM, Crouch RJ, Conti MA, Adelstein RS, Walker JE, Holt IJ (2011) Actin and myosin contribute to mammalian mitochondrial DNA maintenance. *Nucleic Acids Res* **39:** 5098-5108

Ribas V, Garcia-Ruiz C, Fernandez-Checa JC (2014) Glutathione and mitochondria. *Frontiers in pharmacology* **5:** 151

Richman PG, Meister A (1975) Regulation of gamma-glutamyl-cysteine synthetase by nonallosteric feedback inhibition by glutathione. *J Biol Chem* **250:** 1422-1426

Robinson AJ, Kunji ER (2006) Mitochondrial carriers in the cytoplasmic state have a common substrate binding site. *Proceedings of the National Academy of Sciences of the United States of America* **103:** 2617-2622

Santel A, Frank S, Gaume B, Herrler M, Youle RJ, Fuller MT (2003) Mitofusin-1 protein is a generally expressed mediator of mitochondrial fusion in mammalian cells. *J Cell Sci* **116:** 2763-2774

Satoh M, Kuroiwa T (1991) Organization of multiple nucleoids and DNA molecules in mitochondria of a human cell. *Experimental cell research* **196:** 137-140

Satrustegui J, Pardo B, Del Arco A (2007) Mitochondrial transporters as novel targets for intracellular calcium signaling. *Physiological reviews* **87:** 29-67

Schagger H, Pfeiffer K (2000) Supercomplexes in the respiratory chains of yeast and mammalian mitochondria. *Embo J* **19:** 1777-1783

Schlame M, Ren M (2006) Barth syndrome, a human disorder of cardiolipin metabolism. *FEBS Lett* **580:** 5450-5455

Schlame M, Rua D, Greenberg ML (2000) The biosynthesis and functional role of cardiolipin. *Progress in lipid research* **39:** 257-288

Scorrano L, Ashiya M, Buttle K, Weiler S, Oakes SA, Mannella CA, Korsmeyer SJ (2002) A distinct pathway remodels mitochondrial cristae and mobilizes cytochrome c during apoptosis. *Dev Cell* **2:** 55-67

Sen A, Damm VT, Cox RT (2013) Drosophila clueless is highly expressed in larval neuroblasts, affects mitochondrial localization and suppresses mitochondrial oxidative damage. *PLoS One* **8:** e54283

Sesaki H, Jensen RE (2001) UGO1 encodes an outer membrane protein required for mitochondrial fusion. *J Cell Biol* **152:** 1123-1134

Sheridan C, Delivani P, Cullen SP, Martin SJ (2008) Bax- or Bak-induced mitochondrial fission can be uncoupled from cytochrome C release. *Mol Cell* **31:** 570-585

Sheridan C, Martin SJ (2010) Mitochondrial fission/fusion dynamics and apoptosis. *Mitochondrion* **10:** 640-648

Shutt T, Geoffrion M, Milne R, McBride HM (2012) The intracellular redox state is a core determinant of mitochondrial fusion. *EMBO reports* **13:** 909-915

Simbeni R, Pon L, Zinser E, Paltauf F, Daum G (1991) Mitochondrial membrane contact sites of yeast. Characterization of lipid components and possible involvement in intramitochondrial translocation of phospholipids. *J Biol Chem* **266:** 10047-10049

Smirnova E, Griparic L, Shurland DL, van der Bliek AM (2001) Dynamin-related protein Drp1 is required for mitochondrial division in mammalian cells. *Molecular biology of the cell* **12:** 2245-2256

Song Z, Chen H, Fiket M, Alexander C, Chan DC (2007) OPA1 processing controls mitochondrial fusion and is regulated by mRNA splicing, membrane potential, and Yme1L. *The Journal of cell biology* **178:** 749-755

Song Z, Ghochani M, McCaffery JM, Frey TG, Chan DC (2009) Mitofusins and OPA1 mediate sequential steps in mitochondrial membrane fusion. *Molecular biology of the cell* **20:** 3525-3532

Soubannier V, Vaillier J, Paumard P, Coulary B, Schaeffer J, Velours J (2002) In the absence of the first membrane-spanning segment of subunit 4(b), the yeast ATP synthase is functional but does not dimerize or oligomerize. *J Biol Chem* **277:** 10739-10745

Spelbrink JN, Li FY, Tiranti V, Nikali K, Yuan QP, Tariq M, Wanrooij S, Garrido N, Comi G, Morandi L, Santoro L, Toscano A, Fabrizi GM, Somer H, Croxen R, Beeson D, Poulton J, Suomalainen A, Jacobs HT, Zeviani M, Larsson C (2001) Human mitochondrial DNA deletions associated with mutations in the gene encoding Twinkle, a phage T7 gene 4-like protein localized in mitochondria. *Nat Genet* **28:** 223-231

Sperka-Gottlieb CD, Hermetter A, Paltauf F, Daum G (1988) Lipid topology and physical properties of the outer mitochondrial membrane of the yeast, Saccharomyces cerevisiae. *Biochim Biophys Acta* **946:** 227-234

Spinazzi M, Cazzola S, Bortolozzi M, Baracca A, Loro E, Casarin A, Solaini G, Sgarbi G, Casalena G, Cenacchi G, Malena A, Frezza C, Carrara F, Angelini C, Scorrano L, Salviati L, Vergani L (2008) A novel deletion in the GTPase domain of OPA1 causes defects in mitochondrial morphology and distribution, but not in function. *Human molecular genetics* **17:** 3291-3302

St-Pierre J, Lin J, Krauss S, Tarr PT, Yang R, Newgard CB, Spiegelman BM (2003) Bioenergetic analysis of peroxisome proliferator-activated receptor gamma coactivators 1alpha and 1beta (PGC-1alpha and PGC-1beta) in muscle cells. *J Biol Chem* **278:** 26597-26603

Stewart JD, Hudson G, Yu-Wai-Man P, Blakeley EL, He L, Horvath R, Maddison P, Wright A, Griffiths PG, Turnbull DM, Taylor RW, Chinnery PF (2008) OPA1 in multiple mitochondrial DNA deletion disorders. *Neurology* **71:** 1829-1831

Sukhorukov VM, Bereiter-Hahn J (2009) Anomalous diffusion induced by cristae geometry in the inner mitochondrial membrane. *PLoS One* **4:** e4604

Suthanthiran M, Anderson ME, Sharma VK, Meister A (1990) Glutathione regulates activation-dependent DNA synthesis in highly purified normal human T lymphocytes stimulated via the CD2 and CD3 antigens. *Proceedings of the National Academy of Sciences of the United States of America* **87:** 3343-3347

Szabadkai G, Simoni AM, Chami M, Wieckowski MR, Youle RJ, Rizzuto R (2004) Drp-1-dependent division of the mitochondrial network blocks intraorganellar Ca2+ waves and protects against Ca2+-mediated apoptosis. *Mol Cell* **16:** 59-68

Taguchi N, Ishihara N, Jofuku A, Oka T, Mihara K (2007) Mitotic phosphorylation of dynamin-related GTPase Drp1 participates in mitochondrial fission. *J Biol Chem* **282:** 11521-11529

Takai D, Isobe K, Hayashi J (1999) Transcomplementation between different types of respiration-deficient mitochondria with different pathogenic mutant mitochondrial DNAs. *J Biol Chem* **274:** 11199-11202

Takamatsu C, Umeda S, Ohsato T, Ohno T, Abe Y, Fukuoh A, Shinagawa H, Hamasaki N, Kang D (2002) Regulation of mitochondrial D-loops by transcription factor A and single-stranded DNA-binding protein. *EMBO Rep* **3:** 451-456

Tanaka A, Cleland MM, Xu S, Narendra DP, Suen DF, Karbowski M, Youle RJ (2010) Proteasome and p97 mediate mitophagy and degradation of mitofusins induced by Parkin. *J Cell Biol* **191:** 1367-1380

Tang S, Le PK, Tse S, Wallace DC, Huang T (2009) Heterozygous mutation of Opa1 in Drosophila shortens lifespan mediated through increased reactive oxygen species production. *PLoS One* **4:** e4492

Tashiro A, Zhao C, Gage FH (2006) Retrovirus-mediated single-cell gene knockout technique in adult newborn neurons in vivo. *Nature protocols* **1:** 3049-3055

Taylor PM (2014) Role of amino acid transporters in amino acid sensing. *Am J Clin Nutr* **99:** 223S-230S

Taylor RW, Turnbull DM (2005) Mitochondrial DNA mutations in human disease. *Nat Rev Genet* **6:** 389-402

Teslaa T, Teitell MA (2015) Pluripotent stem cell energy metabolism: an update. *Embo J* **34:** 138-153

Tondera D, Grandemange S, Jourdain A, Karbowski M, Mattenberger Y, Herzig S, Da Cruz S, Clerc P, Raschke I, Merkwirth C, Ehses S, Krause F, Chan DC, Alexander C, Bauer C, Youle R, Langer T, Martinou JC (2009) SLP-2 is required for stress-induced mitochondrial hyperfusion. *Embo J* **28:** 1589-1600

Trinkle-Mulcahy L (2012) Resolving protein interactions and complexes by affinity purification followed by label-based quantitative mass spectrometry. *Proteomics* **12:** 1623-1638

Tyurin VA, Tyurina YY, Osipov AN, Belikova NA, Basova LV, Kapralov AA, Bayir H, Kagan VE (2007) Interactions of cardiolipin and lyso-cardiolipins with cytochrome c and tBid: conflict or assistance in apoptosis. *Cell Death Differ* **14:** 872-875

Van Goethem G, Dermaut B, Lofgren A, Martin JJ, Van Broeckhoven C (2001) Mutation of POLG is associated with progressive external ophthalmoplegia characterized by mtDNA deletions. *Nat Genet* **28:** 211-212

Verstreken P, Ly CV, Venken KJ, Koh TW, Zhou Y, Bellen HJ (2005) Synaptic mitochondria are critical for mobilization of reserve pool vesicles at Drosophila neuromuscular junctions. *Neuron* **47:** 365-378

Vidoni S, Zanna C, Rugolo M, Sarzi E, Lenaers G (2013) Why mitochondria must fuse to maintain their genome integrity. *Antioxid Redox Signal* **19:** 379-388

Vives-Bauza C, Zhou C, Huang Y, Cui M, de Vries RL, Kim J, May J, Tocilescu MA, Liu W, Ko HS, Magrane J, Moore DJ, Dawson VL, Grailhe R, Dawson TM, Li C, Tieu K, Przedborski S (2010) PINK1-dependent recruitment of Parkin to mitochondria in mitophagy. *Proceedings of the National Academy of Sciences of the United States of America* **107:** 378-383

Vogel F, Bornhovd C, Neupert W, Reichert AS (2006) Dynamic subcompartmentalization of the mitochondrial inner membrane. *The Journal of cell biology* **175:** 237-247

von der Malsburg K, Muller JM, Bohnert M, Oeljeklaus S, Kwiatkowska P, Becker T, Loniewska-Lwowska A, Wiese S, Rao S, Milenkovic D, Hutu DP, Zerbes RM, Schulze-Specking A, Meyer HE, Martinou JC, Rospert S, Rehling P, Meisinger C, Veenhuis M, Warscheid B, van der Klei IJ, Pfanner N, Chacinska A, van der Laan M (2011) Dual role of mitofilin in mitochondrial membrane organization and protein biogenesis. *Developmental cell* **21:** 694-707

Wang H, Song P, Du L, Tian W, Yue W, Liu M, Li D, Wang B, Zhu Y, Cao C, Zhou J, Chen Q (2011) Parkin ubiquitinates Drp1 for proteasome-dependent degradation: implication of dysregulated mitochondrial dynamics in Parkinson disease. *J Biol Chem* **286:** 11649-11658

Wang J, Xiong S, Xie C, Markesbery WR, Lovell MA (2005) Increased oxidative damage in nuclear and mitochondrial DNA in Alzheimer's disease. *J Neurochem* **93:** 953-962

Wang Y, Bogenhagen DF (2006) Human mitochondrial DNA nucleoids are linked to protein folding machinery and metabolic enzymes at the mitochondrial inner membrane. *J Biol Chem* **281:** 25791-25802

Wanschers BF, Szklarczyk R, van den Brand MA, Jonckheere A, Suijskens J, Smeets R, Rodenburg RJ, Stephan K, Helland IB, Elkamil A, Rootwelt T, Ott M, van den Heuvel L, Nijtmans LG, Huynen MA (2014) A mutation in the human CBP4 ortholog UQCC3 impairs complex III assembly, activity and cytochrome b stability. *Human molecular genetics* **23:** 6356-6365

Wasilewski M, Semenzato M, Rafelski SM, Robbins J, Bakardjiev AI, Scorrano L (2012) Optic atrophy 1-dependent mitochondrial remodeling controls steroidogenesis in trophoblasts. *Curr Biol* **22:** 1228-1234

Waterham HR, Koster J, van Roermund CW, Mooyer PA, Wanders RJ, Leonard JV (2007) A lethal defect of mitochondrial and peroxisomal fission. *N Engl J Med* **356:** 1736-1741

Weber TA, Koob S, Heide H, Wittig I, Head B, van der Bliek A, Brandt U, Mittelbronn M, Reichert AS (2013) APOOL is a cardiolipin-binding constituent of the

Mitofilin/MINOS protein complex determining cristae morphology in mammalian mitochondria. *PLoS One* **8:** e63683

Wibom R, Lasorsa FM, Tohonen V, Barbaro M, Sterky FH, Kucinski T, Naess K, Jonsson M, Pierri CL, Palmieri F, Wedell A (2009) AGC1 deficiency associated with global cerebral hypomyelination. *N Engl J Med* **361:** 489-495

Wiedemann FR, Manfredi G, Mawrin C, Beal MF, Schon EA (2002) Mitochondrial DNA and respiratory chain function in spinal cords of ALS patients. *J Neurochem* **80:** 616-625

Wikstrom M (2004) Cytochrome c oxidase: 25 years of the elusive proton pump. *Biochim Biophys Acta* **1655:** 241-247

Wilkins HM, Brock S, Gray JJ, Linseman DA (2014) Stable over-expression of the 2-oxoglutarate carrier enhances neuronal cell resistance to oxidative stress via Bcl-2-dependent mitochondrial GSH transport. *J Neurochem* **130:** 75-86

Wilkins HM, Kirchhof D, Manning E, Joseph JW, Linseman DA (2013) Mitochondrial glutathione transport is a key determinant of neuronal susceptibility to oxidative and nitrosative stress. *J Biol Chem* **288:** 5091-5101

Williams T, Courchet J, Viollet B, Brenman JE, Polleux F (2011) AMP-activated protein kinase (AMPK) activity is not required for neuronal development but regulates axogenesis during metabolic stress. *Proceedings of the National Academy of Sciences of the United States of America* **108:** 5849-5854

Wittig I, Braun HP, Schagger H (2006) Blue native PAGE. *Nature protocols* **1:** 418-428

Wittig I, Meyer B, Heide H, Steger M, Bleier L, Wumaier Z, Karas M, Schagger H (2010) Assembly and oligomerization of human ATP synthase lacking mitochondrial subunits a and A6L. *Biochim Biophys Acta* **1797:** 1004-1011

Wittig I, Schagger H (2009) Supramolecular organization of ATP synthase and respiratory chain in mitochondrial membranes. *Biochim Biophys Acta* **1787:** 672-680

Woodfield K, Ruck A, Brdiczka D, Halestrap AP (1998) Direct demonstration of a specific interaction between cyclophilin-D and the adenine nucleotide translocase confirms their role in the mitochondrial permeability transition. *Biochem J* **336 (Pt 2):** 287-290

Wu Z, Puigserver P, Andersson U, Zhang C, Adelmant G, Mootha V, Troy A, Cinti S, Lowell B, Scarpulla RC, Spiegelman BM (1999) Mechanisms controlling mitochondrial biogenesis and respiration through the thermogenic coactivator PGC-1. *Cell* **98:** 115-124

Wurm CA, Jakobs S (2006) Differential protein distributions define two sub-compartments of the mitochondrial inner membrane in yeast. *FEBS Lett* **580:** 5628-5634

Xavier JM, Rodrigues CM, Sola S (2015) Mitochondria: Major Regulators of Neural Development. *The Neuroscientist : a review journal bringing neurobiology, neurology and psychiatry*

Yamaguchi R, Lartigue L, Perkins G, Scott RT, Dixit A, Kushnareva Y, Kuwana T, Ellisman MH, Newmeyer DD (2008) Opa1-mediated cristae opening is Bax/Bak and BH3 dependent, required for apoptosis, and independent of Bak oligomerization. *Molecular Cell* **31:** 557-569

Yan N, Meister A (1990) Amino acid sequence of rat kidney gamma-glutamylcysteine synthetase. *J Biol Chem* **265:** 1588-1593

Yang L, Long Q, Liu J, Tang H, Li Y, Bao F, Qin D, Pei D, Liu X (2015a) Mitochondrial fusion provides an 'initial metabolic complementation' controlled by mtDNA. *Cellular and molecular life sciences : CMLS*

Yang RF, Sun LH, Zhang R, Zhang Y, Luo YX, Zheng W, Zhang ZQ, Chen HZ, Liu DP (2015b) Suppression of Mic60 compromises mitochondrial transcription and oxidative phosphorylation. *Scientific reports* **5:** 7990

Yokoyama Y, Beckman JS, Beckman TK, Wheat JK, Cash TG, Freeman BA, Parks DA (1990) Circulating xanthine oxidase: potential mediator of ischemic injury. *Am J Physiol* **258:** G564-570

Yoon Y, Krueger EW, Oswald BJ, McNiven MA (2003) The mitochondrial protein hFis1 regulates mitochondrial fission in mammalian cells through an interaction with the dynamin-like protein DLP1. *Mol Cell Biol* **23:** 5409-5420

Yu-Wai-Man P, Chinnery PF (2013) Dominant optic atrophy: novel OPA1 mutations and revised prevalence estimates. *Ophthalmology* **120:** 1712-1712 e1711

Yu-Wai-Man P, Griffiths PG, Gorman GS, Lourenco CM, Wright AF, Auer-Grumbach M, Toscano A, Musumeci O, Valentino ML, Caporali L, Lamperti C, Tallaksen CM, Duffey P, Miller J, Whittaker RG, Baker MR, Jackson MJ, Clarke MP, Dhillon B, Czermin B, Stewart JD, Hudson G, Reynier P, Bonneau D, Marques W, Jr., Lenaers G, McFarland R, Taylor RW, Turnbull DM, Votruba M, Zeviani M, Carelli V, Bindoff LA, Horvath R, Amati-Bonneau P, Chinnery PF (2010) Multi-system neurological disease is common in patients with OPA1 mutations. *Brain* **133:** 771-786

Zhang DX, Gutterman DD (2007) Mitochondrial reactive oxygen species-mediated signaling in endothelial cells. *Am J Physiol Heart Circ Physiol* **292:** H2023-2031

Zhang M, Mileykovskaya E, Dowhan W (2002) Gluing the respiratory chain together. Cardiolipin is required for supercomplex formation in the inner mitochondrial membrane. *J Biol Chem* **277:** 43553-43556

Zhao J, Lendahl U, Nister M (2013) Regulation of mitochondrial dynamics: convergences and divergences between yeast and vertebrates. *Cellular and molecular life sciences : CMLS* **70:** 951-976

Zhong Q, Putt DA, Xu F, Lash LH (2008) Hepatic mitochondrial transport of glutathione: studies in isolated rat liver mitochondria and H4IIE rat hepatoma cells. *Archives of biochemistry and biophysics* **474:** 119-127

Zhu Q, Hulen D, Liu T, Clarke M (1997a) The cluA- mutant of Dictyostelium identifies a novel class of proteins required for dispersion of mitochondria. *Proceedings of the National Academy of Sciences of the United States of America* **94:** 7308-7313

Zhu Q, Hulen D, Liu T, Clarke M (1997b) The cluA- mutant of Dictyostelium identifies a novel class of proteins required for dispersion of mitochondria. *Proc Natl Acad Sci U S A* **94:** 7308-7313

Zindy F, Quelle DE, Roussel MF, Sherr CJ (1997) Expression of the p16INK4a tumor suppressor versus other INK4 family members during mouse development and aging. *Oncogene* **15:** 203-211

Zuchner S, Mersiyanova IV, Muglia M, Bissar-Tadmouri N, Rochelle J, Dadali EL, Zappia M, Nelis E, Patitucci A, Senderek J, Parman Y, Evgrafov O, Jonghe PD, Takahashi Y, Tsuji S, Pericak-Vance MA, Quattrone A, Battaloglu E, Polyakov AV, Timmerman V, Schroder JM, Vance JM (2004) Mutations in the mitochondrial GTPase mitofusin 2 cause Charcot-Marie-Tooth neuropathy type 2A. *Nat Genet* **36:** 449-451

Zunino R, Braschi E, Xu L, McBride HM (2009) Translocation of SenP5 from the nucleoli to the mitochondria modulates DRP1-dependent fission during mitosis. *J Biol Chem* **284:** 17783-17795

Appendices

Appendix A: Licences & Permissions

Appendix B:

Patten DA, Wong J, Khacho M, Soubannier V, Mailloux RJ, Pilon-Larose K, MacLaurin JG, Park DS, McBride HM, Trinkle-Mulcahy L, Harper ME, Germain M, Slack RS (2014) OPA1-dependent cristae modulation is essential for cellular adaptation to metabolic demand. Embo J 33: 2676-2691

Appendix C:

Reprinted from: **Patten DA**, Germain M, Kelly MA, Slack RS. Reactive oxygen species: stuck in the middle of neurodegeneration. J Alzheimers Dis. 2010;20 Suppl 2:S357-67. With permission from IOS press.

Appendix D:

Germain M, Nguyen AP, Khacho M, **Patten DA**, Screaton RA, Park DS, Slack RS (2013) LKB1-regulated adaptive mechanisms are essential for neuronal survival following mitochondrial dysfunction. Hum Mol Genet 22: 952-962

Appendix E:

Khacho M, Tarabay M, **Patten D**, Khacho P, MacLaurin JG, Guadagno J, Bergeron R, Cregan SP, Harper ME, Park DS, Slack RS (2014) Acidosis overrides oxygen deprivation to maintain mitochondrial function and cell survival. Nature communications 5: 3550

Appendix A: Licences & Permissions

JOHN WILEY AND SONS LICENSE TERMS AND CONDITIONS

Jul 20, 2015

This Agreement between David A Patten ("You") and John Wiley and Sons ("John Wiley and Sons") consists of your license details and the terms and conditions provided by John Wiley and Sons and Copyright Clearance Center.

License Number	3673200525594
License date	Jul 20, 2015
Licensed Content Publisher	John Wiley and Sons
Licensed Content Publication	The EMBO Journal
Licensed Content Title	OPA1-dependent cristae modulation is essential for cellular adaptation to metabolic demand
Licensed Content Author	David A Patten,Jacob Wong,Mireille Khacho,Vincent Soubannier,Ryan J Mailloux,Karine Pilon-Larose,Jason G MacLaurin,David S Park,Heidi M McBride,Laura Trinkle-Mulcahy,Mary-Ellen Harper,Marc Germain,Ruth S Slack
Licensed Content Date	Oct 8, 2014
Pages	16
Type of use	Dissertation/Thesis
Requestor type	Author of this Wiley article
Format	Electronic
Portion	Full article
Will you be translating?	No
Title of your thesis / dissertation	The role of OPA1 and interacting proteins in mitochondrial function
Expected completion date	Aug 2015
Expected size (number of pages)	203
Requestor Location	[redacted] [redacted] Attn: David A Patten
Billing Type	Invoice
Billing Address	David A Patten [redacted] [redacted] Attn: David A Patten

[redacted]

Total 0.00 CAD

Terms and Conditions

TERMS AND CONDITIONS

This copyrighted material is owned by or exclusively licensed to John Wiley & Sons, Inc. or one of its group companies (each a"Wiley Company") or handled on behalf of a society with which a Wiley Company has exclusive publishing rights in relation to a particular work (collectively "WILEY"). By clicking □accept□ in connection with completing this licensing transaction, you agree that the following terms and conditions apply to this transaction (along with the billing and payment terms and conditions established by the Copyright Clearance Center Inc., ("CCC's Billing and Payment terms and conditions"), at the time that you opened your Rightslink account (these are available at any time at http://myaccount.copyright.com).

Terms and Conditions

- The materials you have requested permission to reproduce or reuse (the "Wiley Materials") are protected by copyright.
- You are hereby granted a personal, non-exclusive, non-sub licensable (on a stand-alone basis), non-transferable, worldwide, limited license to reproduce the Wiley Materials for the purpose specified in the licensing process. This license is for a one-time use only and limited to any maximum distribution number specified in the license. The first instance of republication or reuse granted by this licence must be completed within two years of the date of the grant of this licence (although copies prepared before the end date may be distributed thereafter). The Wiley Materials shall not be used in any other manner or for any other purpose, beyond what is granted in the license. Permission is granted subject to an appropriate acknowledgement given to the author, title of the material/book/journal and the publisher. You shall also duplicate the copyright notice that appears in the Wiley publication in your use of the Wiley Material. Permission is also granted on the understanding that nowhere in the text is a previously published source acknowledged for all or part of this Wiley Material. Any third party content is expressly excluded from this permission.
- With respect to the Wiley Materials, all rights are reserved. Except as expressly granted by the terms of the license, no part of the Wiley Materials may be copied, modified, adapted (except for minor reformatting required by the new Publication), translated, reproduced, transferred or distributed, in any form or by any means, and no derivative works may be made based on the Wiley Materials without the prior permission of the respective copyright owner. You may not alter, remove or suppress in any manner any copyright, trademark or other notices displayed by the Wiley Materials. You may not license, rent, sell, loan, lease, pledge, offer as security, transfer or assign the Wiley Materials on a stand-alone basis, or any of the rights granted to you hereunder to any other person.
- The Wiley Materials and all of the intellectual property rights therein shall at all times remain the exclusive property of John Wiley & Sons Inc, the Wiley Companies, or their respective licensors, and your interest therein is only that of having possession of

and the right to reproduce the Wiley Materials pursuant to Section 2 herein during the continuance of this Agreement. You agree that you own no right, title or interest in or to the Wiley Materials or any of the intellectual property rights therein. You shall have no rights hereunder other than the license as provided for above in Section 2. No right, license or interest to any trademark, trade name, service mark or other branding ("Marks") of WILEY or its licensors is granted hereunder, and you agree that you shall not assert any such right, license or interest with respect thereto.

- NEITHER WILEY NOR ITS LICENSORS MAKES ANY WARRANTY OR REPRESENTATION OF ANY KIND TO YOU OR ANY THIRD PARTY, EXPRESS, IMPLIED OR STATUTORY, WITH RESPECT TO THE MATERIALS OR THE ACCURACY OF ANY INFORMATION CONTAINED IN THE MATERIALS, INCLUDING, WITHOUT LIMITATION, ANY IMPLIED WARRANTY OF MERCHANTABILITY, ACCURACY, SATISFACTORY QUALITY, FITNESS FOR A PARTICULAR PURPOSE, USABILITY, INTEGRATION OR NON-INFRINGEMENT AND ALL SUCH WARRANTIES ARE HEREBY EXCLUDED BY WILEY AND ITS LICENSORS AND WAIVED BY YOU

- WILEY shall have the right to terminate this Agreement immediately upon breach of this Agreement by you.

- You shall indemnify, defend and hold harmless WILEY, its Licensors and their respective directors, officers, agents and employees, from and against any actual or threatened claims, demands, causes of action or proceedings arising from any breach of this Agreement by you.

- IN NO EVENT SHALL WILEY OR ITS LICENSORS BE LIABLE TO YOU OR ANY OTHER PARTY OR ANY OTHER PERSON OR ENTITY FOR ANY SPECIAL, CONSEQUENTIAL, INCIDENTAL, INDIRECT, EXEMPLARY OR PUNITIVE DAMAGES, HOWEVER CAUSED, ARISING OUT OF OR IN CONNECTION WITH THE DOWNLOADING, PROVISIONING, VIEWING OR USE OF THE MATERIALS REGARDLESS OF THE FORM OF ACTION, WHETHER FOR BREACH OF CONTRACT, BREACH OF WARRANTY, TORT, NEGLIGENCE, INFRINGEMENT OR OTHERWISE (INCLUDING, WITHOUT LIMITATION, DAMAGES BASED ON LOSS OF PROFITS, DATA, FILES, USE, BUSINESS OPPORTUNITY OR CLAIMS OF THIRD PARTIES), AND WHETHER OR NOT THE PARTY HAS BEEN ADVISED OF THE POSSIBILITY OF SUCH DAMAGES. THIS LIMITATION SHALL APPLY NOTWITHSTANDING ANY FAILURE OF ESSENTIAL PURPOSE OF ANY LIMITED REMEDY PROVIDED HEREIN.

- Should any provision of this Agreement be held by a court of competent jurisdiction to be illegal, invalid, or unenforceable, that provision shall be deemed amended to achieve as nearly as possible the same economic effect as the original provision, and the legality, validity and enforceability of the remaining provisions of this Agreement shall not be affected or impaired thereby.

- The failure of either party to enforce any term or condition of this Agreement shall not constitute a waiver of either party's right to enforce each and every term and condition of this Agreement. No breach under this agreement shall be deemed waived or excused by either party unless such waiver or consent is in writing signed by the party granting such waiver or consent. The waiver by or consent of a party to a breach of any provision of this Agreement shall not operate or be construed as a waiver of or consent to any other or subsequent breach by such other party.

- This Agreement may not be assigned (including by operation of law or otherwise) by you without WILEY's prior written consent.

- Any fee required for this permission shall be non-refundable after thirty (30) days from receipt by the CCC.

- These terms and conditions together with CCC□s Billing and Payment terms and conditions (which are incorporated herein) form the entire agreement between you and WILEY concerning this licensing transaction and (in the absence of fraud) supersedes all prior agreements and representations of the parties, oral or written. This Agreement may not be amended except in writing signed by both parties. This Agreement shall be binding upon and inure to the benefit of the parties' successors, legal representatives, and authorized assigns.

- In the event of any conflict between your obligations established by these terms and conditions and those established by CCC□s Billing and Payment terms and conditions, these terms and conditions shall prevail.

- WILEY expressly reserves all rights not specifically granted in the combination of (i) the license details provided by you and accepted in the course of this licensing transaction, (ii) these terms and conditions and (iii) CCC□s Billing and Payment terms and conditions.

- This Agreement will be void if the Type of Use, Format, Circulation, or Requestor Type was misrepresented during the licensing process.

- This Agreement shall be governed by and construed in accordance with the laws of the State of New York, USA, without regards to such state□s conflict of law rules. Any legal action, suit or proceeding arising out of or relating to these Terms and Conditions or the breach thereof shall be instituted in a court of competent jurisdiction in New York County in the State of New York in the United States of America and each party hereby consents and submits to the personal jurisdiction of such court, waives any objection to venue in such court and consents to service of process by registered or certified mail, return receipt requested, at the last known address of such party.

WILEY OPEN ACCESS TERMS AND CONDITIONS

Wiley Publishes Open Access Articles in fully Open Access Journals and in Subscription journals offering Online Open. Although most of the fully Open Access journals publish

[redacted]

open access articles under the terms of the Creative Commons Attribution (CC BY) License only, the subscription journals and a few of the Open Access Journals offer a choice of Creative Commons Licenses:: Creative Commons Attribution (CC-BY) license Creative Commons Attribution Non-Commercial (CC-BY-NC) license and Creative Commons Attribution Non-Commercial-NoDerivs (CC-BY-NC-ND) License. The license type is clearly identified on the article.

Copyright in any research article in a journal published as Open Access under a Creative Commons License is retained by the author(s). Authors grant Wiley a license to publish the article and identify itself as the original publisher. Authors also grant any third party the right to use the article freely as long as its integrity is maintained and its original authors, citation details and publisher are identified as follows: [Title of Article/Author/Journal Title and Volume/Issue. Copyright (c) [year] [copyright owner as specified in the Journal]. Links to the final article on Wiley□s website are encouraged where applicable.

The Creative Commons Attribution License

The Creative Commons Attribution License (CC-BY) allows users to copy, distribute and transmit an article, adapt the article and make commercial use of the article. The CC-BY license permits commercial and non-commercial re-use of an open access article, as long as the author is properly attributed.

The Creative Commons Attribution License does not affect the moral rights of authors, including without limitation the right not to have their work subjected to derogatory treatment. It also does not affect any other rights held by authors or third parties in the article, including without limitation the rights of privacy and publicity. Use of the article must not assert or imply, whether implicitly or explicitly, any connection with, endorsement or sponsorship of such use by the author, publisher or any other party associated with the article.

For any reuse or distribution, users must include the copyright notice and make clear to others that the article is made available under a Creative Commons Attribution license, linking to the relevant Creative Commons web page.

To the fullest extent permitted by applicable law, the article is made available as is and without representation or warranties of any kind whether express, implied, statutory or otherwise and including, without limitation, warranties of title, merchantability, fitness for a particular purpose, non-infringement, absence of defects, accuracy, or the presence or absence of errors.

Creative Commons Attribution Non-Commercial License

The Creative Commons Attribution Non-Commercial (CC-BY-NC) License permits use, distribution and reproduction in any medium, provided the original work is properly cited and is not used for commercial purposes.(see below)

Creative Commons Attribution-Non-Commercial-NoDerivs License

The Creative Commons Attribution Non-Commercial-NoDerivs License (CC-BY-NC-ND) permits use, distribution and reproduction in any medium, provided the original work is

properly cited, is not used for commercial purposes and no modifications or adaptations are made. (see below)

Use by non-commercial users

For non-commercial and non-promotional purposes, individual users may access, download, copy, display and redistribute to colleagues Wiley Open Access articles, as well as adapt, translate, text- and data-mine the content subject to the following conditions:

- The authors' moral rights are not compromised. These rights include the right of "paternity" (also known as "attribution" - the right for the author to be identified as such) and "integrity" (the right for the author not to have the work altered in such a way that the author's reputation or integrity may be impugned).
- Where content in the article is identified as belonging to a third party, it is the obligation of the user to ensure that any reuse complies with the copyright policies of the owner of that content.
- If article content is copied, downloaded or otherwise reused for non-commercial research and education purposes, a link to the appropriate bibliographic citation (authors, journal, article title, volume, issue, page numbers, DOI and the link to the definitive published version on **Wiley Online Library**) should be maintained. Copyright notices and disclaimers must not be deleted.
- Any translations, for which a prior translation agreement with Wiley has not been agreed, must prominently display the statement: "This is an unofficial translation of an article that appeared in a Wiley publication. The publisher has not endorsed this translation."

Use by commercial "for-profit" organisations

Use of Wiley Open Access articles for commercial, promotional, or marketing purposes requires further explicit permission from Wiley and will be subject to a fee. Commercial purposes include:

- Copying or downloading of articles, or linking to such articles for further redistribution, sale or licensing;
- Copying, downloading or posting by a site or service that incorporates advertising with such content;
- The inclusion or incorporation of article content in other works or services (other than normal quotations with an appropriate citation) that is then available for sale or licensing, for a fee (for example, a compilation produced for marketing purposes, inclusion in a sales pack)
- Use of article content (other than normal quotations with appropriate citation) by for-profit organisations for promotional purposes

[redacted]

- Linking to article content in e-mails redistributed for promotional, marketing or educational purposes;
- Use for the purposes of monetary reward by means of sale, resale, licence, loan, transfer or other form of commercial exploitation such as marketing products
- Print reprints of Wiley Open Access articles can be purchased from: corporatesales@wiley.com

Further details can be found on Wiley Online Library
http://olabout.wiley.com/WileyCDA/Section/id-410895.html

Other Terms and Conditions:

v1.9

Questions? customercare@copyright.com or +1-855-239-3415 (toll free in the US) or +1-978-646-2777.

Print Close

From: **Carry Koolbergen** ([redacted])
Sent: August-07-15 5:32:30 AM
To: Dave Patten ([redacted])

Dear Dave Patten,

We hereby grant you permission to reproduce the below mentioned material in **print and electronic format** at no charge subject to the following conditions:

If any part of the material to be used (for example, figures) has appeared in our publication with credit or acknowledgement to another source, permission must also be sought from that source. If such permission is not obtained then that material may not be included in your publication/copies.

Suitable acknowledgement to the source must be made, either as a footnote or in a reference list at the end of your publication, as follows:

"Reprinted from Publication title, Vol number, Author(s), Title of article, Pages No., Copyright (Year), with permission from IOS Press".

This permission is granted for non-exclusive world **English** rights only. For other languages please reapply separately for each one required.

Reproduction of this material is confined to the purpose for which permission is hereby given.

Yours sincerely

Carry Koolbergen (Mrs.)
Contracts, Rights & Permissions Coordinator
Not in the office on Wednesdays

IOS Press BV
[redacted]
Tel.: [redacted]
Fax: [redacted]
Email: [redacted]

URL: [redacted]
Twitter: [redacted]
G+: [redacted]
Facebook: [redacted]

[redacted] 2015-08-16

OXFORD UNIVERSITY PRESS LICENSE
TERMS AND CONDITIONS

Jul 20, 2015

This is a License Agreement between David A Patten ("You") and Oxford University Press ("Oxford University Press") provided by Copyright Clearance Center ("CCC"). The license consists of your order details, the terms and conditions provided by Oxford University Press, and the payment terms and conditions.

All payments must be made in full to CCC. For payment instructions, please see information listed at the bottom of this form.

License Number	3673210321487
License date	Jul 20, 2015
Licensed content publisher	Oxford University Press
Licensed content publication	Human Molecular Genetics
Licensed content title	LKB1-regulated adaptive mechanisms are essential for neuronal survival following mitochondrial dysfunction:
Licensed content author	Marc Germain, Angela P. Nguyen, Mireille Khacho, David A. Patten, Robert A. Screaton, David S. Park, Ruth S. Slack
Licensed content date	03/01/2013
Type of Use	Thesis/Dissertation
Institution name	None
Title of your work	The role of OPA1 and interacting proteins in mitochondrial function
Publisher of your work	n/a
Expected publication date	Aug 2015
Permissions cost	0.00 USD
Value added tax	0.00 USD
Total	0.00 USD
Total	0.00 USD
Terms and Conditions	

STANDARD TERMS AND CONDITIONS FOR REPRODUCTION OF MATERIAL FROM AN OXFORD UNIVERSITY PRESS JOURNAL

1. Use of the material is restricted to the type of use specified in your order details.

2. This permission covers the use of the material in the English language in the following territory: world. If you have requested additional permission to translate this material, the terms and conditions of this reuse will be set out in clause 12.

3. This permission is limited to the particular use authorized in (1) above and does not allow you to sanction its use elsewhere in any other format other than specified above, nor does it

apply to quotations, images, artistic works etc that have been reproduced from other sources which may be part of the material to be used.

4. No alteration, omission or addition is made to the material without our written consent. Permission must be re-cleared with Oxford University Press if/when you decide to reprint.

5. The following credit line appears wherever the material is used: author, title, journal, year, volume, issue number, pagination, by permission of Oxford University Press or the sponsoring society if the journal is a society journal. Where a journal is being published on behalf of a learned society, the details of that society must be included in the credit line.

6. For the reproduction of a full article from an Oxford University Press journal for whatever purpose, the corresponding author of the material concerned should be informed of the proposed use. Contact details for the corresponding authors of all Oxford University Press journal contact can be found alongside either the abstract or full text of the article concerned, accessible from www.oxfordjournals.org Should there be a problem clearing these rights, please contact journals.permissions@oup.com

7. If the credit line or acknowledgement in our publication indicates that any of the figures, images or photos was reproduced, drawn or modified from an earlier source it will be necessary for you to clear this permission with the original publisher as well. If this permission has not been obtained, please note that this material cannot be included in your publication/photocopies.

8. While you may exercise the rights licensed immediately upon issuance of the license at the end of the licensing process for the transaction, provided that you have disclosed complete and accurate details of your proposed use, no license is finally effective unless and until full payment is received from you (either by Oxford University Press or by Copyright Clearance Center (CCC)) as provided in CCC's Billing and Payment terms and conditions. If full payment is not received on a timely basis, then any license preliminarily granted shall be deemed automatically revoked and shall be void as if never granted. Further, in the event that you breach any of these terms and conditions or any of CCC's Billing and Payment terms and conditions, the license is automatically revoked and shall be void as if never granted. Use of materials as described in a revoked license, as well as any use of the materials beyond the scope of an unrevoked license, may constitute copyright infringement and Oxford University Press reserves the right to take any and all action to protect its copyright in the materials.

9. This license is personal to you and may not be sublicensed, assigned or transferred by you to any other person without Oxford University Press's written permission.

10. Oxford University Press reserves all rights not specifically granted in the combination of (i) the license details provided by you and accepted in the course of this licensing transaction, (ii) these terms and conditions and (iii) CCC's Billing and Payment terms and conditions.

11. You hereby indemnify and agree to hold harmless Oxford University Press and CCC, and their respective officers, directors, employs and agents, from and against any and all claims arising out of your use of the licensed material other than as specifically authorized pursuant to this license.

[redacted]

12. Other Terms and Conditions:

v1.4

Title: Acidosis overrides oxygen deprivation to maintain mitochondrial function and cell survival

Author: Mireille Khacho, Michelle Tarabay, David Patten, Pamela Khacho, Jason G. MacLaurin, Jennifer Guadagno

Publication: Nature Communications

Publisher: Nature Publishing Group

Date: Apr 1, 2014

Logged in as:
David Patten

LOGOUT

Creative Commons

The request you have made is considered to be non-commercial/educational. As the article you have requested has been distributed under a Creative Commons license (Attribution-Noncommercial), you may reuse this material for non-commercial/educational purposes without obtaining additional permission from Nature Publishing Group, providing that the author and the original source of publication are fully acknowledged(please see the article itself for the license version number). You may reuse this material without obtaining permission from Nature Publishing Group, providing that the author and the original source of publication are fully acknowledged, as per the terms of the license. For license terms, please see http://creativecommons.org/

BACK CLOSE WINDOW

ELSEVIER LICENSE
TERMS AND CONDITIONS

Jul 20, 2015

This is a License Agreement between David A Patten ("You") and Elsevier ("Elsevier") provided by Copyright Clearance Center ("CCC"). The license consists of your order details, the terms and conditions provided by Elsevier, and the payment terms and conditions.

All payments must be made in full to CCC. For payment instructions, please see information listed at the bottom of this form.

Supplier	Elsevier Limited The Boulevard,Langford Lane Kidlington,Oxford,OX5 1GB,UK
Registered Company Number	1982084
Customer name	David A Patten
Customer address	[redacted]
License number	3673210701951
License date	Jul 20, 2015
Licensed content publisher	Elsevier
Licensed content publication	Molecular Aspects of Medicine
Licensed content title	The mitochondrial transporter family SLC25: Identification, properties and physiopathology
Licensed content author	Ferdinando Palmieri
Licensed content date	April–June 2013
Licensed content volume number	34
Licensed content issue number	2-3
Number of pages	20
Start Page	465
End Page	484
Type of Use	reuse in a thesis/dissertation
Intended publisher of new work	other
Portion	figures/tables/illustrations
Number of figures/tables/illustrations	1
Format	print
Are you the author of this Elsevier article?	No

[redacted]

Will you be translating?	No
Original figure numbers	Figure 1
Title of your thesis/dissertation	The role of OPA1 and interacting proteins in mitochondrial function
Expected completion date	Aug 2015
Estimated size (number of pages)	203
Elsevier VAT number	GB 494 6272 12
Permissions price	0.00 USD
VAT/Local Sales Tax	0.00 USD / 0.00 GBP
Total	0.00 USD
Terms and Conditions	

INTRODUCTION

1. The publisher for this copyrighted material is Elsevier. By clicking "accept" in connection with completing this licensing transaction, you agree that the following terms and conditions apply to this transaction (along with the Billing and Payment terms and conditions established by Copyright Clearance Center, Inc. ("CCC"), at the time that you opened your Rightslink account and that are available at any time at http://myaccount.copyright.com).

GENERAL TERMS

2. Elsevier hereby grants you permission to reproduce the aforementioned material subject to the terms and conditions indicated.

3. Acknowledgement: If any part of the material to be used (for example, figures) has appeared in our publication with credit or acknowledgement to another source, permission must also be sought from that source. If such permission is not obtained then that material may not be included in your publication/copies. Suitable acknowledgement to the source must be made, either as a footnote or in a reference list at the end of your publication, as follows:

"Reprinted from Publication title, Vol /edition number, Author(s), Title of article / title of chapter, Pages No., Copyright (Year), with permission from Elsevier [OR APPLICABLE SOCIETY COPYRIGHT OWNER]." Also Lancet special credit - "Reprinted from The Lancet, Vol. number, Author(s), Title of article, Pages No., Copyright (Year), with permission from Elsevier."

4. Reproduction of this material is confined to the purpose and/or media for which permission is hereby given.

5. Altering/Modifying Material: Not Permitted. However figures and illustrations may be altered/adapted minimally to serve your work. Any other abbreviations, additions, deletions and/or any other alterations shall be made only with prior written authorization of Elsevier Ltd. (Please contact Elsevier at permissions@elsevier.com)

[redacted]

6. If the permission fee for the requested use of our material is waived in this instance, please be advised that your future requests for Elsevier materials may attract a fee.

7. Reservation of Rights: Publisher reserves all rights not specifically granted in the combination of (i) the license details provided by you and accepted in the course of this licensing transaction, (ii) these terms and conditions and (iii) CCC's Billing and Payment terms and conditions.

8. License Contingent Upon Payment: While you may exercise the rights licensed immediately upon issuance of the license at the end of the licensing process for the transaction, provided that you have disclosed complete and accurate details of your proposed use, no license is finally effective unless and until full payment is received from you (either by publisher or by CCC) as provided in CCC's Billing and Payment terms and conditions. If full payment is not received on a timely basis, then any license preliminarily granted shall be deemed automatically revoked and shall be void as if never granted. Further, in the event that you breach any of these terms and conditions or any of CCC's Billing and Payment terms and conditions, the license is automatically revoked and shall be void as if never granted. Use of materials as described in a revoked license, as well as any use of the materials beyond the scope of an unrevoked license, may constitute copyright infringement and publisher reserves the right to take any and all action to protect its copyright in the materials.

9. Warranties: Publisher makes no representations or warranties with respect to the licensed material.

10. Indemnity: You hereby indemnify and agree to hold harmless publisher and CCC, and their respective officers, directors, employees and agents, from and against any and all claims arising out of your use of the licensed material other than as specifically authorized pursuant to this license.

11. No Transfer of License: This license is personal to you and may not be sublicensed, assigned, or transferred by you to any other person without publisher's written permission.

12. No Amendment Except in Writing: This license may not be amended except in a writing signed by both parties (or, in the case of publisher, by CCC on publisher's behalf).

13. Objection to Contrary Terms: Publisher hereby objects to any terms contained in any purchase order, acknowledgment, check endorsement or other writing prepared by you, which terms are inconsistent with these terms and conditions or CCC's Billing and Payment terms and conditions. These terms and conditions, together with CCC's Billing and Payment terms and conditions (which are incorporated herein), comprise the entire agreement between you and publisher (and CCC) concerning this licensing transaction. In the event of any conflict between your obligations established by these terms and conditions and those established by CCC's Billing and Payment terms and conditions, these terms and conditions shall control.

14. Revocation: Elsevier or Copyright Clearance Center may deny the permissions described in this License at their sole discretion, for any reason or no reason, with a full refund payable to you. Notice of such denial will be made using the contact information provided by you. Failure to receive such notice will not alter or invalidate the denial. In no event will Elsevier

or Copyright Clearance Center be responsible or liable for any costs, expenses or damage incurred by you as a result of a denial of your permission request, other than a refund of the amount(s) paid by you to Elsevier and/or Copyright Clearance Center for denied permissions.

LIMITED LICENSE

The following terms and conditions apply only to specific license types:

15. **Translation**: This permission is granted for non-exclusive world **English** rights only unless your license was granted for translation rights. If you licensed translation rights you may only translate this content into the languages you requested. A professional translator must perform all translations and reproduce the content word for word preserving the integrity of the article. If this license is to re-use 1 or 2 figures then permission is granted for non-exclusive world rights in all languages.

16. **Posting licensed content on any Website**: The following terms and conditions apply as follows: Licensing material from an Elsevier journal: All content posted to the web site must maintain the copyright information line on the bottom of each image; A hyper-text must be included to the Homepage of the journal from which you are licensing at http://www.sciencedirect.com/science/journal/xxxxx or the Elsevier homepage for books at http://www.elsevier.com; Central Storage: This license does not include permission for a scanned version of the material to be stored in a central repository such as that provided by Heron/XanEdu.

Licensing material from an Elsevier book: A hyper-text link must be included to the Elsevier homepage at http://www.elsevier.com . All content posted to the web site must maintain the copyright information line on the bottom of each image.

Posting licensed content on Electronic reserve: In addition to the above the following clauses are applicable: The web site must be password-protected and made available only to bona fide students registered on a relevant course. This permission is granted for 1 year only. You may obtain a new license for future website posting.

17. **For journal authors:** the following clauses are applicable in addition to the above:

Preprints:

A preprint is an author's own write-up of research results and analysis, it has not been peer-reviewed, nor has it had any other value added to it by a publisher (such as formatting, copyright, technical enhancement etc.).

Authors can share their preprints anywhere at any time. Preprints should not be added to or enhanced in any way in order to appear more like, or to substitute for, the final versions of articles however authors can update their preprints on arXiv or RePEc with their Accepted Author Manuscript (see below).

If accepted for publication, we encourage authors to link from the preprint to their formal publication via its DOI. Millions of researchers have access to the formal publications on ScienceDirect, and so links will help users to find, access, cite and use the best available

[redacted]

version. Please note that Cell Press, The Lancet and some society-owned have different preprint policies. Information on these policies is available on the journal homepage.

Accepted Author Manuscripts: An accepted author manuscript is the manuscript of an article that has been accepted for publication and which typically includes author-incorporated changes suggested during submission, peer review and editor-author communications.

Authors can share their accepted author manuscript:

- immediately
  - via their non-commercial person homepage or blog
  - by updating a preprint in arXiv or RePEc with the accepted manuscript
  - via their research institute or institutional repository for internal institutional uses or as part of an invitation-only research collaboration work-group
  - directly by providing copies to their students or to research collaborators for their personal use
  - for private scholarly sharing as part of an invitation-only work group on commercial sites with which Elsevier has an agreement
- after the embargo period
  - via non-commercial hosting platforms such as their institutional repository
  - via commercial sites with which Elsevier has an agreement

In all cases accepted manuscripts should:

- link to the formal publication via its DOI
- bear a CC-BY-NC-ND license - this is easy to do
- if aggregated with other manuscripts, for example in a repository or other site, be shared in alignment with our hosting policy not be added to or enhanced in any way to appear more like, or to substitute for, the published journal article.

Published journal article (JPA): A published journal article (PJA) is the definitive final record of published research that appears or will appear in the journal and embodies all value-adding publishing activities including peer review co-ordination, copy-editing, formatting, (if relevant) pagination and online enrichment.

Policies for sharing publishing journal articles differ for subscription and gold open access articles:

[redacted]

Subscription Articles: If you are an author, please share a link to your article rather than the full-text. Millions of researchers have access to the formal publications on ScienceDirect, and so links will help your users to find, access, cite, and use the best available version.

Theses and dissertations which contain embedded PJAs as part of the formal submission can be posted publicly by the awarding institution with DOI links back to the formal publications on ScienceDirect.

If you are affiliated with a library that subscribes to ScienceDirect you have additional private sharing rights for others' research accessed under that agreement. This includes use for classroom teaching and internal training at the institution (including use in course packs and courseware programs), and inclusion of the article for grant funding purposes.

Gold Open Access Articles: May be shared according to the author-selected end-user license and should contain a CrossMark logo, the end user license, and a DOI link to the formal publication on ScienceDirect.

Please refer to Elsevier's posting policy for further information.

18. **For book authors** the following clauses are applicable in addition to the above: Authors are permitted to place a brief summary of their work online only. You are not allowed to download and post the published electronic version of your chapter, nor may you scan the printed edition to create an electronic version. **Posting to a repository:** Authors are permitted to post a summary of their chapter only in their institution's repository.

19. **Thesis/Dissertation**: If your license is for use in a thesis/dissertation your thesis may be submitted to your institution in either print or electronic form. Should your thesis be published commercially, please reapply for permission. These requirements include permission for the Library and Archives of Canada to supply single copies, on demand, of the complete thesis and include permission for Proquest/UMI to supply single copies, on demand, of the complete thesis. Should your thesis be published commercially, please reapply for permission. Theses and dissertations which contain embedded PJAs as part of the formal submission can be posted publicly by the awarding institution with DOI links back to the formal publications on ScienceDirect.

Elsevier Open Access Terms and Conditions

You can publish open access with Elsevier in hundreds of open access journals or in nearly 2000 established subscription journals that support open access publishing. Permitted third party re-use of these open access articles is defined by the author's choice of Creative Commons user license. See our open access license policy for more information.

Terms & Conditions applicable to all Open Access articles published with Elsevier:

Any reuse of the article must not represent the author as endorsing the adaptation of the article nor should the article be modified in such a way as to damage the author's honour or reputation. If any changes have been made, such changes must be clearly indicated.

[redacted]

The author(s) must be appropriately credited and we ask that you include the end user license and a DOI link to the formal publication on ScienceDirect.

If any part of the material to be used (for example, figures) has appeared in our publication with credit or acknowledgement to another source it is the responsibility of the user to ensure their reuse complies with the terms and conditions determined by the rights holder.

Additional Terms & Conditions applicable to each Creative Commons user license:

CC BY: The CC-BY license allows users to copy, to create extracts, abstracts and new works from the Article, to alter and revise the Article and to make commercial use of the Article (including reuse and/or resale of the Article by commercial entities), provided the user gives appropriate credit (with a link to the formal publication through the relevant DOI), provides a link to the license, indicates if changes were made and the licensor is not represented as endorsing the use made of the work. The full details of the license are available at http://creativecommons.org/licenses/by/4.0.

CC BY NC SA: The CC BY-NC-SA license allows users to copy, to create extracts, abstracts and new works from the Article, to alter and revise the Article, provided this is not done for commercial purposes, and that the user gives appropriate credit (with a link to the formal publication through the relevant DOI), provides a link to the license, indicates if changes were made and the licensor is not represented as endorsing the use made of the work. Further, any new works must be made available on the same conditions. The full details of the license are available at http://creativecommons.org/licenses/by-nc-sa/4.0.

CC BY NC ND: The CC BY-NC-ND license allows users to copy and distribute the Article, provided this is not done for commercial purposes and further does not permit distribution of the Article if it is changed or edited in any way, and provided the user gives appropriate credit (with a link to the formal publication through the relevant DOI), provides a link to the license, and that the licensor is not represented as endorsing the use made of the work. The full details of the license are available at http://creativecommons.org/licenses/by-nc-nd/4.0. Any commercial reuse of Open Access articles published with a CC BY NC SA or CC BY NC ND license requires permission from Elsevier and will be subject to a fee.

Commercial reuse includes:

- Associating advertising with the full text of the Article
- Charging fees for document delivery or access
- Article aggregation
- Systematic distribution via e-mail lists or share buttons

Posting or linking by commercial companies for use by customers of those companies.

20. **Other Conditions**:

[redacted]

v1.7

Questions? customercare@copyright.com or +1-855-239-3415 (toll free in the US) or +1-978-646-2777.

Appendix B:

Published online: October 8, 2014

Article

SOURCE DATA TRANSPARENT PROCESS

THE EMBO JOURNAL

OPA1-dependent cristae modulation is essential for cellular adaptation to metabolic demand

David A Patten[1], Jacob Wong[1], Mireille Khacho[1], Vincent Soubannier[2], Ryan J Mailloux[3], Karine Pilon-Larose[1], Jason G MacLaurin[1], David S Park[1], Heidi M McBride[2], Laura Trinkle-Mulcahy[1], Mary-Ellen Harper[3], Marc Germain[4,**] & Ruth S Slack[1,*]

Abstract

Cristae, the organized invaginations of the mitochondrial inner membrane, respond structurally to the energetic demands of the cell. The mechanism by which these dynamic changes are regulated and the consequences thereof are largely unknown. Optic atrophy 1 (OPA1) is the mitochondrial GTPase responsible for inner membrane fusion and maintenance of cristae structure. Here, we report that OPA1 responds dynamically to changes in energetic conditions to regulate cristae structure. This cristae regulation is independent of OPA1's role in mitochondrial fusion, since an OPA1 mutant that can still oligomerize but has no fusion activity was able to maintain cristae structure. Importantly, OPA1 was required for resistance to starvation-induced cell death, for mitochondrial respiration, for growth in galactose media and for maintenance of ATP synthase assembly, independently of its fusion activity. We identified mitochondrial solute carriers (SLC25A) as OPA1 interactors and show that their pharmacological and genetic blockade inhibited OPA1 oligomerization and function. Thus, we propose a novel way in which OPA1 senses energy substrate availability, which modulates its function in the regulation of mitochondrial architecture in a SLC25A protein-dependent manner.

Keywords ATP synthase; cristae; mitochondria; OPA1; SLC25A
Subject Categories Membrane & Intracellular Transport; Metabolism
DOI 10.15252/embj.201488349 | Received 27 February 2014 | Revised 28 August 2014 | Accepted 29 August 2014 | Published online 8 October 2014
The EMBO Journal (2014) 33: 2676–2691

Introduction

Mitochondria are vital to a number of important cell functions including energy production through oxidative phosphorylation (OXPHOS), calcium buffering and apoptotic signalling. These dynamic organelles constantly modify their architecture and undergo fission and fusion. Mitochondrial fusion is mediated by the two outer membrane mitofusins (MFN1 and MFN2) (Chen *et al*, 2003) and the inner membrane optic atrophy 1 (OPA1) (Meeusen *et al*, 2006). Mitochondrial fusion and fission are important processes for cell survival during a variety of stressors (Tondera *et al*, 2009; Gomes *et al*, 2011) and are dysregulated or disrupted in a number of human pathologies (Alexander *et al*, 2000; Delettre *et al*, 2000; Zuchner *et al*, 2004). Mitochondria also undergo internal cristae changes. Cristae, being invaginations of the inner membrane, form internal compartments which are connected to the inner boundary membrane (IBM) by tight cristae junctions. Cristae possess different proteins than the IBM arguing that they are functionally distinct compartments (Vogel *et al*, 2006; Wurm & Jakobs, 2006). Tight cristae, and their junctions, may restrict diffusion of small molecules and membrane proteins into and out of cristae (Mannella, 2006b; Sukhorukov & Bereiter-Hahn, 2009).

Changes in inner membrane topology have been documented during apoptosis, as cristae junction widening is required to mobilize cytochrome *c* stores for release upon outer membrane permeabilization (Scorrano *et al*, 2002; Germain *et al*, 2005; Frezza *et al*, 2006). Cristae structural changes during non-cell death stimuli have also been reported for many decades, but their regulation and function remain elusive. For example, isolated liver mitochondria display different reversible ultrastructure conformations according to their energetic state (Hackenbrock, 1966). Hackenbrock named these two states *orthodox* and *condensed*, where condensed mitochondria have a compacted matrix with enlarged cristae and orthodox mitochondria have a less dense matrix with compacted cristae. Similarly, starvation increases mitochondrial length and the number of cristae (Gomes *et al*, 2011), suggesting that mitochondria regulate their shape to adjust their activity with metabolic conditions (Mannella, 2006a). Furthermore, it was recently shown that cristae shape regulates respiration through the assembly of respiratory chain supercomplexes (Cogliati *et al*, 2013).

In addition to fusion, OPA1 and Mgm1, the yeast homologue of OPA1, are required for cristae structure as their disruption

1 Department of Cellular & Molecular Medicine, University of Ottawa, Ottawa, ON, Canada
2 Montreal Neurological Institute, McGill University, Montreal, QC, Canada
3 Department of Biochemistry, Microbiology & Immunology, University of Ottawa, Ottawa, ON, Canada
4 Département de Biologie Médicale, Université du Québec à Trois-Rivières, Trois-Rivières, QC, Canada
*Corresponding author. Tel: +1 613 562 5800; E-mail: rslack@uottawa.ca
**Corresponding author. Tel: +1 819 376 5011 x3330; E-mail: marc.germain1@uqtr.ca

drastically affects cristae morphology (Amutha *et al*, 2004; Frezza *et al*, 2006; Meeusen *et al*, 2006). Maintenance of cristae structure by OPA1 requires its oligomerization since during apoptosis, disruption of OPA1 oligomers is necessary for cristae opening and cytochrome *c* mobilization (Frezza *et al*, 2006). In fact, cytochrome *c* release and apoptosis could be inhibited by expressing mutant OPA1(Q297V), which mimics OPA1's GTP-bound state and remains self-assembled (Yamaguchi *et al*, 2008). However, the impact of physiological metabolic changes on OPA1 assembly, cristae and mitochondrial respiration is unknown.

Here, we demonstrate that OPA1 dynamically regulates cristae shape in healthy cells and that this process is required to maintain mitochondrial activity under conditions of low-energy substrate availability. Specifically, lack of energy substrates induced OPA1 oligomerization and narrowing of cristae, which was required to promote ATP synthase assembly and to maintain ATP-linked respiration. Importantly, these changes were independent of mitochondrial fusion and essential for cell survival. We also identified a group of mitochondrial solute carriers that interact with OPA1 to regulate its function. Taken together, our results demonstrate that OPA1-dependent modulation of cristae structure is necessary for cellular adaptation to energy substrate availability and is required for cell growth and survival.

Results

OPA1 responds rapidly and reversibly to metabolic demand

Although mitochondrial structural changes in response to energetic states have been documented for decades, their regulation and functional significance have remained largely unknown. To ask whether cristae structure responds to changes in nutrient conditions, mouse embryonic fibroblasts (MEFs) were starved with EBSS for 2 h and cristae were measured. We observed a significant thinning of cristae width and mitochondrial width in response to starvation (Fig 1A). While untreated cells had an average cristae width of 17.6 nm, starved cells had an average width of only 11.9 nm. Since the deoligomerization of OPA1 regulates cristae widening during cell death signalling (Frezza *et al*, 2006), we assessed the oligomerization status of OPA1 in response to starvation. Starved MEFs exhibited significantly more oligomerized OPA1 than fed controls (Fig 1B and D). At longer time points, we also observed that mitochondria elongate from an average length of 3.3 to 4.2 μm, $P = 0.022$ (distribution in Fig 1C). This previously documented elongation has been substantiated by a decrease in mitochondrial fission through DRP-1 inhibition leading to unopposed mitochondrial fusion (Gomes *et al*, 2011; Rambold *et al*, 2011). Unlike elongation, the oligomerization of OPA1 in response to starvation was rapid (within 1 h) and preceded activation of the autophagic pathway as indicated by p62 degradation (Fig 1D). Furthermore, changes in OPA1 oligomerization were rapidly reversible, since incubation of starved MEFs for only 30 min in recovery media (regular growth media) reversed the increase in oligomerized OPA1 (Fig 1E). Together, these data suggest that changes in OPA1 oligomers are linked to changes in cristae structure not only during cell death as previously demonstrated (Frezza *et al*, 2006), but also in healthy cells following changes in energy substrate availability.

To assess how OPA1 responds to changes in fuel substrate availability, we turned to an *in vitro* system. Isolated mitochondria were incubated in the absence or the presence of ETC substrates and crosslinked. When mitochondria were fed with complex I and II substrates (malate plus glutamate or succinate, respectively), OPA1 oligomerization was dramatically reduced compared to no substrate, starved controls [Fig 2A (EDC crosslinking) and Supplementary Fig S1A (BMH crosslinking)]. As we would predict, the same concentration of glucose, the principal glycolysis substrate, had no effect on OPA1 oligomerization (Fig 2A). As in starved cells, OPA1 oligomerization was rapidly reversible upon the addition or removal of complex I substrates (Fig 2B). Next, we asked whether changes in OPA1 oligomerization correlated with altered mitochondrial structure. This was assessed by mitochondrial inter-cristae cytochrome *c* retention, as a readout of cristae structure, since an increase in releasable cytochrome *c* following outer membrane solubilization correlates with wider cristae (Scorrano *et al*, 2002; Wasilewski *et al*, 2012). Following the addition of a low concentration of digitonin to specifically solubilize the outer membrane [1 μg/μg mitochondria, at 0.1% w/v—experimentally determined (Supplementary Fig S1B)], significantly more cytochrome *c* was mobilized when mitochondria were incubated in the presence of complex I and II substrates, compared to the absence of substrates (Fig 2C). Furthermore, this increase in cytochrome *c* mobilization, indicative of cristae widening, was reversible (Supplementary Fig S1C), correlating with the decrease in OPA1 oligomerization and a decrease in orthodox mitochondria, which demonstrates tighter cristae morphology (Supplementary Fig S1D and E). The regulation of cytochrome *c* retention was OPA1 dependent, since mitochondria from OPA1 KO cells had very high levels of mobilized cytochrome *c* independently of the presence of complex I substrates (Fig 2D). We next asked whether the substrate-dependent changes in OPA1 oligomerization were secondary to changes in electron transport chain (ETC) activity. To this end, we added rotenone, a complex I poison, and CCCP, a mitochondrial uncoupler, to the mitochondrial preparations. Neither rotenone nor CCCP altered OPA1 oligomerization (Fig 2E and F), suggesting that OPA1 responds to energy substrate availability upstream of changes in mitochondrial respiration and ETC function.

These studies reveal a strict correlation between energy substrate level, cristae structure and OPA1 oligomerization in which mitochondria enriched with substrates show low levels of OPA1 oligomers and mobilized cytochrome *c* from cristae stores, and starved mitochondria show high levels of OPA1 oligomers and tight cristae. We next sought out the physiological relevance of this cristae regulation as well as the mechanism by which OPA1 senses energy substrate availability.

OPA1 is required for regulation of cristae structure and cell survival during starvation

To address the physiological importance of OPA1-dependent cristae remodelling in response to changes in energy substrate conditions, we first asked whether OPA1 KO cells, devoid of cristae, could survive cellular starvation. While WT MEFs were minimally affected by 6 h of EBSS starvation, OPA1 KO MEFs showed a dramatic increase in cell death, as recently published (Fig 3A, Supplementary Fig S2A and B) (Gomes *et al*, 2011). As survival of starved cells has

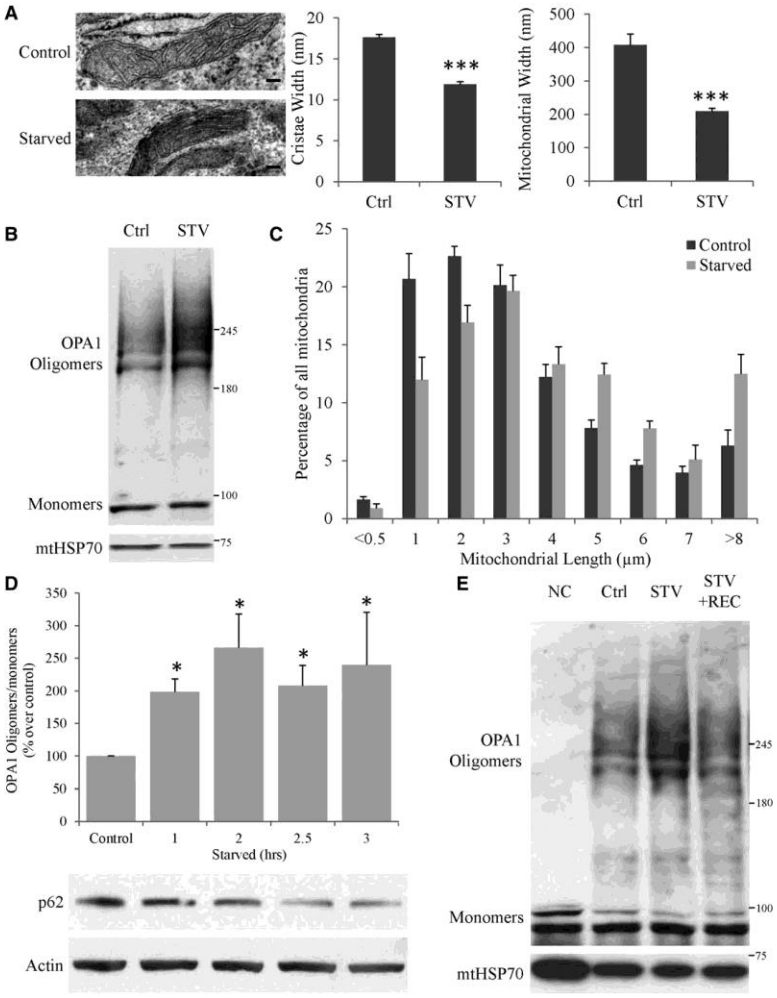

Figure 1. Cristae condense, mitochondria elongate and OPA1 oligomerizes rapidly and reversibly during cell starvation.

A MEFs were starved (STV) or not (Ctrl) for 2 h, fixed with 2% PFA and 1.6% glutaraldehyde and analysed by EM. Cristae and mitochondrial width were quantified from mitochondria and cristae within 10 cells from two independent cultures (n = 20). Scale bars: 100 nm.

B Cells were starved or not for 2 h and crosslinked with BMH (1 mM), and OPA1 oligomerization was analysed by gradient gel Western blot.

C MEFs were starved for 4 h and fixed, and mitochondrial length was measured by immunofluorescence using Tom20 antibodies (averages ± SEM of three independent experiments).

D Time-course experiment of EBSS starvation on OPA1 oligomerization status as performed in (B) (averages ± SEM of four independent experiments). Whole-cell lysates of a parallel experiment were analysed by Western blot.

E After 2 h of EBSS starvation, MEFs were recovered (REC) in regular growth media for 30 min or not and OPA1 oligomers were then analysed as above. A non-crosslinked control (NC) is also included.

Data information: Student's t-tests were performed relative to control, $^*P < 0.05$, $^{***}P < 0.005$.
Source data are available online for this figure.

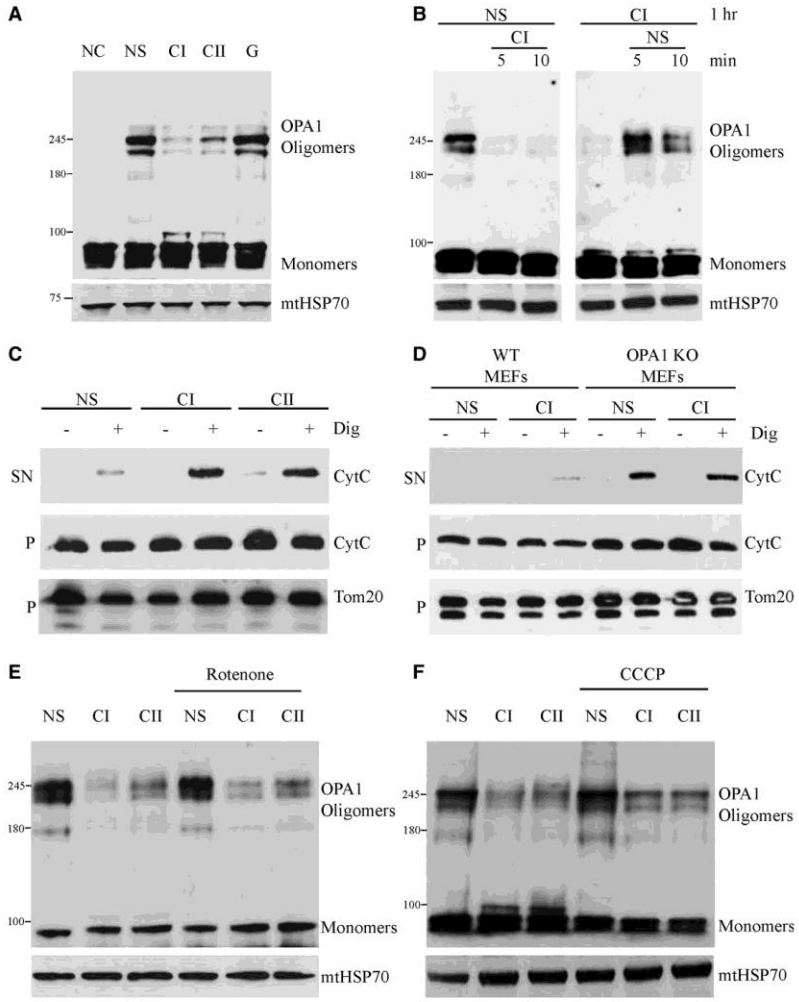

Figure 2. OPA1 responds to energy substrate availability and responds by oligomerizing and maintaining cytochrome c in isolated mitochondria.

A OPA1 oligomerization was analysed in isolated mouse liver mitochondria incubated with or without the indicated ETC substrates (NC: non-crosslinked control; NS: no substrate control; CI: complex I, malate and glutamate; CII: complex II, succinate; G: glucose control; all at 5 mM each) for 1 h at 37°C and subsequently crosslinked with EDC for 30 min at room temperature. OPA1 oligomers were then analysed by gradient gel Western blot.

B Mitochondria were incubated with or without complex I substrates, spun down and resuspended in the indicated buffer for 5 and 10 min and analysed as above.

C Mitochondrial ultrastructure was analysed as the distribution of intercristal cytochrome *c* from liver mitochondria and solubilized with low digitonin concentrations (1 μg/μg mitochondria, 0.1%). Mobilized cytochrome *c* was separated by centrifugation and visualized by Western blot analysis where released cytochrome *c* was redistributed from the pellet (P) to the supernatant (SN) fraction.

D Cytochrome *c* mobilization was analysed on mitochondria isolated from WT and OPA1 KO MEFs treated as indicated.

E Liver mitochondria were incubated with or without indicated substrates as above with or without rotenone (2 μM), an ETC complex I poison.

F Liver mitochondria were incubated with or without indicated substrates as above with or without CCCP (10 μM), a mitochondrial uncoupler.

Source data are available online for this figure.

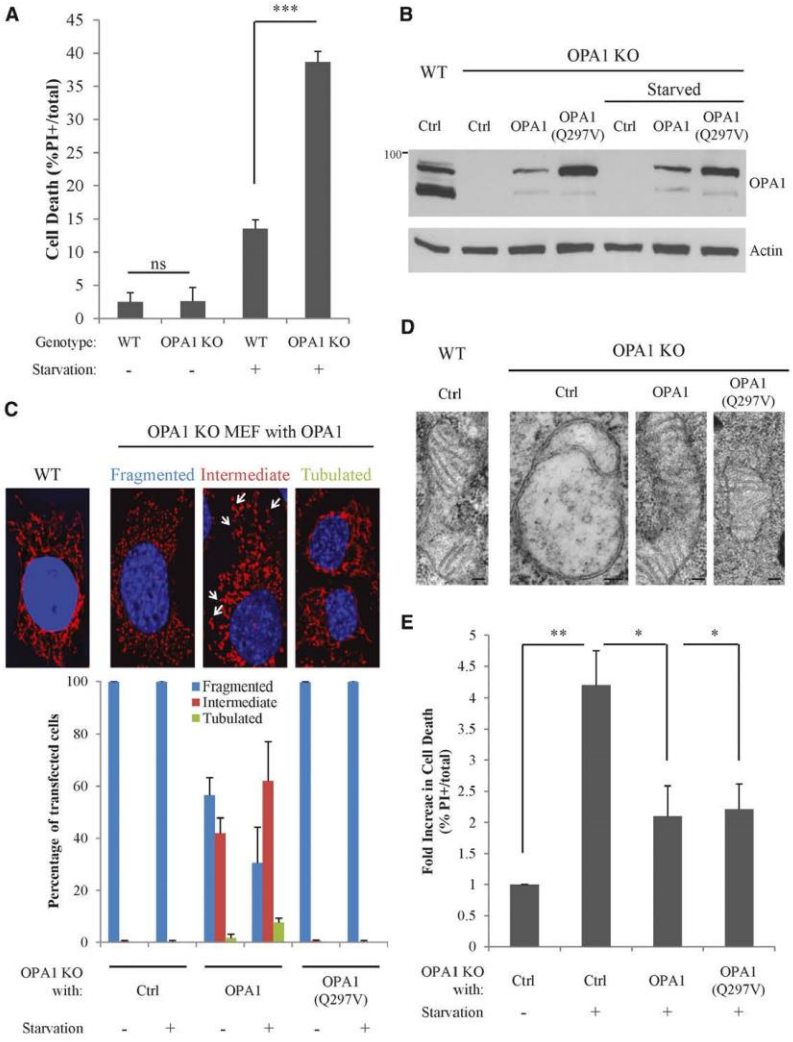

Figure 3. OPA1 is required for resistance to starvation-induced cell death independently of its fusion activity.

A Cell death of WT and OPA1 KO cells starved or not for 6 h was analysed with propidium iodide (PI) and Hoechst (averages ± SEM of four independent experiments).

B Representative Western blot of OPA1 expression in the transient transfection experiments performed in (C–E).

C OPA1 KO MEFs were transiently transfected for 48 h with the indicated plasmids, and mitochondrial length was binned according to the top panels by immunofluorescence where cells that had any long mitochondria were binned as intermediate (averages ± SEM of three independent experiments).

D Representative EM of mitochondria from cells transfected as indicated. Scale bars: 100 nm.

E OPA1 KO MEFs were transfected as indicated for 48 h and starved or not for 6 h, and cell death was analysed as in (A) (averages ± SEM of four independent experiments).

Data information: Student's *t*-tests were performed as indicated, $*P < 0.05$, $**P < 0.01$ and $***P < 0.005$.
Source data are available online for this figure.

been suggested to require mitochondrial elongation through unopposed fusion (Gomes *et al*, 2011), we isolated the roles of fusion and cristae structure using a mutant form of OPA1 that fails to mediate fusion. OPA1(Q297V) mimics the GTP-bound state of OPA1, allowing oligomerization, but defective in GTPase activity, which is required to mediate fusion (Misaka *et al*, 2002; Yamaguchi *et al*, 2008). To assess their ability to rescue mitochondrial fusion and cristae structure, isoform 1 of WT OPA1 or isoform 1 of OPA1(Q297V) was reintroduced in OPA1 KO MEFs by transient transfections, resulting in the expression of mostly the long form with some cleaved short form (Fig 3B). While WT OPA1 rescued fusion, the OPA1(Q297V) mutant was completely fusion incompetent, despite that it was expressed at slightly higher levels than WT OPA1 (Fig 3B and C). To assess whether OPA1(Q297V) can rescue the cristae structural defects seen in OPA1 KO cells, we performed transmission electron microscopy (EM). Both WT and OPA1(Q297V) rescued the severe cristae defects found in OPA1 KO MEFs (Fig 3D) and rescued survival of OPA1 KO MEFs during starvation (Fig 3E, Supplementary Fig S2C). These results suggest that OPA1 protects against starvation-induced cell death independently of its fusion activity.

OPA1 maintains mitochondrial function independently of its fusion activity

The rescue of cristae structure and cell survival by OPA1 and a fusion-incompetent mutant suggests that cristae modulation is a key determinant of cellular survival under changing energetic demands. To assess whether OPA1-mediated cristae alterations alone can affect cellular metabolism, we generated MEFs stably expressing OPA1 or OPA1(Q297V), resulting in high expression of both the long and short isoforms of OPA1 (Fig 4A). As in the transient system, OPA1(Q297V) rescued cristae structure in OPA1-deficient MEFs but not mitochondrial fusion (Supplementary Fig S3A and B). In addition, both WT and OPA1(Q297V) oligomerized and responded to substrate-level changes in isolated mitochondria from stable cell lines (Fig 4B).

To address how OPA1-mediated control of cristae modulates mitochondrial energetics, we assessed cellular oxygen consumption characteristics after OPA1 reintroduction using the Seahorse XF-24 analyzer (Fig 4C–E). Under fuel-rich conditions, a modest difference in ATP-linked respiration (the difference between the initial resting respiration and the respiration in the presence of oligomycin, a complex V inhibitor) was observed between WT and OPA1 KO MEFs (Fig 4C, Supplementary Fig S4A and B). However, starvation increased the difference in ATP-linked oxygen consumption between WT and OPA1 KO cells (Fig 4D, Supplementary Fig S4A and B), consistent with a requirement for OPA1 to maintain mitochondrial ATP levels under starvation (Gomes *et al*, 2011). We next addressed whether OPA1(Q297V) rescued oxygen consumption. Under resting (fed) conditions, only expression of the WT form of OPA1 significantly increased ATP-linked respiration of OPA1 KO MEFs (Fig 4C and quantified in E). However, after starvation, both the WT and OPA1(Q297V) significantly increased ATP-linked oxygen consumption (Fig 4D and E). Only WT OPA1 reintroduction completely rescued maximal respiration (oligomycin and FCCP, a mitochondrial uncoupler) and thus the reserve capacity (the difference between the resting and maximal respiration) (Fig 4E). These functional studies demonstrate that the critical role of OPA1 in regulating mitochondrial metabolism is fusion independent; however, mitochondrial fusion is required for full maximal oxygen consumption, possibly through maintenance of mtDNA (see below), which may be important following other various stressors.

To further investigate the role of cristae and mitochondrial fusion in mitochondrial function, cells were grown in a galactose medium in which they must rely on OXPHOS for ATP production (Aguer *et al*, 2011; Cogliati *et al*, 2013). While WT and OPA1 KO MEFs grew at similar rates in glucose media, OPA1 KO cells were growth retarded in galactose media compared to WT MEFs (Fig 4F). In fact, in the third week of growth in galactose media, it took more than twice as long for OPA1 KO cells to double their numbers (Supplementary Fig S5). Reintroducing WT or OPA1(Q297V) rescued growth retardation in OPA1 KO MEFs (Fig 4F, Supplementary Fig S5), providing further evidence that OPA1 can maintain mitochondrial function to support cell growth, independently of mitochondrial fusion.

As Mgm1 and OPA1 are required for the assembly of the ATP synthase (Amutha *et al*, 2004; Gomes *et al*, 2011), we asked whether this assembly is modified by energy substrate availability and in a fusion-independent fashion. To this end, Blue-Native PAGE (BN-PAGE) was performed on isolated mitochondria treated with substrates affecting OPA1 oligomerization and cytochrome *c* retention. When mitochondria are fed with complex I substrates, which decrease OPA1 oligomers (Fig 2), both ATP synthase oligomers and monomers are decreased (Fig 5A), without a decrease in ATP5A subunits themselves (Fig 5B). BN-PAGE analysis in whole cells demonstrated that in WT MEFS, all ATP synthase subunits were assembled to form the monomer (very little dimer was detected); however, OPA1 KO MEFs had substantially less assembled ATP synthase monomers and an increase in free F_1 (Fig 5C). Reconstitution with either WT OPA1 or OPA1(Q297V) increased ATP synthase assembly, most notably when cells were forced to rely on OXPHOS for ATP production (galactose media, Fig 5C and D). While WT OPA1 completely rescued the assembly of the F_1 portion into F_1F_o monomers, OPA1(Q297V) cells still exhibited a significant level of free F_1, even in galactose media (Fig 5C and D). The persistence of free F_1 correlated with the inability of OPA1(Q297V) to rescue the loss of mtDNA caused by OPA1 deletion (Fig 5E), consistent with the requirement of mitochondrial fusion for mtDNA maintenance (Chen *et al*, 2010). While all of the subunits of the F_1 are nuclear-encoded, the F_o portion contains two subunits, ATP6 and ATP8, encoded by mtDNA. Since OPA1 KO and OPA1(Q297V) cells have decreased mtDNA levels, unassembled F_1 is likely due to a lack of mitochondrial-encoded F_o subunits. Interestingly, human mutations affecting expression of both mtDNA F_o subunits demonstrate increased free F_1 relative to monomer by BN-PAGE (Jonckheere *et al*, 2008; Pitceathly *et al*, 2012). Indeed, decreased levels of the mtDNA-encoded F_o subunit ATP6 in OPA1 KO and OPA1(Q297V) cells were confirmed by RT–PCR (Fig 5F). Since the OPA1(Q297V) mutant was unable to rescue mtDNA or mtDNA-encoded transcripts, here we propose a novel fusion-independent role of OPA1 on ATP synthase stability. Thus, assembly of a functional F_1F_o monomer depends dually on OPA1 for its stability and for fusion-dependent, mtDNA-encoded F_o subunit expression (Fig 5G).

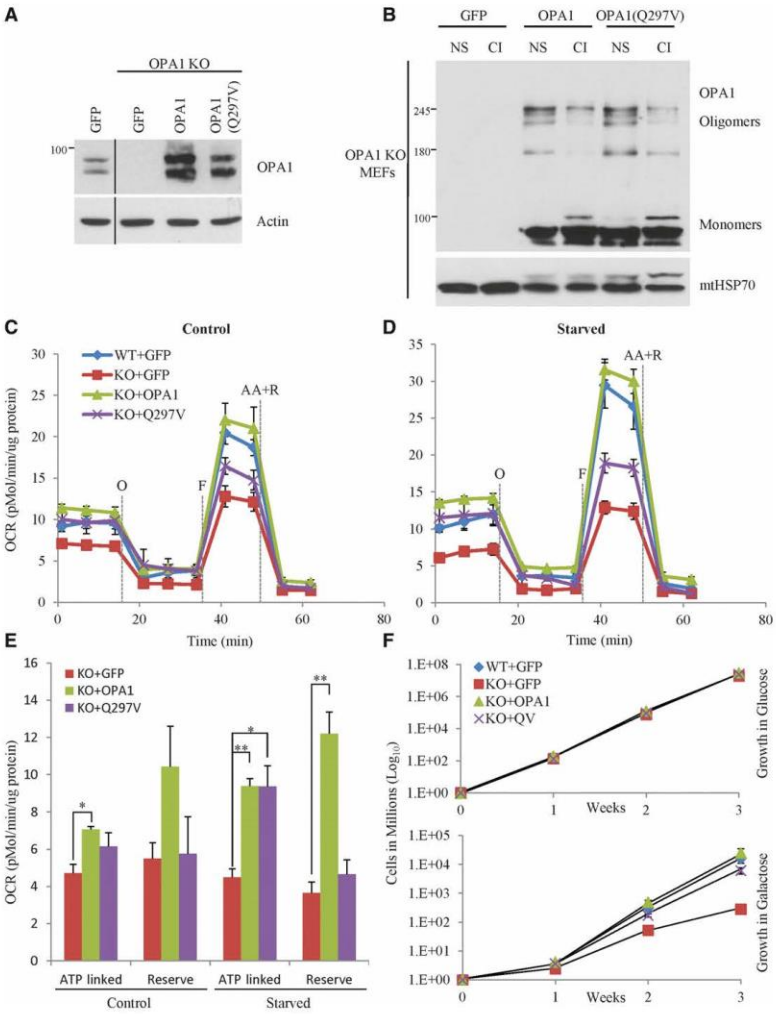

Figure 4. OPA1 regulates mitochondrial metabolism independently of mitochondrial fusion.

A WT and OPA1 knockout MEFs were infected with viruses encoding GFP, OPA1 or OPA1(Q297V) with dual promoters expressing GFP to allow for puromycin selection and FACS sorting cells for GFP expression. The resulting cultures were lysed, analysed by Western blot analysis and used for all subsequent experiments.

B OPA1 oligomers were analysed from isolated mitochondria incubated with no substrate or complex I substrates.

C, D To assess the impact of the fusion-incompetent OPA1 mutant on mitochondrial bioenergetics, we studied cells in the Seahorse XF-24 analyzer. Cells were plated on Seahorse TC plates 24 h prior to analysis, washed and incubated for 15 min in modified KRB and analysed. Cells in (D) were pre-starved for 2 h before analysis. At the indicated times, oligomycin (O), FCCP (F) and antimycin A (AA) with rotenone (R) were injected (averages ± SEM of three independent experiments).

E Quantification of ATP-linked OCR (resting OCR minus oligomycin-insensitive OCR) and reserve OCR (maximal minus resting) in (C) and (D).

F Long-term cell cultures were grown in glucose (top panel) or galactose media (bottom panel). Cells were passaged as required, medium was changed every 3 days if required, and cell number was determined once per week (averages ± SEM of four independent experiments).

Data information: Student's *t*-tests were performed relative to control, $*P < 0.05$ $**P < 0.01$.
Source data are available online for this figure.

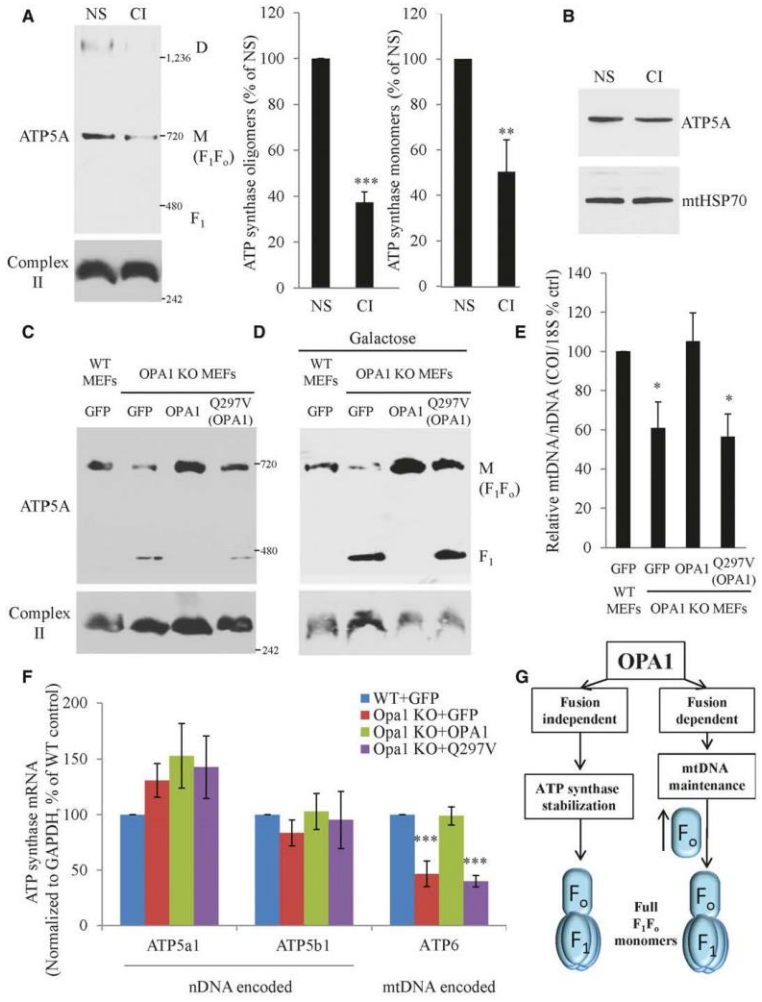

Figure 5. The dual role of OPA1 in regulating the ATP synthase.

A Isolated mitochondria incubated with complex I substrates were analysed by BN-PAGE and blotted for ATP5A of the ATP synthase. The oligomers [mostly dimers (D)] and monomer (M) of the ATP synthase were quantified as relative to complex II monomer (averages ± SEM of five independent experiments).

B Isolated liver mitochondria incubated with or without complex I in parallel with (A), lysed and analysed for ATP5A by straight Western blot.

C, D Long-term cultures of control cells (C) or cells grown for 1–2 weeks in galactose (D) were extracted for BN-PAGE directly from cells and blotted for ATP5A and complex II.

E DNA was extracted from long-term cultures, and mtDNA was analysed by qPCR relative to nDNA (averages ± SEM of three independent experiments).

F RNA was extracted from long-term cultures, and nuclear and mtDNA-encoded ATP synthase transcripts were analysed by RT–PCR (averages ± SEM of four independent experiments).

G Schematic diagram demonstrates the dual roles of OPA1 on the F_1F_o ATP synthase where OPA1 regulates the stabilization of the ATP synthase independently of its fusion activity and regulates mtDNA stability which is required for ATP6 (F_o subunit) expression and thus full F_1F_o ATP synthase assembly.

Data information: Student's *t*-tests were performed relative to control, $*P < 0.05$, $**P < 0.01$ and $***P < 0.005$.
Source data are available online for this figure.

Solute carriers interact with OPA1 and regulate its sensing of mitochondrial energy substrates

Our results revealed that OPA1 responds to changes in fuel substrate conditions by modifying its oligomerization and that this is required for the adaptation and survival of cells during starvation. To determine the mechanism by which substrate levels modify OPA1 function, we performed a proteomics screen in search of OPA1 interacting factors. Stable isotope labelling of amino acids in cell culture (SILAC) combined with immunoprecipitation and mass spectroscopy was used as a quantitative and sensitive technique to identify novel OPA1 protein interactors that may be required for substrate sensing (Trinkle-Mulcahy, 2012) (Supplementary Fig S6A). A log SILAC ratio of 1 was set as the cut-off for validation since it gave a confidence interval of 95% (Supplementary Fig S6B). Of the 35 hits above a log SILAC ratio of 1, 18 (51%) were mitochondrial, 8 were ribosomal and 9 were either unknown or neither mitochondrial nor ribosomal (Supplementary Fig S6 and Supplementary Table S1). Highly relevant to fuel substrate sensing, a number of mitochondrial carrier proteins (SLC25A) were identified as OPA1-interacting proteins. Mitochondrial solute carriers are mitochondrial inner membrane proteins that catalyze the transfer of diverse substrates across the mitochondrial inner membrane [for a review see (Palmieri, 2013)]. Importantly, some of these solute carriers are involved in shuttling the mitochondrial substrates utilized in Fig 2, namely malate and succinate by SLC25A10 [the dicarboxylate carrier (DIC)], malate by SLC25A11 [the oxoglutarate carrier (OGC)] and glutamate by SLC25A12 and SLC25A13 [the aspartate/glutamate carriers 1 (AGC1) and 2 (AGC2)]. Given the requirement for OPA1-mediated cristae regulation in response to starvation, we asked whether these solute carriers were responsible for modulating OPA1 in response to substrate concentrations.

To first validate the OPA1–SLC25A protein interactions, C-terminally 3×flag-tagged solute carrier protein constructs (AGC1, AGC2, OGC and DIC) were overexpressed in MEFs and their mitochondrial localization was confirmed by immunofluorescence (Supplementary Fig S7A). Immunoprecipitation of tagged AGC1, AGC2, OGC and DIC revealed an interaction with endogenous OPA1 (Fig 6A), in line with the SILAC experiment where tagged OPA1 immunoprecipitated endogenous SLC25A proteins. Furthermore, immunoprecipitation of endogenous OPA1 from both isolated MEF and liver mitochondria also revealed an interaction with endogenous OGC but not other control mitochondrial proteins (Fig 6B, Supplementary Fig S7B). In addition, the interaction between OPA1 and OGC was decreased by 59.4% ± 10.7 (SEM, $n = 3$) when an OGC competitive inhibitor (phenylsuccinate) was added to the immunoprecipitation buffer suggestive of a dynamic interaction (Fig 6B, Supplementary Fig S7B). To further study this interaction and the role of solute carriers in the regulation of OPA1 assembly and function, we used both a genetic and pharmaceutical approach. To deplete OGC, MEFs were subjected to two rounds of siRNA transfection for a total of 120 h (Fig 6C). Neither OGC depletion nor OGC overexpression had an observable effect on mitochondrial length (Supplementary Fig S8A and B). In addition to mitochondrial length, OGC depletion had no effect on gross mitochondrial structure (Supplementary Fig S9A), OCR rates in regular growth conditions (Fig 6F and H) or cell survival in starvation (Supplementary Fig S9B and C), indicating that decreasing OGC levels does not disrupt overall mitochondrial structure and function. As our hypothesis is that OGC and other SLC25A proteins regulate OPA1 under changing substrate levels, we then measured the response of siOGC mitochondria to substrate availability *in vitro*. Incubation of siOGC mitochondria in the absence of substrates reduced OPA1 oligomerization, also reducing the difference in OPA1 oligomerization between fed and no substrate conditions (Fig 6D, Supplementary Fig S9D). Additionally, when isolated mitochondria were incubated in the absence of energy substrates, siOGC mitochondria were unable to retain as much cytochrome *c*, indicative of their inability to respond to changing substrate levels (Fig 6E, Supplementary Fig S9C). Next, we investigated the consequences of OGC depletion on the response to starvation. Starvation of siOGC cells significantly reduced their ATP-linked oxygen consumption rate (Fig 6G and H), indicating an impaired response to changes in substrate availability. In addition, siOGC cells displayed a modest but reproducible decrease in cell growth in galactose media (Fig 6I). These results indicate that OGC plays a role in the adaptation of mitochondria to changing energy substrate levels, possibly by regulating OPA1 oligomerization.

To confirm that OPA1 senses substrate availability through the SLC25A proteins, we utilized competitive inhibitors of the DIC and OGC in order to mimic substrate binding in the complete absence of actual energy substrates. Strikingly, both the DIC inhibitor butylmalonate (BM) and the OGC inhibitor phenylsuccinate (PhS) alone drastically reduced OPA1 oligomerization, mirroring the OPA1 response to substrate-rich conditions (Fig 7A). Again, this correlated with increased mobilization of cytochrome *c* stores, indicative of an increased cristae width (Fig 7B). Finally, since OPA1 regulates ATP synthase stability, we investigated the effect of the SLC25A inhibitors on the ATP synthase. Strikingly, both the dimer and the monomer of the ATP synthase were drastically decreased following incubation with BM or PhS (Fig 7C). Importantly, the decrease in ATP synthase and increase in cytochrome *c* mobilization were specific, as cytochrome *c* was not mobilized in the absence of digitonin (Fig 7B), complex II was not altered (Fig 7C), and BM and PhS did not alter total ATP5A levels (Fig 7D).

Altogether, these results indicate that OPA1 responds to changes in fuel substrate levels, influenced by SLC25A proteins, altering mitochondrial function through its role in cristae regulation and ATP synthase assembly.

Discussion

Cristae structural changes have been documented decades ago (Hackenbrock, 1966, 1968a,b), but our understanding of how these changes occur and their functional consequence is largely unknown. Here, we demonstrate a novel mechanism by which cristae are physiologically regulated. Changes in energy substrate availability are sensed by mitochondrial SLC25A transporters, which in turn regulate OPA1 oligomerization. OPA1 oligomerization is then required to modulate cristae width and regulate assembly of the ATP synthase, in a mitochondrial fusion-independent manner. The physiological importance of this mechanism is highlighted by the demonstration that a fusion-incompetent form of OPA1(Q297V) rescued OCR, ATP synthase assembly and cell growth of OPA1 KO MEFs in galactose media, which forces mitochondrial respiration for ATP production.

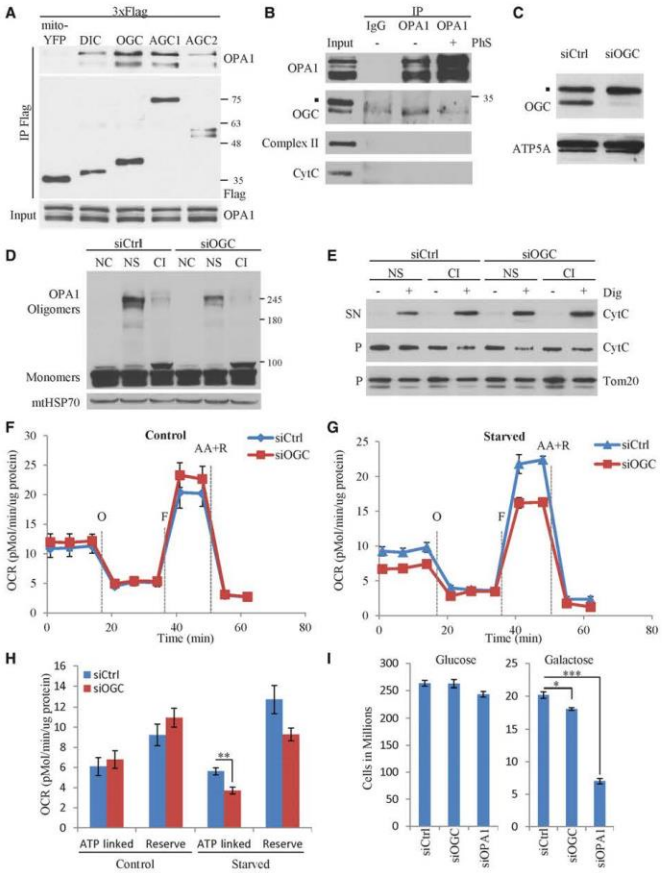

Figure 6. OPA1 interacts with SLC25 proteins that regulate OPA1's response to starvation.

A Mito-YFP-3×flag, DIC-3×flag, OGC-3×flag, AGC1-3×flag and AGC2-3×flag constructs were transiently transfected into MEFs. Twenty-four hours post-transfection, cells were lysed, immunoprecipitated with anti-flag antibodies and analysed by Western blot.

B Endogenous OPA1 was immunoprecipitated from MEF mitochondrial lysates with or without 15 mM phenylsuccinate (PhS), and the eluted samples were analysed by Western blot. Complex II and cytochrome *c* were used as negative controls.

C Representative OGC knockdown for experiments in (D–H) (see also Supplementary Figs S8B and S9A–E). MEFs were transfected twice with siOGC for 120 h total, and mitochondrial lysates were analysed by Western blot.

D Isolated mitochondria from siOGC-treated cells were incubated with the indicated ETC substrates (NC: non-crosslinked control; NS: no substrate control; CI: complex I, malate and glutamate at 5 mM each) for 30 min at 37°C and crosslinked with EDC, and OPA1 oligomers were then analysed by gradient gel Western blot.

E Isolated mitochondria from siOGC and siCtrl cells were incubated in no substrate or complex I buffers for 30 min and analysed for cytochrome *c* retention.

F, G SiOGC and siCtrl cells were plated onto Seahorse TC plates 24 h prior to analysis, washed and incubated for 15 min in modified KRB and analysed by the XF analyzer. Cells in (G) were pre-starved for 2 h before analyses. At the indicated times, oligomycin (O), FCCP (F) and antimycin A (AA) with Rotenone (R) were injected.

H Quantification of ATP-linked (resting OCR minus oxygen leak) and reserve OCR (maximal minus resting OCR) in (F) and (G) (averages ± SEM of four independent experiments).

I MEFs were grown for 1 week in galactose media, to revert to a more oxidative phenotype, or in regular glucose media, and these cells (1×10^5) were transfected with either siCtrl, siOGC or siOPA1 and maintained in their respective media. Cells were then left to grow, passaged when required, and cell number in regular growth medium (left panel) or galactose media (right panel) was counted 6 days later (averages ± SEM of 4 independent experiments).

Data information: Student's *t*-tests were performed as indicated: $*P < 0.05$, $**P < 0.01$, $***P < 0.005$. ▪ indicates a background band in (B) and (C).
Source data are available online for this figure.

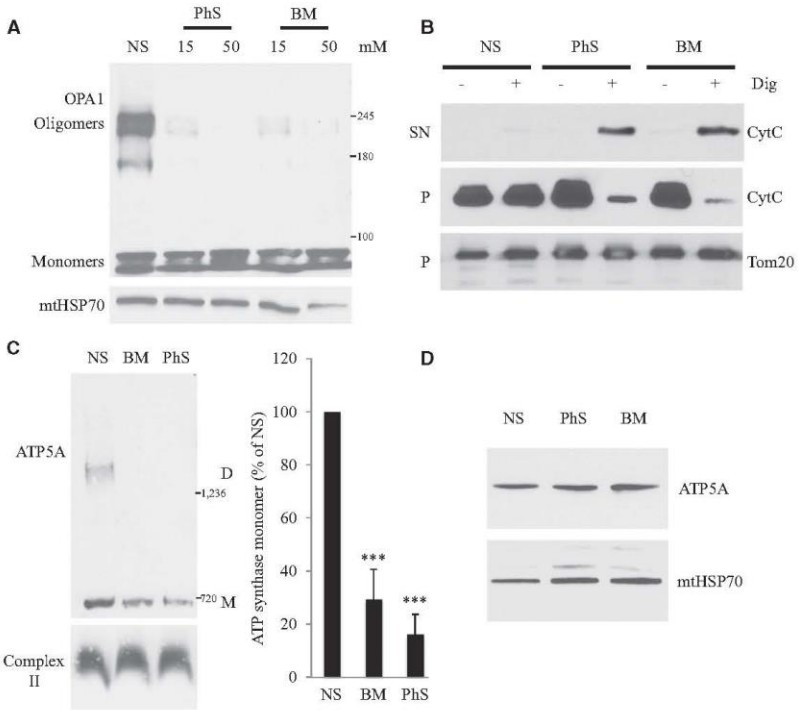

Figure 7. Pharmacological blockade of SLC25A proteins drastically inhibit OPA1 oligomerization and function.

A Isolated liver mitochondria were incubated with phenylsuccinate (PhS) or butylmalonate (BM), and OPA1 oligomerization was assessed as previously.

B Mouse liver mitochondria were incubated with 50 mM PhS or BM, and then, cytochrome *c* retention was analysed where released CytC was mobilized from the pellet (P) to the supernatant (SN) fraction.

C Mouse liver mitochondria were incubated with 50 mM PhS or BM, and lysates were analysed by BN-PAGE. ATP synthase monomers were quantified (right panel) relative to complex II monomer (averages ± SEM of 6 independent experiments).

D Mouse liver mitochondria were prepared and incubated in parallel with 7C and analysed by regular Western blot for ATP5A.

Data information: Student's *t*-tests were performed relative to control, ***$P < 0.005$.
Source data are available online for this figure.

Although it is known that OPA1 oligomers disassemble during cell death leading to release of proapoptotic factors (Frezza *et al*, 2006) and that OPA1 oligomer disruption by cristae remodelling results in impaired respiration (Cogliati *et al*, 2013), physiological changes in OPA1 oligomers and their role in regulating cristae structure under non-cell death conditions remained poorly understood. Here, we demonstrated in both cells and isolated mitochondria that starvation increases OPA1 oligomers rapidly and reversibly, correlating with tighter cristae width. These substrate-dependent changes in OPA1 oligomers were upstream/independent of ETC function and membrane potential, known regulators of OPA1 processing and its fusion function (Song *et al*, 2007; Mishra *et al*, 2014). By taking advantage of the OPA1(Q297V) mutant, we showed that, independently of mitochondrial fusion, OPA1 can maintain cristae structure and mitochondrial activity and adapt to the lack of nutrients during starvation. Our study therefore demonstrates that the roles of OPA1 in mitochondrial fusion and cristae maintenance can be separated and that cristae can be maintained in the absence of mitochondrial fusion.

How oligomerized OPA1 regulates cristae structure is still largely unknown. One proposed mechanism is through the oligomerization of two long and one short isomer of OPA1 (Frezza *et al*, 2006), although OPA1 oligomerization could also promote its interaction with other protein complexes required for cristae formation. In support of this hypothesis, our SILAC-based interaction screens revealed interactions with several factors critical for cristae structure maintenance: the ATP synthase, prohibitin, mitofilin, CHCHD3, Sam50 and the adenonucleotide transporters. In fact, recent groundbreaking studies have revealed protein complexes required for cristae maintenance termed MINOS, MitOS or MICOS (Harner *et al*, 2011; Hoppins *et al*, 2011; von der Malsburg *et al*, 2011). Indeed,

disruption of these components may lead to cristae loss, decreased ETC complexes and a decrease in respiration. In addition, since it has been demonstrated that ATP synthase oligomerization mediates cristae morphogenesis (Paumard *et al*, 2002; Habersetzer *et al*, 2013), it is possible that OPA1 oligomer-dependent changes regulate the ATP synthase which then alters cristae structure. In any case, the fact that OPA1 interacts with cristae maintenance components, as well as the ATP synthase, highlights its central role in the coordinated regulation of mitochondrial structure and function.

One of the ways in which cristae structure may regulate ETC function is by controlling local substrate concentrations. From computer modelling experiments, it has been proposed that these changes in cristae structure may regulate the diffusion of metabolites (Mannella, 2006b). Scorrano's group has shown that OPA1 is required for the regulation of respiratory chain supercomplex assembly (Cogliati *et al*, 2013). These ETC supercomplexes may increase the efficiency of electron transfer and ATP production and may decrease the toxic accumulation of reactive oxygen species (Wittig & Schagger, 2009; Lenaz & Genova, 2012). Here, we present non-cell death manipulations of healthy cells or mitochondria to demonstrate that OPA1 regulates ATP synthase expression and the stabilization of the functional monomer, independently of OPA1 fusion activity. The starvation-induced rescue of ATP synthase assembly by OPA1 and OPA1(Q297V) clearly supports a major role for these complexes in fine-tuning mitochondrial function according to nutrient availability. However, we cannot exclude that part of the prosurvival role of OPA1(Q297V) is in preventing the release of proapoptotic factors from mitochondria, as previously suggested under apoptotic conditions (Yamaguchi *et al*, 2008). Interestingly, the OPA1(Q297V) mutant still responds to changes in fuel substrate availability without GTPase activity, potentially mimicking GTP binding (Yamaguchi *et al*, 2008), suggesting that OPA1 oligomerization is upstream of GTP binding and hydrolysis.

We identified members of the SLC25A family of mitochondrial solute carriers being required for OPA1 oligomerization in response to changes in energy substrate levels. Since their pharmacological and genetic ablation resulted in disruption of OPA1 oligomers and cytochrome *c* mobilization, outside of transporting their respective substrates, SLC25As could represent a novel class of inner membrane-shaping proteins. While our results suggest that OGC interacts with OPA1, we cannot exclude the possibility that it affects OPA1 indirectly, by modulating some undefined mitochondrial process. Moreover, the mechanism governing how SLC25A proteins transport their cargo as well as relay information to OPA1 still remains to be determined. Work on other more characterized solute carriers, the amino acid transporters, suggests that they may act as sensors in addition to carrier functions by activating different cellular signalling pathways [reviewed in (Taylor, 2014)]. The transfer of this idea to SLC25A proteins is of interest, considering the effect of OGC depletion and SLC25 inhibition on OPA1 oligomerization and function. Additionally, since the effect on OPA1 oligomerization and cytochrome *c* mobilization with these drugs was so robust, it would be interesting to investigate whether targeting SLC25As represent a novel mechanism to adjust the cell death programme.

In conclusion, we propose a model in which OPA1 senses the presence of mitochondrial fuel substrates upstream and independently of ETC activity itself. These substrates lead to OPA1 oligomerization and tightening of cristae. These ultrastructural changes are accompanied by increased assembly of the ATP synthase which promotes the efficiency or capacity for ATP produced by oxidative phosphorylation. We believe that these cristae structural changes may be required for other physiological adaptations, which warrants further investigation. Finally, our findings strengthen the link between OPA1 and cristae maintenance and suggest another mechanism by which the cell can respond to its metabolic supply.

Materials and Methods

Cell culture, transfections and viral production

HeLa and MEF cells were cultured in DMEM supplemented with 10% FBS (Wisent), 50 μg/ml penicillin and streptomycin and 2 mM glutamine (Gibco). Galactose media were prepared from glucose-/pyruvate-free DMEM supplemented as above with 10 mM galactose (Sigma). Cells were transfected using Lipofectamine 2000 (Invitrogen) or with the indicated siRNA using siLentFect (Bio-Rad) according to the manufacturer's protocol. Viral vectors were prepared as previously described (Tashiro *et al*, 2006; Jahani-Asl *et al*, 2011). All constructs used are listed in Supplementary Table S2.

To generate the long-term expression cultures, OPA1 KO cells were infected with viruses encoding for WT OPA1, OPA1(Q297V) or GFP as control and WT cells were infected with control GFP. Following transduction, cells were selected with puromycin and FACS sorted for GFP expression. These cell lines were maintained and used between 4 and 12 weeks after stable expression for all experiments.

Mitochondrial isolation

Mouse liver was dissected from young CD-1 or C57BL/6 mice euthanized with sodium pentobarbital. Cells or mouse liver were rinsed with PBS and lysed in mitochondrial isolation buffer (200 mM mannitol, 70 mM sucrose, 10 mM HEPES, pH 7.4, 1 mM EGTA). The isolation was performed in its entirety on ice or at 4°C. Cells were homogenized with a 25-G needle 15 times, while liver was Dounce-homogenized 10 times. Nuclei and cell debris were pelleted by centrifugation at 1,000 rpm for 9 min. The supernatant was then centrifuged at 9,000 rpm for 9 min to pellet mitochondria. These two spins are repeated to further enrich mitochondria in this heavy membrane fraction. Mitochondrial purity was confirmed by Western blot and EM.

Western blot analysis

Western blots were performed as previously described (Germain *et al*, 2013), with the following antibodies: mouse anti-actin and anti-flag (Sigma-Aldrich); mouse anti-OPA1 and anti-cytochrome *c* (BD Bioscience); mouse anti-p62 (SQSTM1) and rabbit anti-TOM20 (Santa Cruz Biotechnologies); mouse anti-ATP5A and anti-Complex II (Invitrogen); and mouse anti-mtHSP70 (ABR Bioreagents) and rabbit anti-OGC (Abcam).

Analysis of OPA1 oligomers

To analyse rapid changes in OPA1 oligomerization in whole cells, we used the cell-permeable BMH (Thermo Scientific) (1 mM) for

20 min at 37°C. After crosslinking, cells were quenched and washed in PBS with 0.1% beta-mercaptoethanol (BME) twice. Cells were then lysed in lysis buffer with BME and subjected to Western blot on NuPAGE Novex 3–8% Tris-acetate gradient gels (Life Technologies). For mitochondrial experiments, isolated liver or MEF mitochondria were suspended in the indicated buffer (200 mM sucrose, 10 mM Tris-Mops pH 7.4, 2 mM K_2HPO_4, 0.080 mM ADP, 10 μM EGTA-Tris) at 0.5–1 μg of mitochondrial protein/μl. Substrates and drugs were also added or not as follows: malate, glutamate, succinate and glucose (5 mM) (Sigma); rotenone (2 μM) (Sigma); and carbonylcyanide-3-chlorophenylhydrazone (CCCP) (10 μM) (Sigma). All drugs and substrates were adjusted to pH 7.4. Samples were then incubated on a 37°C heating block for 30 min or 1 h. After incubation, EDC (1 mM) (Thermo Scientific) or BMH (10 mM) was added for 30 min at room temperature and quenched with BME. Samples were then analysed by gradient gel Western blot.

Cytochrome c retention assay

As a read-out for changes in mitochondrial ultrastructure, mitochondria were assayed for their ability to retain cytochrome *c*. Mitochondria were incubated as described and then incubated with low digitonin (1 mg/mg of protein at 0.1%), at 4°C for 30 min to mobilize their inner cristae stores dependent on cristae ultrastructure. Mitochondria are then centrifuged for 10 min at 10,000 rpm (4°C) to separate the released proteins. The resulting supernatants and pellets (volume equivalents from 12.5 μg of starting mitochondria) were analysed by Western blot.

Immunofluorescence and cell death assays

Cells were washed twice with PBS and fixed with 4% paraformaldehyde for 20 min and analysed with the indicated primary antibodies. Coverslips were then washed and incubated with their corresponding secondary antibodies (anti-mouse and anti-rabbit Alexa Fluor 488/Alexa Fluor 594). Hoechst stain (Sigma) was added with the secondary antibody where noted to visualize the nucleus. Coverslips were then washed and mounted using Gel Mount Aqueous mounting medium (Sigma).

To analyse cell death during starvation, 24 h after transfection, cells were starved for 6 h and stained using propidium iodide (PI) and Hoescht stain for 20 min. All dead (Pi^+) were counted and expressed as a percentage of all cells ($Hoescht^+$). Cell death was also quantified as the percentage of condensed nuclei to total nuclei. Images were taken of at least six fields of view on a 20× objective, containing an average of 200 cells each (> 1,000 cells total).

Immunoprecipitations

Twenty-four hours following transfection, cells were lysed (50 mM Tris–HCl, 150 mM NaCl, 1 mM EDTA, 1% Triton X-100 and 1:1,000 PIC at pH 7.4), and proteins (2 mg) were immunoprecipitated with ANTI-FLAG M2 magnetic beads (Sigma-Aldrich) according to the manufacturers protocol. Samples were incubated overnight and the beads were washed four times with TBS (50 mM Tris–HCl, 150 mM NaCl and 1:1,000 PIC at pH 7.4). Immunoprecipitated protein was then eluted from the magnetic beads twice with elution buffer (50 mM Tris–HCl and 150 mM NaCl, at pH 7.4 containing 150 ng/μl FLAG peptides). Endogenous immunoprecipitation of OPA1 was performed on isolated MEF or liver mitochondria with CHAPS containing buffer (50 mM Tris–HCl, 150 mM NaCl, 1 mM EDTA, 1% CHAPS and 1:1,000 PIC at pH 7.4) at 4°C overnight with no antibody, normal mouse IgG, or mouse monoclonal anti-OPA1 (BD Biosciences). OPA1 complexes were then immunoprecipitated with 20 μl of A/G magnetic beads (Pierce) at RT for 1 h, washed with TBS four times, eluted with SDS loading dye for 20 min and analysed by Western blot.

Transmission electron microscopy

To analyse rapid cristae structure changes during cell starvation, cells were adhered to square glass coverslips, grown to confluence, treated and rapidly fixed with a combination of 2% paraformaldehyde and 1.6% glutaraldehyde. Fixed cells were floated off their cover slips, and samples were processed as previously described (Jahani-Asl *et al*, 2011). For structural quantification, the cristae diameter and mitochondrial width were measured from all mitochondria from ten cells for each condition in two independent cultures. For analysis of cristae structure in isolated mitochondria, mitochondria were treated as indicated, fixed with 2% glutaraldehyde for 20 min at RT and analysed by EM.

Blue-native analysis of ETC complexes

ATP synthase assembly was analysed from whole cells and isolated mitochondria by Blue-Native PAGE (BN-PAGE) electrophoresis according to Wittig *et al* (2006). The digitonin extraction and BN-PAGE electrophoresis were performed entirely on ice or at 4°C. Cells were grown on 100-mm plates, washed with PBS and scraped in PBS. Cells were pelleted at 3,000 rpm for 5 min, or mitochondria were pelleted at 9,000 rpm for 9 min and resuspended in digitonin extraction buffer (50 mM imidazole/HCl pH 7.0, 50 mM NaCl, 5 mM 6-aminohexanoic acid, 1 mM EDTA with 1% digitonin). Final protein to digitonin ratios were 1:4 w/w for cells and 1:8 w/w for mitochondria. Protein was extracted on ice for 1 h (for cells) or 30 min (for mitochondria) and cleared at 14,000 rpm for 30 min. Protein was quantified and 150 μg of protein (or 75 μg from mitochondria) was loaded with 5% glycerol and 1:10 dye:digitonin ratio of Coomassie blue G-250 in 500 mM 6-aminohexanoic acid onto home-made 3–13% large gels. Gels were run 2 h in a high Coomassie blue G-250 cathode buffer at 150 V at 4°C and then switched to a low G-250 buffer overnight at 4°C. Pictures of the gels were taken to confirm proper loading, and gels were transferred to nitrocellulose membrane at 500 mA for 2 h. The resulting membranes were Western blotted as per above.

mtDNA and mRNA quantification

DNA was extracted by phenol–chloroform–isoamylalcohol extraction according to Guo *et al* (2009), followed by qPCR with SYBR Green FastMix (Quanta Biosciences) according to the manufacturer's protocol with the indicated primers in Supplementary Table S2. RNA was extracted with TRIzol (Life Technologies) and analysed by RT–PCR according to Gomes *et al* (2013) with the indicated primers in Supplementary Table S2.

Analysis of oxygen consumption rates

To assess mitochondrial respiration, oxygen consumption was measured with the XF24 Analyzer (Seahorse Biosciences). Cells (50,000 experimentally optimized) were seeded onto 24-well XF24 cell culture plates. On the following day, cells were starved or not for 2 h. Cells were then washed and incubated with modified Kreb's Ringer Buffer (KRB) (KRB: 128 mM NaCl, 4.8 mM KCl, 1.2 mM KH_2PO_4, 1.2 mM $MgSO_4$, 25 mM $CaCl_2$, 0.1% BSA (fatty acid free); completed on the day of the experiment with 10 mM glucose and 1 mM sodium pyruvate and pH 7.4) for 15 min at 37°C prior to cartridge loading in the XF Analyser. Following resting respiration, cells were treated sequentially with: oligomycin (0.2 μg/μl), for nonphosphorylating OCR; FCCP (1 μM), for maximal OCR; and antimycin A (2.5 μM) with rotenone (1 μM), for extramitochondrial OCR. Measurements were taken over 2-min intervals, proceeded by a 2-min mixing and a 2-min incubation. Three measurements were taken for the resting OCR, three for nonphosphorylating OCR, two for maximal OCR and two for extramitochondrial OCR. All data were compiled by the XF software, normalized to protein levels per well and analysed with Microsoft Excel.

Stable isotope labelling with amino acids in cell culture (SILAC) coupled Immunoprecipitation and mass spectrometry

SILAC-coupled immunoprecipitation and MS was performed as previously described (Trinkle-Mulcahy, 2012). HeLa cells were grown in DMEM minus arginine and lysine, supplemented with 10% dialysed FBS, 100 U/ml penicillin/streptomycin and either 'light' L-arginine and L-lysine or 'heavy' L-arginine ^{13}C and L-lysine 4,4,5,5-D4. Cells were grown and passaged for 10 days to allow for incorporation of isotopic amino acids. Cells were then transduced with control adenovirus (mito-YFP) in the light conditions and with OPA1-YFP adenovirus in the heavy condition. Cells were harvested 24 h after transduction and lysed in RIPA buffer (50 mM Tris–HCl pH 7.5, 150 mM NaCl, 1% NP-40, 0.5% deoxycholate and protease inhibitors). Proteins were immunoprecipitated with GFP-Trap_A (Chromotek) and combined during immunoprecipitation washes and eluted together. Proteins were then reduced with 10 mM DTT, alkylated with 50 mM iodoacetamide and separated on pre-cast SDS–PAGE gels (Invitrogen). Bands were cut and digested with trypsin, and peptides were recovered. Peptides were analysed by liquid chromatography–mass spectrometry (LC-MS) using an LTQ-Oribitrap mass MS system coupled to a Dionex 3000 nano-LC system. Raw data files were analysed using the UniProt human database. Quantitation was performed using the MaxQuant software package (Cox & Mann, 2008). Positive OPA1 interactors were identified as being enriched in the heavy condition.

Supplementary information for this article is available online: http://emboj.embopress.org

Acknowledgments

We would like to acknowledge Peter Rippstein from the Ottawa Heart Institute for the preparation of EM samples as well as technical assistance, Delphine Chamousset for technical assistance with SILAC experiments, Dr. Ilona Skerjanc for essential equipment and Delphie Dugal-Tessier for reviewing the manuscript. WT and OPA1 KO MEFs were a kind gift from Dr. Luca Scorrano.

This work was supported by grants to R.S.S. from the Canadian Institutes of Health Research (MOP50471), the Heart and Stroke Foundation of Canada (T7185) and the Brain Canada/Krembil Foundation, and by a grant to M.E.H. from the Canadian Institutes of Health Research (MOP57810). D.A.P. was supported by scholarships from the Shelby Hayter Pass the Baton Graduate Fellowship from the Parkinson's Research Consortium, Ontario Graduate Scholarship and a Focus on Stroke Doctoral Research Award from the Heart and Stroke Foundation. M.G. was supported by a Parkinson's Society of Canada Research Fellowship. J.W. was supported by a Ontario Graduate Scholarship. M.K. was supported by a Focus on Stroke Fellowship from the Heart and Stroke Society of Canada.

Author contributions

DAP and RSS performed conception and design of experiments, data acquisition, analysis and interpretation of data, and drafting and revising the manuscript. MG and JW contributed to the conception and design of experiments, data acquisition, analysis and interpretation of data and revision of the manuscript. MK, VS and RM contributed to the design of experiments, interpretation of data and revision of the manuscript. KPL contributed to the design of experiments, data acquisition and interpretation of results. JM contributed to the design of experiments and data acquisition. DSP, HM, LTM and MEH contributed to the design of experiments, contributed critical reagents and revised the manuscript.

Conflict of interest

The authors declare that they have no conflict of interest.

References

Aguer C, Gambarotta D, Mailloux RJ, Moffat C, Dent R, McPherson R, Harper ME (2011) Galactose enhances oxidative metabolism and reveals mitochondrial dysfunction in human primary muscle cells. *PLoS ONE* 6: e28536

Alexander C, Votruba M, Pesch UE, Thiselton DL, Mayer S, Moore A, Rodriguez M, Kellner U, Leo-Kottler B, Auburger G, Bhattacharya SS, Wissinger B (2000) OPA1, encoding a dynamin-related GTPase, is mutated in autosomal dominant optic atrophy linked to chromosome 3q28. *Nat Genet* 26: 211 215

Amutha B, Gordon DM, Gu Y, Pain D (2004) A novel role of Mgm1p, a dynamin-related GTPase, in ATP synthase assembly and cristae formation/maintenance. *Biochem J* 381: 19 23

Chen H, Detmer SA, Ewald AJ, Griffin EE, Fraser SE, Chan DC (2003) Mitofusins Mfn1 and Mfn2 coordinately regulate mitochondrial fusion and are essential for embryonic development. *J Cell Biol* 160: 189 200

Chen H, Vermulst M, Wang YE, Chomyn A, Prolla TA, McCaffery JM, Chan DC (2010) Mitochondrial fusion is required for mtDNA stability in skeletal muscle and tolerance of mtDNA mutations. *Cell* 141: 280 289

Cogliati S, Frezza C, Soriano ME, Varanita T, Quintana-Cabrera R, Corrado M, Cipolat S, Costa V, Casarin A, Gomes LC, Perales-Clemente E, Salviati L, Fernandez-Silva P, Enriquez JA, Scorrano L (2013) Mitochondrial cristae shape determines respiratory chain supercomplexes assembly and respiratory efficiency. *Cell* 155: 160 171

Cox J, Mann M (2008) MaxQuant enables high peptide identification rates, individualized p.p.b.-range mass accuracies and proteome-wide protein quantification. *Nat Biotechnol* 26: 1367 1372

Delettre C, Lenaers G, Griffoin JM, Gigarel N, Lorenzo C, Belenguer P, Pelloquin L, Grosgeorge J, Turc-Carel C, Perret E, Astarie-Dequeker C,

Lasquellec L, Arnaud B, Ducommun B, Kaplan J, Hamel CP (2000) Nuclear gene OPA1, encoding a mitochondrial dynamin-related protein, is mutated in dominant optic atrophy. *Nat Genet* 26: 207 210

Frezza C, Cipolat S, Martins de Brito O, Micaroni M, Beznoussenko GV, Rudka T, Bartoli D, Polishuck RS, Danial NN, De Strooper B, Scorrano L (2006) OPA1 controls apoptotic cristae remodeling independently from mitochondrial fusion. *Cell* 126: 177 189

Germain M, Mathai JP, McBride HM, Shore GC (2005) Endoplasmic reticulum BIK initiates DRP1-regulated remodelling of mitochondrial cristae during apoptosis. *EMBO J* 24: 1546 1556

Germain M, Nguyen AP, Khacho M, Patten DA, Screaton RA, Park DS, Slack RS (2013) LKB1-regulated adaptive mechanisms are essential for neuronal survival following mitochondrial dysfunction. *Hum Mol Genet* 22: 952 962

Gomes LC, Di Benedetto G, Scorrano L (2011) During autophagy mitochondria elongate, are spared from degradation and sustain cell viability. *Nat Cell Biol* 13: 589 598

Gomes AP, Price NL, Ling AJ, Moslehi JJ, Montgomery MK, Rajman L, White JP, Teodoro JS, Wrann CD, Hubbard BP, Mercken EM, Palmeira CM, de Cabo R, Rolo AP, Turner N, Bell EL, Sinclair DA (2013) Declining NAD(+) induces a pseudohypoxic state disrupting nuclear-mitochondrial communication during aging. *Cell* 155: 1624 1638

Guo W, Jiang L, Bhasin S, Khan SM, Swerdlow RH (2009) DNA extraction procedures meaningfully influence qPCR-based mtDNA copy number determination. *Mitochondrion* 9: 261 265

Habersetzer J, Larrieu I, Priault M, Salin B, Rossignol R, Brethes D, Paumard P (2013) Human F1F0 ATP synthase, mitochondrial ultrastructure and OXPHOS impairment: a (super-)complex matter? *PLoS ONE* 8: e75429

Hackenbrock CR (1966) Ultrastructural bases for metabolically linked mechanical activity in mitochondria. I. Reversible ultrastructural changes with change in metabolic steady state in isolated liver mitochondria. *J Cell Biol* 30: 269 297

Hackenbrock CR (1968a) Chemical and physical fixation of isolated mitochondria in low-energy and high-energy states. *Proc Natl Acad Sci USA* 61: 598 605

Hackenbrock CR (1968b) Ultrastructural bases for metabolically linked mechanical activity in mitochondria. II. Electron transport-linked ultrastructural transformations in mitochondria. *J Cell Biol* 37: 345 369

Harner M, Korner C, Walther D, Mokranjac D, Kaesmacher J, Welsch U, Griffith J, Mann M, Reggiori F, Neupert W (2011) The mitochondrial contact site complex, a determinant of mitochondrial architecture. *EMBO J* 30: 4356 4370

Hoppins S, Collins SR, Cassidy-Stone A, Hummel E, Devay RM, Lackner LL, Westermann B, Schuldiner M, Weissman JS, Nunnari J (2011) A mitochondrial-focused genetic interaction map reveals a scaffold-like complex required for inner membrane organization in mitochondria. *J Cell Biol* 195: 323 340

Jahani-Asl A, Pilon-Larose K, Xu W, MacLaurin JG, Park DS, McBride HM, Slack RS (2011) The mitochondrial inner membrane GTPase, optic atrophy 1 (Opa1), restores mitochondrial morphology and promotes neuronal survival following excitotoxicity. *J Biol Chem* 286: 4772 4782

Jonckheere AI, Hogeveen M, Nijtmans LG, van den Brand MA, Janssen AJ, Diepstra JH, van den Brandt FC, van den Heuvel LP, Hol FA, Hofste TG, Kapusta L, Dillmann U, Shamdeen MG, Smeitink JA, Rodenburg RJ (2008) A novel mitochondrial ATP8 gene mutation in a patient with apical hypertrophic cardiomyopathy and neuropathy. *J Med Genet* 45: 129 133

Lenaz G, Genova ML (2012) Supramolecular organisation of the mitochondrial respiratory chain: a new challenge for the mechanism and control of oxidative phosphorylation. *Adv Exp Med Biol* 748: 107 144

von der Malsburg K, Muller JM, Bohnert M, Oeljeklaus S, Kwiatkowska P, Becker T, Loniewska-Lwowska A, Wiese S, Rao S, Milenkovic D, Hutu DP, Zerbes RM, Schulze-Specking A, Meyer HE, Martinou JC, Rospert S, Rehling P, Meisinger C, Veenhuis M, Warscheid B *et al* (2011) Dual role of mitofilin in mitochondrial membrane organization and protein biogenesis. *Dev Cell* 21: 694 707

Mannella CA (2006a) The relevance of mitochondrial membrane topology to mitochondrial function. *Biochim Biophys Acta* 1762: 140 147

Mannella CA (2006b) Structure and dynamics of the mitochondrial inner membrane cristae. *Biochim Biophys Acta* 1763: 542 548

Meeusen S, DeVay R, Block J, Cassidy-Stone A, Wayson S, McCaffery JM, Nunnari J (2006) Mitochondrial inner-membrane fusion and crista maintenance requires the dynamin-related GTPase Mgm1. *Cell* 127: 383 395

Misaka T, Miyashita T, Kubo Y (2002) Primary structure of a dynamin-related mouse mitochondrial GTPase and its distribution in brain, subcellular localization, and effect on mitochondrial morphology. *J Biol Chem* 277: 15834 15842

Mishra P, Carelli V, Manfredi G, Chan DC (2014) Proteolytic cleavage of Opa1 stimulates mitochondrial inner membrane fusion and couples fusion to oxidative phosphorylation. *Cell Metab* 19: 630 641

Palmieri F (2013) The mitochondrial transporter family SLC25: identification, properties and physiopathology. *Mol Aspects Med* 34: 465 484

Paumard P, Vaillier J, Coulary B, Schaeffer J, Soubannier V, Mueller DM, Brethes D, di Rago JP, Velours J (2002) The ATP synthase is involved in generating mitochondrial cristae morphology. *EMBO J* 21: 221 230

Pitceathly RD, Murphy SM, Cottenie E, Chalasani A, Sweeney MG, Woodward C, Mudanohwo EE, Hargreaves I, Heales S, Land J, Holton JL, Houlden H, Blake J, Champion M, Flinter F, Robb SA, Page R, Rose M, Palace J, Crowe C *et al* (2012) Genetic dysfunction of MT-ATP6 causes axonal Charcot-Marie-Tooth disease. *Neurology* 79: 1145 1154

Rambold AS, Kostelecky B, Elia N, Lippincott-Schwartz J (2011) Tubular network formation protects mitochondria from autophagosomal degradation during nutrient starvation. *Proc Natl Acad Sci USA* 108: 10190 10195

Scorrano L, Ashiya M, Buttle K, Weiler S, Oakes SA, Mannella CA, Korsmeyer SJ (2002) A distinct pathway remodels mitochondrial cristae and mobilizes cytochrome *c* during apoptosis. *Dev Cell* 2: 55 67

Song Z, Chen H, Fiket M, Alexander C, Chan DC (2007) OPA1 processing controls mitochondrial fusion and is regulated by mRNA splicing, membrane potential, and Yme1L. *J Cell Biol* 178: 749 755

Sukhorukov VM, Bereiter-Hahn J (2009) Anomalous diffusion induced by cristae geometry in the inner mitochondrial membrane. *PLoS ONE* 4: e4604

Tashiro A, Zhao C, Gage FH (2006) Retrovirus-mediated single-cell gene knockout technique in adult newborn neurons in vivo. *Nat Protoc* 1: 3049 3055

Taylor PM (2014) Role of amino acid transporters in amino acid sensing. *Am J Clin Nutr* 99: 223S 230S

Tondera D, Grandemange S, Jourdain A, Karbowski M, Mattenberger Y, Herzig S, Da Cruz S, Clerc P, Raschke I, Merkwirth C, Ehses S, Krause F, Chan DC, Alexander C, Bauer C, Youle R, Langer T, Martinou JC (2009) SLP-2 is required for stress-induced mitochondrial hyperfusion. *EMBO J* 28: 1589 1600

Trinkle-Mulcahy L (2012) Resolving protein interactions and complexes by affinity purification followed by label-based quantitative mass spectrometry. *Proteomics* 12: 1623 1638

Vogel F, Bornhovd C, Neupert W, Reichert AS (2006) Dynamic subcompartmentalization of the mitochondrial inner membrane. *J Cell Biol* 175: 237 247

Wasilewski M, Semenzato M, Rafelski SM, Robbins J, Bakardjiev AI, Scorrano L (2012) Optic atrophy 1-dependent mitochondrial remodeling controls steroidogenesis in trophoblasts. *Curr Biol* 22: 1228 1234

Wittig I, Braun HP, Schagger H (2006) Blue native PAGE. *Nat Protoc* 1: 418 428

Wittig I, Schagger H (2009) Supramolecular organization of ATP synthase and respiratory chain in mitochondrial membranes. *Biochim Biophys Acta* 1787: 672 680

Wurm CA, Jakobs S (2006) Differential protein distributions define two sub-compartments of the mitochondrial inner membrane in yeast. *FEBS Lett* 580: 5628 5634

Yamaguchi R, Lartigue L, Perkins G, Scott RT, Dixit A, Kushnareva Y, Kuwana T, Ellisman MH, Newmeyer DD (2008) Opa1-mediated cristae opening is Bax/Bak and BH3 dependent, required for apoptosis, and independent of Bak oligomerization. *Mol Cell* 31: 557 569

Zuchner S, Mersiyanova IV, Muglia M, Bissar-Tadmouri N, Rochelle J, Dadali EL, Zappia M, Nelis E, Patitucci A, Senderek J, Parman Y, Evgrafov O, Jonghe PD, Takahashi Y, Tsuji S, Pericak-Vance MA, Quattrone A, Battaloglu E, Polyakov AV, Timmerman V *et al* (2004) Mutations in the mitochondrial GTPase mitofusin 2 cause Charcot-Marie-Tooth neuropathy type 2A. *Nat Genet* 36: 449 451

Appendix C:

Journal of Alzheimer's Disease 20 (2010) S357–S367
DOI 10.3233/JAD-2010-100498
IOS Press

Review

Reactive Oxygen Species: Stuck in the Middle of Neurodegeneration

David A. Patten[1], Marc Germain[1], Melissa A. Kelly and Ruth S. Slack*
Department of Cellular and Molecular Medicine, University of Ottawa, Ottawa, ON, Canada

Accepted 5 April 2010

Abstract. Neuronal cell loss associated with neurodegeneration has recently been linked to mitochondrial dysfunction. Electron transport chain defects and reactive oxygen species (ROS) production are emerging as important players in the etiology of neurodegenerative diseases. Proper management of ROS and disposal of damaged cellular components are vital to the survival and function of neurons. Proteins involved in these pathways are often mutated in neurodegenerative diseases such as Alzheimer's disease, Parkinson's disease, amyotrophic lateral sclerosis, and Huntington's disease. In this review, we will discuss the roles of ROS in normal physiology, how changes in ROS production affect neuronal survival in neurodegenerative diseases, and the recent advances in mitochondrial antioxidants as potential therapeutics.

Keywords: Apoptosis, autophagy, mitochondria, neurodegeneration, reactive oxygen species

INTRODUCTION

Neurodegenerative diseases are characterized by the progressive loss of specific neuronal populations. Accumulation of protein aggregates occurs in the affected neuronal populations and has been suggested to be at the origin of their demise, at least under some circumstances. Accumulating evidence suggests, however, that mitochondrial dysfunction also plays an important role in the etiology of neurodegenerative diseases. The management of mitochondrial reactive oxygen species (ROS) and the damage they cause is emerging as a major contributor to neuronal loss in Alzheimer's disease (AD), Parkinson's disease (PD), amyotrophic lateral sclerosis (ALS), and Huntington's disease (HD). In this review, we will discuss the roles of ROS in normal physiology as well as the causes and consequences of mitochondrial-generated ROS in neurodegenerative diseases.

REACTIVE OXYGEN SPECIES

ROS are a group of small oxygen-containing free radicals that are extremely reactive due to their unpaired valence electrons. ROS are generally formed by the primary ROS superoxide (O_2^-), which is chiefly converted to hydrogen peroxide (H_2O_2) by superoxide dismutases (SOD) but may also be protonated to form hydroperoxyl radicals (HO_2^-). H_2O_2 can be transformed into a number of other ROS including hydroxyl radicals (OH), hydroxyl anions (HO-), singlet oxygen ($^1O_2$) and hypochlorite (ClO^-). There are many generators of cellular ROS including the mitochondrion, nicotinamide adenine dinucleotide phosphate (NADPH) oxidase (reviewed in [1]), xanthine oxidase [2], and uncoupled endothelial nitric oxide synthase (eNOS) [3]. In the majority of cell types, the mitochondrion is the major source of ROS. Superoxide production, due to inefficiencies in oxidative phosphorylation, accounts for

[1]These authors contributed equally to this work.

*Correspondence to: Ruth S. Slack, Ph.D., Ottawa Health Research Institute, University of Ottawa, 451 Smyth Road, Ottawa, ON, Canada K1H 8M5. Tel.: +1 613 562 5800, ext. 8458; Fax: +1 613 562 5403; E-mail: rslack@uottawa.ca.

ISSN 1387-2877/10/$27.50

up to 2% of the total oxygen consumed by mitochondria [4]. Mitochondrial-generated ROS (mtROS) are mainly produced at complex I and complex III of the electron transport chain, although a total of nine sites have been identified [5]. Complex I produces superoxide solely in the matrix while complex III generates superoxide in both the matrix and the intermembrane space [6].

One cannot discuss ROS without discussing its clearance. Cells possess a number of antioxidant defenses chiefly to protect the cell from oxidative stress, but are also involved in other functions including cellular signaling. As a charged molecule, superoxide is generally membrane impermeable and is a particularly damaging molecule. It is, however, rapidly converted to H_2O_2 by superoxide dismutases: copper/zinc superoxide dismutase (SOD1) in the cytoplasm and mitochondrial intermembrane space; and by manganese superoxide dismutase (SOD2) in the mitochondrial matrix [7]. The importance of superoxide detoxification is highlighted by the fact that SOD2 knockout mice live only weeks [8]. H_2O_2, however, is membrane permeable and is likely the main signaling molecule in ROS-mediated pathways. H_2O_2 is detoxified in cells by glutathione peroxidase (GPx), and in some cases by catalase, to form water [7]. Prolonged high levels of ROS that surpass the cell's antioxidant capacity result in oxidative stress.

ROS AS SIGNALING MOLECULES

Although high ROS concentrations are damaging to lipids, proteins, and DNA, there is a large body of evidence demonstrating that low and intermediary levels of ROS are physiologically important (reviewed in [9] and [10]). NADPH oxidase-derived ROS (noxROS), for instance, have been well characterized in the cardiovascular field for their role in cell signaling. NADPH oxidases are a group of enzyme complexes highly expressed in phagocytes and cardiovascular tissue, which catalyze the reduction of oxygen to form superoxide. In phagocytes, NADPH oxidase produces large bursts of ROS, killing foreign organisms as part of the immune defense system [11]. In cardiovascular tissue, however, NADPH oxidase produces relatively less ROS at a slow and sustained rate, serving as intracellular signaling molecules [12]. NADPH activity is regulated by growth factors, vasoactive agents, and cytokines: the signaling of which results in the assembly and activation of the complex. Increased noxROS result in the activation of key survival pathways, notably mitogen-activated protein kinase (MAPK) pathways and the phosphoinositide 3-kinase (PI3K)/Akt pathway [10], presumably through the oxidation of key cysteine residues. Depending on the stimulus, activation of these pathways may induce cell growth, apoptosis, proliferation, migration, or smooth muscle contraction [13]. Increased noxROS is involved in the development of cardiovascular disease through activation of these pro-survival pathways. For example, noxROS play a pivotal role in vascular remodeling implicated in angiotensin II (Ang II)-dependent hypertension (reviewed in [14]).

In addition to the activation of the aforementioned signaling pathways, ROS are also involved in activation of transcription factors that regulate cellular responses to ROS. One of the first responses to increased ROS is the upregulation of antioxidant defenses. Nrf2 is a major transcription factor activated by oxidative stress regulating expression of several important antioxidant proteins such as superoxide dismutases, peroxiredoxins, glutathione peroxidases, and heme oxygenases ([15] and reviewed in [16]). Nrf2 is normally kept inactive by interacting with Keap1 in the cytosol where it is targeted for ubiquitin-dependent proteasomal degradation. The interaction between Keap1 and Nrf2 is disrupted with increased ROS production, allowing Nrf2 to translocate to the nucleus and activate transcription [17]. Interestingly, the PD-related gene DJ-1 has been proposed to promote the dissociation of Nrf2 from Keap1, thereby increasing its activity [18].

While Nrf2 plays an important role in regulating antioxidant defenses in response to elevated ROS, other ROS-activated transcription factors, such as hypoxia-inducible factors (HIFs), control several aspects of cellular functions. HIFs are the master transcription factors responsible for the adaptation of cells to low oxygen (hypoxia). HIFs maintain oxygen and energy homeostasis by regulating genes involved in metabolism, proliferation, erythropoiesis, angiogenesis, and cell survival [19]. Active HIF is a heterodimer regulated primarily though degradation or stabilization of its oxygen sensitive α subunit, while its β subunit is constitutively expressed. Under normal oxygen conditions, HIFα is rapidly degraded by the proteasome; however, during hypoxic conditions HIFα is stabilized, dimerizes with HIFβ and activates transcription of its target genes. In addition to oxygen levels, HIFα is also regulated through mtROS [20–22]. Inhibition of mtROS through pharmacological and genetic inhibition of complex III, and through antioxidant treatments, indeed lead to increased HIFα stability [20–22]. mtROS stabilize HIFα by inhibiting HIF prolyl-hydroxylases (PHDs), key en-

zymes responsible for HIF degradation. PHD inhibition by ROS probably occurs via the Fenton reaction which oxidizes Fe^{2+} to Fe^{3+}, where Fe^{2+} is an essential co-factor [23]. Interestingly, recent evidence demonstrates that HIF activation plays a protective role in neurodegenerative diseases (reviewed in [24]). For instance, the PHD inhibitor 3,4-dihydroxybenzoate has recently been shown to protect neurons from the MPTP model of PD both *in vitro* and *in vivo* [25].

Nuclear factor-kappa B (NF-κB) is a second pro-survival transcription factor activated by ROS that regulates several important cellular defense mechanisms. NF-κB activates target genes involved in cellular survival, growth, differentiation, and inflammation. Normally, NF-κB is sequestered in the cytoplasm and held inactive by IκB (inhibitor of κB). Moderate ROS levels lead to phosphorylation and degradation of IκB and therefore the activation of NF-κB [26]. Once activated, NF-κB plays a pro-survival role through the transcriptional activation of anti-apoptotic proteins, such as XIAP and GADD45β [27], and genes involved in decreasing mtROS, most notably SOD2 [28,29]. In addition, NF-κB may play a pro-survival role by inhibiting the JNK and caspase cell death pathways [30]. While moderate ROS levels activate NF-κB, high levels inactivate NF-κB through oxidation of cysteine 62 of its p50 subunit, inhibiting its DNA binding [31].

The p53 tumor suppressor represents a different aspect of ROS-activated transcription factors, as it can promote both survival and death. Cellular damage activates p53, leading to the inhibition of cell cycle or initiation of apoptosis [32]. In addition to these classical roles, p53 also presents a pro-survival role in response to increased ROS levels by upregulating several antioxidants, including glutathione peroxidase [33, 34], SOD2 [34], and ALDH4 [35]. p53 also induces the pentose phosphate shunt through regulating TP53-induced glycolysis and apoptosis regulator (TIGAR) [36]. TIGAR inhibits glycolysis and directs glucose to the pentose phosphate pathway producing NADPH, which is required to reduce glutathione (GSH) and thus lower ROS levels [36]. This antioxidant function of p53 is activated during low cellular stress [37], while high stress and ROS concentrations results in p53-mediated apoptosis through activation of several pro-apoptotic genes such as BH3-only proteins [38] and a series of p53-induced genes (PIGs) [39]. Although the exact mechanism by which p53 senses ROS and responds via either pro-apoptotic or anti-apoptotic functions remains relatively unknown, these differing functions possibly depend on p53 levels, posttranslational modification, and cellular localization [40].

Taken together these studies suggest that while high ROS levels are damaging, low levels play an integral role in pro-survival pathways through both the activation of key signaling pathways and the activation of transcription factors (Fig. 1).

ROS IN NEURODEGENERATIVE DISEASES

Excessively high levels of ROS beyond the clearance capacity of the cell cause oxidative stress, mitochondrial dysfunction, cellular damage, and, in numerous cases, cell death. A range of data suggests that oxidative stress is at the center of various neurodegenerative diseases. Among these diseases, evidence of increased ROS has been reported in ALS [41], HD [42], PD [43, 44], and AD [45,46]. The most direct example is in cases of familial ALS (FALS) in which the antioxidant enzyme SOD1 is mutated [47,48]. Dysfunctional SOD1 causes an increase in oxidative stress, as shown in several animal models of ALS in which mutant human or mouse SOD1 are expressed. The toxicity of SOD1 mutants amounts to more than a disrupted enzymatic function, however, as the mutant protein forms toxic aggregates within mitochondria [49,50], impairing respiration and promoting mitochondrial dysfunction [51]. Increased ROS in FALS is therefore likely the result of a combination of loss of antioxidant function and accumulation of toxic SOD1 aggregates.

ROS generation in neurodegenerative diseases go beyond such a direct effect on antioxidant function, although mitochondrial damage is a recurrent theme. For example, decreased mitochondrial respiration [52], as well as increased ROS and oxidative DNA damage have been reported in HD transgenic mice and in the parietal cortex of human HD brains [42,53,54], while antioxidant treatment with Coenzyme Q_{10} promoted moderate improvement in disease progression and extended survival [55]. However, the best-characterized neurodegenerative disease where mitochondrial dysfunction is linked to ROS production is PD.

The first evidence for a role of ROS in PD came from the observation that human PD brains show signs of mitochondrial dysfunction and oxidative damage in degenerating areas including the substantia nigra [43,44]. This was further substantiated by the identification of several PD-related genes that are associated with mitochondrial function, namely the mitochondrial kinase PTEN-induced putative kinase 1 (PINK1), the E3 ligase Parkin, and the oxidative stress sensor DJ-1 [56]. Specifically, mutations in PINK1 cause mitochondrial

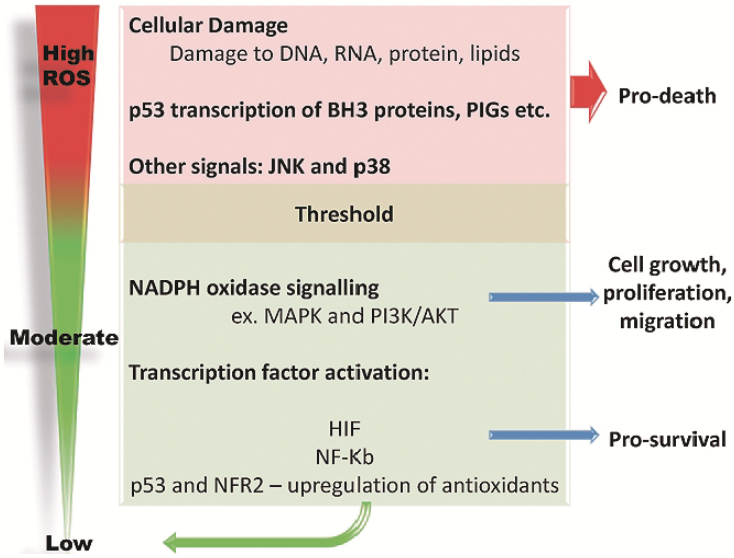

Fig. 1. Model of ROS levels moderating pro-survival and pro-death signaling. Moderate increases in ROS lead to activation of various cell signaling events that are generally pro-survival pathways. Moreover, activation of p53 and NRF2 are important to return the cell to a lower oxidative state by regulating the transcription of antioxidants. When ROS production exceeds a specific threshold (cell and stimulus specific), the cellular response shifts to promote cell death.

dysfunction [57], while loss of Parkin in mouse models has been shown to result in oxidative stress and mitochondrial dysfunction [58]. Recently, loss of DJ-1 in mouse embryonic fibroblasts (MEFs) has been associated with decreased respiration, increased mtROS, and reduced mitochondrial membrane potential [59]. Interestingly, PINK1, Parkin, and DJ-1 potentially interact in a complex to stimulate proteasomal degradation of proteins likely to aggregate, effectively preventing the accumulation of these neurotoxins [60]. The beneficial role of PINK1 and Parkin may also be involved in clearance of damaged mitochondria resulting in additional reductions in ROS (discussed below).

ROS production has also been linked to another key feature of neurodegenerative diseases, namely the accumulation of protein aggregates, although this relationship is complex. For example, expression of PD mutant α-synuclein (a component of Lewy bodies in PD) in mice and neurons is toxic, induces mitochondrial dysfunction, and increases ROS and cell death [61–63]. A second example where accumulation of protein aggregates has been linked to mitochondrial dysfunction and ROS production is in AD. The presence of amyloid-β (Aβ) plaques is a characteristic feature of AD and its accumulation has been linked to oxidative stress, mitochondrial dysfunction, energy failure, synaptic dysfunction, and ultimately neuronal loss [64–66]. Indeed, AD brains show signs of increased ROS including nuclear DNA and mitochondrial DNA (mtDNA) damage [45,46], while mitochondrial accumulation of Aβ reduces oxygen consumption, and decreases mitochondrial electron transport chain activity [64,67]. One other way in which Aβ may affect ROS production is through its effect on mitochondrial dynamics. Mitochondria exist as a highly dynamic network that constantly divide and fuse. Recent evidence suggests that Aβ disrupts this process, leading to mitochondrial fragmentation and increased ROS production [68–70].

The causative role of Aβ in AD, however, remains debated, and it is clear that other aspects of the disease, such as hyperphosphorylation and accumulation of tau, also play an important role in its progression. In that respect, it is interesting to note that while protein aggregates can promote ROS production and mitochondrial dysfunction, ROS may also cause the accumulation of these neurotoxic aggregates, including Aβ [71] and α-synuclein [57,72,73]. This, along with the observation that the increase in ROS production precedes the pathological appearance of Aβ plaques [64,65], suggests that mitochondria dysfunction can be an early event that precedes protein aggregation. It should also be kept in mind, however, that mitochondrial dysfunc-

tion might be secondary to alterations in other pathways that can affect both mitochondrial function and accumulation of toxic proteins. For example, deregulated calcium homeostasis in AD may also play a role in ROS generation, Aβ aggregation, and damage to mitochondria [74–76] with Aβ oligomers further promoting intracellular calcium entry in a deleterious positive feedback loop [77].

Oxidative stress is thus emerging as a common theme in neurodegeneration (Fig. 2), with decreased mitochondrial antioxidants, increased protein aggregation, and increased mitochondrial dysfunction all promoting increased ROS generation. While several pathways (described above) are activated to control ROS production, dysfunctional mitochondria need to be removed to prevent further damage. Recent work has highlighted a role for autophagy in clearance of damaged mitochondria.

AUTOPHAGY AND APOPTOSIS

Macroautophagy (hereafter referred to as autophagy) is a conserved catabolic process allowing for recycling of nutrients during starvation. A basal level of autophagy is required to degrade damaged proteins and organelles. Autophagy is characterized by formation of double-membrane vesicles which deliver the cellular components to be recycled to lysosomes where they are degraded. Autophagosome formation is dependent on a series of conserved autophagy-related (ATG) genes (reviewed in [78]).

A role for autophagy in neurodegenerative diseases was first suggested by the phenotype of the ATG5 and ATG7 (two essential ATG genes) conditional knockouts in the central nervous system, where both models lead to an accumulation of ubiquitin-positive aggregates, neuronal loss, and death of the animals within several weeks of birth [79,80]. More recently, damaged mitochondria have been shown to be specifically removed by autophagy (mitophagy) in a process requiring PINK1 and Parkin, two aforementioned PD-related genes [81–84]. PINK1 is a labile mitochondrial outer membrane kinase that is stabilized on mitochondria that have lost their membrane potential [81,83, 84]. Following this increase in protein levels, PINK1 recruits the ubiquitin E3-ligase Parkin to the damaged mitochondria in a manner dependent on PINK1 kinase activation [81,83,84]. Once on the mitochondrial outer membrane, Parkin ubiquitinates substrates including VDAC1, leading to the recruitment of p62/SQSTM, a ubiquitin binding protein that targets ubiquitinated substrates to autophagosomes for autophagy-dependent degradation [81]. PD-related mutations in either PINK1 or Parkin lead to the accumulation of damaged organelles, increases in dysfunctional mitochondria, and elevated ROS, further damaging the cell.

Failure to properly control ROS production and remove damaged organelles via mitophagy results in accumulation of damage and cell death. At least two types of cell death have been associated with ROS production: apoptosis and necrosis. High levels of ROS, associated with severe cellular damage can lead to necrotic cell death in a process that causes disruption of the cell membrane, causing further inflammation and tissue damage [85]. On the other hand, apoptosis is a tightly controlled process leading to complete removal of the damaged cells without eliciting an inflammatory response [85]. Apoptosis is regulated by a family of related proteins, BCL-2 homologues, that converge on mitochondria to regulate its outer membrane permeability and the release of several pro-apoptotic factors from the intermembrane space (reviewed in [86, 87]). Among these, Apoptosis Inducing Factor (AIF) and Endonuclease G (EndoG) translocate to the nucleus where they cause caspase-independent DNA degradation and cell death [88]. However, the major pathway activated in apoptotic cells relies on the release of cytochrome c [86,87]. Once in the cytosol, cytochrome c activates formation of the apoptosome, a protein complex comprised of cytochrome c, APAF-1 and caspase-9. The apoptosome activates effector caspases, the apoptotic proteases responsible for morphological changes leading to the dismantling of the cellular component. Cytochrome c release is dependent upon activation of two pro-apoptotic BCL-2 homologues, BAX and BAK [86,87]. Anti-apoptotic BCL-2 homologues (BCL-2, MCL-1, BCL-XL, and A1) inhibit apoptosis by blocking BAX/BAK function in healthy cells. The key molecules for BAX/BAK activation are the BH3-only proteins, a third class of BCL-2 homologues. BH3-only proteins induce BAX/BAK activation either through direct interaction (the so-called activator BH3 BID and BIM) or indirectly by inhibiting anti-apoptotic BCL-2 homologues [86,87]. While the exact contribution of each pathway is still debated, it is clear that BH3-only proteins are the upstream activators of cytochrome c release and apoptosis [86,87]. Activation of BH3-only proteins occurs through several mechanisms [86,87]. For example, BID activation is dependent on its cleavage by caspase-8 while BAD is regulated by phosphorylation. However, the main regulatory

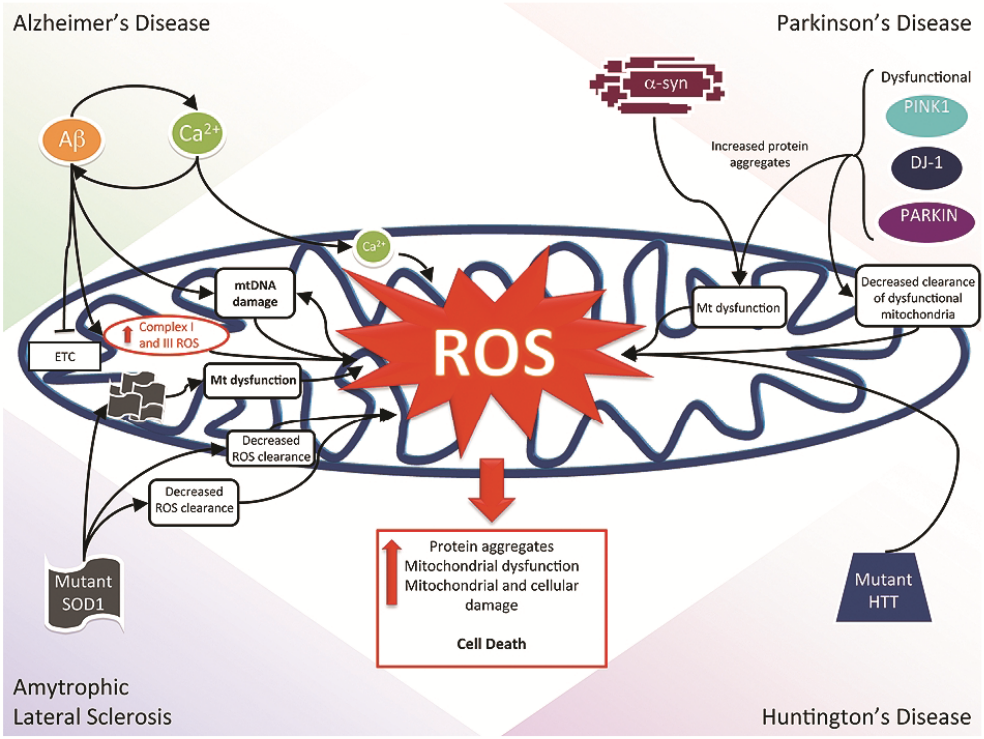

Fig. 2. Schematic of factors affecting mtROS in neurodegenerative diseases. Multiple pathways in neurodegenerative disease converge on the mitochondria to induce the production of mtROS. In the case of AD, Aβ accumulation is toxic to mitochondrial respiration and increases mtDNA damage and mtROS. In addition, deregulated Ca^{2+} levels are also detrimental to proper mitochondrial function. These two components are not mutually exclusive in that Aβ accumulation can deregulate Ca^{2+} levels and vice versa. Mutations in PD-related genes cause protein aggregation leading to mitochondrial dysfunction and oxidative stress. In addition, dysfunctional mitochondria are not appropriately disposed of by mitophagy, further increasing mtROS production. Aberrant levels of the mutant form of the protein huntingtin causes ROS generation in HD. Finally, mutations in SOD1 in FALS hinder ROS clearance and create toxic mitochondrial aggregates. Generation of ROS may in turn lead to further protein aggregation, mitochondrial dysfunction, cell damage, and cell death.

mechanism for several BH3-only proteins is transcriptional regulation. Following several types of cellular injury, including increased ROS, p53 is stabilized and activates expression of at least three BH3-only proteins, namely Noxa, Puma, and human BIK [38,89], providing a link between increased ROS production and induction of apoptosis. As p53 activation also promotes survival under some circumstances, other factors such as JNK and p38 are likely to participate in activation of BH3-only proteins following an increase in ROS. For example, JNK is activated by ROS and phosphorylates several apoptosis-related substrates such as MCL-1 and the BH3-only protein BIM [90,91]. In the case of MCL-1, this results in its proteasome-dependent degradation [91] while JNK-dependent phosphorylation of BIM increases its pro-apoptotic activity [90].

Interestingly, several links exist between autophagy and apoptosis. For example, anti-apoptotic BCL-2 homologues can regulate the activation of autophagy through inhibition of Beclin-1, a protein required for the initiation of autophagosome formation [92,93]. In addition, JNK is activated by starvation (a classical autophagy inducer) and promotes autophagy through several mechanisms including inhibition of BCL-2 [94] and induction of p62 [95]. As discussed above, autophagy is a protective mechanism that promotes disposal of damaged cellular components. However, sustained or excessive autophagy can also lead to autophagic (type II) cell death [96]. Keeping a proper balance between the different aspects of ROS production and clearance (including ROS signaling and autophagic removal of damaged organelles) is therefore key to

maintaining survival of cells with high metabolic rates and long lifespan such as neurons.

MITOCHONDRIAL ANTIOXIDANTS

Since ROS and oxidative damage underlie a large number of human diseases, attempts have been made in administering large doses of antioxidants to patients. Unfortunately, these treatments have been largely unsuccessful, likely due to their limited cellular and mitochondrial uptake. In an attempt to increase uptake and efficacy, a large effort has commenced to develop mitochondrial targeted antioxidants (reviewed in [97]). Mitochondria-targeted ubiquinol (MitoQ), for example, was shown to prevent cell death caused by endogenous oxidative stress hundreds of times more potently than its untargeted homologue [98]. Of note here, MitoQ also inhibited HIF accumulation in hypoxia [22]. Furthermore, MitoQ gave promising results in the cardiovascular field where MitoQ treatment reduced cardiac hypertrophy and improved endothelial function of stroke-prone spontaneously hypertensive rats [99]. MitoQ entered into Phase II clinical trials for the treatment of both PD and hepatitis C in 2008. Results, however, remain to be presented.

Another example of a promising mitochondrial targeted antioxidant is SkQ1 [100], shown to reduce H_2O_2-induced apoptosis in human fibroblasts and HeLa cells [101]. SkQ1 has produced some extraordinary *in vivo* results including restoring vision to blind animals with retinopathy, decreasing lymphomas in $p53^{-/-}$ mice, and prolonging the lifespan of fungi, crustaceans, flies, and mice [101]. Further research will be needed to investigate whether or not SkQ1 can prevent neuronal cell death and if it could be used as a potential treatment in neurodegenerative diseases.

Szeto-Schiller (SS) peptides represent a second class of mitochondrial antioxidants that offer the advantage of localizing to mitochondria irrespective of mitochondrial membrane potential, which may improve their therapeutic potential [102]. SS peptides concentrate 1000-fold to mitochondria, reduce ROS in neuronal cells, and protect cells against neuronal cell death by tert-butyl hydroperoxide [103]. Additionally, in both mouse and human islet cells where mitochondrial dysfunction is at the center of cell death, SS peptides prevented mitochondrial depolarization and apoptosis [104]. *In vivo*, SS peptides are protective in a mouse model of ALS, increasing survival and motor performance, and decreasing cell loss [105]. SS peptides also protect dopaminergic neurons against 1-methyl-4-phenyl-1,2,3,6-tetrahydropyridine (MPTP) neurotoxicity both in cell cultures and in the PD animal model [106].

The links between neurodegenerative diseases and ROS presented above, along with the results obtained using these new antioxidants, present compelling *in vitro* and *in vivo* evidence that ROS underlie neuronal death. These new mitochondrial ROS scavengers therefore represent a promising novel therapeutic approach to the treatment of these diseases.

CONCLUSION

As more efficient and better-tolerated mitochondrial antioxidants become available, there are a number of important matters to consider. First of all, mitochondrial antioxidant treatments may inhibit ROS-dependent apoptosis, but not the underlying mitochondrial defects and may therefore result in other non-ROS mediated cell death pathways. Secondly, since mtROS are involved in beneficial cell signaling, including some pro-survival pathways previously discussed, it will be important to ensure that these pathways are not blocked by these treatments. Perhaps moderate doses of mitochondrial antioxidants will be most efficient since the beneficial pro-survival pathways will remain relatively unaltered. And finally, since oxygen sensing through HIF requires mtROS [20], it would be interesting and important to investigate whether these treatments make mammals more susceptible to cell death following ischemic injury.

Regardless, mitochondrial antioxidants represent a promising avenue for neurodegenerative disease treatments. Research is still needed, however, to fully delineate the missing steps by which neurodegenerative diseases increase mtROS and how mtROS leads to cell death. These studies will potentially present new pharmacological targets upstream or downstream of ROS generation, allowing to target damaging ROS without interfering with physiological ROS signaling.

ACKNOWLEDGMENTS

We would like to thank the life side for providing the title. This work was supported by a grant from the Canadian Institutes of Health Research (CIHR) to RSS. DAP holds a Shelby Hayter Pass the Baton Graduate Fellowship from the Parkinson's Research Consortium.

MG holds a Parkinson's Society of Canada Research Fellowship.

Authors' disclosures available online (http://www.j-alz.com/disclosures/view.php?id=398).

REFERENCES

[1] Babior BM (2000) The NADPH oxidase of endothelial cells. *IUBMB Life* **50**, 267-269.

[2] Yokoyama Y, Beckman JS, Beckman TK, Wheat JK, Cash TG, Freeman BA, Parks DA (1990) Circulating xanthine oxidase: potential mediator of ischemic injury. *Am J Physiol* **258**, G564-G570.

[3] Dijkstra G, Moshage H, van Dullemen HM, de Jager-Krikken A, Tiebosch AT, Kleibeuker JH, Jansen PL, van Goor H (1998) Expression of nitric oxide synthases and formation of nitrotyrosine and reactive oxygen species in inflammatory bowel disease. *J Pathol* **186**, 416-421.

[4] Orrenius S (2007) Reactive oxygen species in mitochondria-mediated cell death. *Drug Metab Rev* **39**, 443-455.

[5] Andreyev AY, Kushnareva YE, Starkov AA (2005) Mitochondrial metabolism of reactive oxygen species. *Biochemistry* (*Mosc*) **70**, 200-214.

[6] Muller FL, Liu Y, Van Remmen H (2004) Complex III releases superoxide to both sides of the inner mitochondrial membrane. *J Biol Chem* **279**, 49064-49073.

[7] Zhang DX, Gutterman DD (2007) Mitochondrial reactive oxygen species-mediated signaling in endothelial cells. *Am J Physiol Heart Circ Physiol* **292**, H2023-2031.

[8] Lebovitz RM, Zhang H, Vogel H, Cartwright J, Jr., Dionne L, Lu N, Huang S, Matzuk MM (1996) Neurodegeneration, myocardial injury, and perinatal death in mitochondrial superoxide dismutase-deficient mice. *Proc Natl Acad Sci U S A* **93**, 9782-9787.

[9] Valko M, Leibfritz D, Moncol J, Cronin MT, Mazur M, Telser J (2007) Free radicals and antioxidants in normal physiological functions and human disease. *Int J Biochem Cell Biol* **39**, 44-84.

[10] Groeger G, Quiney C, Cotter TG (2009) Hydrogen peroxide as a cell-survival signaling molecule. *Antioxid Redox Signal* **11**, 2655-2671.

[11] Babior BM (2004) NADPH oxidase. *Curr Opin Immunol* **16**, 42-47.

[12] Griendling KK, Sorescu D, Ushio-Fukai M (2000) NAD(P)H oxidase: role in cardiovascular biology and disease. *Circ Res* **86**, 494-501.

[13] Lassegue B, Griendling KK (2010) NADPH oxidases: functions and pathologies in the vasculature. *Arterioscler Thromb Vasc Biol* **30**, 653-661.

[14] Paravicini TM, Touyz RM (2008) NADPH oxidases, reactive oxygen species, and hypertension: clinical implications and therapeutic possibilities. *Diabetes Care* **31 Suppl 2**, S170-S180.

[15] Lee JM, Calkins MJ, Chan K, Kan YW, Johnson JA (2003) Identification of the NF-E2-related factor-2-dependent genes conferring protection against oxidative stress in primary cortical astrocytes using oligonucleotide microarray analysis. *J Biol Chem* **278**, 12029-12038.

[16] de Vries HE, Witte M, Hondius D, Rozemuller AJ, Drukarch B, Hoozemans J, van Horssen J (2008) Nrf2-induced antioxidant protection: a promising target to counteract ROS-mediated damage in neurodegenerative disease? *Free Radic Biol Med* **45**, 1375-1383.

[17] Itoh K, Wakabayashi N, Katoh Y, Ishii T, O'Connor T, Yamamoto M (2003) Keap1 regulates both cytoplasmic-nuclear shuttling and degradation of Nrf2 in response to electrophiles. *Genes Cells* **8**, 379-391.

[18] Clements CM, McNally RS, Conti BJ, Mak TW, Ting JP (2006) DJ-1, a cancer- and Parkinson's disease-associated protein, stabilizes the antioxidant transcriptional master regulator Nrf2. *Proc Natl Acad Sci U S A* **103**, 15091-15096.

[19] Semenza GL (2003) Targeting HIF-1 for cancer therapy. *Nat Rev Cancer* **3**, 721-732.

[20] Brunelle JK, Bell EL, Quesada NM, Vercauteren K, Tiranti V, Zeviani M, Scarpulla RC, Chandel NS (2005) Oxygen sensing requires mitochondrial ROS but not oxidative phosphorylation. *Cell Metab* **1**, 409-414.

[21] Guzy RD, Hoyos B, Robin E, Chen H, Liu L, Mansfield KD, Simon MC, Hammerling U, Schumacker PT (2005) Mitochondrial complex III is required for hypoxia-induced ROS production and cellular oxygen sensing. *Cell Metab* **1**, 401-408.

[22] Bell EL, Klimova TA, Eisenbart J, Moraes CT, Murphy MP, Budinger GR, Chandel NS (2007) The Qo site of the mitochondrial complex III is required for the transduction of hypoxic signaling via reactive oxygen species production. *J Cell Biol* **177**, 1029-1036.

[23] Bell EL, Klimova T, Chandel NS (2008) Targeting the mitochondria for cancer therapy: regulation of hypoxia-inducible factor by mitochondria. *Antioxid Redox Signal* **10**, 635-640.

[24] Correia SC, Moreira PI (2010) Hypoxia-inducible factor 1: a new hope to counteract neurodegeneration? *J Neurochem* **112**, 1-12.

[25] Lee DW, Rajagopalan S, Siddiq A, Gwiazda R, Yang L, Beal MF, Ratan RR, Andersen JK (2009) Inhibition of prolyl hydroxylase protects against 1-methyl-4-phenyl-1,2,3,6-tetrahydropyridine-induced neurotoxicity: model for the potential involvement of the hypoxia-inducible factor pathway in Parkinson disease. *J Biol Chem* **284**, 29065-29076.

[26] Kamata H, Manabe T, Oka S, Kamata K, Hirata H (2002) Hydrogen peroxide activates IkappaB kinases through phosphorylation of serine residues in the activation loops. *FEBS Lett* **519**, 231-237.

[27] Pahl HL (1999) Activators and target genes of Rel/NF-kappaB transcription factors. *Oncogene* **18**, 6853-6866.

[28] Das KC, Lewis-Molock Y, White CW (1995) Activation of NF-kappa B and elevation of MnSOD gene expression by thiol reducing agents in lung adenocarcinoma (A549) cells. *Am J Physiol* **269**, L588-602.

[29] Gloire G, Piette J (2009) Redox regulation of nuclear post-translational modifications during NF-kappaB activation. *Antioxid Redox Signal* **11**, 2209-2222.

[30] Bubici C, Papa S, Dean K, Franzoso G (2006) Mutual cross-talk between reactive oxygen species and nuclear factor-kappa B: molecular basis and biological significance. *Oncogene* **25**, 6731-6748.

[31] Toledano MB, Leonard WJ (1991) Modulation of transcription factor NF-kappa B binding activity by oxidation-reduction *in vitro*. *Proc Natl Acad Sci U S A* **88**, 4328-4332.

[32] Vousden KH, Lane DP (2007) p53 in health and disease. *Nat Rev Mol Cell Biol* **8**, 275-283.

[33] Tan M, Li S, Swaroop M, Guan K, Oberley LW, Sun Y (1999) Transcriptional activation of the human glutathione peroxidase promoter by p53. *J Biol Chem* **274**, 12061-12066.

[34] Hussain SP, Amstad P, He P, Robles A, Lupold S, Kaneko I, Ichimiya M, Sengupta S, Mechanic L, Okamura S, Hofseth LJ, Moake M, Nagashima M, Forrester KS, Harris CC (2004) p53-induced up-regulation of MnSOD and GPx but not catalase increases oxidative stress and apoptosis. *Cancer Res* **64**, 2350-2356.

[35] Yoon KA, Nakamura Y, Arakawa H (2004) Identification of ALDH4 as a p53-inducible gene and its protective role in cellular stresses. *J Hum Genet* **49**, 134-140.

[36] Bensaad K, Tsuruta A, Selak MA, Vidal MN, Nakano K, Bartrons R, Gottlieb E, Vousden KH (2006) TIGAR, a p53-inducible regulator of glycolysis and apoptosis. *Cell* **126**, 107-120.

[37] Sablina AA, Budanov AV, Ilyinskaya GV, Agapova LS, Kravchenko JE, Chumakov PM (2005) The antioxidant function of the p53 tumor suppressor. *Nat Med* **11**, 1306-1313.

[38] Vousden KH, Lu X (2002) Live or let die: the cell's response to p53. *Nat Rev Cancer* **2**, 594-604.

[39] Polyak K, Xia Y, Zweier JL, Kinzler KW, Vogelstein B (1997) A model for p53-induced apoptosis. *Nature* **389**, 300-305.

[40] Liu B, Chen Y, St Clair DK (2008) ROS and p53: a versatile partnership. *Free Radic Biol Med* **44**, 1529-1535.

[41] Ferrante RJ, Browne SE, Shinobu LA, Bowling AC, Baik MJ, MacGarvey U, Kowall NW, Brown RH, Jr., Beal MF (1997) Evidence of increased oxidative damage in both sporadic and familial amyotrophic lateral sclerosis. *J Neurochem* **69**, 2064-2074.

[42] Browne SE, Bowling AC, MacGarvey U, Baik MJ, Berger SC, Muqit MM, Bird ED, Beal MF (1997) Oxidative damage and metabolic dysfunction in Huntington's disease: selective vulnerability of the basal ganglia. *Ann Neurol* **41**, 646-653.

[43] Schulz JB, Beal MF (1994) Mitochondrial dysfunction in movement disorders. *Curr Opin Neurol* **7**, 333-339.

[44] Alam ZI, Jenner A, Daniel SE, Lees AJ, Cairns N, Marsden CD, Jenner P, Halliwell B (1997) Oxidative DNA damage in the parkinsonian brain: an apparent selective increase in 8-hydroxyguanine levels in substantia nigra. *J Neurochem* **69**, 1196-1203.

[45] Wang J, Xiong S, Xie C, Markesbery WR, Lovell MA (2005) Increased oxidative damage in nuclear and mitochondrial DNA in Alzheimer's disease. *J Neurochem* **93**, 953-962.

[46] Mecocci P, MacGarvey U, Beal MF (1994) Oxidative damage to mitochondrial DNA is increased in Alzheimer's disease. *Ann Neurol* **36**, 747-751.

[47] Rosen DR, Siddique T, Patterson D, Figlewicz DA, Sapp P, Hentati A, Donaldson D, Goto J, O'Regan JP, Deng HX, et al. (1993) Mutations in Cu/Zn superoxide dismutase gene are associated with familial amyotrophic lateral sclerosis. *Nature* **362**, 59-62.

[48] Zimmerman MC, Oberley LW, Flanagan SW (2007) Mutant SOD1-induced neuronal toxicity is mediated by increased mitochondrial superoxide levels. *J Neurochem* **102**, 609-618.

[49] Boillee S, Vande Velde C, Cleveland DW (2006) ALS: a disease of motor neurons and their nonneuronal neighbors. *Neuron* **52**, 39-59.

[50] Vijayvergiya C, Beal MF, Buck J, Manfredi G (2005) Mutant superoxide dismutase 1 forms aggregates in the brain mitochondrial matrix of amyotrophic lateral sclerosis mice. *J Neurosci* **25**, 2463-2470.

[51] Ferri A, Cozzolino M, Crosio C, Nencini M, Casciati A, Gralla EB, Rotilio G, Valentine JS, Carri MT (2006) Familial ALS-superoxide dismutases associate with mitochondria and shift their redox potentials. *Proc Natl Acad Sci U S A* **103**, 13860-13865.

[52] Gu M, Gash MT, Mann VM, Javoy-Agid F, Cooper JM, Schapira AH (1996) Mitochondrial defect in Huntington's disease caudate nucleus. *Ann Neurol* **39**, 385-389.

[53] Bogdanov MB, Andreassen OA, Dedeoglu A, Ferrante RJ, Beal MF (2001) Increased oxidative damage to DNA in a transgenic mouse model of Huntington's disease. *J Neurochem* **79**, 1246-1249.

[54] Perez-Severiano F, Santamaria A, Pedraza-Chaverri J, Medina-Campos ON, Rios C, Segovia J (2004) Increased formation of reactive oxygen species, but no changes in glutathione peroxidase activity, in striata of mice transgenic for the Huntington's disease mutation. *Neurochem Res* **29**, 729-733.

[55] Ferrante RJ, Andreassen OA, Dedeoglu A, Ferrante KL, Jenkins BG, Hersch SM, Beal MF (2002) Therapeutic effects of coenzyme Q10 and remacemide in transgenic mouse models of Huntington's disease. *J Neurosci* **22**, 1592-1599.

[56] Bueler H (2010) Mitochondrial dynamics, cell death and the pathogenesis of Parkinson's disease. *Apoptosis*, in press.

[57] Liu W, Vives-Bauza C, Acin-Perez R, Yamamoto A, Tan Y, Li Y, Magrane J, Stavarache MA, Shaffer S, Chang S, Kaplitt MG, Huang XY, Beal MF, Manfredi G, Li C (2009) PINK1 defect causes mitochondrial dysfunction, proteasomal deficit and alpha-synuclein aggregation in cell culture models of Parkinson's disease. *PLoS One* **4**, e4597.

[58] Palacino JJ, Sagi D, Goldberg MS, Krauss S, Motz C, Wacker M, Klose J, Shen J (2004) Mitochondrial dysfunction and oxidative damage in parkin-deficient mice. *J Biol Chem* **279**, 18614-18622.

[59] Krebiehl G, Ruckerbauer S, Burbulla LF, Kieper N, Maurer B, Waak J, Wolburg H, Gizatullina Z, Gellerich FN, Woitalla D, Riess O, Kahle PJ, Proikas-Cezanne T, Kruger R (2010) Reduced basal autophagy and impaired mitochondrial dynamics due to loss of Parkinson's disease-associated protein DJ-1. *PLoS One* **5**, e9367.

[60] Xiong H, Wang D, Chen L, Choo YS, Ma H, Tang C, Xia K, Jiang W, Ronai Z, Zhuang X, Zhang Z (2009) Parkin, PINK1, and DJ-1 form a ubiquitin E3 ligase complex promoting unfolded protein degradation. *J Clin Invest* **119**, 650-660.

[61] Tanaka Y, Engelender S, Igarashi S, Rao RK, Wanner T, Tanzi RE, Sawa A, V LD, Dawson TM, Ross CA (2001) Inducible expression of mutant alpha-synuclein decreases proteasome activity and increases sensitivity to mitochondria-dependent apoptosis. *Hum Mol Genet* **10**, 919-926.

[62] Devi L, Raghavendran V, Prabhu BM, Avadhani NG, Anandatheerthavarada HK (2008) Mitochondrial import and accumulation of alpha-synuclein impair complex I in human dopaminergic neuronal cultures and Parkinson disease brain. *J Biol Chem* **283**, 9089-9100.

[63] Martin LJ, Pan Y, Price AC, Sterling W, Copeland NG, Jenkins NA, Price DL, Lee MK (2006) Parkinson's disease alpha-synuclein transgenic mice develop neuronal mitochondrial degeneration and cell death. *J Neurosci* **26**, 41-50.

[64] Manczak M, Anekonda TS, Henson E, Park BS, Quinn J, Reddy PH (2006) Mitochondria are a direct site of A beta accumulation in Alzheimer's disease neurons: implications for free radical generation and oxidative damage in disease progression. *Hum Mol Genet* **15**, 1437-1449.

[65] Caspersen C, Wang N, Yao J, Sosunov A, Chen X, Lustbader JW, Xu HW, Stern D, McKhann G, Yan SD (2005) Mitochondrial Abeta: a potential focal point for neuronal metabolic dysfunction in Alzheimer's disease. *FASEB J* **19**, 2040-2041.

[66] Querfurth HW, LaFerla FM (2010) Alzheimer's disease. *N Engl J Med* **362**, 329-344.

[67] Casley CS, Canevari L, Land JM, Clark JB, Sharpe MA (2002) Beta-amyloid inhibits integrated mitochondrial respiration and key enzyme activities. *J Neurochem* **80**, 91-100.
[68] Wang X, Su B, Lee HG, Li X, Perry G, Smith MA, Zhu X (2009) Impaired balance of mitochondrial fission and fusion in Alzheimer's disease. *J Neurosci* **29**, 9090-9103.
[69] Yu T, Robotham JL, Yoon Y (2006) Increased production of reactive oxygen species in hyperglycemic conditions requires dynamic change of mitochondrial morphology. *Proc Natl Acad Sci U S A* **103**, 2653-2658.
[70] Wang X, Su B, Siedlak SL, Moreira PI, Fujioka H, Wang Y, Casadesus G, Zhu X (2008) Amyloid-beta overproduction causes abnormal mitochondrial dynamics via differential modulation of mitochondrial fission/fusion proteins. *Proc Natl Acad Sci U S A* **105**, 19318-19323.
[71] Karuppagounder SS, Xu H, Shi Q, Chen LH, Pedrini S, Pechman D, Baker H, Beal MF, Gandy SE, Gibson GE (2009) Thiamine deficiency induces oxidative stress and exacerbates the plaque pathology in Alzheimer's mouse model. *Neurobiol Aging* **30**, 1587-1600.
[72] Esteves AR, Arduino DM, Swerdlow RH, Oliveira CR, Cardoso SM (2009) Oxidative stress involvement in alpha-synuclein oligomerization in Parkinson's disease cybrids. *Antioxid Redox Signal* **11**, 439-448.
[73] Batelli S, Albani D, Rametta R, Polito L, Prato F, Pesaresi M, Negro A, Forloni G (2008) DJ-1 modulates alpha-synuclein aggregation state in a cellular model of oxidative stress: relevance for Parkinson's disease and involvement of HSP70. *PLoS One* **3**, e1884.
[74] Sheehan JP, Swerdlow RH, Miller SW, Davis RE, Parks JK, Parker WD, Tuttle JB (1997) Calcium homeostasis and reactive oxygen species production in cells transformed by mitochondria from individuals with sporadic Alzheimer's disease. *J Neurosci* **17**, 4612-4622.
[75] LaFerla FM (2002) Calcium dyshomeostasis and intracellular signalling in Alzheimer's disease. *Nat Rev Neurosci* **3**, 862-872.
[76] Isaacs AM, Senn DB, Yuan M, Shine JP, Yankner BA (2006) Acceleration of amyloid beta-peptide aggregation by physiological concentrations of calcium. *J Biol Chem* **281**, 27916-27923.
[77] Alberdi E, Sanchez-Gomez MV, Cavaliere F, Perez-Samartin A, Zugaza JL, Trullas R, Domercq M, Matute C (2010) Amyloid beta oligomers induce Ca(2+) dysregulation and neuronal death through activation of ionotropic glutamate receptors. *Cell Calcium* **47**, 264-272.
[78] He C, Klionsky DJ (2009) Regulation mechanisms and signaling pathways of autophagy. *Annu Rev Genet* **43**, 67-93.
[79] Hara T, Nakamura K, Matsui M, Yamamoto A, Nakahara Y, Suzuki-Migishima R, Yokoyama M, Mishima K, Saito I, Okano H, Mizushima N (2006) Suppression of basal autophagy in neural cells causes neurodegenerative disease in mice. *Nature* **441**, 885-889.
[80] Komatsu M, Waguri S, Chiba T, Murata S, Iwata J, Tanida I, Ueno T, Koike M, Uchiyama Y, Kominami E, Tanaka K (2006) Loss of autophagy in the central nervous system causes neurodegeneration in mice. *Nature* **441**, 880-884.
[81] Geisler S, Holmstrom KM, Skujat D, Fiesel FC, Rothfuss OC, Kahle PJ, Springer W (2010) PINK1/Parkin-mediated mitophagy is dependent on VDAC1 and p62/SQSTM1. *Nat Cell Biol* **12**, 119-131.
[82] Narendra D, Tanaka A, Suen DF, Youle RJ (2008) Parkin is recruited selectively to impaired mitochondria and promotes their autophagy. *J Cell Biol* **183**, 795-803.
[83] Vives-Bauza C, Zhou C, Huang Y, Cui M, de Vries RL, Kim J, May J, Tocilescu MA, Liu W, Ko HS, Magrane J, Moore DJ, Dawson VL, Grailhe R, Dawson TM, Li C, Tieu K, Przedborski S (2010) PINK1-dependent recruitment of Parkin to mitochondria in mitophagy. *Proc Natl Acad Sci U S A* **107**, 378-383.
[84] Narendra DP, Jin SM, Tanaka A, Suen DF, Gautier CA, Shen J, Cookson MR, Youle RJ (2010) PINK1 is selectively stabilized on impaired mitochondria to activate Parkin. *PLoS Biol* **8**, e1000298.
[85] Festjens N, Vanden Berghe T, Vandenabeele P (2006) Necrosis, a well-orchestrated form of cell demise: signalling cascades, important mediators and concomitant immune response. *Biochim Biophys Acta* **1757**, 1371-1387.
[86] Chipuk JE, Moldoveanu T, Llambi F, Parsons MJ, Green DR (2010) The BCL-2 Family Reunion. *Mol Cell* **37**, 299-310.
[87] Youle RJ, Strasser A (2008) The BCL-2 protein family: opposing activities that mediate cell death. *Nat Rev Mol Cell Biol* **9**, 47-59.
[88] Cho BB, Toledo-Pereyra LH (2008) Caspase-independent programmed cell death following ischemic stroke. *J Invest Surg* **21**, 141-147.
[89] Mathai JP, Germain M, Marcellus RC, Shore GC (2002) Induction and endoplasmic reticulum location of BIK/NBK in response to apoptotic signaling by E1A and p53. *Oncogene* **21**, 2534-2544.
[90] Hubner A, Barrett T, Flavell RA, Davis RJ (2008) Multisite phosphorylation regulates Bim stability and apoptotic activity. *Mol Cell* **30**, 415-425.
[91] Morel C, Carlson SM, White FM, Davis RJ (2009) Mcl-1 integrates the opposing actions of signaling pathways that mediate survival and apoptosis. *Mol Cell Biol* **29**, 3845-3852.
[92] Maiuri MC, Le Toumelin G, Criollo A, Rain JC, Gautier F, Juin P, Tasdemir E, Pierron G, Troulinaki K, Tavernarakis N, Hickman JA, Geneste O, Kroemer G (2007) Functional and physical interaction between Bcl-X(L) and a BH3-like domain in Beclin-1. *EMBO J* **26**, 2527-2539.
[93] Pattingre S, Tassa A, Qu X, Garuti R, Liang XH, Mizushima N, Packer M, Schneider MD, Levine B (2005) Bcl-2 antiapoptotic proteins inhibit Beclin 1-dependent autophagy. *Cell* **122**, 927-939.
[94] Wei Y, Pattingre S, Sinha S, Bassik M, Levine B (2008) JNK1-mediated phosphorylation of Bcl-2 regulates starvation-induced autophagy. *Mol Cell* **30**, 678-688.
[95] Puissant A, Robert G, Fenouille N, Luciano F, Cassuto JP, Raynaud S, Auberger P (2010) Resveratrol promotes autophagic cell death in chronic myelogenous leukemia cells via JNK-mediated p62/SQSTM1 expression and AMPK activation. *Cancer Res* **70**, 1042-1052.
[96] Scarlatti F, Granata R, Meijer AJ, Codogno P (2009) Does autophagy have a license to kill mammalian cells? *Cell Death Differ* **16**, 12-20.
[97] Smith RA, Adlam VJ, Blaikie FH, Manas AR, Porteous CM, James AM, Ross MF, Logan A, Cocheme HM, Trnka J, Prime TA, Abakumova I, Jones BA, Filipovska A, Murphy MP (2008) Mitochondria-targeted antioxidants in the treatment of disease. *Ann N Y Acad Sci* **1147**, 105-111.
[98] Jauslin ML, Meier T, Smith RA, Murphy MP (2003) Mitochondria-targeted antioxidants protect Friedreich Ataxia fibroblasts from endogenous oxidative stress more effectively than untargeted antioxidants. *FASEB J* **17**, 1972-1974.
[99] Graham D, Huynh NN, Hamilton CA, Beattie E, Smith RA, Cocheme HM, Murphy MP, Dominiczak AF (2009) Mitochondria-targeted antioxidant MitoQ10 improves en-

dothelial function and attenuates cardiac hypertrophy. *Hypertension* **54**, 322-328.

[100] Antonenko YN, Roginsky VA, Pashkovskaya AA, Rokitskaya TI, Kotova EA, Zaspa AA, Chernyak BV, Skulachev VP (2008) Protective effects of mitochondria-targeted antioxidant SkQ in aqueous and lipid membrane environments. *J Membr Biol* **222**, 141-149.

[101] Skulachev VP, Anisimov VN, Antonenko YN, Bakeeva LE, Chernyak BV, Erichev VP, Filenko OF, Kalinina NI, Kapelko VI, Kolosova NG, Kopnin BP, Korshunova GA, Lichinitser MR, Obukhova LA, Pasyukova EG, Pisarenko OI, Roginsky VA, Ruuge EK, Senin, II, Severina, II, Skulachev MV, Spivak IM, Tashlitsky VN, Tkachuk VA, Vyssokikh MY, Yaguzhinsky LS, Zorov DB (2009) An attempt to prevent senescence: a mitochondrial approach. *Biochim Biophys Acta* **1787**, 437-461.

[102] Zhao K, Zhao GM, Wu D, Soong Y, Birk AV, Schiller PW, Szeto HH (2004) Cell-permeable peptide antioxidants targeted to inner mitochondrial membrane inhibit mitochondrial swelling, oxidative cell death, and reperfusion injury. *J Biol Chem* **279**, 34682-34690.

[103] Zhao K, Luo G, Giannelli S, Szeto HH (2005) Mitochondria-targeted peptide prevents mitochondrial depolarization and apoptosis induced by tert-butyl hydroperoxide in neuronal cell lines. *Biochem Pharmacol* **70**, 1796-1806.

[104] Thomas DA, Stauffer C, Zhao K, Yang H, Sharma VK, Szeto HH, Suthanthiran M (2007) Mitochondrial targeting with antioxidant peptide SS-31 prevents mitochondrial depolarization, reduces islet cell apoptosis, increases islet cell yield, and improves posttransplantation function. *J Am Soc Nephrol* **18**, 213-222.

[105] Petri S, Kiaei M, Damiano M, Hiller A, Wille E, Manfredi G, Calingasan NY, Szeto HH, Beal MF (2006) Cell-permeable peptide antioxidants as a novel therapeutic approach in a mouse model of amyotrophic lateral sclerosis. *J Neurochem* **98**, 1141-1148.

[106] Yang L, Zhao K, Calingasan NY, Luo G, Szeto HH, Beal MF (2009) Mitochondria targeted peptides protect against 1-methyl-4-phenyl-1,2,3,6-tetrahydropyridine neurotoxicity. *Antioxid Redox Signal* **11**, 2095-2104.

Appendix D:

Human Molecular Genetics, 2013, Vol. 22, No. 5 **952–962**
doi:10.1093/hmg/dds500
Advance Access published on November 27, 2012

LKB1-regulated adaptive mechanisms are essential for neuronal survival following mitochondrial dysfunction

Marc Germain[1,†], Angela P. Nguyen[1], Mireille Khacho[1], David A. Patten[1], Robert A. Screaton[2,3], David S. Park[1] and Ruth S. Slack[1,*]

[1]Department of Cellular and Molecular Medicine, Faculty of Medicine, [2]Department of Pediatrics and CMM, University of Ottawa, 451 Smyth Road, Ottawa, Ontario K1H 8M5, Canada and [3]Children's Hospital of Eastern Ontario Research Institute, University of Ottawa, 401 Smyth Road, Ottawa K1H 8L1, Canada

Received October 11, 2011; Revised and Accepted November 22, 2012

Mitochondrial dysfunction plays an important role in the etiology of neurodegenerative diseases. However, the progressive nature of neuronal loss in genetic models of mitochondrial dysfunction suggests the presence of compensatory mechanisms promoting neuronal survival under these conditions. Here, we identified the energy metabolism kinase LKB1 as a key regulator of the compensatory mechanisms activated in neurons, following mitochondrial dysfunction. To accomplish this, we have created an *in vivo* neurodegenerative model based on the deletion of the mitochondrial protein apoptosis-inducing factor (AIF) in postmitotic neurons. Loss of mitochondrial function caused by AIF deletion induced several adaptive mechanisms, including increased glycolysis and mitochondrial biogenesis. Importantly, the activation of these adaptive mechanisms was abrogated by the deletion of one allele of LKB1, resulting in impaired neuronal survival. Because loss of mitochondrial function is a central mechanism implicated in neurodegenerative diseases, modulation of LKB1-dependent pathways may represent an important strategy to preserve neuronal survival and function.

INTRODUCTION

Neurodegenerative diseases are characterized by a progressive loss of neurons that often affects specific neuronal populations. In recent years, mitochondrial dysfunction has emerged as a key factor contributing to this neuronal cell death in diseases such as Alzheimer's disease (AD), Parkinson's disease (PD) and amyotrophic lateral sclerosis [reviewed in (1–4)]. For example, loss of function of complex I of the electron transport chain (ETC) is an important feature of PD, whereas amyloid-β disrupts mitochondrial function, contributing to neuronal loss in AD (2,5).

To better understand the role of mitochondrial dysfunction in neurodegenerative diseases, several animal models of mitochondria loss of function have been generated. These include ablation of complex I (Ndufs4) and complex IV (Cox10) subunits (6,7), as well as loss of the mitochondrial transcription factor A (8), all of which cause severe defects in oxidative phosphorylation (OXPHOS). Another example is apoptosis-inducing factor (AIF), an evolutionary conserved mitochondrial protein that plays an essential role in the maintenance of mitochondrial structure and function and the downregulation of which causes neurodegeneration in mice (9) and a severe mitochondrial encephalomyopathy when mutated in humans (10). Of note, while most animal models of loss of mitochondrial function show robust primary mitochondrial defects, the rate of neuronal loss is generally more progressive and limited to specific neuronal populations. Although this selective vulnerability of neurons has been proposed to be linked to differences in neuronal metabolism [reviewed in (4)], the underlying causes remain poorly understood. In fact, while the activation of several cell death pathways has been characterized as a consequence of mitochondrial dysfunction, the nature and regulation of adaptive pathways allowing certain neuronal populations to survive under these circumstances remain an important question.

The serine/threonine kinase LKB1 is a master regulator of energy metabolism, restricting cell growth under energy

*To whom correspondence should be addressed. Email: rslack@uottawa.ca
†Present address: Département de Chimie-Biologie, Université du Québec à Trois-Rivières, Trois-Rivières, G9A 5H7, Canada.

stress conditions through the regulation 14 kinases that act on processes such as cell polarity, cell growth and metabolism (11,12). Among these, the best characterized LKB1 substrate is the AMP-dependent protein kinase AMPK, a kinase that regulates autophagy and prevents cell growth by inhibiting mammalian target of rapamycin (mTOR) (11,12). Given the key role of LKB1 in cellular adaptation to energy stress, it is an attractive candidate for the regulation of metabolically driven adaptive processes. Indeed, recent evidence suggests that LKB1 plays an important role in adapting skeletal muscle metabolic function in response to exercise (13,14). However, the role of LKB1 in the adult brain under basal conditions or following mitochondrial dysfunction remains an important question, as neurons differ significantly from muscle in their metabolic needs [reviewed in (15,16)].

We used the conditional deletion of AIF as a neurodegenerative model to study the role of LKB1 in the adaptive response of neurons to mitochondrial dysfunction. Although AIF deletion in postmitotic neurons resulted in mitochondrial fragmentation and loss of OXPHOS function, as previously observed in other tissues (17–20), no neuronal loss was observed in the cortex of 90 days old AIF KO (AKO) mice. This neuronal survival was dependent on the activation of several LKB1-dependent adaptive mechanisms, including increased glucose metabolism and mitochondrial biogenesis. Consequently, loss of one allele of LKB1 significantly increased cell death that was observed in the cortex of AKO animals. Altogether, these results demonstrate that LKB1 plays a critical role in neuronal adaptation to mitochondrial dysfunction. Because loss of mitochondrial function is an important aspect of neurodegenerative diseases, manipulation of LKB1-dependent pathways could provide new tools to promote neuronal survival in this context.

RESULTS

AIF deletion in postmitotic neurons disrupts mitochondrial function

The mitochondrial inner membrane protein AIF is essential for the maintenance of mitochondrial function and morphology and its loss causes mitochondrial fragmentation and decreased levels of ETC proteins (17–20). As loss of AIF affects both functional and structural aspects of mitochondrial function, we used AIF deletion in postmitotic neurons to address the neuronal response to mitochondrial dysfunction. AIF-floxed mice (18) were crossed with mice expressing Cre under the control of the CamkIIα promoter, resulting in recombination of the floxed AIF allele (null allele) in the cortex, the hippocampus and the striatum (AKO mice) (Fig. 1A) (21). AIF deletion in the cortex was confirmed by western blot (Fig. 1B), and neuron-specific loss of mitochondrial AIF immunostaining was confirmed by immunohistochemistry in the cortex (Fig. 1C), striatum and hippocampus (not shown). Loss of AIF resulted in mitochondrial fragmentation that was accompanied by mitochondrial swelling, as evidenced by the double labeling of mitochondria with the mitochondrial outer membrane protein TOM20 and the matrix protein mtHSP70 (Fig. 1E, quantified in D). This loss of mitochondrial structure was correlated with decreased levels of NDUFA9 (complex I), Core2 (complex III) and COX IV (complex IV), but not SDHA (complex II) (Fig. 1B, quantified in F). Altogether, these results indicate that AKO recapitulates the mitochondrial defects previously reported upon AIF deletion in other tissues (17–20).

To address the consequences of mitochondrial dysfunction caused by AIF deletion on the survival of different neuronal populations, we first examined the general brain morphology in 90-day-old AKO by cresyl violet staining and visualization of cortical processes by MAP2 staining (Fig. 2A). Consistent with the greater sensitivity of striatal neurons to mitochondrial dysfunction (22), a small but significant neuronal loss (15%) was observed in AKO striatum (Fig. 2B) when compared with their littermate controls. In contrast, there were neither gross morphological changes nor significant neuronal loss in the cortex or the hippocampus of AKO animals (Fig. 2A, C and D), two other structures where Cre is expressed (21) (data not shown). AKO cortical thickness was, however, reduced by 15% (Fig. 2E). Given that AKO animals had the same number of cortical neurons as their wild-type (WT) littermates, we explored the possibility that the reduced cortical thickness was the result of decreased cell size. Neuronal cell body volume was indeed significantly reduced in AKO cortical layers II/III, and a similar trend was observed in layer V neurons (Fig. 2F), suggesting that the reduced cortical thickness is the consequence of decreased neuronal cell body volume.

As the absence of cell loss in the cortex could be the consequence of a delayed appearance of mitochondrial dysfunction, we evaluated cortical expression of AIF and complex I subunit NDUFA9 at different ages. AIF loss was evident as early as 30 days after birth, whereas loss of NDUFA9 was clearly apparent in 60 days old animals (Fig. 3A). However, NDUFA9 levels were also decreased in some 30-day-old AKO by western blot (Fig. 3B, levels for four different AKO are plotted) and partially decreased in affected neurons by immunohistochemistry (Fig. 3C). Altogether, these data suggest that AKO mitochondria are dysfunctional by 60 days of age at the latest and that AKO cortical neurons can, thus, survive at least a month with dysfunctional mitochondria. Of note, loss of mitochondrial complexes, including Core2, was most evident in layer V neurons ($Oct6^{+}$) (Fig. 4A, D; quantified in B) that normally express the highest levels of several mitochondrial markers in their cell body (Fig. 4E, quantified in B). Interestingly, these neurons are also more sensitive to the loss of the transcriptional co-activator PGC1α (23,24), an important regulator of mitochondrial biogenesis.

Activation of adaptive mechanisms in AKO cortical neurons

Recent evidence suggests a role of proteins involved in the regulation of metabolism in promoting neuronal survival under metabolic stress, although their physiological regulation in this context is not well understood. For example, PGC1α levels are decreased in several neurodegenerative diseases, and its reintroduction in neurons from disease models is protective (25). As layer V neurons are the most affected in both AKO and PGC1α KO animals, we quantified PGC1α levels following AIF deletion. More precisely, to discriminate

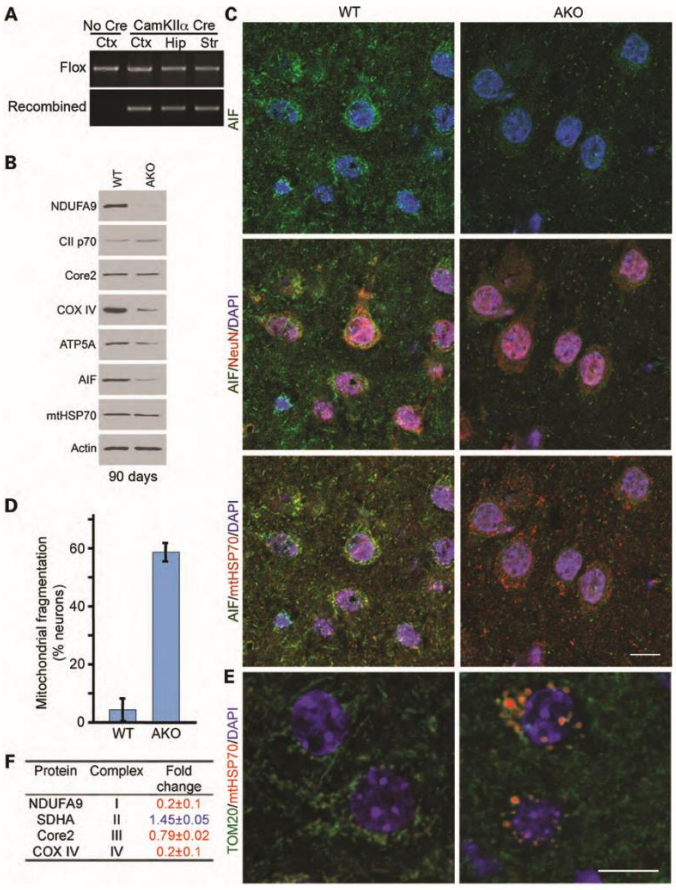

Figure 1. Loss of mitochondrial function in apoptosis-inducing factor (AIF) null neurons. (**A**) PCR analysis of recombination at the *Aif* locus in 60-day-old AKO animals showing recombination in the presence of the Cre recombinase. Note that recombination occurs in the cortex (Ctx), hippocampus (Hip) and striatum (Str). (**B**) Expression levels of various components of the ETC in the cortices of 90 days old WT and AKO animals. The following antibodies were used: NDUFA9 (complex I), SDHA (complex II), Core2 (complex III), Cox IV (complex IV) and ATP5A (ATP synthase). mtHSP70 was used as a mitochondrial loading control. (**C**) Neuron-specific loss of AIF in AKO mice. AIF expression was analyzed in the cortex of AKO animals by staining with an AIF-specific antibody (green) and an antibody against the neuronal marker NeuN (middle panels; red) or the mitochondrial marker mtHSP70 (lower panels; red), along with the nuclear stain DAPI (blue). Scale bar 10 μm. Representative images are shown. (**D** and **E**) Mitochondrial fragmentation in AKO neurons. Mitochondria in the cortex of AKO animals were visualized by co-staining with the outer membrane TOM20 (green) and the matrix protein mtHSP70 (red). Confocal images were taken using a 63 × objective (E) and quantified in (D). Scale bar 10 μm. Representative images are shown in (E). (**F**) Protein levels from the western blots in (A) were quantified using Image J. The measurements from three animals per genotype were normalized to actin levels and expressed as fold change over WT ± SD.

potential layer-specific responses, PGC1α levels were analyzed by immunohistochemistry and not western blot. Loss of AIF resulted in the upregulation of PGC1α specifically in layer V neurons ($Oct6^+$ cells; Fig. 5A, quantified in B), suggesting a link between the increased sensitivity of these neurons to the loss of mitochondrial markers and their requirement for mitochondrial biogenesis. A second example of a metabolic enzyme promoting neuronal survival following mitochondrial dysfunction is HKII, the enzyme regulating the first, rate limiting, step of glycolysis (26). Interestingly, HKII levels were also increased in AKO cortical neurons (Fig. 5A, quantified in C).

Several metabolic pathways are regulated upon loss of ATP production in a fashion that depends on the activation of

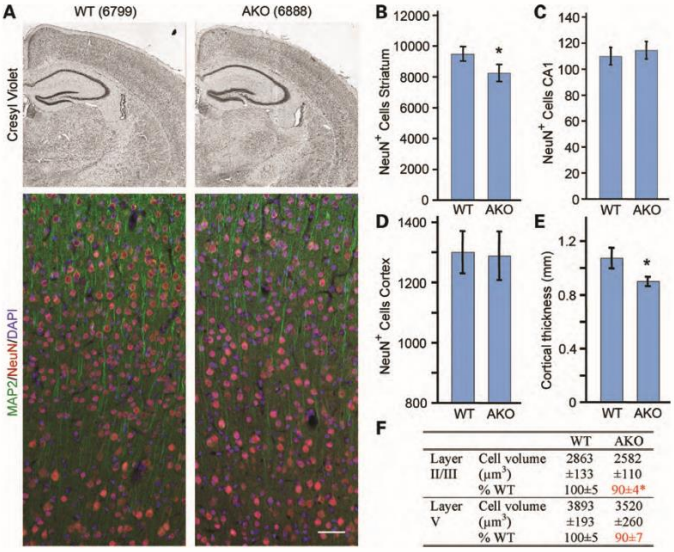

F

		WT	AKO
Layer II/III	Cell volume (μm^3)	2863 ±133	2582 ±110
	% WT	100±5	90±4*
Layer V	Cell volume (μm^3)	3893 ±193	3520 ±260
	% WT	100±5	90±7

Figure 2. AKO brain morphology. (**A**) Brain sections of 90 days old animals were stained with cresyl violet and imaged using a 5× objective. Several images were used to create the composite images shown (top). Sections were also stained with antibodies against the dendritic marker MAP2 and the neuronal marker NeuN, with the nuclear stain DAPI (blue) and imaged using a confocal microscope equipped with a 20× objective (bottom). Scale bar 50 μm. Representative images are shown. (**B–D**) Neuronal numbers are decreased in the striatum (B) but not the hippocampus (C) and cortex (D) of AKO animals. (**B**) The number of NeuN-positive cells was counted in images from the striatum taken using a 20× objective. The total number of neurons per section was then estimated from the average of at least two images and the total area of the striatum. Data are expressed as the total number of $NeuN^+$ cells per section in at least three animals per genotype + SD. $^*P < 0.05$. Alternatively, the number of NeuN-positive cells was counted from a section of the CA1 taken with a 40× objective (C) or in 10× composite images of the cortex encompassing all six neuronal layers (D). Data are expressed as the total number of $NeuN^+$ cells per image in at least three animals per genotype ± SD. (**E**) Cortical thickness was measured in the same sections as in (D). Data from least three animals per genotype ± SD. $^*P < 0.05$. (**F**) Decreased neuronal cell body volume in AKO neurons. Cell body volume was estimated from stacks of NeuN-stained neurons from 90 days old animals taken using a confocal microscope. Data are expressed as the average neuronal cell body volume in least three animals per genotype ± SD. $^*P < 0.05$.

AMPK. In this way, AMPK reestablishes cellular energy balance by promoting ATP synthesis, while shutting down energy-consuming processes such as mTOR-dependent protein translation (11,12). Interestingly, loss of AIF also induced AMPK activation, as determined by its phosphorylation on residue S172 (Fig. 4D). This correlated with a reduction in mTOR activity, as determined by decreased phosphorylation of the mTOR substrate 4eBP1 (Fig. 5D). Altogether, our results suggest that loss of AIF triggers the activation of several compensatory mechanisms promoting the survival of cortical neurons.

LKB1 regulates the adaptive mechanisms induced by mitochondrial loss of function

LKB1 is an evolutionary conserved kinase that regulates energy metabolism through the control of key cellular processes such as cell polarity, cell growth, mitochondrial biogenesis and glucose metabolism (Fig. 6I). This occurs in ways that are both dependent and independent of AMPK, its best characterized substrate (11,12,27). Of note, PGC1α and HKII, activated as a consequence of AIF deletion, are both regulated in an LKB1-dependent manner in skeletal muscle (13,14). However, as metabolic control is significantly different in neurons and muscle (15,16), whether LKB1 regulates compensatory mechanisms in a similar fashion in cortical neurons remains unknown. Therefore, we determined the role of LKB1 in the activation of these compensatory mechanisms by conditionally deleting LKB1 (28) in AKO animals (using CamKIIα Cre). Strikingly, loss of only one allele of LKB1 was sufficient to decrease both LKB1 levels and AMPK phosphorylation in the cortex of 10 days old animals (Fig. 6A), suggesting an important role for LKB1 in this context. Given that complete deletion of LKB1 leads to loss of axonal growth in neural precursors (29,30) and that AMPK phosphorylation was notably decreased in LKB1 heterozygotes, we used a LKB1 heterozygote for all subsequent experiments. These animals were similar to their littermate controls in all aspects tested, including axonal tracts (Fig. 6B), clearly distinguishing them from the embryonic phenotype previously reported (29,30).

To address the role of LKB1 in the regulation of the adaptive mechanisms activated by the loss of AIF, we first quantified PGC1α expression in response to LKB1 deletion. The decrease in LKB1 expression in the LKB1 heterozygote did not affect

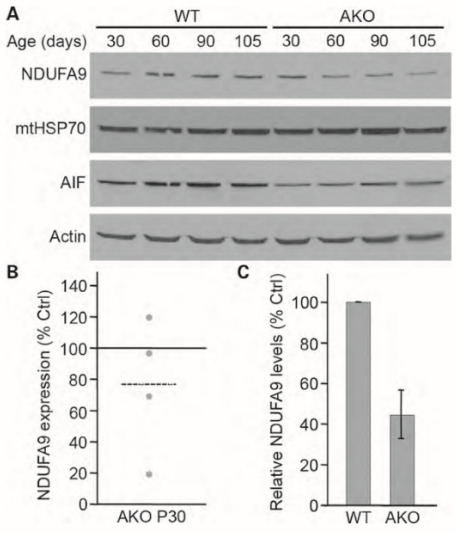

Figure 3. Time course of loss of mitochondrial function in AKO animals. (**A**) Expression levels of AIF and the complex I subunit NDUFA9 in the cortices of WT and AKO animals of the indicated ages. (**B**) NDUFA9 levels were quantified using Image J by normalizing to actin levels and expressed as percentage of change over WT in 30-day-old animals. Individual animals are plotted. (**C**) NDUFA9 levels were quantified by co-staining of cortical sections from 30-day-old animals with antibodies against NDUFA9 and the mitochondrial outer membrane marker TOM20 expressed as percentage of change over WT. Data from at least three animals per genotype ± SD. $^{*}P < 0.01$.

basal PGC1α expression (Fig. 6C). However, the increase in PGC1α expression previously noted in AKO Oct6^{+} neurons was abolished following the deletion of one allele of LKB1 (Fig. 6C).

To further substantiate PGC1α activation, we quantified the expression of SOD1, a cytosolic PGC1α target gene (31). A cytosolic target was chosen because levels of mitochondrial proteins might not reflect their transcription, due to degradation following mitochondrial dysfunction. Consistent with PGC1α activation, SOD1 levels were increased in AKO mice, and this was abrogated by the deletion of one allele of LKB1 (Fig. 6D). Altogether, these results indicate a role for LKB1 in the activation of PGC1α triggered by mitochondrial dysfunction in the absence of AIF.

Given the importance of glycolysis for ATP production in the absence of functional mitochondria, we next addressed changes in glucose metabolism, following AIF deletion. GLUT3, a glucose transporter expressed in the CNS specifically in neurons, was previously shown to be upregulated following energy stress (32). GLUT3 levels were indeed increased in AKO cortical neurons (Fig. 6F), similar to the increase observed for the glycolitic enzyme HKII (Fig. 5A and C). Strikingly, although the deletion of one allele of LKB1 did not significantly alter the basal expression of these proteins, it abrogated the increase caused by AIF deletion (Fig. 6E and F). This suggests that LKB1 plays an important role in the regulation of glycolysis, following mitochondrial dysfunction in cortical neurons.

Finally, given that cell size is usually controlled by mTOR, a master regulator of protein translation that is inhibited in AKO animals (Fig. 5D), we addressed the contribution of LKB1 in the regulation of cell size. Loss of one allele of LKB1 prevented the reduction in cell size caused by AIF deletion in layer II/III neurons (Fig. 6G), consistent with a role for LKB1. However, LKB1 deletion did not prevent the decrease in cell volume observed in layer V neurons (Fig. 6H). Given that our results suggest an important role for LKB1 in the metabolic adaptation to mitochondrial dysfunction and that layer V and VI neurons are more sensitive to energy stress, the inability of LKB1 deletion to rescue layer V neurons' cell body volume could result from the induction of cell death in these neurons. Therefore, we determined the effect of the loss of one allele of LKB1, and the abrogation of the compensatory mechanisms it regulates, on the survival of cortical neurons.

LKB1 regulates cortical neuronal survival, following mitochondrial dysfunction

Although AKO mice had the same number of cortical neurons than their WT littermates, loss of one allele of LKB1 in conjunction with AIF deletion (AKOL) caused a 10% reduction in the number of cortical neurons (Fig. 7A), suggesting that deletion of one allele of LKB1 sensitizes neurons to cell death following deletion of AIF. To specifically address the apoptotic cell loss, we analyzed caspase-3 activation in the cortex of AIF KO mice that were either WT or heterozygous for LKB1. Surprisingly, given the absence of neuronal loss in the AKO, some active caspase-3(AC3)-positive cells were observed in AKO layer V neurons starting at 90 days (Fig. 7B). However, as no significant changes in AC3 were observed before 90 days, this time point represents the onset of neuronal loss in AKO neurons. This interpretation is supported by the cell death data in the AKOL animals. Although deletion of one allele of LKB1 did not cause an increase in AC3-positive cells in the presence of AIF, apoptotic cell death occurred significantly earlier (60 days) in AKOL and increased at a greater rate than their AKO littermates (Fig. 7B). This is consistent with the observed neuronal loss in AKOL brains (Fig. 7A). As with AKO animals, most AC3-positive cells in the double mutant were also positive for the layer V marker Oct6 (Fig. 7C), further indicating that the defects are neuron specific. The data are also in agreement with the greater sensitivity of layer V neurons to cell death under energy stress (23,24) and the decreased cell volume of AKOL layer V neurons when compared with layer II/III neurons (Fig. 6G). Indeed, deletion of one allele of LKB1 in AKO animals was associated with a significant decrease in the number of layer V (Oct6^{+}) neurons when compared with AKO, for which we did not observe a significant loss at 90 days (Fig. 7D). Altogether, these results indicate that the activation of LKB1-regulated pathways is required for survival of AIF null neurons. Therefore, our results suggest that LKB1 plays an important role in neuronal adaptation to mitochondrial dysfunction and could, thus, be a key protein in the regulation of neuronal survival in the context of neurodegenerative diseases.

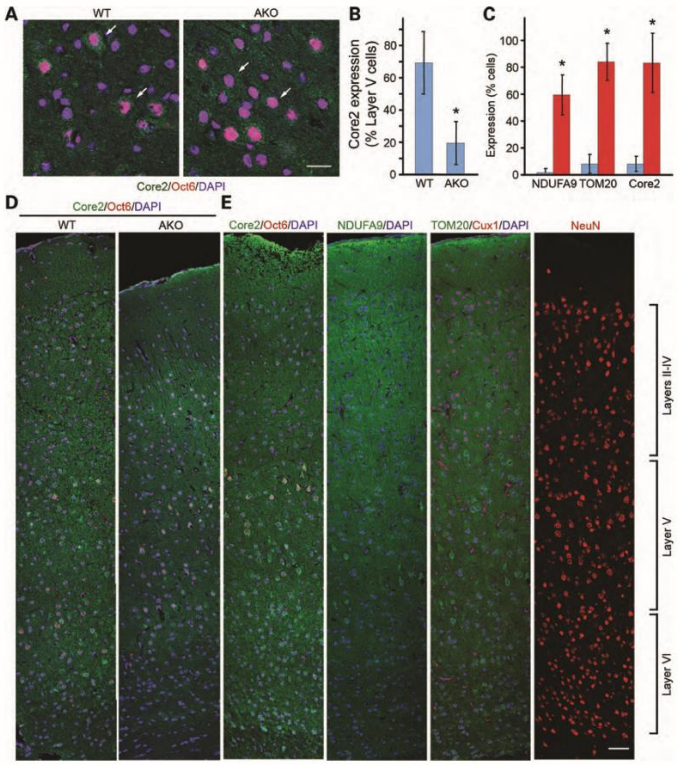

Figure 4. Differential expression of mitochondrial proteins in cortical layers. Brain sections from WT and AKO were stained for an antibody against the complex III subunit Core2 (green) and the layer V marker Oct6 (red), and confocal images were taken using a 63× (**A**) or 40× (**D**) objective. The arrows in (A) denote Oct6$^-$ cells. Several images were used to create the composite images shown in (D). Core2 expression from (A) was quantified in (**B**). Alternatively (**E**), sections from adult WT mice (105 days old) were stained with the indicated antibodies and analyzed as in (D). Data were quantified in (**C**). Representative images are shown. Scale bars 20 μm (D) and 50 μm (E and **F**).

DISCUSSION

Loss of mitochondrial function is a major characteristic of many neurodegenerative diseases. For example, while mutations in mitochondrial proteins such as ETC components or proteins involved in mitochondrial dynamics often cause neurodegeneration, sporadic cases of AD and PD are also linked to altered mitochondrial function (1–3). Similarly, human mutations in the mitochondrial protein AIF cause a severe mitochondrial encephalomyopathy (10). We have now used CamKIIα Cre to delete AIF and cause mitochondrial dysfunction in postmitotic neurons, thereby creating a novel model of neurodegeneration. However, as with many models of mitochondrial loss of function in neurons (6–9), neuronal loss following AIF deletion was progressive and limited to a specific neuronal population (striatum).

This neuronal survival is the consequence of the activity of energy metabolism kinase LKB1. Specifically, we demonstrated here that LKB1 plays a critical role in the regulation of neuronal survival, following the loss of mitochondrial function by activating several compensatory mechanisms that promote adaptation to energy stress. Thus, AIF deletion triggered the LKB1-dependent upregulation of mitochondrial biogenesis and glycolysis, compensatory mechanisms that were abrogated by the deletion of one allele of LKB1. By preventing the activation of these compensatory mechanisms, loss of LKB1 caused the death of these neurons, highlighting the critical role of this protein in metabolic stress adaptation and neuronal survival.

Previous work has indicated that LKB1 is a master regulator of energy metabolism under energy stress conditions (11,12). Indeed, a role for LKB1 in maintaining muscle metabolic

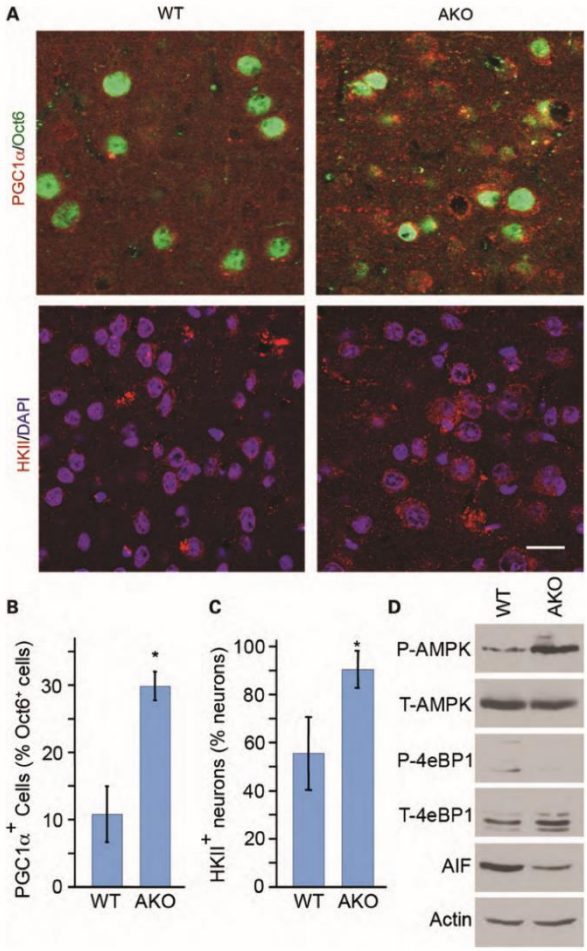

Figure 5. AIF deletion in cortical neurons activates compensatory metabolic pathways. (**A**) PGC1α and HKII are upregulated in AKO layer V neurons. Sections from 90 days old animals were stained for PGC1α (red), the layer V marker Oct6 (green) and the nuclear stain DAPI (blue). Alternatively, sections were stained for HKII (red) and DAPI (blue). Sections were imaged with a 63× objective using a confocal microscope. Scale bar 10 μm. Representative images are shown. Data were quantified in (**B**) for PGC1α and (**C**) for HKII from at least three animals per genotype ± SD. $^{*}P < 0.05$. (**D**) Expression levels of phospho-AMPK and phospho-4eBP1 in the cortices of 90 days old WT and AKO animals.

function during exercise has been previously suggested (13,14). However, as the regulation of ATP production differs greatly in neurons and muscle (15,16), the role of LKB1 in the adult brain remains unknown. Indeed, the main function of LKB1 that has been described in neurons is during development, through the regulation of axon formation (29,30). Nevertheless, in contrast to the dramatic *in vivo* loss of axons when LKB1 is deleted in neuronal progenitors (29,30), we did not observe obvious axonal defects (Fig. 6B). This suggests that LKB1 controls distinct cellular functions in precursors and differentiated cells, with a greater role of metabolic regulation of survival in postmitotic neurons. This would be consistent with the more important role of autophagy previously observed in postmitotic neurons, when compared with neural precursors (33).

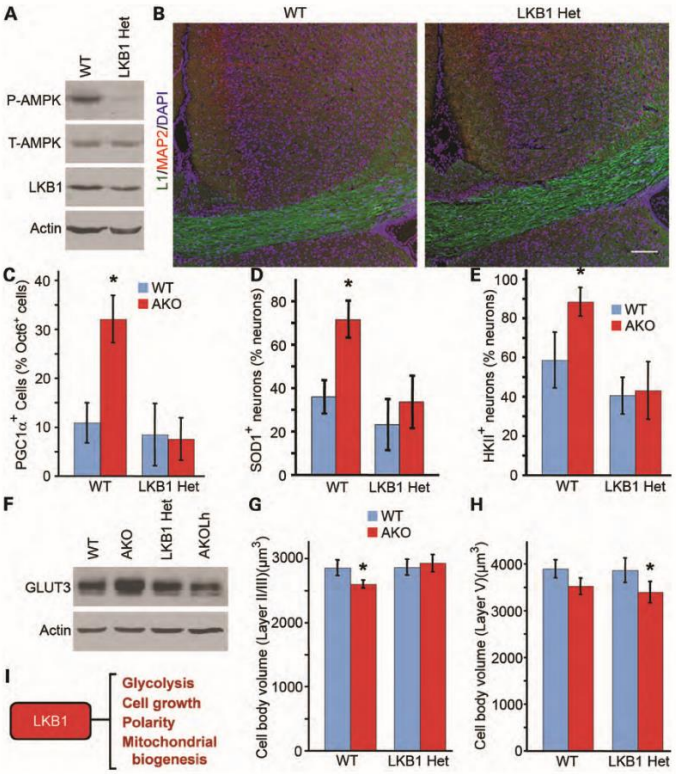

Figure 6. The compensatory mechanisms activated in AKO cortical neurons are LKB1 dependent. (**A**) Expression levels of phospho-AMPK in the cortices of 10 days old WT and LKB1 heterozygote animals. (**B**) Axonal staining in 10 days old LKB1 heterozygote animals. Sections were stained for the axonal marker L1 (green) and the dendritic marker MAP2 (red), along with the nuclear stain DAPI (blue). Confocal images were taken using a 63× objective. Scale bar 100 μm. Representative images are shown. (**C**) Quantification of PGC1α in layer V neurons in 90 days old animals of the indicated genotypes. Data from at least three animals per genotype are expressed as percentage of $Oct6^+$ neurons that are also positive for nuclear PGC1α + SD. $^*P < 0.005$. (**D**) Quantification of SOD1 in layer V neurons in 90 days old animals of the indicated genotypes. Data from at least three animals per genotype are expressed as percentage of neurons that are positive for SOD1 + SD. $^*P < 0.01$. (**E**) The number of HKII-expressing neurons was quantified in 63× images from layer V of 90 days old animals with the indicated genotypes. Data are expressed as percentage of $NeuN^+$ cells that are also positive for HKII in at least three animals per genotype ± SD. $^*P < 0.05$. (**F**) Expression levels of the neuronal glucose transporter GLUT3 in the cortices of 90 days old animals with the indicated pheonotype. (**G** and **H**) Quantification of neuronal cell body volume in layer II/III (G) and layer V (H) neurons. Cell body volume was estimated from stacks of NeuN-stained neurons from 90 days old animals taken using a confocal microscope. Data are expressed as the average neuronal cell body volume in three animals per genotype + SD. $^*P < 0.05$. (**I**) Schematic representation of different pathways regulated in a LKB1-dependent manner.

AIF deletion leads to loss of ETC components and decreased ATP production (17–19). It is, therefore, noteworthy that the compensatory mechanisms activated in an LKB1-dependent manner following AIF deletion play key roles in promoting ATP production. For example, GLUT3 and HKII both promote increased glycolysis, through glucose uptake and activation of a rate-limiting step of glycolysis, respectively. In addition, it has previously been reported that the activation of PGC1α can partially alleviate the mitochondrial dysfunction caused by the loss of ETC components (34). Together, these mechanisms likely promote the survival of AKO neurons by maintaining ATP production, despite the loss of mitochondrial function characterizing these cells. Interestingly, mitochondrial HKII has recently been shown to regulate BAX recruitment to mitochondria, thereby inhibiting cytochrome c release and apoptosis (26). It is, therefore, possible that, in addition to regulating ATP production, these pathways promote cell survival by regulating more directly the apoptotic machinery.

Given the importance of mitochondrial dysfunction in neurodegenerative diseases, the role of LKB1 in neuronal

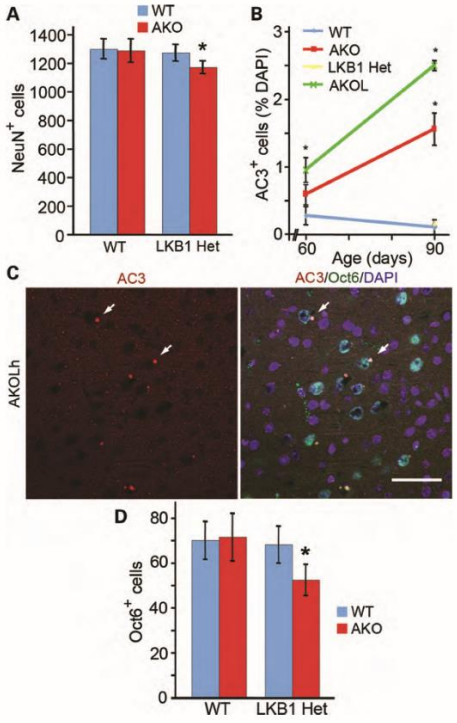

Figure 7. Increased cell death in AKO mice lacking one allele of LKB1. (**A**) Decreased number of cortical neurons in AKO animals lacking one allele of LKB1 (AKOL). The number of NeuN-positive cells was counted in 10× composite images of the cortex encompassing all six neuronal layers. Data are expressed as the total number of $NeuN^+$ cells per image in at least three animals per genotype ± SD. $^*P < 0.05$. (**B**) Increased AC3 staining in AKOL. Data are expressed as the percentage of total cells (DAPI positive) that are caspase-3 positive in at least three animals per genotype ± SD. $^*P < 0.005$. (**C**) AC3-positive neurons are found specifically in layer V. Sections from AKOL animals were stained for AC3, the layer V marker Oct6 and imaged using a 40× objective on a confocal microscope. Scale bar 50 μm. A representative image is shown. Arrows denote examples of AC3-positive layer V cells. (**D**) Decreased number of $Oct6^+$ layer V neurons in AKO animals lacking one allele of LKB1. Data were analyzed as in (B). $^*P < 0.05$.

adaptation to mitochondrial dysfunction could be highly relevant to these diseases. It is, therefore, noteworthy that several lines of evidence point to a causal relationship between mitochondrial dysfunction and other important features of neurodegenerative diseases such as increased reactive oxygen species (ROS) and accumulation of misfolded proteins (2,3). Although this relationship is complex and not yet fully understood, it raises the possibility that the LKB1 pathway also promotes neuronal survival, following accumulation of ROS or misfolded proteins, a possibility that clearly warrants further investigation.

MATERIALS AND METHODS

Animals

All experiments were approved by the University of Ottawa's Animal Care Ethics Committee adhering to the Guidelines of the Canadian Council on Animal Care. To generate forebrain-specific AIF KO mice, the previously described floxed AIF mice on a FVBN background (18) were crossed with CamKIIα-Cre mice (C57Bl/6) (21). AIF mice were also crossed with LKB1 conditional mice [from Dr Ronald DePinho (28)]. To minimize phenotypic variations that could result from the mixed background, the mice were kept on this FVBN/C57Bl/6 background for at least six generations before analyzing the mice, and littermates were used as controls for all experiments. Animals were genotyped according to standard protocols with previously published primers for AIF, LKB1 and Cre.

Tissue processing and immunohistochemistry

Mice were euthanized with a lethal injection of sodium pentobarbitol. For immunohistochemistry, mice were perfused with 1× PBS followed by fresh cold 4% paraformaldehyde (PFA). Brains were then removed, postfixed overnight in 4% PFA, cryoprotected in 20% sucrose in 1× PBS and frozen. Sections were collected as 14 μm coronal cryosections on Superfrost Plus® slides (Fisher Scientific). For western blot analysis, brains were removed, cortices dissected and flash frozen in liquid nitrogen.

Brain sections were analyzed by immunohistochemistry using AlexaFluor and Cy3 secondary antibodies (Jackson ImmunoResearch Laboratories, Inc.). Images were taken using a Zeiss 510 meta confocal microscope. Where noted, composite images were created by juxtaposing multiple higher resolution images in Adobe Photoshop. All quantification was done blind on at least three sections per brain. Layer V neurons were identified as $Oct6^+$ neurons, whereas the most superficial neurons were considered layer II/III. To measure the neuronal cell body volume, sections were aligned using the anterior commissure and stained with an antibody against the neuronal marker NeuN, which stains both the nuclei and cytosol of neurons. Z stacks were then taken using a 63× objective on a Zeiss 510 meta confocal microscope, and the surface area was calculated for each neuron in every z section using Image J. Because the sections were thin (14 μm), the volume was estimated by measuring the four bigger area of each cell multiplied by the z stack thickness. To quantify in an unbiased way the expression of proteins basally expressed in neurons, but for which the expression was altered in AKO neurons, the intensity of the immunofluorescent signal in the cell body was compared with that of an area outside cell bodies. A neuron with a 2-fold difference was considered positive.

Antibodies and immunoblots

The following antibodies were used: mouse anti-LDH_H and mouse anti-actin (Sigma-Aldrich); goat anti HKII, goat anti-Oct6, rabbit anti-MAP2, mouse anti-LKB1, rabbit anti-GLUT3, rabbit anti-PGC1α, goat anti-AIF, rabbit anti-SOD1 and rabbit anti-TOM20 (Santa Cruz Biotechnologies); mouse

anti-Core2, mouse anti-NDUFA9, mouse anti-SDHA (complex II p70) and mouse anti-COX IV (Invitrogen); rabbit anti-phospho-AMPK, rabbit anti-AMPK, rabbit anti-phospho-4eBP1, rabbit anti-4eBP1 and rabbit anti-active caspase-3 (Cell Signaling Technologies); mouse anti-NeuN (Chemicon); rabbit anti-NeuN (EnCor Biotechnologies Inc.); rat anti-L1 (Millipore); mouse anti-ATP5A (Mitosciences); and mouse anti-mtHSP70 (ABR Bioreagents).

Tissue was resuspended in 2% SDS, 62.5 mM Tris pH 6.8, 10% glycerol and boiled for 10 min. Alternatively, for phospho antibodies, tissue was lyzed in 10 mM Tris–HCl, pH 7.9, 150 mM NaCl, 1 mM EDTA, 1% Triton X-100 supplemented with protease inhibitors mixture (Sigma-Aldrich) and phosphatase inhibitors. For immunoblot analysis, proteins were subjected to SDS PAGE, transferred to nitrocellulose membranes and blotted with specific antibodies. Blots were incubated with HRP-conjugated secondary antibodies and visualized by enhanced chemiluminescence (Amersham Biosciences). Western blot quantification was performed using the Image J software and normalizing to actin levels.

AUTHORS' CONTRIBUTIONS

M.G., A.P.N., M.K., D.A.P., D.S.P. and R.S.S. designed research; M.G. and A.P.N performed research; M.G. and R.S.S. analyzed data and wrote the paper; and R.A.S. contributed critical reagents.

ACKNOWLEDGEMENTS

We thank Linda Jiu for tissue preparation. Microscopy equipment was funded through the Centre for Stroke Recovery.

Conflict of Interest statement. None declared.

FUNDING

This work was supported by grants from the Canadian Institutes of Health Research (CIHR) and Heart and Stroke Foundation of Canada to R.S.S. R.A.S. holds the Canada Research Chair in Apoptotic Signalling. M.G. holds a Parkinson's Society of Canada Research Fellowship. M.K. holds a Focus on Stroke Fellowship from the Heart and Stroke Society of Canada. D.A.P. holds a Shelby Hayter Pass, the Baton Graduate Fellowship from the Parkinson's Research Consortium and an Ontario Graduate Scholarship.

REFERENCES

1. Nunnari, J. and Suomalainen, A. (2012) Mitochondria: in sickness and in health. *Cell*, **148**, 1145–1159.
2. Patten, D.A., Germain, M., Kelly, M.A. and Slack, R.S. (2010) Reactive oxygen species: stuck in the middle of neurodegeneration. *J. Alzheimers Dis.*, **20** (Suppl. 2), S357–S367.
3. Moran, M., Moreno-Lastres, D., Marin-Buera, L., Arenas, J., Martin, M.A. and Ugalde, C. (2012) Mitochondrial respiratory chain dysfunction: implications in neurodegeneration. *Free Radic. Biol. Med.*, **53**, 595–609.
4. Dubinsky, J.M. (2009) Heterogeneity of nervous system mitochondria: location, location, location. *Exp. Neurol.*, **218**, 293–307.
5. Fukui, H. and Moraes, C.T. (2008) The mitochondrial impairment, oxidative stress and neurodegeneration connection: reality or just an attractive hypothesis? *Trends Neurosci.*, **31**, 251–256.
6. Fukui, H., Diaz, F., Garcia, S. and Moraes, C.T. (2007) Cytochrome c oxidase deficiency in neurons decreases both oxidative stress and amyloid formation in a mouse model of Alzheimer's disease. *Proc. Natl. Acad. Sci. USA*, **104**, 14163–14168.
7. Quintana, A., Kruse, S.E., Kapur, R.P., Sanz, E. and Palmiter, R.D. (2010) Complex I deficiency due to loss of Ndufs4 in the brain results in progressive encephalopathy resembling Leigh syndrome. *Proc. Natl. Acad. Sci. USA*, **107**, 10996–11001.
8. Ekstrand, M.I., Terzioglu, M., Galter, D., Zhu, S., Hofstetter, C., Lindqvist, E., Thams, S., Bergstrand, A., Hansson, F.S., Trifunovic, A. *et al.* (2007) Progressive parkinsonism in mice with respiratory-chain-deficient dopamine neurons. *Proc. Natl. Acad. Sci. USA*, **104**, 1325–1330.
9. Klein, J.A., Longo-Guess, C.M., Rossmann, M.P., Seburn, K.L., Hurd, R.E., Frankel, W.N., Bronson, R.T. and Ackerman, S.L. (2002) The harlequin mouse mutation downregulates apoptosis-inducing factor. *Nature*, **419**, 367–374.
10. Ghezzi, D., Sevrioukova, I., Invernizzi, F., Lamperti, C., Mora, M., D'Adamo, P., Novara, F., Zuffardi, O., Uziel, G. and Zeviani, M. (2010) Severe X-linked mitochondrial encephalomyopathy associated with a mutation in apoptosis-inducing factor. *Am. J. Hum. Genet.*, **86**, 639–649.
11. Mihaylova, M.M. and Shaw, R.J. (2011) The AMPK signalling pathway coordinates cell growth, autophagy and metabolism. *Nat. Cell Biol.*, **13**, 1016–1023.
12. Shackelford, D.B. and Shaw, R.J. (2009) The LKB1-AMPK pathway: metabolism and growth control in tumour suppression. *Nat. Rev. Cancer*, **9**, 563–575.
13. Thomson, D.M., Hancock, C.R., Evanson, B.G., Kenney, S.G., Malan, B.B., Mongillo, A.D., Brown, J.D., Hepworth, S., Fillmore, N., Parcell, A.C. *et al.* (2010) Skeletal muscle dysfunction in muscle-specific LKB1 knockout mice. *J. Appl. Physiol.*, **108**, 1775–1785.
14. Thomson, D.M., Porter, B.B., Tall, J.H., Kim, H.J., Barrow, J.R. and Winder, W.W. (2007) Skeletal muscle and heart LKB1 deficiency causes decreased voluntary running and reduced muscle mitochondrial marker enzyme expression in mice. *Am. J. Physiol. Endocrinol. Metab.*, **292**, E196–E202.
15. Belanger, M., Allaman, I. and Magistretti, P.J. (2011) Brain energy metabolism: focus on astrocyte-neuron metabolic cooperation. *Cell Metab.*, **14**, 724–738.
16. Draoui, N. and Feron, O. (2011) Lactate shuttles at a glance: from physiological paradigms to anti-cancer treatments. *Dis. Model Mech.*, **4**, 727–732.
17. Cheung, E.C., Joza, N., Steenaart, N.A., McClellan, K.A., Neuspiel, M., McNamara, S., MacLaurin, J.G., Rippstein, P., Park, D.S., Shore, G.C. *et al.* (2006) Dissociating the dual roles of apoptosis-inducing factor in maintaining mitochondrial structure and apoptosis. *EMBO J.*, **25**, 4061–4073.
18. Joza, N., Oudit, G.Y., Brown, D., Benit, P., Kassiri, Z., Vahsen, N., Benoit, L., Patel, M.M., Nowikovsky, K., Vassault, A. *et al.* (2005) Muscle-specific loss of apoptosis-inducing factor leads to mitochondrial dysfunction, skeletal muscle atrophy, and dilated cardiomyopathy. *Mol. Cell. Biol.*, **25**, 10261–10272.
19. Pospisilik, J.A., Knauf, C., Joza, N., Benit, P., Orthofer, M., Cani, P.D., Ebersberger, I., Nakashima, T., Sarao, R., Neely, G. *et al.* (2007) Targeted deletion of AIF decreases mitochondrial oxidative phosphorylation and protects from obesity and diabetes. *Cell*, **131**, 476–491.
20. Vahsen, N., Cande, C., Briere, J.J., Benit, P., Joza, N., Larochette, N., Mastroberardino, P.G., Pequignot, M.O., Casares, N., Lazar, V. *et al.* (2004) AIF deficiency compromises oxidative phosphorylation. *EMBO J.*, **23**, 4679–4689.
21. Casanova, E., Fehsenfeld, S., Mantamadiotis, T., Lemberger, T., Greiner, E., Stewart, A.F. and Schutz, G. (2001) A CamKIIalpha iCre BAC allows brain-specific gene inactivation. *Genesis*, **31**, 37–42.
22. Pickrell, A.M., Fukui, H., Wang, X., Pinto, M. and Moraes, C.T. (2011) The striatum is highly susceptible to mitochondrial oxidative phosphorylation dysfunctions. *J. Neurosci.*, **31**, 9895–9904.
23. Ma, D., Li, S., Lucas, E.K., Cowell, R.M. and Lin, J.D. (2010) Neuronal inactivation of peroxisome proliferator-activated receptor gamma coactivator 1alpha (PGC-1alpha) protects mice from diet-induced obesity and leads to degenerative lesions. *J. Biol. Chem.*, **285**, 39087–39095.

24. Lin, J., Wu, P.H., Tarr, P.T., Lindenberg, K.S., St-Pierre, J., Zhang, C.Y., Mootha, V.K., Jager, S., Vianna, C.R., Reznick, R.M. *et al.* (2004) Defects in adaptive energy metabolism with CNS-linked hyperactivity in PGC-1alpha null mice. *Cell*, **119**, 121–135.
25. Jones, A.W., Yao, Z., Vicencio, J.M., Karkucinska-Wieckowska, A. and Szabadkai, G. (2012) PGC-1 family coactivators and cell fate: roles in cancer, neurodegeneration, cardiovascular disease and retrograde mitochondria-nucleus signalling. *Mitochondrion*, **12**, 86–99.
26. Gimenez-Cassina, A., Lim, F., Cerrato, T., Palomo, G.M. and Diaz-Nido, J. (2009) Mitochondrial hexokinase II promotes neuronal survival and acts downstream of glycogen synthase kinase-3. *J. Biol. Chem.*, **284**, 3001–3011.
27. Krock, B., Skuli, N. and Simon, M.C. (2011) The tumor suppressor LKB1 emerges as a critical factor in hematopoietic stem cell biology. *Cell Metab.*, **13**, 8–10.
28. Bardeesy, N., Sinha, M., Hezel, A.F., Signoretti, S., Hathaway, N.A., Sharpless, N.E., Loda, M., Carrasco, D.R. and DePinho, R.A. (2002) Loss of the Lkb1 tumour suppressor provokes intestinal polyposis but resistance to transformation. *Nature*, **419**, 162–167.
29. Barnes, A.P., Lilley, B.N., Pan, Y.A., Plummer, L.J., Powell, A.W., Raines, A.N., Sanes, J.R. and Polleux, F. (2007) LKB1 and SAD kinases define a pathway required for the polarization of cortical neurons. *Cell*, **129**, 549–563.
30. Shelly, M., Cancedda, L., Heilshorn, S., Sumbre, G. and Poo, M.M. (2007) LKB1/STRAD promotes axon initiation during neuronal polarization. *Cell*, **129**, 565–577.
31. St Pierre, J., Drori, S., Uldry, M., Silvaggi, J.M., Rhee, J., Jager, S., Handschin, C., Zheng, K., Lin, J., Yang, W. *et al.* (2006) Suppression of reactive oxygen species and neurodegeneration by the PGC-1 transcriptional coactivators. *Cell*, **127**, 397–408.
32. Weisova, P., Concannon, C.G., Devocelle, M., Prehn, J.H. and Ward, M.W. (2009) Regulation of glucose transporter 3 surface expression by the AMP-activated protein kinase mediates tolerance to glutamate excitation in neurons. *J. Neurosci.*, **29**, 2997–3008.
33. Germain, M., Nguyen, A.P., Le Grand, J.N., Arbour, N., Vanderluit, J.L., Park, D.S., Opferman, J.T. and Slack, R.S. (2011) MCL-1 is a stress sensor that regulates autophagy in a developmentally regulated manner. *EMBO J.*, **30**, 395–407.
34. Srivastava, S., Diaz, F., Iommarini, L., Aure, K., Lombes, A. and Moraes, C.T. (2009) PGC-1alpha/beta induced expression partially compensates for respiratory chain defects in cells from patients with mitochondrial disorders. *Hum. Mol. Genet.*, **18**, 1805–1812.

Appendix E:

nature COMMUNICATIONS

ARTICLE

Received 28 Dec 2013 | Accepted 5 Mar 2014 | Published 1 Apr 2014

DOI: 10.1038/ncomms4550 OPEN

Acidosis overrides oxygen deprivation to maintain mitochondrial function and cell survival

Mireille Khacho[1], Michelle Tarabay[1], David Patten[1,*], Pamela Khacho[1,*], Jason G. MacLaurin[1], Jennifer Guadagno[2], Richard Bergeron[1,3], Sean P. Cregan[2], Mary-Ellen Harper[4], David S. Park[1] & Ruth S. Slack[1]

Sustained cellular function and viability of high-energy demanding post-mitotic cells rely on the continuous supply of ATP. The utilization of mitochondrial oxidative phosphorylation for efficient ATP generation is a function of oxygen levels. As such, oxygen deprivation, in physiological or pathological settings, has profound effects on cell metabolism and survival. Here we show that mild extracellular acidosis, a physiological consequence of anaerobic metabolism, can reprogramme the mitochondrial metabolic pathway to preserve efficient ATP production regardless of oxygen levels. Acidosis initiates a rapid and reversible homeostatic programme that restructures mitochondria, by regulating mitochondrial dynamics and cristae architecture, to reconfigure mitochondrial efficiency, maintain mitochondrial function and cell survival. Preventing mitochondrial remodelling results in mitochondrial dysfunction, fragmentation and cell death. Our findings challenge the notion that oxygen availability is a key limiting factor in oxidative metabolism and brings forth the concept that mitochondrial morphology can dictate the bioenergetic status of post-mitotic cells.

[1] Department of Cellular and Molecular Medicine, Faculty of Medicine, University of Ottawa, Ottawa, Ontario K1H 8M5, Canada. [2] Department of Physiology and Pharmacology, J. Allyn Taylor Centre for Cell Biology, Robarts Research Institute, The University of Western Ontario, London, Ontario N6A 5B7, Canada. [3] Ottawa Hospital Research Institute, Ottawa, Ontario K1H 8M5, Canada. [4] Department of Biochemistry, Microbiology and Immunology, University of Ottawa, Ottawa, Ontario K1H 8M5, Canada. * These authors contributed equally to this work. Correspondence and requests for materials should be addressed to R.S.S. (email: rslack@uottawa.ca).

Long-term survival of post-mitotic cells, which have a limited regenerative capacity, is essential to ensure continued biological function of an organism. In recent years, it has become apparent that the decline of post-mitotic cells, during aging, neurodegenerative diseases and ischemic disorders, is generally associated with mitochondrial dysfunction[1,2]. Mitochondria are essential organelles for energy production, regulation of signalling cascades and cell death[3]. These organelles form a dynamic interconnecting network through continuous cycles of fission and fusion events[4]. The regulation of mitochondrial morphology is closely coupled to cell survival and metabolic adaptation during stress[5–7]. For example, aberrant mitochondrial fission has been observed in many disease and injury models and considered a key contributor to mitochondrial dysfunction and cell death[8–10]. In these settings, inhibition of mitochondrial fission or enhancing mitochondrial fusion restores cell viability[11–14]. These observations highlight the importance in the regulation of mitochondrial dynamics as a strategy to promote cellular survival.

A common characteristic of high-energy-demanding post-mitotic cells, such as neurons, muscle and cardiomyocytes, is their dependence on a continuous supply of energy for sustained cellular function and viability. For this reason, contemporary eukaryotic cells are highly dependent on oxygen and functional mitochondria for the efficient generation of ATP through oxidative phosphorylation[15,16]. In this context, it can be appreciated how limitations in oxygen availability, or hypoxia, have profound physiological effects. Low oxygen levels cause major changes in mitochondrial structure and dynamics, ultimately leading to defective mitochondrial function, reduced ATP supply and activation of cell death pathways[17–19]. Importantly, a defective mitochondrial function induced by hypoxic stress is observed in diverse complex disorders such as type-2 diabetes mellitus, Alzheimer's disease, cardiac and brain ischemia/reperfusion injury and tissue inflammation[17]. The fate of post-mitotic cells subjected to physiological or pathological settings of hypoxia is thus entirely reliant on their ability to respond and adapt to changing environments and stress conditions. Consequently, understanding oxygen sensing and response mechanisms in cells and tissues has been at the forefront of research for many years with the aim of exploiting adaptive strategies to promote cell survival.

An essential and often neglected aspect of hypoxia is the accumulation of lactic acid as the end product of glycolysis. Excess H^+ ions resulting from an increased glycolytic rate are pumped outside the cell, inevitably causing acidification of the extracellular milieu. Physiological levels of acidosis in regions subjected to limited oxygen availability, such as the ischemic penumbra following a stroke, can range within the pH values of 6.0–6.5 depending on the severity of the insult[20–22]. A long-standing debate in biology is the effect of acidosis on cell survival. Although extracellular acidosis is historically viewed as a mere toxic byproduct of fermentation that is detrimental to cells, it is now clinically recognized as a protective agent when present at mild levels (pH 6.5 and above)[21,23–35]. In this regard, although several reports have clearly demonstrated the protective nature of mild acidosis, the underlying molecular mechanisms are still poorly understood. Furthermore, the role of mitochondria, being central to cell survival and death, has surprisingly never been addressed in this perspective. Here we show the unexpected observation that mild acidosis triggers massive morphological reorganization of mitochondria in post-mitotic cells, triggered by a dual programme that both activates fusion and cristae remodelling while inhibiting mitochondrial fragmentation. Activation of this reversible homeostatic programme reconfigures mitochondrial bioenergetics to allow for the persistence of efficient ATP production through oxidative phosphorylation despite oxygen limitations. Our work reveals a novel and physiological mechanism that can control the metabolic status of cells and protect mitochondrial-reliant post-mitotic cells following a hypoxic insult, by reprogramming mitochondrial morphology and functional efficiency.

Results

Acidosis triggers mitochondrial elongation during hypoxia. As mitochondria are central in the cell death that is instigated during hypoxic stress, we investigated mitochondrial morphology in this setting. Cortical neurons were chosen for these experiments since they are a major population affected by hypoxic stress and thus represent a biologically relevant system for the study of adaptive mechanisms in post-mitotic cells. For our studies, we developed an *in vitro* model that mimics the physiological microenvironment found under hypoxic conditions, such as the penumbral region following an ischemic brain injury. This model recapitulates the low oxygen/glucose environment and takes into account that ischemic tissues or hypoxic cells normally acidify their extracellular milieu as a physiological consequence of anaerobic glycolysis. For this, a low glucose media was buffered in a manner to accommodate physiological acidification of the extracellular milieu when neurons are incubated at 1% O_2 (termed acidosis-permissive media (AP)). The control condition utilizes a low glucose media that maintains a stable neutral pH (pH 7.2) throughout experimentation (termed standard media (SD)). Mitochondria from cultured cortical neurons subjected to hypoxic conditions in a neutral pH environment had severely fragmented mitochondria as observed through immuno-fluorescence staining of the outer mitochondrial membrane protein Tom20 (Fig. 1a and quantified in Fig. 1b). Mitochondrial fragmentation was observed before signs of cell death or changes in neuronal morphology (Supplementary Fig. 1). Unexpectedly, neurons subjected to hypoxia but allowed to undergo physiological extracellular acidification (measured pH post experiment was 6.5) exhibited massive mitochondrial elongation compared with control (Fig. 1a and quantified in Fig. 1b). Elongated mitochondria were observed in the cell body of cortical neurons and spanned along the axons (Fig. 1c). Mitochondrial elongation was also observed in cultured cerebellar granular neurons (CGNs; Fig. 1d,e) and *in vivo* hippocampal slice preparations (Fig. 1f,g), as well as in differentiated C2C12 myotubes (Supplementary Fig. 2), suggesting that this is a general phenomenon. Interestingly, acidosis-mediated mitochondrial elongation was not observed in proliferative cells, such as primary and transformed mouse embryonic fibroblast cells (MEF), C2C12 myoblasts, Cos7, HeLa and several cancer cell lines, including MCF-7, A549 and P19, suggesting that this response is unique to post-mitotic cells (Supplementary Fig. 2).

The acidosis-dependent alteration in mitochondrial morphology is pH-specific and elongation of mitochondria was only observed at a pH threshold value between 6.65 and 6.45 (Fig. 2a,b and Supplementary Fig. 3), representing mildly acidic conditions as observed in physiological settings of hypoxic stress. In contrast, cells within a neutral (pH 7.2–6.8) or severely acidic (pH 6.0) extracellular environment during hypoxia exhibited significant mitochondrial fragmentation (Fig. 2a,b and Supplementary Fig. 3). Acidosis-mediated mitochondrial elongation is a rapid process whereby the onset of elongation occurred at about 3-h post-treatment (Fig. 2c,d and Supplementary Fig. 4). This opposed the hypoxia-mediated mitochondrial fragmentation that occurs in neutral conditions beginning 3 h following treatment (Fig. 2c and Supplementary Fig. 4). In addition, although acidosis generally occurs as a consequence of increased glycolysis

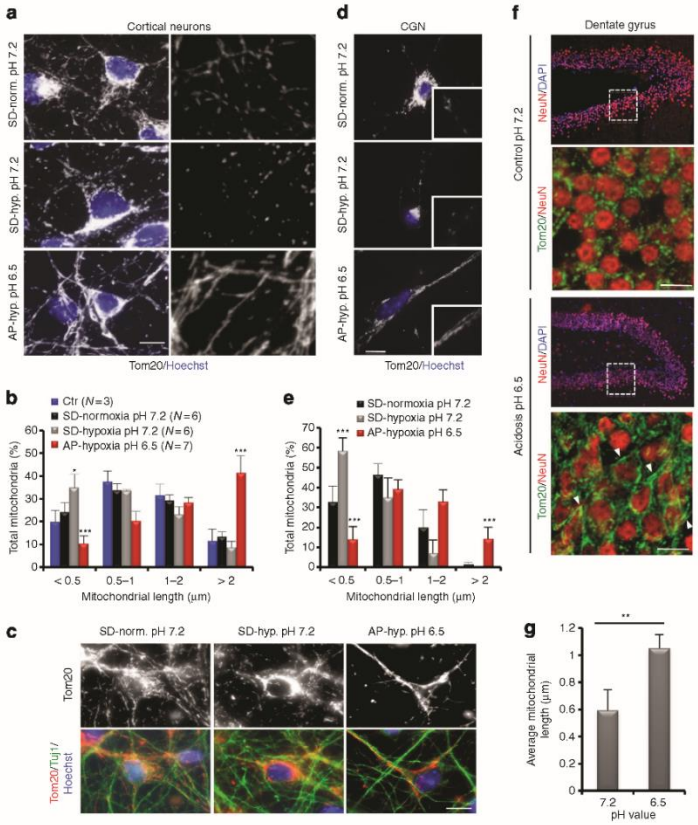

Figure 1 | Extracellular acidification restructures mitochondria in post-mitotic cells. (**a**) Representative confocal images of mitochondrial morphology in cultured cortical neurons following 18-h incubation at normoxic (Norm.) or hypoxic (Hyp.) conditions in SD or AP media. Mitochondria were visualized by Tom20 immunofluorescence. Panels on the right represent zoomed views of the mitochondria. (**b**) Mitochondrial length from (**a**) was quantified and binned into different length categories. Represented as mean and s.d. (*n* values indicated on graph). Ctr = control; represents neurons incubated in neurobasal media. (**c**) Representative images of mitochondrial morphology, revealed by Tom20 staining, in Tuj1+ cortical neurons at the indicated conditions. (**d** and **e**) Mitochondrial morphology in cultured CGN after 18-h incubation at the indicated conditions. Insets in (**d**) are zoomed views of mitochondria. (**e**) Mean and s.d. ($n = 3$) of mitochondrial length data in (**d**). (**f** and **g**) Mitochondrial morphology in *ex vivo* hippocampal slice preparations incubated in normoxia for 4 h at the indicated conditions. Neurons were immunostained with NeuN (neuronal-specific nuclear protein) and Tom20 (mitochondria). Panels showing Tom20/NeuN staining are zoomed views of the boxed area within the hippocampus. Arrowheads indicate elongated mitochondria. (**g**) Average mitochondrial length and s.d. were plotted for the indicated conditions. $^{*}P < 0.05$; $^{**}P < 0.01$; $^{***}P < 0.001$ (Student's *t*-test). For all images scale = 10 µm.

during limited oxygen availability, its effect on mitochondrial morphology was in fact independent of oxygen. Incubation of cortical neurons in media set to pH 6.5 in the presence of oxygen (normoxia) resulted in a significant increase in mitochondrial length compared with control (Fig. 2e). To further confirm the direct affect of acidosis on mitochondrial length, the contribution of low glucose levels in the experimental paradigm, which represents a more physiologically relevant setting, was assessed. The effect of acidosis on mitochondrial length was not a consequence of decreased glucose availability since mitochondrial elongation persisted in the presence of high glucose levels (Fig. 2f and Supplementary Fig. 5). Thus, mitochondrial elongation in these settings is directly mediated by acidosis and is not a consequence of an induced starvation response. This is supported by the observation that the limited glucose availability in these experiments was not sufficient to activate autophagy (Supplementary Fig. 6) such as that observed during complete glucose starvation, where there is a marked increase in LC3II, degradation of p62 and loss of outer membrane Tom20 due to mitophagy (Supplementary Fig. 6). These results demonstrate that acidosis alone is sufficient to promote mitochondrial elongation. Acidosis-driven elongation is also a reversible process. Mitochondria remain elongated regardless of oxygen levels, confirming that this process is oxygen-independent (Fig. 2g,h

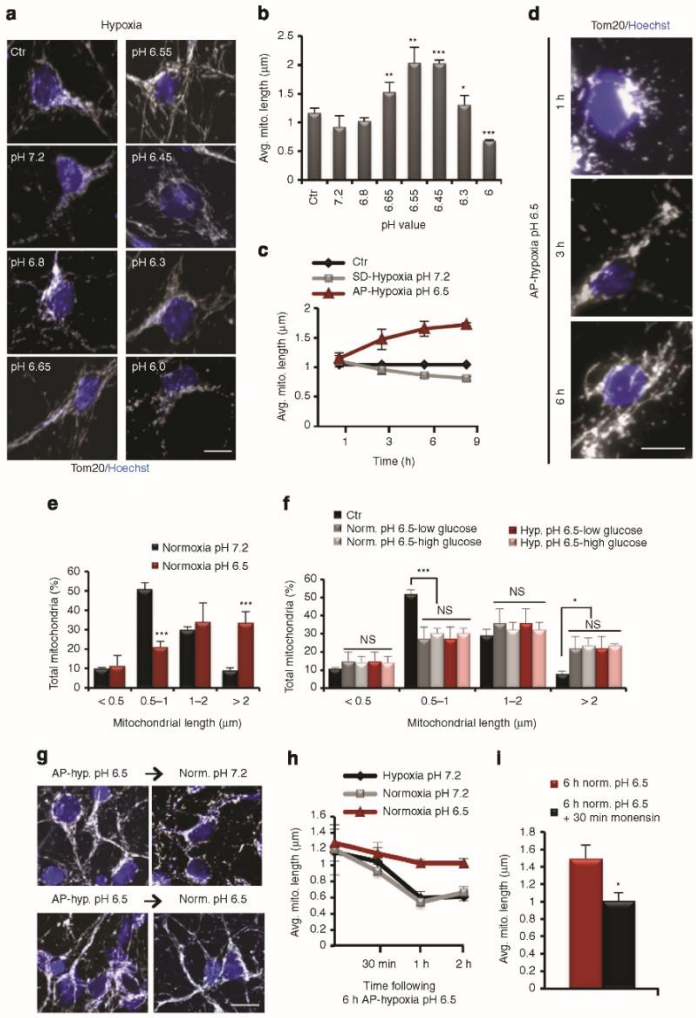

Figure 2 | Acidosis-mediated mitochondrial elongation is pH-specific, rapid, reversible and O_2- and glucose-independent. (**a**) Representative confocal images of mitochondrial morphology in cultured cortical neurons following incubation at fixed pH values in hypoxia. Ctr = control; represents neurons incubated in neurobasal media. (**b**) Average mitochondrial length and s.d. ($n = 3$) were plotted for the indicated pH values. (**c**) Average mitochondrial length and s.d. ($n = 3$) over time at indicated conditions. (**d**) Immunofluorescence of Tom20 (mitochondria) showing the change in mitochondrial length in cortical neurons by physiological acidosis at the indicated times. (**e**) Mean and s.d. ($n = 3$) of mitochondrial length distribution during normoxic conditions at indicated pH values for 6 h. (**f**) Mean and s.d. ($n = 3$) of mitochondrial length distribution during normoxic or hypoxic conditions in the presence of low (5.5 mM) or high (25 mM) glucose levels for 6 h. (**g** and **h**) Analysis of mitochondrial morphology after 6-h incubation in AP-Hypoxia pH 6.5 and following reoxygenation at the indicated pH values. (**h**) Graph of the change in average mitochondrial length (s.d., $n = 3$) at the indicated conditions following a 6-h incubation in AP-Hypoxia pH 6.5. (**i**) Average mitochondrial length and s.d. ($n = 3$) were plotted for the indicated conditions. ns = not significant, $^*P < 0.05$; $^{**}P < 0.01$; $^{***}P < 0.001$ (Student's *t*-test). For all images scale = 10 µm.

and Supplementary Fig. 7). However, mitochondria revert back to a fragmented phenotype following neutralization of the extracellular pH both under hypoxic or reoxygenation conditions (Fig. 2g,h and Supplementary Fig. 7). In fact, the level of fragmentation following reoxygenation in a neutral context was very rapid (within 30 min) and was quite severe (Fig. 2h

and Supplementary Fig. 7). In order to gain insight as to how extracellular acidosis can relay an intracellular signal to modify mitochondrial morphology, pH changes within the intracellular environment were examined. Analysis of intracellular pH changes using the ratiometric fluorescent indicator BCECF-AM (Supplementary Fig. 8a) showed that a decrease in extracellular pH as used in our studies (pH 6.5) was sufficient to cause a reduction in intracellular pH (Supplementary Fig. 8b) and is consistent with previous reports showing that intracellular pH can be modified by the extracellular milieu[36,37]. Furthermore, neutralization of the intracellular pH using the Na+/H+ exchanger Monensin (Supplementary Fig. 8c) rapidly reverses the mitochondrial elongation phenotype that was instigated by extracellular acidosis (Fig. 2i and Supplementary Fig. 8d,e). Together, these results demonstrate a pH-dependent regulation of mitochondrial morphology that is oxygen- and glucose-independent and is reversible.

Acidosis inhibits DRP1-mediated mitochondrial fission. Mitochondrial fragmentation is a prominent phenotype during hypoxic stress conditions as observed here (Figs 1a,b and 2c) and in previous studies[19,38,39]. However, physiological acidification appears to prevent hypoxia-induced mitochondrial fragmentation. An essential component of the mitochondrial fission machinery, the dynamin protein DRP1, is a cytosolic factor that is recruited to mitochondria upon activation[40]. As expected, localization analysis of endogenous DRP1 showed a pronounced increase in mitochondrial-specific DRP1 foci during hypoxia-neutral conditions that correlate with the observed increase in fragmentation (Fig. 3a,b). Interestingly, a decrease in the number of DRP1 foci per unit length of mitochondria was observed during acidosis (Fig. 3a,b). A decline in mitochondrial DRP1 during acidosis was not due to changes in total cellular protein expression of DRP1 (Fig. 3c) but was reminiscent of the decreased number of mitochondrial DRP1 foci observed in the presence of the selective inhibitor of DRP1-mediated mitochondrial fission, Mdivi-1(ref. 41; Fig. 3d). Analysis of DRP1 protein interactions revealed that in cultured cortical neurons DRP1 associates with Fis1 but not Mff, two previously identified DRP1-binding proteins (Supplementary Fig. 9a)[42]. Furthermore, immunoprecipitation of endogenous DRP1 at the onset of mitochondrial elongation by acidosis revealed a decreased level of interaction between DRP1 and Fis1, a mitochondrial DRP1-binding protein important for DRP1 recruitment and fission[42,43]. The decrease in DRP1–Fis1 interaction was similar to what is observed following treatment with forskolin, an inhibitor of fission through its activation of PKA-mediated phosphorylation and inhibition of DRP1 recruitment to mitochondria (Fig. 3e and Supplementary Fig. 9b,d). These data suggest that acidosis inhibits DRP1-mediated fission during hypoxia. Although PKA-dependent phosphorylation at Ser637 represents a major regulatory sight for DRP1 activation[44], we did not observe a change in the phosphorylation status of DRP1 at Ser637. Moreover, inhibition of the PKA pathway did not affect acidosis-mediated mitochondrial elongation nor did activation of this pathway affects mitochondrial morphology during hypoxia (Supplementary Fig. 9b,d). Furthermore, the phosphorylation status of DRP1 at Ser616, a common target of DRP1 regulation during oxidative stress[45], was not altered at the time point where mitochondrial elongation is observed (Supplementary Fig. 9c). Thus, mild acidosis prevents mitochondrial fragmentation under hypoxic conditions through the PKA and CDK1/PKCδ-independent regulation of DRP1 activation and recruitment to mitochondria.

Mitochondrial fusion by acidosis depends on the SIMH pathway. The degree and rate of elongation observed during acidosis suggested the possibility of a pH-dependent enhancement in mitochondrial fusion activity, in addition to suppression of the fission pathway. This was tested in live neurons, infected

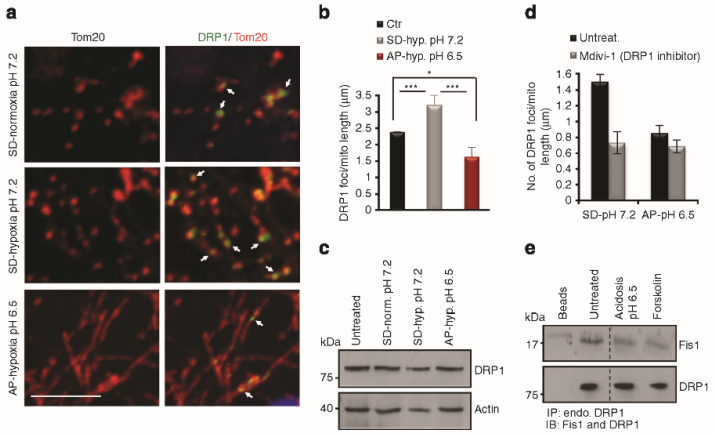

Figure 3 | Mild acidosis inhibits DRP1-mediated mitochondrial fission. (**a**) Colocalization of DRP1 foci at mitochondria by immunofluorescence of DRP1 and Tom20 in cortical neurons using confocal imaging. Arrows show DRP1 foci localized at mitochondria. Scale = 5 µm. (**b**) Quantification of the number of DRP1 foci colocalized to mitochondria and represented as mean and s.d. ($n=3$). (**c**) Western blot of the indicated proteins from whole cell lysates of cultured cortical neurons following 6-h incubation at the indicated conditions. (**d**) Quantification of the number of DRP1 foci colocalized to mitochondria following 6-h hypoxic incubation in SD or AP media in the presence or absence of the fission inhibitor Mdivi-1. (**e**) Western blot of indicated proteins following incubation for 3 h at the indicated conditions and immunoprecipitation of endogenous (endo.) DRP1 using anti-DRP1 antibody.

with a mitochondrial matrix targeted photo-activatable green-fluorescent protein (GFP) lentivirus (PA-Oct-GFP), following 3 h of incubation at pH 7.2 or 6.5 under normoxic conditions, representing the onset of elongation in the absence of hypoxia-induced fission. The rate of dilution and spread of the photo-converted GFP molecules are used as a measure of fusion activity. Time-lapse imaging of the activated mitochondrial GFP signal demonstrated an increase in mitochondrial fusion in neurons subjected to mild acidosis (Fig. 4a,b and Supplementary Fig. 10). Examination of mitochondrial mass further confirmed that mitochondrial elongation during acidosis is a result of enhanced fusion activity rather than increased mitochondrial biogenesis

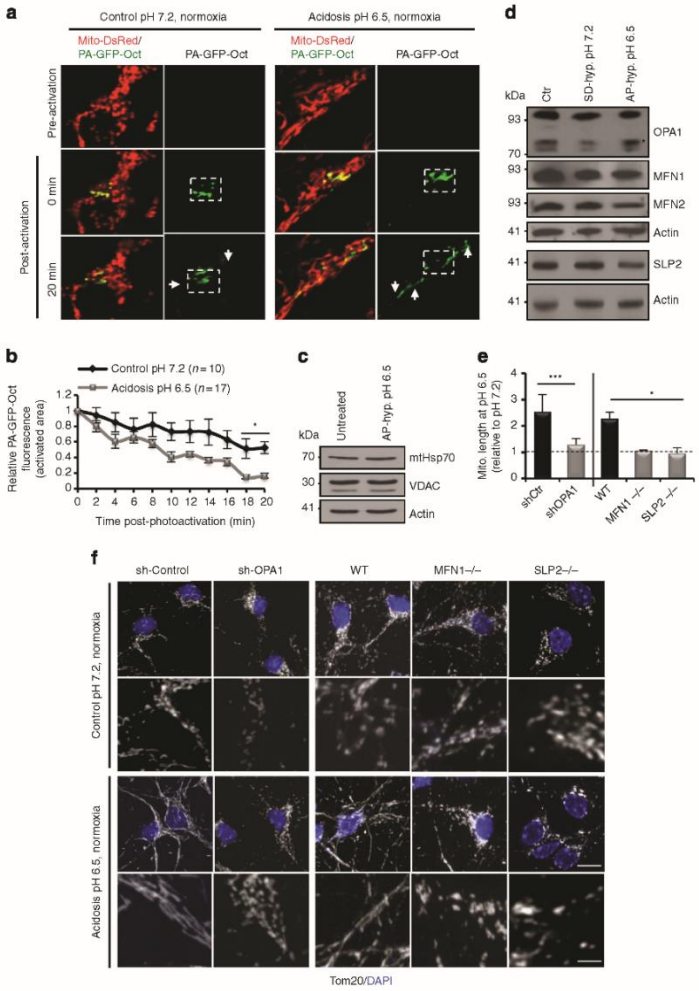

Figure 4 | Mild acidosis regulates mitochondrial dynamics. (**a**) Representative images of mitochondrial fusion over time (indicated in minutes) following activation of exogenously expressed PA-GFP-Oct. Boxes indicate photo-activated regions and arrows indicate spread of the GFP signal within mitochondria (revealed by exogenous expression of Mito-DsRed). (**b**) Quantification of mitochondrial fusion in cortical neurons as a loss of GFP fluorescence in the activated region. Data represent the mean and s.d. of $n=10$ (control) and $n=17$ (experimental) from three independent experiments. (**c** and **d**) Western blot of the indicated proteins from whole-cell lysates of cortical neurons incubated for 6 h at the indicated conditions. Asterisk indicates s-OPA1. (**e**) Mean and s.d. ($n=3$) of mitochondrial length during acidosis, of the indicated genotypes, relative to control conditions. (**f**) Representative images of mitochondrial morphology from cortical neurons of the indicated genotypes following 6-h incubation in MES-buffered media at the indicated conditions. Bottom panel of each condition is a zoom view of mitochondria. Scale = 10 μm. $^{*}P<0.05$; $^{***}P<0.001$ (Student's *t*-test).

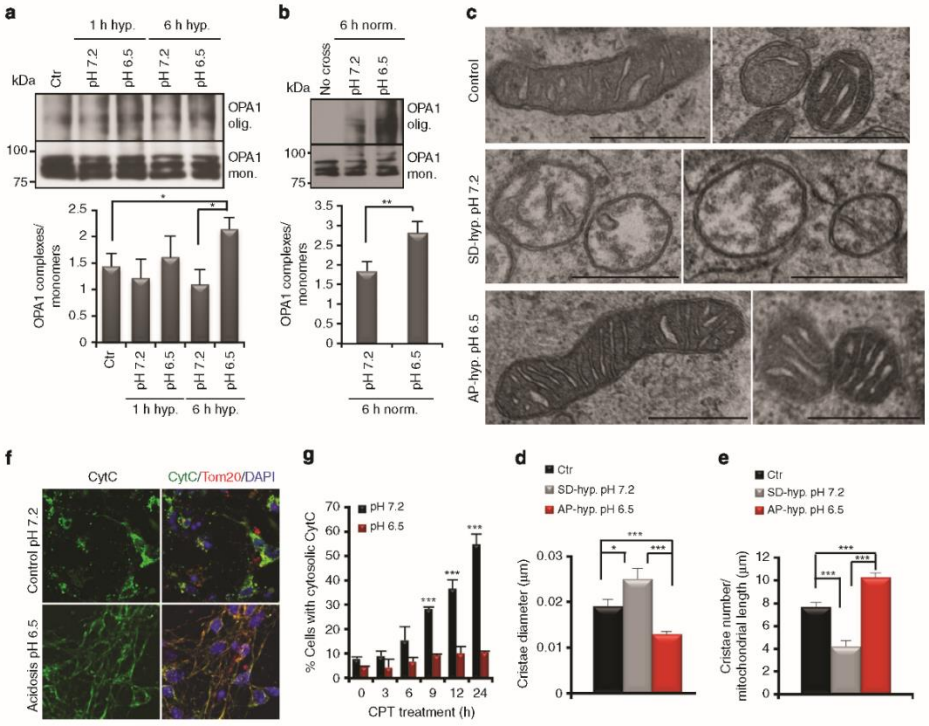

Figure 5 | Mild acidosis regulates cristae architecture. (**a**,**b**) Western blot of OPA1 oligomers and monomers from lysates of BMH crosslinking in live cortical neurons at the indicated conditions. OPA1 western blot has been spliced to better clarify where monomeric and oligomerized Opa1 appear. Graphs represent the mean and s.d. ($n=3$) quantification of OPA1 oligomer:monomer ratio. (**c**–**e**) Representative EM images of mitochondrial ultrastructure following 6-h incubation at the indicated conditions. Scale = 500 nm. Graphs in (**d**,**e**) represent mean and s.e.m ($n=10$) for quantification of cristae diameter and cristae number. Ctr = control represents neurons incubated in neurobasal media. (**f**,**g**) Representative images and quantification (mean and s.d., $n=4$) of CytC localization following CPT treatment in MES-buffered media at pH 7.2 or 6.5 in normoxia. $^{*}P<0.05$; $^{**}P<0.01$; $^{***}P<0.001$ (Student's *t*-test).

since the levels of resident mitochondrial proteins HSP70 and VDAC were unchanged (Fig. 4c). Mitochondrial elongation during acidosis does not appear to be activated through increased expression levels of core fusion proteins OPA1 and MFN1/2 (refs 46–48; Fig. 4d). Moreover, addition of the protein synthesis inhibitor cycloheximide did not prevent acidosis-mediated mitochondrial elongation or significantly alter mitochondrial length during control conditions, suggesting that acidosis may regulate mitochondrial dynamics at the post-translational level (Supplementary Fig. 11). To further decipher the molecular mechanism enabling enhanced fusion activity, we examined the possibility that acidosis activates the stress-induced mitochondrial hyperfusion (SIMH) pathway[7]. We found that removal of the key molecular components of the mitochondrial fusion machinery and the SIMH pathway, OPA1, MFN1 and SLP2, rendered neurons unresponsive to acidosis-induced mitochondrial elongation in normoxia (Fig. 4e,f). Together, these data demonstrate that mild acidosis enhances mitochondrial fusion, requires an intact fusion machinery and suggests a specific role for the SIMH pathway in the hyperfusion observed by mild acidosis during hypoxic stress.

Acidosis regulates cristae remodelling during stress. The internal structures of mitochondria, the cristae, are also dynamic and can undergo OPA1-dependent remodelling during stress conditions[49,50]. OPA1 oligomeric complexes, consisting of both membrane-bound long (l-OPA1) and soluble short forms (s-OPA1) of OPA1 in the intermembrane space, have been associated with inner membrane morphology, tightness of the cristae junctions, as well as sequestration of Cytochrome *c* (Cyt*C*) within the cristae[46,49,51,52]. We found that the relative amount of s-OPA1 was altered following 6 h of hypoxic treatment (Fig. 4d) and OPA1-specific oligomeric complexes were disrupted as early as 1 h after treatment (Fig. 5a and Supplementary Fig. 12). However, a mild decrease in the extracellular pH during hypoxia rescued both the levels of s-OPA1 and OPA1 oligomeric complexes (Figs 4d and 5a). Acidosis also increased OPA1 oligomeric complexes under normoxic conditions (Fig. 5b). This suggested that acidosis not only changes mitochondrial length but it may also alter cristae morphology. Examination of mitochondrial ultrastructure using transmission electron microscopy (TEM) revealed that mitochondrial ultrastructure, which is severely disrupted during hypoxia, was preserved by

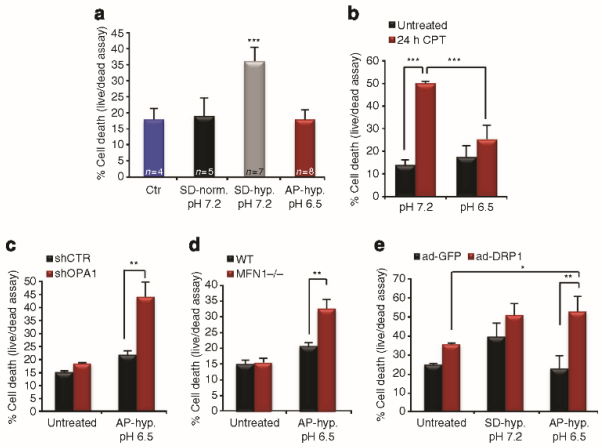

Figure 6 | Acidosis-mediated mitochondrial remodelling protects neurons from cell death during hypoxic stress. (**a**) Quantification of cell death of cortical neurons as mean and s.d. (*n* values indicate independent experiments) following 30-h incubation in SD or AP media at the indicated conditions. (**b**) Mean and s.d. ($n=3$) of neuronal cell death analysis following 24-h treatment with CPT in MES-buffered media at pH 7.2 or 6.5 in normoxia. (**c**) Quantification of cell death in neurons infected with lentivirus encoding a scrambled (shCTR) or OPA1-specific (shOPA1) shRNA following 30 h in SD or AP media at the indicated conditions (mean and s.d., $n=3$). (**d**) Mean and s.d. ($n=4$) of cell death quantification in WT (wild-type) or MFN1-deficient (MFN1 $-/-$) cortical neurons following 30-h incubation in SD or AP media at the indicated conditions. (**e**) Quantification of cell death in neurons infected with adenovirus-encoding GFP or DRP1-YFP following 30-h incubation in SD or AP media at the indicated conditions (mean and s.d., $n=3$). $^{*}P<0.05$; $^{**}P<0.01$; $^{***}P<0.001$ (Student's *t*-test).

acidosis (Fig. 5c–e). During hypoxia-neutral conditions, where aberrant mitochondrial fragmentation is observed, there is a severe disruption of mitochondrial ultrastructure leading to a significant increase in cristae diameter as well as a reduction in cristae number (Fig. 5c–e). More importantly, a mild decrease in the pH during hypoxia not only rescued this defect but also resulted in a significant tightness of the cristae diameter and increased cristae number, relative to control (Fig. 5c–e). These data suggest a role for acidosis in cristae maintenance and remodelling. This was further confirmed through an indirect examination of cristae remodelling by measuring the degree of CytC release following an apoptotic stimulus, which can provide information related to the tightness of the cristae junctions[49,53]. Treatment of neurons with Camptothecin (CPT), a DNA-damaging agent that triggers the apoptotic cell death pathway, revealed that mitochondrial restructuring by acidosis renders cells resistant to CytC release (Fig. 5f,g), in the presence of apoptosis signalling as indicated by BAX activation (Supplementary Fig. 13). Together, these data demonstrate that mild acidosis modulates mitochondrial dynamics as well as cristae architecture. Furthermore, these data suggest that acidosis prevents the intramitochondrial remodelling, as a result of OPA1 oligomer destabilization, that is associated with mitochondrial fragmentation and cell death signalling.

Mitochondrial restructuring protects cells in hypoxia. Several studies have demonstrated the protective effect of mild acidosis during ischemic conditions. Importantly, this observation was recapitulated in our model of ischemia. A significant increase in cell death is observed in hypoxia under neutral conditions; however, a physiological decrease in the extracellular pH (pH 6.5) protects neurons from death (Fig. 6a). Interestingly, acidosis rendered neurons resistant to other damaging agents such as CPT (Fig. 6b), suggesting that cells subjected to mild changes in extracellular pH can sustain survival under different modes of stress. The observation that mild acidosis in our system also promotes mitochondrial remodelling suggests that this may be the underlying mechanism of cellular protection previously observed at similar pH levels. To confirm this hypothesis, we tested neuronal survival during hypoxia–acidosis where we prevented the impact of acidosis on mitochondrial dynamics. The protective effect of acidosis was reversed in the absence of the essential fusion machinery. Acute RNA interference-mediated loss of OPA1 expression or genetic ablation of MFN1 prevented acidosis-mediated mitochondrial elongation (Fig. 4e,f) and was sufficient to increase cell death during hypoxia even in the presence of acidosis (Fig. 6c,d). Moreover, overexpression of the mitochondrial fission protein DRP1, in wild-type neurons, resulted in a significant increase in cell death during hypoxia–acidosis (Fig. 6e). These data demonstrate that the restructuring of mitochondria during stress is a major player in the protective effect of mild acidosis.

Reprogrammed mitochondria maintain ATP production in hypoxia. A prominent response to cellular hypoxic stress is mitochondrial fragmentation, and loss of mitochondrial membrane potential and dysfunction[17,19]. Since acidosis prevents hypoxia-induced mitochondrial fragmentation and cell death, we wanted to investigate the status of mitochondrial integrity and function. We found that mild acidosis maintains mitochondrial membrane potential during hypoxia (Fig. 7a, and Supplementary Fig. 14). Maintenance of mitochondrial membrane potential requires a protonmotive force that is generated by the electron transport chain through respiration or, in pathological situations, by ATP hydrolysis via the F_1F_0-ATPase (ATP synthase). A highly polarized membrane potential suggests that either mitochondrial

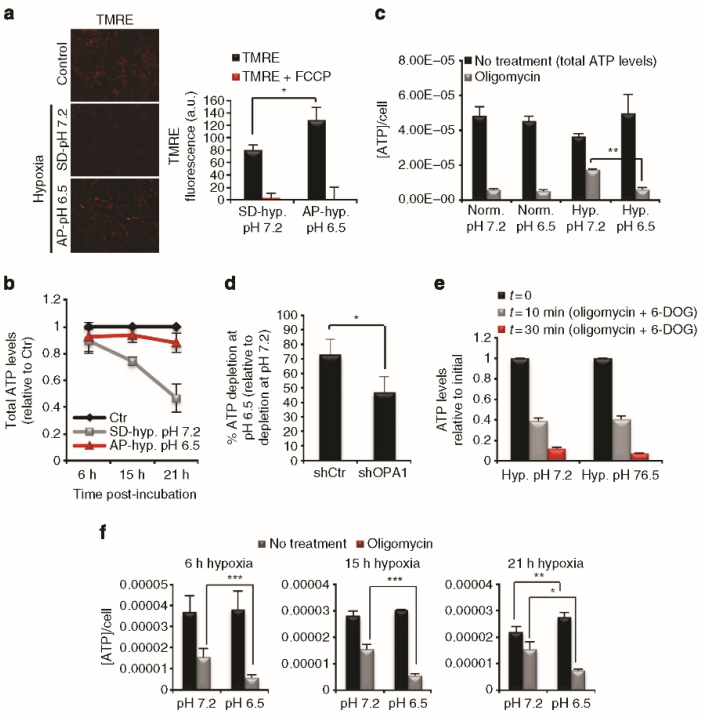

Figure 7 | Acidosis maintains mitochondrial function during hypoxic stress. (**a**) TMRE staining and quantification of fluorescence intensity following 18-h incubation in SD or AP media in hypoxia. Mean and s.d. ($n=3$ from three independent experiments). The uncoupler FCCP, which dissipates the membrane potential, is used to show specificity of the measured TMRE fluorescence. (**b**) Total ATP levels relative to normoxic control (in black). Mean and s.d. ($n=5$). (**c**) Total ATP concentration per cell at steady state (black) and after 1-h oligomycin treatment (grey) following 6 h of treatment at the indicated conditions. Mean and s.d. ($n=3$ replicates from six independent experiments). (**d**) Quantification of the amount of ATP depletion following 1-h oligomycin treatment in cortical neurons infected with lentivirus encoding a scrambled control (shCtr) or OPA1-specific shRNA (shOPA1). Mean and s.d. ($n=3$ replicates from three independent experiments). (**e**) ATP levels per cell relative to initial values (black) following oligomycin and 6-DOG treatment. Mean and s.d. ($n=3$ replicates from three independent experiments). (**f**) Total ATP levels per cell at steady state (black) and after 1-h oligomycin treatment (grey). Graphs represent mean and s.d. of $n=3$ replicates from six independent experiments. $^{*}P<0.05$; $^{**}P<0.01$; $^{***}P<0.001$ (Student's *t*-test).

respiratory function was preserved by mild acidosis or that the membrane potential was maintained by the reversal of the ATP synthase, which would result in ATP consumption. Interestingly, total ATP levels were sustained for an extended period in hypoxia if cells underwent physiological acidification (Fig. 7b), suggesting that ATP hydrolysis by the ATP synthase was not a central contributing factor in maintaining membrane potential.

It is well established that mitochondrial function and the generation of ATP through oxidative phosphorylation (OXPHOS) is impaired during hypoxic conditions, causing cells to shift to anaerobic glycolysis[54]. Although this shift in metabolism is important for cell survival during acute hypoxic stress, glycolysis represents a much less efficient mode of ATP production, and over the long run it is reasonable to conceive how this can pose an energy deficit in high-energy-demanding cells such as neurons. The remodelling of mitochondria, as well as maintained membrane potential and ATP levels by acidosis, led us to postulate that acidosis may also preserve mitochondrial function during hypoxic conditions. Intriguingly, we found that addition of oligomycin, an ATP synthase inhibitor that blocks mitochondrial ATP production, resulted in a significant depletion, of ~90%, in total ATP levels during hypoxia–acidosis conditions, to the same extent as that observed during normoxia (at pH 7.2 and 6.5; Fig. 7c). This is in contrast to what is observed under hypoxia-neutral conditions whereby oligomycin treatment following short-term hypoxia (6 h) results in only about 50% decrease in ATP levels, suggesting the use of a non-mitochondrial ATP production pathway (that is, glycolysis). Preventing mitochondrial fusion and disrupting cristae structure during acidosis, through acute loss of OPA1 expression, resulted in decreased oligomycin-sensitive ATP depletion at pH 6.5 (Fig. 7d). The increased level of ATP depletion in wild-type neurons, observed in the presence of oligomycin during acidosis, was not due to an elevation in ATP utilization since arrest of both ATP production pathways using 6-deoxyglucose (6-DOG; glycolysis inhibitor) and oligomycin showed a similar rate of ATP consumption over time during hypoxia at pH 7.2 and 6.5 (Fig. 7e). Given that an increase in consumption cannot account

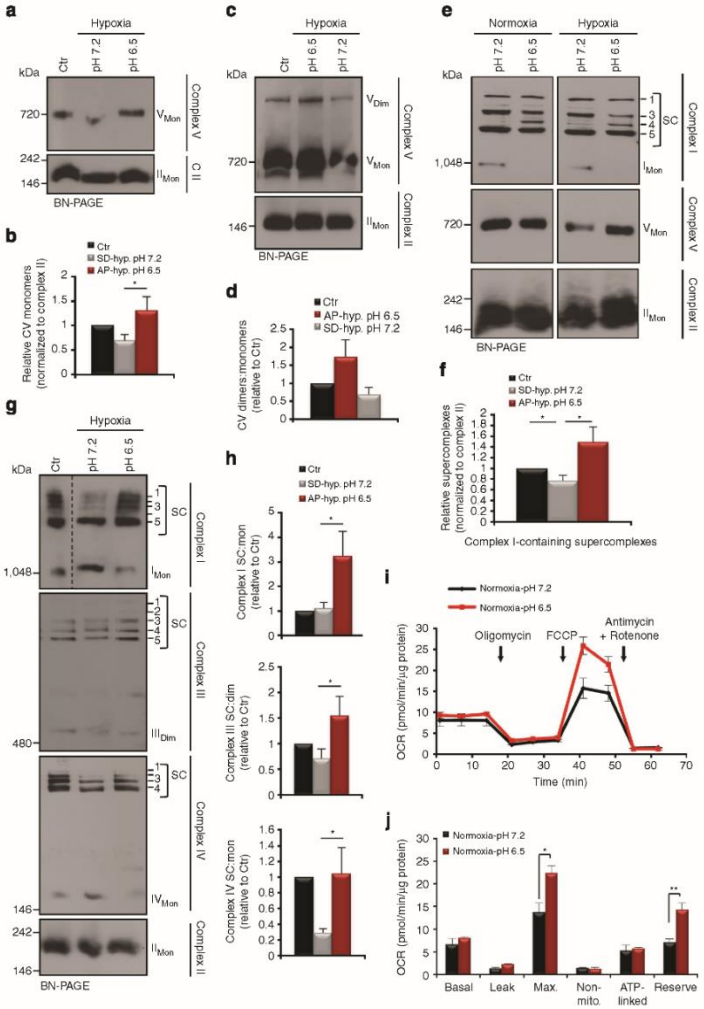

Figure 8 | Acidosis instigates an adaptive reprogramming of mitochondrial respiratory efficiency. (**a**–**d**) Representative BN-PAGE of Complex V (ATP synthase) (**a**) monomers (whole cells) and (**c**) dimers (isolated mitochondria) in cortical neurons following 6-h treatment in the indicated conditions. In (**c**), longer exposure of the membrane was required to visualize the dimeric Complex V. Graphs represent mean and s.e.m of (**b**) $n=5$ and (**d**) $n=3$ independent experiments. Mon = monomers, Dim = dimers, and CV = Complex V. (**e**) Representative BN-PAGE of the indicated respiratory complexes using anti-NDUFA9 (Complex-I), anti-ATP5a (Complex-V) and anti-Core2 (Complex-II). Cortical neurons were treated for 6 h in the indicated conditions. SC 1–5 = supercomplex assembly. (**f**) Quantification of relative assembly of supercomplexes visualized using anti-NDUFA9 (Complex-I). Mean and s.e.m of $n=4$ independent experiments. (**g**,**h**) Representative BN-PAGE of the indicated respiratory complexes using anti-NDUFA9 (Complex-I), anti-UQCRC2 (Complex-III), anti-Complex IV subunit 1 (Complex-IV) and anti-Core2 (Complex-II) following 6 h in the indicated conditions. Graphs in (**h**) are mean and s.e.m of $n=6$ (Complex-I), $n=4$ (Complex-III) and $n=3$ (Complex-IV) independent experiments. (**i**,**j**) OCR in cortical neurons using a Seahorse XF24 Extracellular Flux Analyzer. Mean and s.d. ($n=4$ replicates from three independent experiments). $^{*}P<0.05$; $^{**}P<0.01$; $^{***}P<0.001$ (Student's t-test).

for the significant depletion of ATP in the presence of oligomycin, this suggests that cells in acidosis rely less on the glycolytic ATP generation pathway and supports the idea that acidosis preserves mitochondrial function and sustains OXPHOS during hypoxia. This observation was quite surprising considering that oxygen availability is historically viewed as a limiting factor

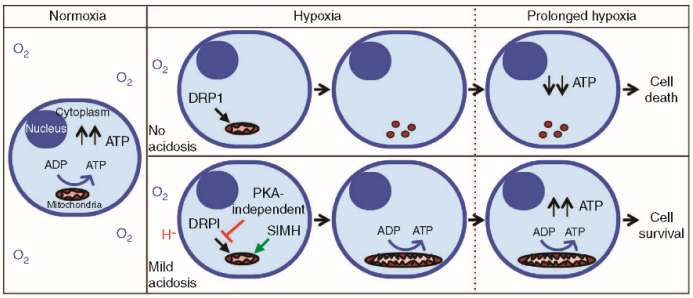

Figure 9 | Mitochondrial restructuring by mild acidosis determines cellular bioenergetics during hypoxia. The cartoon depicts the cascade of events following a decrease in oxygen levels and the role of mild acidosis in triggering mitochondrial restructuring and reprogramming to determine cellular bioenergetics and cell fate. Upper row: hypoxia causes mitochondrial fragmentation, loss of efficient ATP production and eventual cell death. Lower row: mild acidosis during hypoxia prevents DRP1-mediated fission and promotes mitochondrial elongation (in a SIMH-dependent manner) and cristae remodelling to maintain ATP levels and cell survival. In our model and experiments, 'no acidosis' and 'mild acidosis' indicate an extracellular pH of 7.2 and 6.5, respectively; 'hypoxia' indicates incubation at 1% oxygen for 0–12 h, and 'prolonged hypoxia' is considered following 12–21 h of incubation at 1% oxygen.

for mitochondrial ATP generation through mitochondrial respiration. More importantly, a pH-dependent shift in the bioenergetic status of neurons was observed over time, whereby cells in hypoxia at pH 7.2 relied increasingly on oligomycin-insensitive ATP production (that is, glycolysis) while neurons allowed to undergo physiological acidification relied on mitochondrial-dependent ATP production (Fig. 7f). Thus, acidosis sustains efficient mitochondrial ATP production during prolonged hypoxia (Fig. 7f).

An alteration in the metabolic profile of cells in hypoxia–acidosis implies an adaptation of the electron transport chain (ETC) components to maximize mitochondrial efficiency during limited oxygen availability. Several studies have reported the adverse effect of hypoxia on the expression and activity of ETC complexes as well as supercomplex disassembly[55,56]. Expression analysis of subunits encompassing the ETC complexes during acute hypoxia revealed maintained expression of Complex I subunit NDUFA9 as well as ATP synthase subunit ATP5a by mild acidosis (Supplementary Fig. 15). Blue native PAGE (BN-PAGE) analysis of the respiratory chain complexes showed a destabilization of the monomeric ATP synthase multiprotein complex during hypoxia, which is rescued by acidosis (Fig. 8a,b). Only a minor proportion of the ATP synthase is present in its dimeric form in neurons used during our experiments (Fig. 8c and Supplementary Fig. 16). Nonetheless, longer exposure of BN-PAGE from whole cells or BN-PAGE performed on isolated mitochondria revealed a higher molecular weight band corresponding to dimeric forms of the ATP synthase predominantly in hypoxia–acidosis conditions (Fig. 8c,d and Supplementary Fig. 16), indicating a distinct rise in the stability of the enzyme superassembly. The individual multiprotein complexes of the ETC can further associate into super-complexes, known as respirasomes[57,58]. It has been proposed that supercomplex assembly could stabilize the single complexes, enhance the electron flow between complexes and limit generation of oxygen radicals[59–63]. In addition, a distinct role for cristae shape has been recently shown to affect supercomplex assembly and respiratory efficiency[64]. Examination of higher order respiratory complex assembly by BN-PAGE showed a distinct reorganization of Complex I-containing supercomplexes by acidosis regardless of oxygen levels (Fig. 8e), resulting in loss of monomeric complex I and enhanced supercomplex assembly (complex I supercomplex:monomer ratio; Fig. 8h), as well as an increase in the relative levels (Fig. 8f). Detailed analysis of the respiratory supercomplexes showed maintained assembly of Complexes 1, III and IV into supercomplexes in the presence of acidosis during hypoxic conditions (Fig. 8g,h). We hypothesized that the acidosis-mediated changes to the OXPHOS complexes would be accompanied by an enhancement in the respiratory capacity of mitochondria. To test this hypothesis, the bioenergetic profile of mitochondria was assessed in intact neurons exposed to normoxic conditions at pH 7.2 and 6.5. First, basal cellular and mitochondrial oxygen consumption rate (OCR) was similar in both conditions (Fig. 8i,j). Next, the mitochondrial respiration capacity was determined using the uncoupler FCCP, which stimulates maximal mitochondrial respiration by dissipating the mitochondrial membrane potential. We found that acidosis significantly enhances the ability of mitochondria to increase their maximal respiratory capacity (Fig. 8i,j). In addition, analysis of mitochondrial reserve capacity, which signifies the ability of mitochondria to further engage in the production of ATP through OXPHOS, revealed a significant increase at pH 6.5 (Fig. 8i,j). These data coupled with data obtained from ATP studies provide evidence that acidosis maintains mitochondrial function during hypoxic stress. This is achieved through an adaptive reprogramming of mitochondrial respiratory efficiency that occurs as a result of changes in the mitochondrial ultrastructure and cristae shape, respiratory supercomplex assembly and maintenance of monomeric ATP synthase.

Discussion

The ability of post-mitotic cells to adapt and survive physiological or pathological stress, such as that imposed by oxygen deprivation, has been a long-standing question in biology. Here we report that mild extracellular acidosis, a biological consequence of anaerobic metabolism during hypoxia, restructures the mitochondrial network as an adaptive mechanism to enhance mitochondrial function and promote cellular survival. Mitochondrial remodelling by acidosis, through the activation of a dual programme that modulates mitochondrial dynamics and architecture, represents a novel and physiological pathway that sustains mitochondrial integrity and ATP production despite oxygen limitations. Preventing this reversible and homeostatic process results in mitochondrial dysfunction, fragmentation and

cell death. We provide a mechanism underlying the protective nature of mild acidosis, identify a novel physiological regulator of mitochondrial dynamics in post-mitotic cells and propose a role for mitochondrial morphology in the bioenergetic status of cells.

Survival of post-mitotic cells is highly dependent on a sufficient supply of energy to uphold the exhaustive demands incurred by complex molecular networks. The switch to anaerobic metabolism, albeit a critical cellular metabolic adaptation of hypoxic cells, cannot compensate for the loss of mitochondrial respiration during prolonged hypoxia[54,65,66]. As a result, cells faced with prolonged hypoxia will inevitably endure energy failure and cell death if not counteracted with an increase in energy supply. Data presented here demonstrate that post-mitotic cells have evolved a rapid and reversible mechanism to uphold efficient ATP production, via mitochondrial remodelling, that is regulated by acidosis. This is, to our knowledge, the first ascribed function for this metabolic product of anaerobic respiration historically associated with clinical resistance during ischemic insults. We propose a model whereby a threshold accumulation of extracellular protons, acquired through an initial increase in the glycolytic rate during hypoxia, would relay a signal back to mitochondria, potentially via changes in intracellular pH, in order to modulate mitochondrial bioenergetics (Fig. 9).

In recent years, mitochondrial structure and dynamics have emerged as a fundamental aspect for biological life. Our work further highlights this concept in demonstrating the protective nature of mitochondrial restructuring during stress. In addition, we provide a link between mitochondrial morphology and cristae architecture with the metabolic state of cells. The data presented in this study suggest that mitochondrial remodelling can instigate a systemic reconfiguration of mitochondrial efficiency to extract more ATP per oxygen molecule. In essence, acidosis-mediated reorganization of mitochondrial efficiency can override oxygen limitations and allow for the persistence of mitochondrial respiration in an anaerobic environment. This observation refines the well-established role of oxygen as a limiting factor for oxidative phosphosphorylation and puts forth the idea that mitochondrial reprogramming can dictate the bioenergetics of the cell. In view of these findings, the capability of post-mitotic cells to sense and adapt to anaerobic conditions by inducing anaerobic mitochondrial respiration should emerge as a central research theme in the study of physiological and pathological situations that relates to oxygen and energy homeostasis.

Methods

Mice, primary neuronal cultures and cell lines. To generate dorsal telencephalon-specific *MFN1* conditional mutant mice, floxed *MFN1* (Jackson Laboratories) and *Emx1-cre* heterozygous females were bred with floxed *MFN1* homozygous and *MFN2* heterozygous males. Telencephalon-specific *SLP2* conditional mutants were generated by breeding floxed *SLP2* homozygous females with *Foxg1-cre* male mice (provided by Dr Sean Cregan). Cortical neurons were cultured from CD1 wild-type female and male mice (Charles River) and *MFN1* or *SLP2* conditional knockout mice at embryonic day 14.5 or 15.5 (ref. 67). CGNs were cultured from CD1 mice at postnatal day 7 or 8 (ref. 13). All experiments were approved by the University of Ottawa's Animal Care ethics committee adhering to the Guidelines of the Canadian Council on Animal Care. Neurons were maintained in culture for 3–5 days before experimentation. MCF-7 breast carcinoma, A549 lung carcinoma, P19 embryonic teratocarcinoma, Cos7 African green monkey kidney fibroblasts, HeLa and C2C12 myoblasts were obtained from ATCC (Manassas, VA, USA). Primary and transformed MEFs were generated from CD1 mice on embryonic day 13.5. *In vitro* differentiation of C2C12 myoblasts into multinucleated myotubes was performed by replacing fetal bovine serum (FBS)-containing DMEM with DMEM containing 2% horse serum when myoblasts were at 80% confluency. Media were changed every second day for about 7 days until multinucleated myotubes were formed.

Cell culture. The plating density for each cell population was chosen to optimize the rate of physiological extracellular acidification during hypoxic conditions. Cortical neurons and CGNs were seeded on plates (with or without coverslips) coated with 0.01 mg ml^{-1} poly-D-lysine (BD Bioscience) for all experiments. Cortical neurons were plated onto four-well plates, 35- and 60-mm dishes with 4.0×10^5, 3.0×10^6 and 9.0×10^6 neurons, respectively, and maintained in Neurobasal media (Gibco) that contained 2% B27 (Gibco), 1% N2 (Gibco), 0.6 mM L-glutamine (Gibco) and 1% Pen-Strep (Sigma). CGNs were plated in four- or 12-well plates with 4×10^5 and 8×10^5, respectively, and maintained in DMEM (Wisent Inc.) that contained 10% dialysed FBS (Sigma), 25 mM KCl, 2 mM glutamine (Invitrogen), 25 mM glucose and 0.1 mg ml^{-1} gentamycin (Sigma). MCF-7 and MEFs were plated in 35-mm dishes with 7×10^5 cells and maintained in DMEM containing 5% FBS and 1% Pen-Strep. All cells were maintained at 37 °C under 5% CO_2 environment until experimentation. Hypoxia was achieved by incubation in a hypoxic chamber at 37 °C under a 1% O_2, 5% CO_2 and N_2-balanced atmosphere. Acidosis experiments were conducted as previously described[68], with modifications. For acidosis experiments mimicking physiological conditions, SD or AP media was utilized. Buffer-free and low glucose (5.5 mM) medium (DMEM; Gibco) was freshly prepared and supplemented with B27 and N2 for post-mitotic neurons or 5% FBS for replicating cells. The level of physiological acidification of the extracellular environment is proportional to the cell density and the buffering capacity of the media. $NaHCO_3$ was added at 10 mM (post-mitotic cells) or 35 mM (replicating cells) and the pH was adjusted with HCl to 7.2 (SD media) or 6.5 (AP media). Air was bubbled into both media at 22 °C, which stabilizes the pH at 7.2. Culture media were aspirated and cells were washed $\times 2$ in buffer-free low glucose DMEM to remove all traces of highly buffered culture media. Cells were then placed in AP or SD media. AP media slowly reverted to its original set pH under hypoxia, whereas the SD medium remained at pH 7.2. For acute acidosis experiments in hypoxia or normoxia, 30 mM of MES was used as a buffer and the pH was set and stabilized at the required value.

Viruses and materials. Recombinant adenoviral vectors carrying the DRP1-YFP or GFP expression cassette were prepared using the AdEasy system[12]. Lentivirus vectors carrying photoactivable GFP-ornithine carbamyltransferase (PA-GFP-Oct), Mito-DsRed, shRNA scramble control (shCtr sequence; 5′-CAACAAGATGAAG AGCACCAA-3′), and mouse-specific short-hairpin RNA (shRNA) OPA1 (shOPA1 sequence; 5′-GCCTGACTTTATATGGGAAAT-3′) were prepared using the ViraPower lentiviral expression system (Invitrogen)[13]. For lentiviruses and adenoviruses, neurons were transduced with 2 MOI (multiplicity of infection) or 50–100 MOI, respectively, at time of plating. For all experiments using viruses, neurons were infected with adenovirus or lentivirus for 72 h before experimentation. Oligomycin (10 μM), 6-deoxyglucose (6-DOG, 6 mM), cycloheximide (100 μg ml^{-1}), CPT (20 μM), mdivi-1 (50 μM), H89 (20 μM), forskolin (25 μM) and Monensin (1 μM) were used where indicated.

Immunofluorescence. Cells seeded on coverslips were fixed with 4% paraformaldehyde in PBS for 20 min at room temperature. Primary antibodies used were Tom20 (Santa Cruz; 1:100), Tuj1 (Covance; 1:10,000), MAP2 (Novus Biologicals; 1:200), NeuN (Millipore; 1:1,000), DLP1 (BD Biosciences; 1:100), Cytochrome *c* (BD Biosciences; 1:100) and Bax (Santa Cruz, 1:100). Cells were incubated for 1 h with a primary antibody solution containing 1% bovine serum albumin (BSA), 0.1% Triton-X-100 in PBS. Cells were washed several times in PBS before 1-h incubation with a secondary 594 or 488 Alexa (Invitrogen; 1:400). Hoechst stain 33342 (Sigma) or 4′,6-diamidino-2-phenylindole (DAPI) was added to visualize nuclei and coverslips were mounted using Immunomount (Thermo Scientific).

Immunohistochemistry. Coronal hippocampal slice preparations (200 μm) were incubated in oxygenated artificial cerebrospinal fluid (ACSF) buffered with PIPES to pH 7.2 or 6.5 for 4 h. Hippocampal slices were fixed for 20 min with ice-cold 4% paraformaldehyde in 1 × PBS and then rinsed twice with 1 × PBS. Slices were incubated in 10% sucrose and embedded in OCT and then sectioned using a microtome to 15-μm sections. Sections were stained with primary antibodies specific to Tom20 and NeuN in 10% normal goat serum-0.1% TritonX/0.1% Tween-20 in PBS overnight at 4 °C followed by 3 × 5 min washes with 1 × PBS. Sections were incubated with secondary antibodies in PBS for 1 h, washed for 5 min, stained with DAPI for 5 min, and then washed with 1 × PBS for 3 × 5 min. Slides were mounted using Immunomount (Thermo Scientific). Representative samples were imaged using a Zeiss Axiovert 100 (Oberkochen, Germany) confocal microscope equipped with a QiCam Digital camera (QImaging Corporation) and Zen software.

Mitochondrial length. Mitochondrial length was assessed by staining with Tom20 (translocase of outer mitochondria). Mitochondrial length was measured by tracing the mitochondria using the ImageJ software. Mitochondrial length was either binned into different categories (< 0.5 μm, 0.5–1 μm, 1–2 μm, > 2 μm) or taken as an average.

Intracellular pH measurements. Changes in intracellular pH was determined utilizing the ratiometric fluorescent intracellular pH indicator BCECF-AM (Invitrogen). Intracellular pH measurements were performed on cultured cortical neurons plated in 96-well black microplates that were treated for 6 h in the

appropriate experimental media and subsequently loaded with BCECF-AM (1 μM) for 30–45 min at 37 °C. A dual-excitation ratio of 480 and 440 nm and fixed emission at 535 nm was used to measure changes in BCECF-AM fluorescence. Since these experiments were designed to determine the effect of extracellular acidosis on intracellular pH, the measurements had to be performed while the cells were maintained in the respective experimental media (that is, media at pH 7.2 or pH 6.5). For this reason, the use of BCECF-AM was first validated by performing a calibration curve, using the high K+ Nigericin technique, to ensure that intracellular changes in pH can be detected in the experimental media. MES-buffered DMEM media was supplemented with 130 mM KCl and the pH was set to 6.0, 6.5, 7.0, 7.5 and 8.0 using KOH. The media of cells previously loaded with BCECF-AM (for 30–45 min) was replaced with the high K+ MES-buffered media supplemented with the ionophore Nigericin (Molecular Probes, 10 μM) and incubated for 10 min to allow for equilibration of the intracellular pH with the controlled extracellular medium. BCECF-AM fluorescence was measured as described above.

Immunoblot. For total cell lysates, cells were washed with PBS, lysed with 4% SDS in PBS, boiled for 5 min and the DNA was sheared by passage through a 26-gauge needle. Primary antibodies recognizing Complex I subunit NDUFA9 (Invitrogen; 1:1,000), Complex II 70-KDa Fp subunit (Invitrogen; 1: 10,000), ATP5a (Abcam; 1:1,000), Complex IV subunit 1 (Invitrogen; 1:1,000), Complex III core protein 2 (UQCRC2, Abcam; 1:1,000), DLP1 (DRP1, BD Transduction Laboratories; 1:1,000), Phoso-DRP1 S637 and S616 (Cell Signaling; 1:1,000), Fis1 (Biovision; 1:500), OPA1 (Abcam; 1:1,000), MFN1 and 2 (Abcam; 1:1,000), VDAC (Abcam; 1:1,000), mitochondrial heat-shock protein 70 (mtHSP70, Thermo Scientific; 1:5,000) and Actin (Santa Cruz; 1:1,000) were used. A secondary antibody conjugated to horseradish peroxidase (Jackson ImmunoResearch) was used and detected using Western Lightning Chemiluminescence Reagent Plus (Perkin Elmer). Representative full-gel bots are shown in Supplementary Fig. 17.

Immunoprecipitation. Cells were lysed in RIPA buffer (50 mM Tris (pH 7.2), 150 mM NaCl, 10% NP40 and 1 mM sodium orthovanadate with a protease inhibitor cocktail (PIC)). Cell lysates were incubated with anti-DRP1 antibody (BD Transduction Laboratories) for 1 h while tumbling at 4 °C, followed by overnight incubation with Sepharose A/G beads blocked in 2% BSA. Beads were washed 4 × in 1 × Tris-buffered saline and eluted by boiling at 95 °C for 4 min.

Time-lapse imaging and mitochondrial fusion assay. Cortical neurons were seeded on 35-mm dishes with coverslip bottoms (MatTek) coated with poly-D-lysine (VWR International) and infected with 2 MOI of the photoactivable GFP tagged to ornithine carbamyltransferase (PA-GFP-Oct) and Mito-DsRed. Following 2-h incubation in MES-buffered media at pH 7.2 or 6.5, plates were mounted in a temperature-controlled chamber (37 °C) and visualized with an LSM-510 confocal laser-scanning microscope (Axiovert 200), with a × 63 oil immersion objective. Mitochondrial fusion assays were performed as described previously with modifications[13]. Briefly, PA-GFP-Oct was first pre-imaged and scanned to ensure that there is no spontaneous activation. PA-GFP-Oct was then photoactivated with a 405-nm laser and the spreading of the signal was imaged every 2 min using a 488-nm line for a total of 22 min. Mito-DsRed was excited at 543 nm and was used a guide to ensure that the ROI for PA-GFP-Oct activation was within the mitochondria. The fusion rate was expressed as a relative measure of pixel intensity at the indicated time over that at $t = 0$ min (where 0 min represents the signal detected after 2 min of photoactivation and equilibration of GFP signal).

OPA1 crosslinking. *In vivo* crosslinking reactions were performed at 37 °C with 10 mM BMH crosslinker (Fisher Scientific) for 20 min. Reactions were terminated by adding 0.001% β-mercaptoethanol. Cells were lysed following crosslinking, and analysed by gradient gel electrophoresis using NuPAGE Novex 3–8% Tris-acetate gradient gels (Life Technologies), followed by western blotting against OPA1.

(TEM) and cristae analyses. Mitochondrial ultrastructure was analysed from whole cells of cultured cortical neurons following 6-h treatment in the appropriate conditions. Briefly, plated neurons were rapidly washed in PBS and harvested by scraping very lightly. Neurons were fixed in 2% gluteraldehyde for 20 min at room temperature and stored immediately at 4 °C for processing as previously described[69]. Cristae analysis was performed using ImageJ and a minimum of 100 mitochondria were analysed. For each individual cristae, the average diameter was measured from three representative regions.

Cytochrome *c* release. Neurons were treated with 20 μM CPT for the indicated times, fixed and stained with cytochrome *c* and Tom20-specific antibodies. For each replicate, a total of 100 neurons were counted from three to five different fields using a Zeiss 510 meta confocal microscope. A diffused cytochrome *c* staining or complete lack of staining was identified as release.

Cell viability assay. Following 30 h of incubation under the indicated conditions, cells were subjected to a live–dead assay (Invitrogen) by staining with calcein (live cells) and ethidium homodimer-1 (dead cells) for 10–15 min at 37 °C. In each replicate, three to five different fields were randomly chosen and imaged per treatment group. Cell death was expressed as a percentage of total cells. Calcein and ethidium homodimer-1 dyes are unaffected by pH as neutralization of an acidic set or acidification of a neutral set immediately before addition of the dyes yielded the same results.

Mitochondrial membrane potential. Neurons were seeded in 96-well black microplates. Following the appropriate treatment, 50 nM TMRE was added and cells were incubated for 30 min at 37 °C under normoxia (control) or hypoxia. FCCP (1 μM) was added to the appropriate wells 10 min before addition of TMRE. Neurons were washed in PBS and TMRE fluoresence was measured in a plate reader at Ex 510 nM an Em 590 nM.

ATP assay. ATP concentrations were measured with the CellTiter-Glo Luminescent Assay (Promega) using a LUMIstar Galaxy luminometer (BMG Labtechnologies) according to the manufacturer's protocol. Data were collected from multiple replicate wells for each experiment. Viability of cells under all conditions was ensured by PI staining.

Blue-native PAGE. ETC supercomplexes and ATP synthase assembly were analysed from whole cells or isolated mitochondria[70]. For whole cells, following the indicated treatments, cells were harvested in PBS on ice, pelleted at 960 *g* for 5 min at 4 °C. For isolated mitochondria, cells were washed with PBS and lysed in mitochondrial isolation buffer (200 mM mannitol, 70 mM sucrose, 10 mM HEPES, pH 7.4, 1 mM EGTA, PIC 1:1,000) on ice using a 25-G needle. Following centrifugation at 110 *g* for 9 min to remove nuclei and cellular debris, the supernatant was centrifuged at 8,600 *g* for 9 min to pellet mitochondria. This differential centrifugation step was repeated to further purify the mitochondrial fraction. For BN-PAGE analysis, pellets of whole cells or isolated mitochondria were resuspended in digitonin extraction buffer (50 mM imidazole/HCl pH 7.0, 50 mM NaCl, 5 mM 6-aminohexanoic acid, 1 mM EDTA and the appropriate ratio of digitonin). A 1% digitonin ratio was used for Complex-1 and supercomplexes, and 2% was used for ATP synthase assembly. One hundred fifty micrograms were loaded with 5% glycerol and 1:10 dye:digitonin ratio of coomassie dye in 500 mM 6-aminohexanoic acid on 3–13% large acrylamide gradient gels. Gels were transferred to nitrocellulose membranes and the resulting membranes were subjected to immunoblotting.

Oxygen consumption. The Seahorse XF24 Extracellular Flux Analyzer (Seahorse Biosciences; North Billerica, MA, USA) was used to measure oxygen consumption in cells. Cortical neurons were seeded onto 24-well Seahorse plates at a density of 1.5×10^5 cells per well. Following treatment, cells were washed with modified Kreb's Ringer Buffer (128 mM NaCl, 4.8 mM KCl, 1.2 mM KH_2PO_4, 1.2 $MgSO_4$, 25 mM $CaCl_2$, 0.1% BSA (fatty acid-free), 10 mM glucose and 1 mM sodium pyruvate, pH 7.4) and placed in Kreb's Ringer Buffer for 15 min at 37 °C before loading into the XF Analyser. Following mesurements of resting respiration, cells were treated sequentially with the following: oligomycin (0.2 μg μl^{-1}), to measure the nonphosphorylating OCR; FCCP (1 μM), to get the maximal OCR; and antimycin A (2.5 μM) and rotenone (1 μM), to measure the extramitochondrial OCR. Each measurement was taken over a 2-min interval followed by 2 min mixing and 2 min incubation. Three measurements were taken for the resting OCR, three after oligomycin treatment, two after FCCP and two after antimycin A and rotenone.

Quantification and statistical analysis. For mitochondrial length measurements, all mitochondria in a field were measured as per condition and a minimum of 1,000 mitochondria were measured for each treatment. For cell death studies, a minimum of 300 cells per field (minimum five fields) were scored for each treatment at the indicated time points. The data represent mean values ± s.d. from three independent experiments ($n = 3$) unless otherwise noted. *P*-values were obtained using a two-tailed Student's *t*-test.

References

1. Lin, M. T. & Beal, M. F. Mitochondrial dysfunction and oxidative stress in neurodegenerative diseases. *Nature* **443,** 787–795 (2006).
2. Terman, A., Kurz, T., Navratil, M., Arriaga, E. A. & Brunk, U. T. Mitochondrial turnover and aging of long-lived postmitotic cells: the mitochondrial-lysosomal axis theory of aging. *Antioxid. Redox. Signal* **12,** 503–535.
3. Newmeyer, D. D. & Ferguson-Miller, S. Mitochondria: releasing power for life and unleashing the machineries of death. *Cell* **112,** 481–490 (2003).
4. Detmer, S. A. & Chan, D. C. Functions and dysfunctions of mitochondrial dynamics. *Nat. Rev. Mol. Cell Biol.* **8,** 870–879 (2007).
5. Youle, R. J. & van der Bliek, A. M. Mitochondrial fission, fusion, and stress. *Science* **337,** 1062–1065 (2012).
6. Gomes, L. C., Di Benedetto, G. & Scorrano, L. During autophagy mitochondria elongate, are spared from degradation and sustain cell viability. *Nat. Cell Biol.* **13,** 589–598 (2011).

7. Tondera, D. *et al.* SLP-2 is required for stress-induced mitochondrial hyperfusion. *EMBO J.* **28,** 1589–1600 (2009).
8. Barsoum, M. J. *et al.* Nitric oxide-induced mitochondrial fission is regulated by dynamin-related GTPases in neurons. *EMBO J.* **25,** 3900–3911 (2006).
9. Frank, S. *et al.* The role of dynamin-related protein 1, a mediator of mitochondrial fission, in apoptosis. *Dev. Cell* **1,** 515–525 (2001).
10. Knott, A. B., Perkins, G., Schwarzenbacher, R. & Bossy-Wetzel, E. Mitochondrial fragmentation in neurodegeneration. *Nat. Rev. Neurosci.* **9,** 505–518 (2009).
11. Scheckhuber, C. Q. *et al.* Reducing mitochondrial fission results in increased life span and fitness of two fungal ageing models. *Nat. Cell Biol.* **9,** 99–105 (2007).
12. Jahani-Asl, A. *et al.* Mitofusin 2 protects cerebellar granule neurons against injury-induced cell death. *J. Biol. Chem.* **282,** 23788–23798 (2007).
13. Jahani-Asl, A. *et al.* The mitochondrial inner membrane GTPase, optic atrophy 1 (Opa1), restores mitochondrial morphology and promotes neuronal survival following excitotoxicity. *J. Biol. Chem.* **286,** 4772–4782 (2011).
14. Wang, J. X. *et al.* miR-499 regulates mitochondrial dynamics by targeting calcineurin and dynamin-related protein-1. *Nat. Med.* **17,** 71–78 (2011).
15. Chandel, N. S., Budinger, G. R. & Schumacker, P. T. Molecular oxygen modulates cytochrome c oxidase function. *J. Biol. Chem.* **271,** 18672–18677 (1996).
16. Wilson, D. F., Rumsey, W. L., Green, T. J. & Vanderkooi, J. M. The oxygen dependence of mitochondrial oxidative phosphorylation measured by a new optical method for measuring oxygen concentration. *J. Biol. Chem.* **263,** 2712–2718 (1988).
17. Solaini, G., Baracca, A., Lenaz, G. & Sgarbi, G. Hypoxia and mitochondrial oxidative metabolism. *Biochim. Biophys. Acta* **1797,** 1171–1177 (2010).
18. Jezek, P. & Plecita-Hlavata, L. Mitochondrial reticulum network dynamics in relation to oxidative stress, redox regulation, and hypoxia. *Int. J. Biochem. Cell Biol.* **41,** 1790–1803 (2009).
19. Zanelli, S. A., Trimmer, P. A. & Solenski, N. J. Nitric oxide impairs mitochondrial movement in cortical neurons during hypoxia. *J. Neurochem.* **97,** 724–736 (2006).
20. Siemkowicz, E. & Hansen, A. J. Brain extracellular ion composition and EEG activity following 10 minutes ischemia in normo- and hyperglycemic rats. *Stroke* **12,** 236–240 (1981).
21. Kaku, D. A., Giffard, R. G. & Choi, D. W. Neuroprotective effects of glutamate antagonists and extracellular acidity. *Science* **260,** 1516–1518 (1993).
22. Meyer, F. B., Anderson, R. E., Sundt, Jr. T. M. & Yaksh, T. L. Intracellular brain pH, indicator tissue perfusion, electroencephalography, and histology in severe and moderate focal cortical ischemia in the rabbit. *J. Cereb. Blood Flow Metab.* **6,** 71–78 (1986).
23. Allen, D. & Westerblad, H. Physiology. Lactic acid--the latest performance-enhancing drug. *Science* **305,** 1112–1113 (2004).
24. Bing, O. H., Brooks, W. W. & Messer, J. V. Heart muscle viability following hypoxia: protective effect of acidosis. *Science* **180,** 1297–1298 (1973).
25. Currin, R. T., Gores, G. J., Thurman, R. G. & Lemasters, J. J. Protection by acidotic pH against anoxic cell killing in perfused rat liver: evidence for a pH paradox. *FASEB J.* **5,** 207–210 (1991).
26. Morimoto, Y., Morimoto, Y., Kerrmotsu, O. & Alojado, F. S. Extracellular acidosis delays cell death against glucose-oxygen deprivation in neuroblastoma x glioma hybrid cells. *Crit. Care. Med.* **25,** 811–817 (1997).
27. Nielsen, O. B., de Paoli, F. & Overgaard, K. Protective effects of lactic acid on force production in rat skeletal muscle. *J. Physiol.* **536,** 161–166 (2001).
28. Pettila, A. & Tramp, B. F. Extracellular acidosis protects Ehrlich ascites tumor cells and rat renal cortex against anoxic injury. *Science* **185,** 277–278 (1974).
29. Lorimangh, G. C. & Sapolsky, R. M. Evolving concepts about the role of acidosis in ischemic neuropathology. *J. Neurochem.* **61,** 793–803 (1993).
30. Tan, Y. Y. *et al.* A novel neuroprotective strategy for ischemic stroke: transient mild acidosis treatment by CO inhalation at reperfusion. *J. Cereb. Blood Flow Metab.* **34,** 275–283 (2013).
31. Inserte, J., Ruiz-Meana, M., Rodriguez-Sinovas, A., Barba, I. & Garcia-Dorado, D. Contribution of delayed intracellular pH recovery to ischemic postconditioning protection. *Antioxid. Redox Signal.* **14,** 923–939 (2011).
32. Fujita, M. *et al.* Prolonged transient acidosis during early reperfusion contributes to the cardioprotective effects of postconditioning. *Am. J. Physiol. Heart Circ. Physiol.* **292,** H2004–H2008 (2007).
33. Lam, T. I. *et al.* Intracellular pH reduction prevents excitotoxic and ischemic neuronal death by inhibiting NADPH oxidase. *Proc. Natl Acad. Sci. USA* **110,** E4362–E4368 (2013).
34. Wu, S. Y. *et al.* Protective effect of hypercapnic acidosis in ischemia-reperfusion lung injury is attributable to upregulation of heme oxygenase 1. *PLoS One* **8,** e74742 (2013).
35. McCarty, M. F. & Whitaker, J. Manipulating tumor acidification as a cancer treatment strategy. *Altern. Med. Rev.* **15,** 264–272 (2010).
36. Bouyer, P. *et al.* Effect of extracellular acid-base disturbances on the intracellular pH of neurones cultured from rat medullary raphe or hippocampus. *J. Physiol.* **559,** 85–101 (2004).
37. Henrich, M. & Buckler, K. J. Effects of anoxia, aglycemia, and acidosis on cytosolic $Mg2+$, ATP, and pH in rat sensory neurons. *Am. J. Physiol. Cell Physiol.* **294,** C280–C291 (2008).
38. Liu, X. & Hajnoczky, G. Altered fusion dynamics underlie unique morphological changes in mitochondria during hypoxia-reoxygenation stress. *Cell Death Differ.* **18,** 1561–1572 (2011).
39. Ong, S. B. *et al.* Inhibiting mitochondrial fission protects the heart against ischemia/reperfusion injury. *Circulation* **121,** 2012–2022 (2010).
40. Smirnova, E., Griparic, L., Shurland, D. L. & van der Bliek, A. M. Dynamin-related protein Drp1 is required for mitochondrial division in mammalian cells. *Mol. Biol. Cell* **12,** 2245–2256 (2001).
41. Cassidy-Stone, A. *et al.* Chemical inhibition of the mitochondrial division dynamin reveals its role in Bax/Bak-dependent mitochondrial outer membrane permeabilization. *Dev. Cell* **14,** 193–204 (2008).
42. Loson, O. C., Song, Z., Chen, H. & Chan, D. C. Fis1, Mff, MiD49, and MiD51 mediate Drp1 recruitment in mitochondrial fission. *Mol. Biol. Cell* **24,** 659–667 (2013).
43. Yoon, Y., Krueger, E. W., Oswald, B. J. & McNiven, M. A. The mitochondrial protein hFis1 regulates mitochondrial fission in mammalian cells through an interaction with the dynamin-like protein DLP1. *Mol. Cell Biol.* **23,** 5409–5420 (2003).
44. Cribbs, J. T. & Strack, S. Reversible phosphorylation of Drp1 by cyclic AMP-dependent protein kinase and calcineurin regulates mitochondrial fission and cell death. *EMBO Rep.* **8,** 939–944 (2007).
45. Qi, X., Disatnik, M. H., Shen, N., Sobel, R. A. & Mochly-Rosen, D. Aberrant mitochondrial fission in neurons induced by protein kinase C{delta} under oxidative stress conditions *in vivo*. *Mol. Biol. Cell* **22,** 256–265 (2011).
46. Meeusen, S. *et al.* Mitochondrial inner-membrane fusion and crista maintenance requires the dynamin-related GTPase Mgm1. *Cell* **127,** 383–395 (2006).
47. Cipolat, S., Martins de Brito, O., Dal Zilio, B. & Scorrano, L. OPA1 requires mitofusin 1 to promote mitochondrial fusion. *Proc. Natl Acad. Sci. USA* **101,** 15927–15932 (2004).
48. Chen, H. *et al.* Mitofusins Mfn1 and Mfn2 coordinately regulate mitochondrial fusion and are essential for embryonic development. *J. Cell Biol.* **160,** 189–200 (2003).
49. Frezza, C. *et al.* OPA1 controls apoptotic cristae remodeling independently from mitochondrial fusion. *Cell* **126,** 177–189 (2006).
50. Frey, T. G. & Mannella, C. A. The internal structure of mitochondria. *Trends Biochem. Sci.* **25,** 319–324 (2000).
51. Olichon, A. *et al.* Loss of OPA1 perturbates the mitochondrial inner membrane structure and integrity, leading to cytochrome c release and apoptosis. *J. Biol. Chem.* **278,** 7743–7746 (2003).
52. Arnoult, D., Grodet, A., Lee, Y. J., Estaquier, J. & Blackstone, C. Release of OPA1 during apoptosis participates in the rapid and complete release of cytochrome c and subsequent mitochondrial fragmentation. *J. Biol. Chem.* **280,** 35742–35750 (2005).
53. Scorrano, L. *et al.* A distinct pathway remodels mitochondrial cristae and mobilizes cytochrome c during apoptosis. *Dev. Cell* **2,** 55–67 (2002).
54. Semenza, G. L. Targeting HIF-1 for cancer therapy. *Nat. Rev. Cancer* **3,** 721–732 (2003).
55. Galkin, A., Abramov, A. Y., Frakich, N., Duchen, M. R. & Moncada, S. Lack of oxygen deactivates mitochondrial complex I: implications for ischemic injury? *J. Biol. Chem.* **284,** 36055–36061 (2009).
56. Piruat, J. I. & Lopez-Barneo, J. Oxygen tension regulates mitochondrial DNA-encoded complex I gene expression. *J. Biol. Chem.* **280,** 42676–42684 (2005).
57. Acin-Perez, R., Fernandez-Silva, P., Peleato, M. L., Perez-Martos, A. & Enriquez, J. A. Respiratory active mitochondrial supercomplexes. *Mol. Cell* **32,** 529–539 (2008).
58. Schagger, H. & Pfeiffer, K. Supercomplexes in the respiratory chains of yeast and mammalian mitochondria. *EMBO J.* **19,** 1777–1783 (2000).
59. Lapuente-Brun, E. *et al.* Supercomplex assembly determines electron flux in the mitochondrial electron transport chain. *Science* **340,** 1567–1570 (2013).
60. Acin-Perez, R. *et al.* Respiratory complex III is required to maintain complex I in mammalian mitochondria. *Mol. Cell* **13,** 805–815 (2004).
61. Diaz, F., Fukui, H., Garcia, S. & Moraes, C. T. Cytochrome c oxidase is required for the assembly/stability of respiratory complex I in mouse fibroblasts. *Mol. Cell Biol.* **26,** 4872–4881 (2006).
62. Schagger, H. Respiratory chain supercomplexes. *IUBMB Life* **52,** 119–128 (2001).
63. Suthammarak, W., Morgan, P. G. & Sedensky, M. M. Mutations in mitochondrial complex III uniquely affect complex I in *Caenorhabditis elegans*. *J. Biol. Chem.* **285,** 40724–40731.
64. Cogliati, S. *et al.* Mitochondrial cristae shape determines respiratory chain supercomplexes assembly and respiratory efficiency. *Cell* **155,** 160–171 (2013).
65. Dkhil, N. *et al.* Hyperpermeability and ATP depletion induced by chronic hypoxia or glycolytic inhibition in Caco-2/8e monolayers. *Am. J. Physiol.* **270,** G1010–G1021 (1996).

66. Iyer, N. V. *et al.* Cellular and developmental control of O2 homeostasis by hypoxia-inducible factor 1 alpha. *Genes Dev.* **12,** 149–162 (1998).
67. Cregan, S. P. *et al.* Bax-dependent caspase-3 activation is a key determinant in p53-induced apoptosis in neurons. *J. Neurosci.* **19,** 7860–7869 (1999).
68. Mekhail, K., Gunaratnam, L., Bonicalzi, M. E. & Lee, S. HIF activation by pI1-dependent nucleolar sequestration of VHL. *Nat. Cell Biol.* **6,** 642–647 (2004).
69. Cheung, E. C. *et al.* Dissociating the dual roles of apoptosis-inducing factor in maintaining mitochondrial structure and apoptosis. *EMBO J.* **25,** 4061–4073 (2006).
70. Wittig, I., Braun, H. P. & Schagger, H. Blue native PAGE. *Nat. Protoc.* **1,** 418–428 (2006).

Acknowledgements

We thank Dr Stephen Lee for critical review of the manuscript, as well as Linda Jui, Peter Rippstein, Vincent Paupe, Alysen Clark and Delphie Dugal-Tessier for excellent technical assistance. This research was funded by grants from the Heart and Stroke Foundation of Canada (HSFO) and Brain Canada/Krembil Foundation to R.S.S. M.K. was supported by fellowships from the Canadian Partnership for Stroke Recovery and the Heart and Stroke Foundation of Canada. D.P. was supported by Ontario Graduate Scholarship (OGS). Equipment was supported by the Canadian Partnership for Stroke Recovery.

Author contributions

All authors reviewed the manuscript. M.K. conceptualized the study, designed and performed experiments, analysed data and wrote the paper; M.T. assisted, performed and analysed experiments; D.P. assisted in the BN-PAGE and Seahorse experiments and interpreted the data; P.K. designed and performed *in vivo* experiments and interpreted the data; J.M. provided technical assistance and generated tools for the study; I.G. performed SLP2 experiments; R.B. supervised *in vivo* experiments; S.P.C. provided the SLP2 conditional mice, supervised and performed SLP2 experiments; M.E.H. provided the Seahorse Analyzer, reagents and interpreted the data; D.P. provided reagents and interpreted the data; and R.S.S. supported and directed the research.

Additional information

Supplementary Information accompanies this paper at http://www.nature.com/naturecommunications

Competing financial interests: The authors declare no competing financial interests.

Reprints and permission information is available online at http://npg.nature.com/reprintsandpermissions/

How to cite this article: Khacho, M. *et al.* Acidosis overrides oxygen deprivation to maintain mitochondrial function and cell survival. *Nat. Commun.* 5:3550 doi: 10.1038/ncomms4550 (2014).